CENTRO DE INVESTIGACIÓN Y DE ESTUDIOS AVANZADOS
DEL INSTITUTO POLITECNICO NACIONAL

Cinvestav

UNIDAD ZACATENCO

DEPARTAMENTO DE GENETICA Y BIOLOGIA MOLECULAR

PARTICIPACIÓN DE LOS TRANSPORTADORES DE GLUTAMATO EN LA SEÑALIZACIÓN GLUTAMATÉRGICA

TESIS

Que Presenta:

M. en C. ZILA BRUMILDA MARTÍNEZ LOZADA

Para obtener el grado de:

DOCTORA EN CIENCIAS

DIRECTOR DE TESIS: DR. ARTURO ORTEGA SOTO

México, D.F. Febrero, 2015

El presente trabajo fue realizado en el laboratorio 31 del Departamento de Toxicología del Centro de Investigación y de Estudios Avanzados del I.P.N. bajo la dirección del Dr. Arturo Ortega Soto y con la asesoría de los Doctores Esther I. López-Bayghen, Rossana Zepeda Hernández, Bulmaro Cisneros Vega, Samuel Zinker Ruzal y Francisco Castelán.

Durante la realización del presente trabajo el autor contó con el apoyo de la beca 300778 del Consejo Nacional para la Ciencia y la Tecnología (CONACYT)

AGRADECIMIENTOS

A mi tutor y amigo, Dr. Arturo Ortega Soto, por su confianza en mi, su paciencia, las múltiples enseñanzas en lo académico y personal, por jalarme las orejas de vez en cuando, y por enseñarme el amor a la ciencia.

A los miembros de mi comité tutorial: Dra. Esther López-Bayghen, Dra. Rossana Zepeda Hernández, Dr. Samuel Zinker Ruzal, Dr. Bulmaro Cisneros Vega y el Dr. Francisco Castelán , por el apoyo brindado, sus valiosas enseñanzas y oportunos comentarios que enriquecen mi formación profesional.

A la Dra. Babette Fuss por abrirme las puertas de su laboratorio, por sus enseñanzas y por su amistad.

Agradezco la asesoría técnica de Luisa Clara Regina Hernández Kelly, Blanca Roció Ibarra López y Luis Ángel Cid Cid, del Departamento de Toxicología, Cinvestav-IPN por el entrenamiento en las metodologías realizadas en este trabajo.

A mis amigos del laboratorio y anexos, Miguel, Carla, Bruno, Edna, Orqui, Beto, Dona, Natalie, Sheila, Luisito, Clarita y Blanquis por hacer mi estancia en el laboratorio mas amena y por relajarme cuando mas lo necesitaba.

A mis padres, Laura y Jordi, mi respaldo, por su amor, su ejemplo, sus oraciones, su confianza, sus sabios consejos; porque a pesar de todo siempre han estado ahí para mi, los amo muchísimo y recuerden "la familia unida jamás será vencida con la ayuda de Dios".

A mi hermana Eda, por ser mi BFPS, por su apoyo incondicional, su amistad, por su alegría, por tener en ella alguien que me escuche siempre. Te amo best. A mi cuñado Luis y a mis sobrinos hermosos, Grethel y David, por su sonrisas, sus abrazos y por recordarme que es lo que realmente vale la pena.

A mi esposo Alain Marc, gracias por esta aventura que estamos empezando, gracias por tu apoyo incondicional en el lab y fuera de el, por estar para mi en las buenas y en las malas, por tu paciencia (se que has necesitado mucha), por los viajes y todo lo que hemos compartido y seguiremos compartiendo. Gracias por soñar junto a mi y por creer en esta familia. Te amo!!!

A Dios, por su respaldo, por ser mi luz, mi fortaleza y mi guía.

… Por ellos y para ellos!

INDICE GENERAL

ABREVIATURAS

a.a	Aminoácidos
AAA	L-α-aminoadipato
ABH	Aspartato-β-hidroxamato
AMPA	ácido α-amino- 3-hidroxi-5-methilisoxazol-4-propionico
CaMKIIβ	Cinasa dependiente de Calcio-Calmodulina IIβ
CGB	Células Gliales de Bergmann
CGM	Células Gliales de Müller
CNQX	6-cyano-7-nitorquinoxalina-2,3-dione
CP	Células de Purkinje
CPCCOEt	7- (hidroximino)ciclopropa[β]cromen-1a-carboxilato etil ester
CPPG	(RS)-a-ciclopropil-4-fosfonofenilglicina
CRD	Dominio Rico en Cisteinas
DAG	Diacilglicerol
D-Asp	D-Aspartato
DHK	Dihidrokainato
EAAC1	Acarreador de aminoácidos excitadores 1
EAATs	Transportadores de aminoácidos excitadores
eEF2K	Cinasa del factor de elongación eucariota 2
EMSA	Ensayo de cambio en la movilidad electroforética
GFAP	Proteína acidica fibrilar glial
GFP	Proteína verde fluorescente
GLAST	Transportador de Glutamato/Aspartato
GLT-1	Transportador de Glutamato 1
iGluRs	Receptores ionotrópicos de glutamato
IP_3	Inositol tri-fosfato
KA	Kainato
KB-R7943	2-[2-[4-(4-Nitrobenziloxi)-fenil]-etil]-iso-tioreamesilato
L-AP4	L-2-amino-4-fosfonobutirato
L-AP5	L-(+)-2-Amino-5-acido-fosfonopentanoico
L-CCG-1	(2S, 1´R, 2´R, 3´R)-2-(2,3-dicarboxiciclopropil) glicina
MAG	glicoproteína asociada a mielina
MBP	Proteína básica de mielina
mGluRs	Receptores metabotrópicos de Glutamato
MOG	Glicoproteína de oligodendrocitos-mielina
mTOR	Blanco de rapamicina de mamíferos
MS	Esclerosis Múltiple
NMDA	ácido N-metil-D-aspartico
NO	Oxido Nítrico
PDC	ácido L-trans-pirrolidina-2,4-dicarboxilico

PDK1	Cinasa dependiente de fosfoinositidos 1
PIP2	L-3-fosfatidilmioinositol-4,5-bifosfato
PKB	Proteína cinasa B
PKC	Proteína cinasa C
PLC	Fosfolipasa C
PLP	proteína proteolipídica
PMSF	Fluoruro de fenilmetil-sulfonilo
PP2	4-amino-5-(4-clorofenil)-7-(dimetiletil)pirazol[3,4-d]pirimidina
$p70^{S6K}$	cinasa de la proteína ribosomal S6 de 70 KDa
SFB	Suero Fetal Bovino
siRNAs	RNAs pequeños interferentes
SNC	Sistema Nervioso Central
t-ACPD	ácido 1-amino-ciclopentano-trans-1,3-dicarboxilico
TBOA	ácido DL-threo-β-benziloxiaspartico
THA	L-treo-β-hidroxi-aspartato
TM	Dominio Transmembranal
TNFα	Factor de necrosis tumoral α
T3MG	ácido-(±)-threo-3-metilglutamico
VFD	Dominio Flytrap Venus
VGCC	Canales de Calcio dependientes de Voltaje
W7	N-(6-aminohexil)-5-cloro-1-naftalensulfonamida
4EBP	Proteína de Unión al factor de elongación 4

INDICE DE FIGURAS INTRODUCCION

INDICE DE FIGURAS RESULTADOS

RESUMEN

El glutamato es el principal neurotransmisor excitador del sistema nervioso central, activa una amplia variedad de cascadas de señalización que regulan la biosíntesis de proteínas a nivel transcripcional y traduccional. La regulación diferencial de genes dependiente de la actividad glutamatérgica ha sido atribuida a la activación de los receptores ionotrópicos y metabotrópicos de este neurotransmisor.

La remoción del glutamato se lleva a cabo a través de transportadores dependientes de Na^+. Estas proteínas se expresan en las células gliales y en las neuronas. En la retina, las células gliales de Müller (CGM) son responsables de la mayor parte de la captura de glutamato a través del transportador de glutamato/aspartato (GLAST/EAAT-1); mientras que en el cerebelo la glía mas abundante, las llamadas células gliales de Bergmann (CGB) remueven el glutamato también gracias a GLAST. Recientemente se ha propuesto que los axones no mielinizados pueden liberar glutamato, el cual es removido por los oligodendrocitos los cuales expresan GLAST, el transportador de Glutamato 1 (GLT-1/EAAT-2), y al acarreador de aminoácidos excitadores 1 (EAAC-1/EAAT3).

Tomando en consideración el acople funcional de las células gliales con las neuronas, se decidió investigar el papel de GLAST como molécula transductora de señales, con este fin, cultivos primarios de CGB y CGM se expusieron a D-Aspartato, análogo del glutamato que no activa los receptores glutamatérgicos pero puede ser transportado por el mismo sistema, y se determino la fosforilación de mTOR, proteína clave en la regulación traduccional. Con el uso de inhibidores específicos se demostró que GLAST actúa como molécula traductora de señales al inducir un influjo de Ca^{2+} mediado por el intercambiador de Na^+/Ca^{2+}, que repercute en regulación traduccional mediante la vía PI3K/Akt/mTOR y en regulación transcripcional al activar la vía CaMKII/MEK/RSK/CREB.

Estos resultados abrieron dos preguntas, GLAST es el único transportador de glutamato con actividad de transductor de señales?, Solo los

transportadores de Glutamato de las células de glía radial son capaces de señalizar? Con el fin de contestar estas preguntas, utilizamos el otro modelo de glía, los oligodendrocitos, y utilizando este modelo fuimos capaces de demostrar que todos los transportadores de glutamato expresados en oligodendrocitos son capaces de inducir cascadas de señalización que repercuten en la maduración morfológica de los oligodendrocitos, a través de la fosforilación de CaMKIIβ.

Los resultados obtenidos añaden un nuevo mediador de los efectos del glutamato y apoyan de manera significativa la participación de las células gliales en la neurotransmisión glutamatérgica.

ABSTRACT

Glutamate, the main excitatory amino acid transmitter triggers a wide variety of signaling cascades that regulate protein biosynthesis at the transcriptional and translational levels. Activity-dependent differential gene expression has been attributed to the activation of ionotropic and metabotropic membrane glutamate receptors.

A family of Na^+-dependent glutamate transporters is responsible for Glutamate uptake from the synaptic cleft. Although these transporter proteins are present in neurons and glia cells, the vast majority of the transport takes place in glial cells. Within the retina, Müller glia cells are responsible for most of glutamate uptake activity through the Na^+-dependent glutamate/aspartate transporter (GLAST/EAAT-1), meanwhile the most abundant glial cells in cerebellum, the Bergmann glial cells, uptake glutamate thought the transporter GLAST. Recently has been suggested that unmyelinated axons release glutamate, which is remove by glutamate transporters expressed in oligodendrocytes, which are at least from three types (EAAT1-3).

Taking into consideration the functional coupling of neurons with glial cells, we decided to investigate a plausible role of GLAST as a signaling molecule. To this end, primary cultures of Müller and Bergmann cells were exposed to D-aspartate, Glutamate analog that do not activate glutamatergic receptors but can be transported by the same system, and the phosphorylation of mTOR, a key translational regulator, was determined. With the use of specific inhibitors we were able to demonstrate that GLAST acts as a signal transducer molecule to induce Ca^{2+} influx through the Na^+/Ca^{2+} exchanger, this impacts translational regulation through the signaling cascade PI3K/Akt/mTOR and transcriptional regulation through CaMKII/MEK/RSK/CREB.

These results open two questions, Is GLAST the only glutamate transporter with transducer signaling activity?, Radial glial glutamate transporters are the only ones with the ability to induce pathways activation? To answer these questions we use other glial cell model, oligodendrocytes. Using this model we were demonstrate that all the glutamate transporters expressed in oligodendrocytes are able to induce pathways activation that impact oligodendrocytes morphology maturation, through CaMKIIβ phosphorylation.

These results add a novel mediator of the glutamate effects particularly important in glia cells and further strengthen the notion of the critical involvement of glia cells in glutamatergic neurotransmission.

INTRODUCCIÓN

El glutamato es el principal neurotransmisor excitador en el sistema nervioso central (SNC) de vertebrados (Watkins and Evans 1981) y está involucrado en la mayoría de las funciones del cerebro incluyendo la cognición, memoria y el aprendizaje (Headley and Grillner 1990). El glutamato juega un papel importante en el desarrollo del SNC, ya que regula la proliferación, migración y sobrevivencia de progenitores neuronales y de las neuronas inmaduras (Guerrini, Blasi et al. 1995). Este neurotransmisor también juega un papel clave en la plasticidad sináptica y en la regulación de la expresión de genes, así como en la muerte neuronal por excitotoxicidad (Thomas and Huganir 2004, Wang, Gong et al. 2007).

En el cerebro el glutamato es sintetizado a partir del α-cetoglutarato, intermediario del ciclo de Krebs (Smith 2002), esta reacción es catalizada por la enzima glutamato deshidrogenasa (Mathews, Van Holde et al. 2000). Para llevar a cabo sus funciones el glutamato se une a receptores específicos que se encuentran en la membrana de células gliales y neuronas. Los receptores a glutamato han sido divididos en dos tipos, receptores glutamatérgicos del tipo ionotrópicos (iGluRs) y receptores glutamatérgicos metabotrópicos (mGluRs). Los primeros se caracterizan por ser canales dependientes de ligando y la formación de un canal iónico; mientras que los mGluRs están acoplados a proteínas G y la transducción de la señal es vía segundos mensajeros (Hollmann and Heinemann 1994).

Receptores glutamatérgicos ionotrópicos

Se caracterizan por formar un canal iónico que se abre por ligando y de acuerdo a los agonistas que los activan se subdividen en Ácido N-metil-D-aspártico (NMDA; GluN1, GluN2A-D y GluN3A,B), Ácido α-amino-3-hidroxi-5-metil-4-isoxazolpropiónico (AMPA; GluA1-4) y Ácido Kaínico (KA; GluK5-7, GluK 1, 2). Esta categoría presenta subunidades proteicas con un dominio N-terminal largo de aproximadamente 45 kDa que reside en la hendidura sináptica en donde interactúa con proteína sinápticas como N-cadherina (Saglietti, Dequidt et al. 2007), un dominio C-terminal

intracelular , 3 segmentos transmembranales y un segmento reentrante (Ozawa, Kamiya et al. 1998).

Recientemente Avalon y Stern Bach aportaron evidencia de un ensamblaje secuencial de canales tetraméricos de los receptores de glutamato ionotrópicos como dímeros de dímeros que permiten el flujo de cationes cuando el Glutamato se une a ellos. Primero se forma una dimerización de las subunidades mediada principalmente por la interacción entre dominios N-terminal compatibles (paso 1. Dímeros de monómeros), ésta primera dimerización es seguida por una segunda dimerización más débil entre dímeros, la cual se forma por la compatibilidad de los dominios de unión al ligando y de los dominios transmembranales de las subunidades, permitiendo así la obtención del tetrámero funcional de los iGluR (Madden 2002).

La formación de los tetrámeros de los iGluRs deriva de las interacciones combinadas entre los dominios transmembrana junto con las interacciones entre el domino N-terminal y los dominios S1S2 (Jin, Singh et al. 2009).

Cuando el glutamato o sus agonistas interactúan con la región S1S2 se abre un poro en la membrana por donde ocurre el flujo de sodio, potasio y/o calcio.

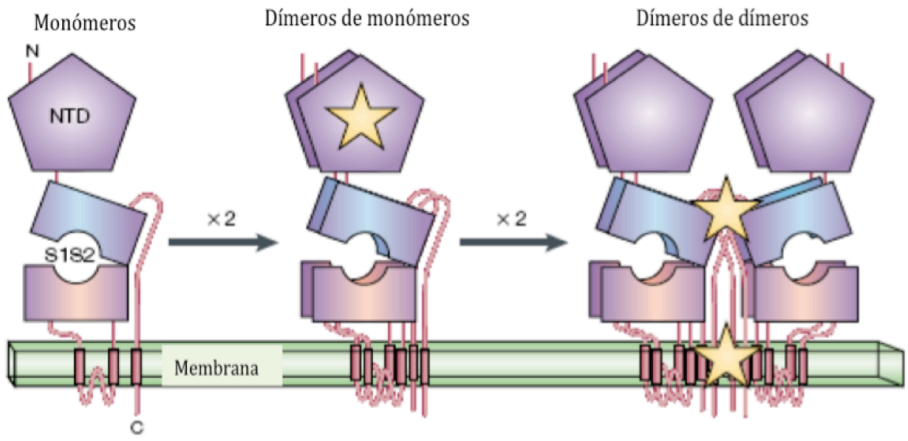

Figura 1. **Ensamblaje de los iGluR (Madden 2002).**

- **Receptores AMPA**

Los receptores AMPA son responsables de la primera despolarización en la neurotransmisión mediada por glutamato y juegan papeles claves en la plasticidad sináptica. Se han asociado los cambios en la fosforilación y distribución celular de los receptores AMPA con cambios en la fuerza sináptica dependientes de actividad a largo plazo como potenciación a largo plazo o depresión a largo plazo (Santos, Carvalho et al. 2009). También se ha involucrado la desregulación de los receptores AMPA en patologías (Kwak and Weiss 2006, Liu, Liao et al. 2006).

Los receptores AMPA responden rápidamente a la aplicación del agonista (1-4ms) y se desensibilizan rápidamente (2-14ms). Son sensibles tanto a AMPA como a KA aunque presentan mayor afinidad al primero, de allí su nombre. Están formados por las subunidades denominadas GluR1 al 4 que poseen cerca de 900 aminoácidos (a.a.) y tienen un peso molecular de cerca de 105 kDa, comparten 68-73% de identidad, comparten cuatro dominios hidrofóbicos: TM1, TM3 y TM4 atraviesan la membrana, mientras que M2 es un segmento reentrante que forma parte del poro del canal. El C-terminal de las subunidades de los receptores AMPA es intracelular y muestra diferencias entre subunidades. Las subunidades de los receptores AMPA pueden combinarse formando homodímeros ó heterodímeros son más permeables a Na^+ y K^+ que a Ca^{2+} esta propiedad reside en la posición 586 de la subunidad GluR2, un residuo de glutamina (Q) aumenta la permeabilidad a Ca^{2+}, mientras que los que presentan arginina (R) son mucho más permeables a Na^+. Este residuo 586, es un sitio de edición del mRNA, el codón de glutamina CAG de la posición 586 es editado por la acción de la enzima adenosina desaminasa a inosina, CIG, que se interpreta como guanina CGG, que codifica para arginina, (Ozawa, Kamiya et al.) Esta edición se presenta en el 99.9% de los casos en el organismo adulto por lo que se concluye que la expresión de la subunidad GluR2 dicta la selectividad de los receptores AMPA, en casos como el de las células gliales de Bergmann (CGB), la ausencia de la subunidad GluR2, supone la presencia de receptores AMPA permeables a Ca^{2+}.

- **Receptores KA**

Los receptores KA son activados por el análogo glutamatérgico KA, de acuerdo con la afinidad a éste, se dividen en receptores KA de baja afinidad y receptores KA de alta afinidad. Los primeros presentan una afinidad a KA de 50nM y están formados por las subunidades GluR5, GluR6 y GluR7. Los receptores KA de alta afinidad, reciben este nombre debido a que su afinidad por KA es de 5nM; se componen de las subunidades KA-1 y KA-2 que interaccionan con las subunidades GluR5-GluR7 para formar canales funcionales (Chittajallu, Braithwaite et al. 1999). Las subunidades GluR7, KA-1 y KA-2 forman canales funcionales si forman complejos con GluR5 y GluR6.

Los receptores KA presentan homología en un 35-40% con los receptores AMPA. Las subunidades GluR5-7 presentan 75-80% de identidad entre ellas y se constituyen de alrededor de 900 a.a., mientras que KA-1 y KA-2 poseen cerca de 970 a.a. con un 70% de identidad entre ellas (Ozawa, Kamiya et al.). El sitio de edición Q/R referido en GluR2, también está presente en GluR5 y GluR6, en esta última existen otros cambios de isoleucina por valina y otro de tirosina por cisteína, en todos los casos favorecen la permeabilidad a Ca^{2+}; así los homodímeros GluR6 son permeables a este ión.

- **Receptores NMDA**

En comparación con los AMPA y KA, los receptores NMDA se caracterizan por responder de forma lenta a glutamato y requieren de D-serina como co-agonista, por lo que presentan un sitio de unión a este aminoácido. La respuesta lenta a glutamato se debe a que estos receptores se inactivan en presencia de Mg^{2+} extracelular. La activación de receptores NMDA es dependiente de voltaje, por lo que el bloqueo con Mg^{2+}.

Los receptores NMDA son altamente permeables a Ca^{2+}, Na^{+} y K^{+}; están conformados por las subunidades NMDAR1, NMDAR2A-D y NMDAR3. Las subunidades NR2 comparten 38-53% de identidad en su secuencia de a.a. y cerca del 72% de homología con NR1. Las subunidades NR3 comparten aproximadamente 50% de identidad aminoacídica, y cerca del 27% con las subunidades NR1 y NR2. Las subunidades NMDAR2 son funcionales si se expresan conjuntamente con las NMDAR1. Cada subunidad consta de 938 a.a. En cuanto al sitio de edición del RNA mensajero (mRNA) Q/R, los receptores NMDA presentan asparagina (N), lo que controla la permeabilidad a Ca^{2+} y el bloqueo por Mg^{2+}. Cuando el residuo N es reemplazado por Q se reduce tanto la permeabilidad a Ca^{2+} como el bloqueo por Mg^{2+}, mientras que el cambio de N por R abate ambas características (Ozawa, Kamiya et al.).

Receptores glutamatérgicos metabotrópicos

Los receptores glutamatérgicos de tipo metabotrópico están formados por proteínas de siete segmentos transmembranales de 854-1179 a.a. Están acoplados a proteínas G y se clasifican en tres grupos de acuerdo a la homología de su secuencia, al tipo de proteína G a la que se encuentran acoplados y por la selectividad al ligando. (Kew and Kemp 2005). Mientras que en cada grupo la homología de secuencia es de mas de 70%, entre grupos la homología es de solo 45% aproximadamente. La superfamilia de mGluRs consiste en 12 miembros codificados por 8 genes, lo cual sucede gracias a múltiples sitios alternativos de corte y empalme en algunos genes de *mGluRs*, mientras que otros genes codifican solo un receptor. Por ejemplo, el gen *mGluR1* codifica 5 isoformas mientras que solo hay una isoforma de *mGluR2* (Willard and Koochekpour 2013).

Los receptores mGluRs contiene un dominio N-terminal extracelular largo, llamado "Dominio flytrap Venus" (VFD), su estructura cristalográfica reveló que el dominio VFD consta de dos lóbulos que se sientan uno encima del otro formando una hendidura entre ellos en la cual se une el

glutamato (Moepps and Fagni 2003). La evidencia sugiere que dos dominios VFD dimerizan juntos. La unión del agonista a uno o ambos VFD induce grandes cambios conformacionales. El dímero VFD existe en tres estados principales: abierto-abierto, abierto-cerrado y cerrado-cerrado (Figura 2). La conformación abierta-abierta (inactiva) es estabilizada por los antagonistas, las conformaciones abierta-cerrada y cerrada-cerrada son inducidas por la unión del ligando a uno o ambos protómeros.

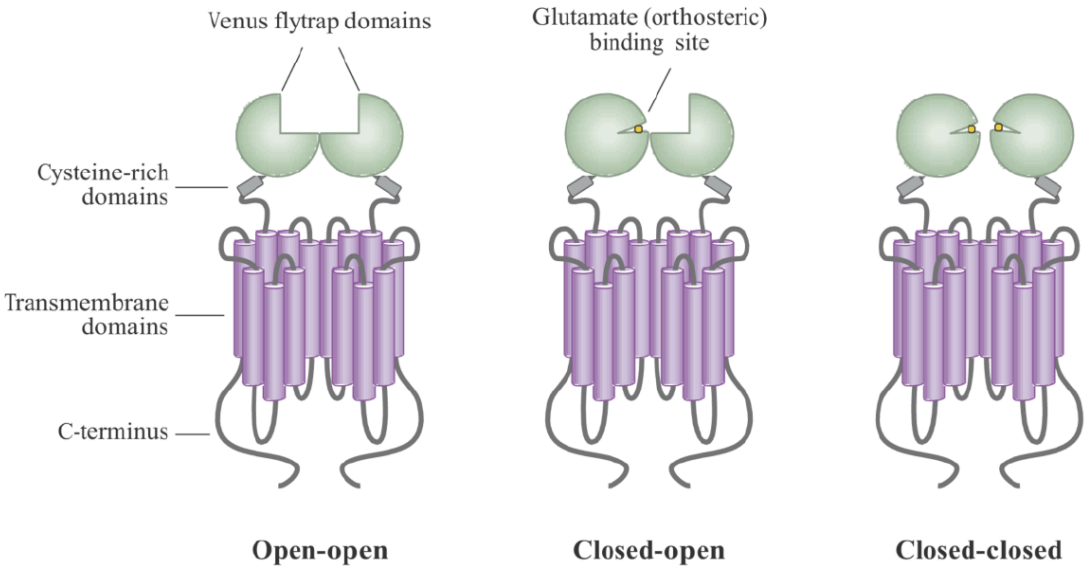

Figura 2 Diagrama esquemático del dímero de los mGluRs en diferentes estados de actividad. Los dímeros de mGluRs contienen dos dominios extracelulares largos llamados VFDs, los cuales unen el glutamato. El dominio rico en cisteína une el dominio VFD a los siete dominios transmembranales, el C-terminal intracelular esta sujeto a corte y empalme alternativo para generar diferentes C-terminales (Niswender and Conn 2010).

Los cambios conformacionales inducidos por la unión del ligando son propagados del dominio VFD al dominio de los siete segmentos transmembranales y al dominio C-terminal por el dominio rico en cisteínas (CRD). El dominio CRD contiene nueve residuos de cisteína críticos, ocho de los cuales se encuentran formando puentes disulfuro. El C-terminal de los mGluRs es un región importante para la modulación de la proteína G a la cual se acoplan. Adicionalmente, esta región de varios mGluRs esta sujeta a corte y empalme alternativo, regulación por fosforilación, e interacciones proteína-proteína moduladoras (Niswender

and Conn 2010).

El grupo I está formado por receptores acoplados a proteínas G_q; se constituye por los receptores mGluR1a-c y mGluR5a-b involucrados en la activación de fosfolipasa C (PLC). La PLC cataliza la conversión de L-3-fosfatidilmioinositol-4,5-bifosfato (PIP_2) a inositol-1,4,5-trifosfato (IP_3) y diacilglicerol (DAG); los productos de esta reacción repercuten en la activación de la proteína cinasa C (PKC) y la liberación de Ca^{2+} en el retículo endoplásmico respectivamente (Ribeiro, Paquet et al. 2010). Estos receptores responden a quisqualato y al ácido 1-amino-ciclopentano-trans-1,3-dicarboxilico (t-ACPD) además de glutamato e ibotenato.

El grupo II está formado por las subunidades mGluR2 y mGluR3, que se acoplan a proteínas G_i, por lo que inhiben a la adenilato ciclasa, reduciendo los niveles de AMPc y responden al agonista (2S, 1´R, 2´R, 3´R)-2-(2,3-dicarboxiciclopropil) glicina (L-CCG-1) y t-ACPD (Nakanishi, Nakajima et al. 1998).

El grupo III se integra por los receptores mGluR4a-b y mGluR6, mGluR7 y mGluR8, acoplados a proteínas G_i. Estos receptores también están involucrados en la inhibición de la Adenilato ciclasa y se caracterizan por ser sensibles a L-2-amino-4-fosfonobutirato (L-AP4) y L-serina-O-fosfato (Ozawa, Kamiya et al.).

Sistemas de captura de glutamato

La activación excesiva de los receptores de glutamato resulta en un fenómeno denominado excitotoxicidad, uno de los principales fenómenos relacionados con enfermedades neurodegenerativas, esta sobre-estimulación lleva a la muerte neuronal (Olney 1969) y de los oligodendrocitos (MacDonald and Fahien 2000).

Se ha demostrado que la activación de receptores ionotrópicos de glutamato incrementa el consumo de energía (Pellerin and Magistretti

1994, Pellerin and Magistretti 1997) debido a que el influjo de Na^+ y Ca^{2+} asociado a la actividad de los receptores. El abatimiento de estos niveles supone una expulsión de los iones en un proceso dependiente de energía (Novelli, Reilly et al. 1988). Adicionalmente, la activación de receptores de glutamato genera especies reactivas de oxígeno (Bondy and Lee 1993). Por lo que, es de importancia crítica que la concentración extracelular de glutamato se mantenga baja.

La única forma rápida de remover el glutamato del líquido extracelular es por captura celular (Balcar and Johnston 1972). La captura de glutamato es realizada por proteínas transportadoras de glutamato las cuales usan el gradiente electroquímico a través de la membrana plasmática para llevar a cabo la captura.

Tanto las neuronas como las células gliales expresan transportadores de glutamato. Algunos de los cuales se encuentran en la membrana plasmática y otros se encuentran intracelularmente.

Existen dos tipos de transportadores de glutamato:

1. *Transportadores de glutamato independientes de sodio ó de baja afinidad con una Km > 500 μM.*
2. *Transportadores de glutamato acoplados a sodio y potasio ó transportadores de aminoácidos excitadores (EAATs), transportadores de alta afinidad con una Km = 1-100 μM.*

- **Transportadores de baja afinidad**

Exhibe valores de Km cercanos a 500 μM (Danbolt 2001) y es un sistema independiente de Na^+ y sensible a la inhibición por D-glutamato (Benjamin and Quastel 1976) y por L-homocisteato (Cox, Headley et al. 1977). Este sistema de captura se ha sugerido para suplementar con aminoácidos a las células cerebrales con propósitos metabólicos.

- **Transportadores de alta afinidad**

Se han identificado cinco subtipos: el transportador de glutamato – aspartato GLAST (EAAT1), el transportador de glutamato 1 GLT-1 (EAAT2), acarreador de aminoácidos excitatorios 1 EAAC1 (EAAT3), transportador de aminoácidos excitatorios 4 (EAAT4) y transportador de aminoácidos excitatorios 5 (EAAT5) (Danbolt 2001). Las cinco proteínas catalizan el transporte de L-glutamato así como de L- y D-aspartato acoplado al transporte de Na^+ y de K^+. El tamaño promedio de los cinco subtipos de transportadores de glutamato varía entre 523 y 527 a.a. y tienen una identidad en la secuencia de aminoácidos del 50 – 60%.

El proceso de captura es llevado a cabo por un gradiente electroquímico a través de la membrana celular. Primeramente de lleva a cabo el co-transporte de un glutamato con tres iones Na^+ y un ion protón hacia el citosol, y después se lleva a cabo el contra-transporte de un ion K^+ requerido para que el transportador regrese a su cara externa, en el estado libre (no ocupado)(Figura 3). (Kanner and Sharon 1978, Roskoski 1979, Barbour, Brew et al. 1988, Sarantis and Attwell 1990, Szatkowski, Barbour et al. 1991). El ciclo de transporte es reversible en todos sus pasos. El proceso de captura es sensible a la temperatura (Wadiche and Kavanaugh 1998).

Los transportadores de glutamato EAAC y GLT-1 tienen la siguiente estequiometria: una molécula de glutamato es tomada junto a tres Na^+ y un H^+ en intercambio por un K^+ (Danbolt 2001). Por lo tanto, dos cargas positivas provocan que el transporte de glutamato tenga un efecto electrogénico en las células (Figura 3). Basado en esta estequiometria ha sido estimado que la energía consumida por los transportadores de glutamato en el córtex cerebelar representa solo cerca del 2% del consumo de energía total en este tejido (Attwell and Laughlin 2001).

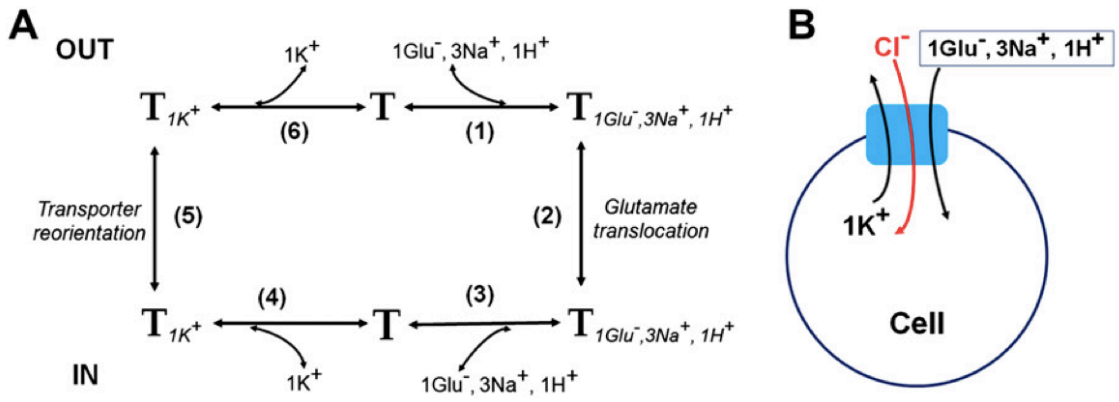

Figura 3 Ciclo de transporte y Estequiometria de los EAATs. (A) Diagrama simplificado del ciclo de transporte mediado por los EAATs. Cuando el glutamato y los iones acoplados (paso 1) se unen a el transportador (T), son translocados (paso 2) y liberados al citosol (paso 3). Después se une el K^+ del lado intracelular (paso 4) y reorienta al transportador que se encuentra libre de sustratos (paso 5), por ultimo el K^+ es liberado fuera de la célula (paso 6). (B) Dibujo que ilustra el acoplamiento iónico de un EAAT. La captura de una molécula de glutamato esta acoplada con el influjo de tres iones Na^+, un H^+ y el eflujo de un ion K^+. Además, los EAATs presentan conductancia aniónica activada por glutamato, que resulta en el influjo de Cl^- bajo condiciones fisiológicas (Jiang and Amara 2011).

Además de transportar glutamato, los EAATs tienen actividad de canales aniónicos (Wadiche, Arriza et al. 1995). La conductancia aniónica es activada por el acoplamiento a Na^+ e incrementa significativamente al agregar glutamato. Sin embargo diversos estudios han demostrado que la corriente aniónica activada por sustrato puede ser llevada a cabo a 4°C o a un potencial de membrana de >70 mV en donde se ha abatido la captura de glutamato (Wadiche and Kavanaugh 1998). Sugiriendo que la actividad del canal aniónico depende de cambios conformacionales diferentes a los requeridos para la captura de glutamato. Los miembros de la familia EAATs contienen seis segmentos transmembranales (TM) formados por α-hélices en el N-terminal, con dos sitios de N-glicosilación localizados en el loop extracelular entre el dominio TM III y IV. Los EAATs contienen un segmento de mas de 50 a.a. entre los segmentos TM4b y TM4c que contienen sitios de N-glicosilación. Las predicciones estructurales para el C-terminal son más ambiguas, en parte porque existen varios residuos cargados en dominios no hidrofóbicos, por lo que la topología del dominio

C-terminal ha sido grandemente debatida. Sin embargo, todos los modelos concuerdan en la existencia de asas re-entrantes, aunque difieren en su número y localización en los dominios TM (Jiang and Amara 2011). Los EAATs forman homo-multímeros, estudios han mostrado que GLT-1 migra como un trímero en SDS-PAGE, mientras que GLAST puede existir como dímeros o trímeros (Haugeto, Ullensvang et al. 1996). Sin embargo aunque la estructura homomultimérica ha sido apoyada por diversos estudios de sedimentación e inmunoprecipitación, cada monómero tiene la capacidad de transportar glutamato.

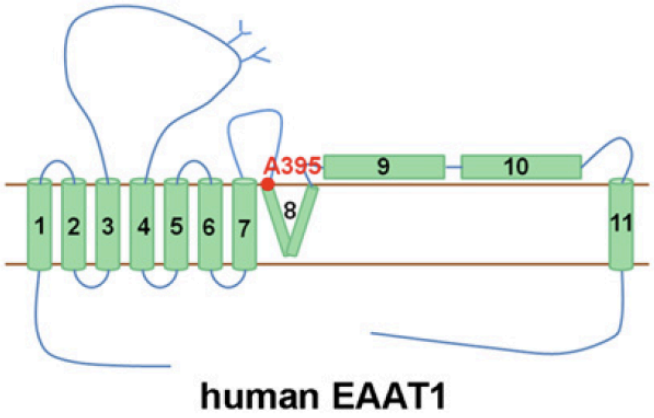

Figura 4 Modelo estructural de los EAATs basado en los resultados obtenidos en estudios por modificaciones de substitución de cisternas usando EAAT1 humano (Jiang and Amara 2011).

Estas proteínas difieren en estructura, propiedades farmacológicas, distribución regional, celular y expresión durante el desarrollo (Robinson and Dowd 1997, Gegelashvili and Schousboe 1998).

GLT-1 y GLAST son los responsables del 80-90% de la captura de glutamato que es atribuida a los cinco subtipos de transportadores (McLennan and Wheal 1976, Schousboe and Hertz 1981). Esto es probablemente validado en todas las regiones del SNC de mamíferos y enfatiza la remoción astroglial de glutamato debido a que las proteínas GLT y GLAST solo se localizan en los astrocitos en el SNC normal y maduro (Haugeto, Ullensvang et al. 1996), con excepción de algunas células epidemales y algunas neuronas en la retina.

GLT-1 y GLAST son los transportadores que se expresan predominantemente en astrocitos; GLT-1 es altamente expresado en el SNC en corteza e hipocampo (Chaudhry, Lehre et al. 1995) la concentración de GLT en hipocampo es de hasta 12,000 moléculas por μm^3 de tejido (Lehre and Danbolt 1998), mientras que la expresión de GLAST es menos abundante en la mayoría de las regiones del cerebro, pero es el principal transportador de glutamato en el cerebelo (Ruiz and Ortega 1995) con una alta densidad de GLAST de hasta 18 000 moléculas por μm^3 de tejido (capa molecular) en las CGB (Lehre and Danbolt 1998) y en la retina en las células gliales de Müller (CGM). EAAC1 es abundante en las neuronas de la corteza, hipocampo y estriado, y su presencia particular en las neuronas inhibidoras como las células de Purkinje pueden reflejar la función de glutamato como precursor de GABA. EAAT4 se localiza principalmente en las dendritas de las neuronas de Purkinje, mientras que EAAT5 se localiza en los fotorreceptores en la retina (Danbolt 2001).

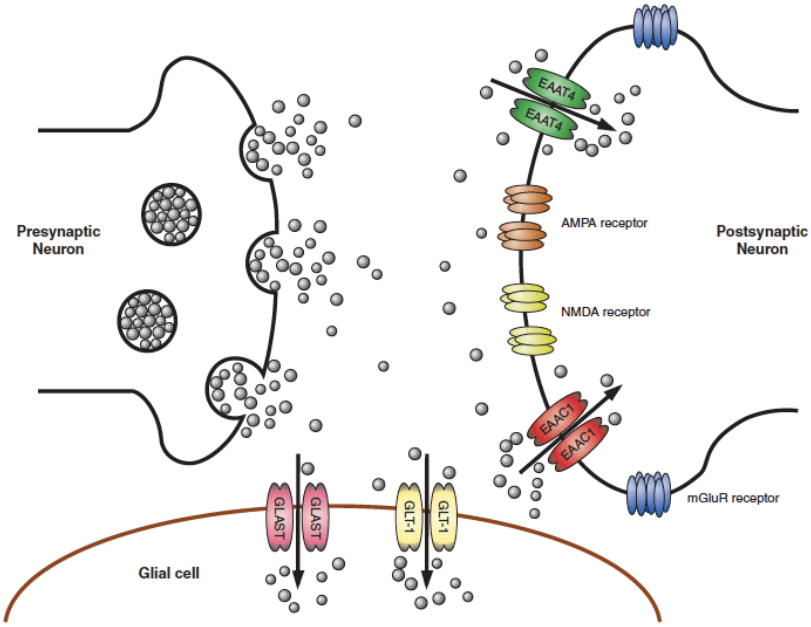

Figura 5 Representación esquemática de una sinapsis glutamatérgica. La liberación sináptica de glutamato provoca la activación de GluRs de diferentes tipos, los cuales se encuentran situados en la neurona post-sináptica, en la terminal pre-sináptica y en las células gliales que rodean esta sinapsis. El glutamato es removido de la hendidura sináptica por transportadores, los cuales, se encuentran enriquecidos en las terminales post-sinápticas y en los procesos de las células gliales. Las neuronas expresan de manera predominante los transportadores EAAC1 y EAAT4, mientras que las células gliales expresan preferencialmente los transportadores "gliales" GLAST y GLT-1 (Gonzalez and Robinson 2004).

En astrocitos, GLAST y GLT-1 exhiben patrones de expresión diferentes: GLAST es el transportador más importante en la captura de glutamato durante el desarrollo, mientras que la expresión de GLT-1 incrementa durante la maduración del SNC (Guillet, Lortet et al. 2002). Se ha demostrado en varias regiones del cerebro y en preparaciones celulares que los transportadores de glutamato difieren cinéticamente, se han establecido las siguientes Km en estudios de clonación para los distintos EAATs: GLAST de rata Km: 77mM, GLT de rata Km: 2mM, EAAC1 de conejo Km: 12mM, y EAAT4 de humano Km: 2.49/0.97mM (Gegelashvili and Schousboe 1998).

Se ha reportado que los transportadores de glutamato son regulados prácticamente a todos los niveles posibles, dentro de estos reportes se ha demostrado que la fosforilación de los transportadores ó proteínas accesorias está implicada en la modulación del tráfico de los transportadores desde compartimentos intracelulares hacia la membrana plasmática y su endocitosis (Duan, Anderson et al. 1999, Guillet, Velly et al. 2005). En células gliales, particularmente en astrocitos y CGB, la regulación de los transportadores de glutamato parece ser tanto en forma dependiente como independiente de los receptores ionotrópicos y metabotrópicos, mediante la activación de cascadas de señalización que involucran proteínas como PKC y PKA (Rana and Hokin 1990, Duan, Anderson et al. 1999, Gonzalez and Ortega 2000, Guillet, Velly et al. 2005).

Los ratones knockout del transportador GLAST, no produce un fenotipo atáxico como era de esperarse dado su expresión en cerebelo; por otra parte, la anatomía cerebelar no estaba visiblemente alterada y el estudio electrofisiológico en el cerebelo no implico un papel fundamental para GLAST en la remoción sináptica del glutamato. Sin embargo, cuando se examinó con más detalle utilizando análisis con rotores de paso y coordinación, los ratones carentes de GLAST no lograron pasar la prueba en la barra rotaria a altas revoluciones, sin embargo a una velocidad baja

realizaron la prueba igual que los controles. Adicionalmente, utilizando una sonda de frío para inducir una lesión traumática, el volumen del edema fue mayor en el cerebelo de los ratones nulos en GLAST que en los controles "wild-type", y el volumen de los edemas de las lesiones traumáticas fue más grande en el cerebelo que en la corteza cerebral (Watase, Hashimoto et al. 1998).

Los ratones knockout de GLT-1 retienen menos del 10% del transporte de glutamato en la corteza cerebral, demostrando que GLT-1 es responsable de la mayoría de la captura del glutamato en el SNC. La perdida subaguda de los transportadores GLT-1, por métodos de anti-sentido, lleva a la parálisis de las extremidad traseras, mientras que los ratones que carecen de GLT-1 desarrollan patología hipocampal, convulsiones y la mayoría muere a las pocas semanas de edad (Tanaka, Watase et al. 1997). Los ratones knockout del transportador EAAC1 desarrollan aminoaciduria dicarboxílica, esto se debe a la perdida de la captura de glutamato y aspartato de los túbulos renales por EAAC1. De manera interesante no se ha observado la perdida neuronal en ninguna de las regiones que normalmente se encuentran enriquecidas en EAAC1 (hipocampo, cerebelo y corteza) (Peghini, Janzen et al. 1997). Los ratones knock-out del transportador EAAT4, no se presentan ningún fenotipo anormal.

Ciclo Glutamato-Glutamina

Los astrocitos contienen en su citoplasma 2-3 mM de glutamato, mientras que las neuronas presentan más de 5 mM. Esta diferencia de concentraciones radica en la presencia de la enzima glutamina sintetasa en los astrocitos, que convierte el glutamato en glutamina, la cual es liberada al medio extracelular para incorporarse a las neuronas.

La glutamina es un aminoácido que se encuentra distribuido de manera ubicua en todos los tejidos de mamíferos, donde actúa como precursor de diversas vías metabólicas, la mayoría de las cuales son similares en el SNC

y en los tejidos periféricos. La Glutamina se encuentra presente normalmente en el fluido extracelular en una concentración cercana a 200-500μM. Esto no compromete la neurotransmisión ya que la glutamina, en contraste con el glutamato, no es tóxica ya que no activa a los receptores de glutamato (Danbolt 2001).

Enfocándonos en el SNC la glutamina es sintetizada a partir de glutamato y amoniaco reacción catalizada por la enzima glutamina sintetasa. La glutamina recién sintetizada es liberada por los astrocitos, transferida a las neuronas e hidrolizada por la enzima glutaminasa, enzima enriquecida en las neuronas, dando lugar a glutamato, el cual es empaquetado en las vesículas sinápticas de la neurona pre-sináptica. Una porción del glutamato puede ser descarboxilado a GABA (ver Figura 6).

Las proteínas que pertenecen a los sistemas A y N muestran localización célula especifica, y son las responsables del transporte de glutamina bien coordinado entre los astrocitos y las neuronas. Los transportadores del sistema A, $SNAT_1$ y $SNAT_2$ son unidireccionales y se localizan en neuronas, catalizando la captura de glutamina. Mientras que los transportadores del sistema N, $SNAT_3$ y $SNAT_5$ son bidireccionales y se localizan en las membranas de los astrocitos mediando el eflujo de la glutamina sintetizada en los astrocitos a partir del glutamato (Chaudhry, Reimer et al. 2002).

La actividad de los transportadores de los sistemas A y N se regulan a nivel transcripcional y traduccional, además se ha reportado que en los transportadores pertenecientes al sistema N su translocación a membrana es regulada mediante fosforilación dependiente de PKCα y γ (Balkrishna, Broer et al. 2010, Nissen-Meyer, Popescu et al. 2011).

A partir de ensayos de resonancia magnética nuclear se ha demostrado que el glutamato es el precursor del 80-90% de la glutamina sintetizada en astrocitos.

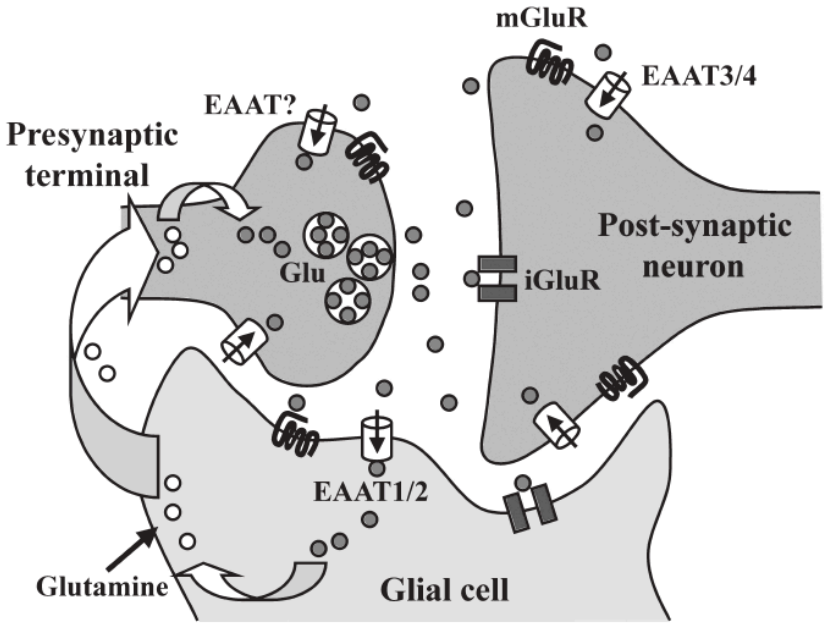

Figura 6 Diagrama del ciclo Glutamato-Glutamina. Glutamato (representado por círculos grises rellenos) es removido de la hendidura sináptica por los EAATs (representados por cilindros) localizados en las neuronas y en las células gliales, en donde es transformado a glutamina (círculos grises vacíos) por la enzima glutamina sintetasa, la glutamina es liberada al espacio extracelular de donde es captada por la terminal pre-sináptica y transformada a glutamato por la enzima glutaminasa, en la neurona pre-sináptica es almacenado en vesículas por el transportador vesicular de glutamato (VGLUT) (O'Shea, Fodera et al. 2002).

Células Gliales

En vertebrados, las células gliales del SNC se clasifican en dos grupos principales: microglía y macroglía. Dentro de sus funciones se encuentran: brindar soporte y estructura al tejido nervioso, a través de producción de mielina para recubrir los axones de las neuronas (oligodendrocitos), remoción de desechos celulares generados por muerte celular o lesiones, actuando también como sistema inmune en el SNC (microglía), en la formación de la barrera hematoencefálica; la glía radial ayuda a la migración neuronal y el crecimiento de los axones. Dentro de las principales funciones de las células gliales se ha descrito la remoción de neurotransmisores liberados por las neuronas durante la neurotransmisión (Kandel, Schwartz et al. 2000). Además de las funciones

de las células gliales mencionadas, se ha demostrado que las células gliales regulan las funciones sinápticas junto a las neuronas, primeramente por su localización y morfología de sus procesos, los cuales envuelven las sinapsis (Witcher, Kirov et al. 2007, Ben Achour and Pascual 2010); y fundamentalmente por las moléculas neuroactivas que pueden liberar, tales como glutamato, ATP, D-Serina, oxido nítrico (NO), radicales libres, citocinas y quimiocinas como el factor de necrosis tumoral alfa (TNF_{α}) e interleucinas (Ben Achour and Pascual 2010).

- **Microglía**

La microglía son células fagocíticas que se movilizan hacia zonas de infección, heridas o por una enfermedad. Estas células surgen de los macrófagos que se encuentran fuera del SNC, y no se relacionan fisiológicamente ni embrionariamente con otras tipos celulares del SNC. Estas células responden a las infecciones, lesiones y convulsiones cambiando sus procesos, a unos mas gruesos y ramificados que los que presentan en estado inactivado, además comienzan a expresar una amplia gama de antígenos.

- **Macroglía**

La macroglía del SNC a su vez se divide en dos grandes grupos astrocitos y oligodendrocitos.

a) Oligodendrocitos

Los oligodendrocitos son las células responsables de la formación de la mielina, una membrana rica en lípidos que rodea los axones de las neuronas, la cual asegura una conducción apropiada de la señal entre axones en el SNC. La perdida de la mielina esta asociada con protección incorrecta del axón lo que con lleva una interrupción en la señalización neuronal, esta se encuentra en la enfermedad desmielinizante esclerosis

múltiple (MS).

Las células precursoras de oligodendrocitos tienen una morfología bipolar pero cuando estas células comienzan a diferenciar empiezan a sufrir cambios en su morfología y en la expresión de diferentes marcadores (lípidos, proteínas, antígenos de superficie o factores de transcripción) que ayudan a diferenciar las diferentes etapas de maduración (Avossa and Pfeiffer 1993, Baumann and Pham-Dinh 2001, Bradl and Lassmann 2010). En el modelo de roedores, varios gangliosidos en la superficie celular de los oligodendrocitos inmaduros son reconocidos por el anticuerpo A2B5 (Raff, Abney et al. 1983, Raff, Abney et al. 1984, Avossa and Pfeiffer 1993, Bradl and Lassmann 2010). Este anticuerpo nos permite caracterizar células precursoras de oligodendrocitos los cuales presentan una morfología unipolar o bipolar, los lípidos reconocidos por este anticuerpo se regulan negativamente cuando estas células comienzan a diferencia a una etapas mas maduras de oligodendrocitos (Raff, Abney et al. 1983, Raff, Abney et al. 1984, Avossa and Pfeiffer 1993, Bradl and Lassmann 2010) (Ver Figura 7). Las células precursoras de oligodendrocitos son altamente migratorias y proliferativas. Para que las células progenitoras de oligodendrocitos maduren es necesaria la expresión de la hormona tiroidea y la falta de factores mitogénicos (Barres, Lazar et al. 1994, Franco, Silvestroff et al. 2008). La maduración de las células progenitoras de oligodendrocitos involucra cambios bioquímicos y morfológicos, los cuales ocurren simultáneamente. Los oligodendrocitos se convierten en células multipolares y son reaccionan al anticuerpo monoclonal O4, el cual se une a un antígeno de superficie no caracterizado (Bansal, Warrington et al. 1989, Bansal and Pfeiffer 1992). Esta es la ultima etapa en el que las células O4+ tienen propiedades proliferativas, a partir de este punto, la etapa post-migratoria se va perdiendo hasta terminar (Warrington and Pfeiffer 1992). La diferenciación de los oligodendrocitos termina cuando comienzan a expresar marcadores de mielina como la proteína básica de mielina (MBP), la proteína proteolipídica (PLP), la glicoproteína asociada a mielina (MAG), la glicoproteína de oligodendrocitos-mielina (MOG), y los galactocerebrosidos que son reconocidos por el anticuerpo O1. En esta

etapa en cultivo se desarrollan hojas de membrana y estas células se clasifican como oligodendrocitos maduros (Bansal, Warrington et al. 1989). Los oligodendrocitos mielinizantes remodelan su red de procesos que se extiende ampliamente y producen membranas de mielina las cuales enrollan en los axones.

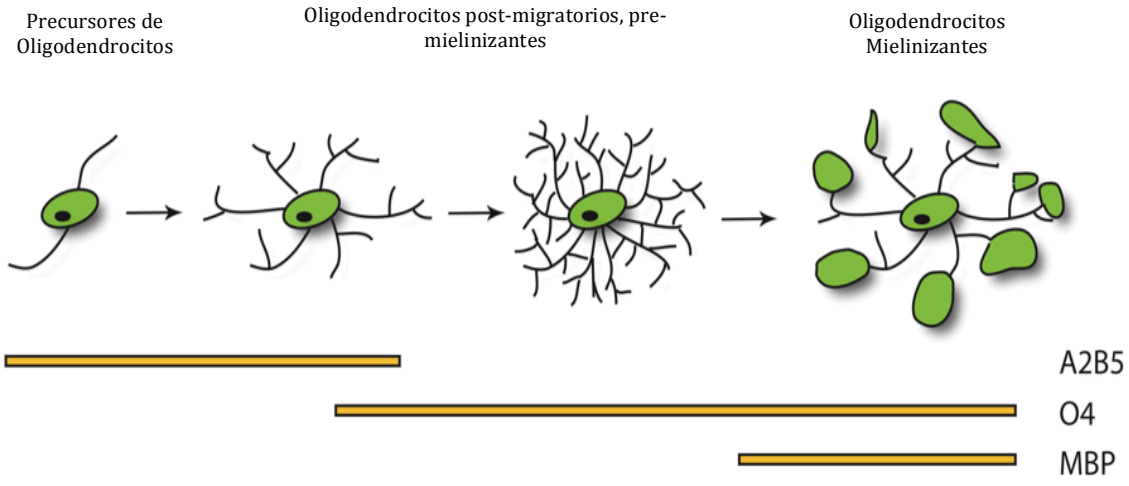

Figura 7 Linaje oligodendrocitico y algunos marcadores expresados en sus diferentes etapas de maduración (Adaptado de Baracskay et al., 2007).

b) Astrocitos

Los astrocitos son la célula glial mas abundante, su nombre deriva de sus cuerpos celulares con forma de estrella e irregulares. Por mucho tiempo se ha creído que estas células tienen un papel meramente de soporte metabólico para las neuronas, sin embargo recientemente se ha demostrado que tienen un papel mucho mas activo en la comunicación en el cerebro, los cuales iremos discutiendo mas adelante. Algunos atrocitos forman pies terminales en la superficie de las neuronas

en el cerebro y en la espina dorsal, los cuales entre otras, tienen la función de brindar nutrientes a estas células. Otros atrocitos colocan sus pies terminales en los vasos sanguíneos del cerebro permitiendo a las células

endoteliales de los vasos sanguíneos formar uniones estrechas, formando así la barrera hematoencefálica.

Los atrocitos también ayudan al mantenimiento de las concentraciones adecuadas de iones potasio en el espacio extracelular entre neuronas. Además, los astrocitos remueven los neurotransmisores de la hendidura sináptica después de un proceso de liberación ayudando a regular la actividad sináptica.

Para comunicarse con las neuronas los astrocitos pueden liberar varias moléculas neuroactivas tales como, glutamato, ATP, D-Serina y oxido nítrico (Ben Achour and Pascual 2010).

c) Glía Radial

En las primeras etapas de desarrollo, la denominada glía radial es uno de los primeros tipos gliales en aparecer. Estas células presentan una morfología bipolar y expresan marcadores específicos como tenascina y vimentina, fundamentalmente para determinar los patrones de migración neuronal. La glía radial expresa genes característicos de astrocitos maduros o reactivos, como la proteína de unión a lípidos, GLAST, la molécula de adhesión TN-C, la enzima glutamina sintetasa, y la proteína de unión a calcio S100β (Malatesta, Appolloni et al. 2008). A partir del nacimiento, estas células inician un proceso denominado "conversión astrocítica", pierden su morfología bipolar, además de la expresión de vicentina y aumenta la expresión de la proteína acídica fibrilar glial (GFAP).

Esta conversión es reversible y regulada por factores secretados por neuronas.

Tanto en el cerebelo como en la retina hay poblaciones de glía radial que permanecen en el individuo adulto: Las CGB en el cerebelo, las CGM en la retina (Lopez-Bayghen and Ortega 2010) y los tanicitos periventriculares del hipotálamo (Bonfanti and Peretto 2007).

- Glía de Bergmann

Las CGB es el tipo de célula glial más abundante en la corteza del cerebelo de los vertebrados adultos y se la considera como un tipo de astrocito especializado. Las CGB no cursan la llamada 'transformación astrocítica' después de la migración neuronal, como normalmente lo hace la glía radial del cerebro en desarrollo, por lo que en el cerebelo maduro la CGB sigue siendo morfológicamente comparable a la glía radial (Sottile, Li et al. 2006).

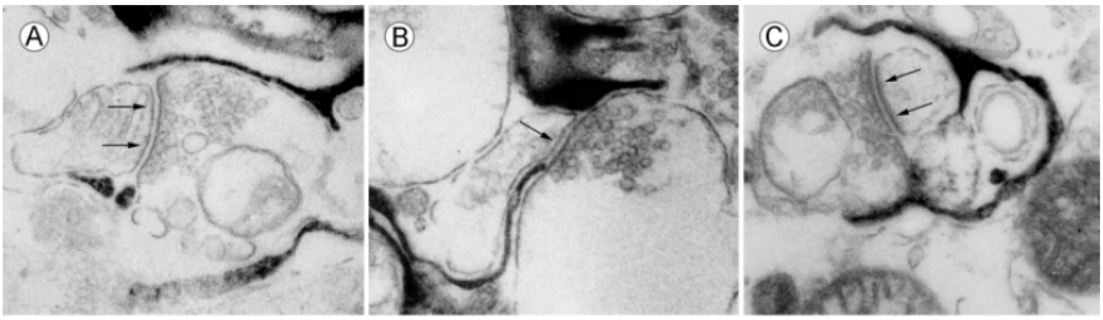

Figura 8 Rebanadas de cerebelo murino adulto, secciones de ME de transmisión. Tres ejemplos (A-C) de coberturas perisinápticas rodeadas por CGB (negro). Las membranas post-sinápticas están marcadas por flechas (Grosche, Kettenmann et al. 2002).

Durante el desarrollo, los procesos de las CGB proveen soporte estructural en la placa cerebelar, sus pies terminales se adhieren para formar una capa continua de glía limitando el cerebelo. Las fibras radiales de las CGB también actúan como una guía esencial para la migración de las células granulares cerebelares (Hatten 1999). Los ratones que presentan defectos en las CGB durante el desarrollo tiene anormalidades severas incluyendo la ruptura pial, una migración neuronal interrumpida y alteraciones en la conectividad (Belvindrah, Nalbant et al. 2006). Además se ha propuesto que las CGB también contribuyen en la elaboración de las dendritas de las células de Purkinje (CP) y en la estabilización de las conexiones sinápticas de esas neuronas. Después de que la morfogénesis cerebelar se encuentra terminada, las CGB permanecen como un soporte estructural importante, pero además tienen papeles adicionales en el mantenimiento, función y plasticidad de la sinapsis (Koirala and Corfas 2010).

En su estado maduro, el soma de la CGB se encuentra en la capa de las CP y sus procesos se proyectan desde este punto hasta la superficie pial, atravesando completamente la capa molecular del cerebelo. Por su localización y morfología, la CGB tiene una estrecha relación con las CP, hasta el punto de que sus procesos involucran casi la totalidad de las sinapsis inhibidoras y excitadoras que la CP establece con otras neuronas del cerebelo. Se ha calculado que existen ocho CGB por cada CP, y que los procesos de una sola de estas células gliales pueden envolver entre 2.142 y 6.358 sinapsis de la capa molecular (Reichenbach, Siegel et al. 1995).

Debido a que las CP integran las diferentes señales generadas en la corteza del cerebelo, la CGB se convierte en un elemento clave para la salida de información del cerebelo y con potencial para regular la comunicación en este sistema.

En la corteza del cerebelo, las CP establecen sinapsis glutamatérgicas con las fibras paralelas (axones de las células granulares) y con las fibras trepadoras. Las sinapsis más abundantes del cerebelo, y de hecho de todo el cerebro, son las que se establecen entre las fibras paralelas y las dendritas de la CP, por lo que el cerebelo es un sistema donde predominan las señales excitadoras. Las sinapsis de las CP se encuentran recubiertas por los procesos de la CGB, los cuales limitan la difusión del glutamato por medio de la actividad de sus transportadores, manteniendo así bajas concentraciones extracelulares de glutamato. Diversos estudios han estimado que de la totalidad de glutamato liberado durante una transmisión sináptica, cerca del 20% es removido por el compartimiento neuronal post-sináptico, mientras que el 80% restante es captado por las CGB (Kirischuk, Kettenmann et al. 2007). Esto es importante debido a que las CP son susceptibles a la excitotoxicidad ocasionada por la excesiva estimulación de sus receptores glutamatérgicos (Slemmer, De Zeeuw et al. 2005). A este respecto, se ha descrito que la función de la CGB es importante para mantener un adecuado funcionamiento del cerebelo, ya que la extirpación de la CGB en ratones adultos y la consecuente ausencia de los transportadores GLAST y GLT1 ocasionan una coordinación motora deficiente, producto de la degeneración de las neuronas de la corteza del

cerebelo (Cui, Allen et al. 2001). Además, la inhibición de la síntesis de los transportadores GLAST y GLT1 *in vivo* a través de la administración de oligonucleótidos anti-sentido eleva las concentraciones extracelulares de glutamato y da lugar a neurodegeneración por excitotoxicidad y parálisis progresiva. Estos estudios sugieren que una función esencial de la CGB es mantener concentraciones de glutamato no tóxicas para las neuronas. Otros trabajos han establecido que el transporte de glutamato llevado a cabo por la CGB limita la difusión del glutamato para impedir una estimulación inespecífica de sinapsis vecinas y regular las corrientes generadas en la CP.

Estudios recientes sugieren que las CGB también tienen papeles más activos en la sinapsis. Las CGB responden a la actividad sináptica con elevaciones de Ca^{2+} (Nimmerjahn, Mukamel et al. 2009), y pueden por lo tanto, modular la transmisión y plasticidad sináptica.

- Glía de Müller

La retina contiene, en adición a las células microgliales, dos formas de células macrogliales, los astrocitos y las CGM (Newman 2001).

Los astrocitos están restringidos a la superficie vitreal de la retina donde están en contacto con los vasos sanguíneos y los manojos de las fibras nerviosas; mientras que las CGM, células gliales radiales especializadas, se extienden a lo largo de la retina y encapsulan las somas neuronales, las dendritas y los axones. Sus pies terminales forman el borde interno (vitreal) de la retina mientras que sus procesos apicales se extienden en la capa fotorreceptora. Las CGM se relacionan con el desarrollo, organización y función de la retina.

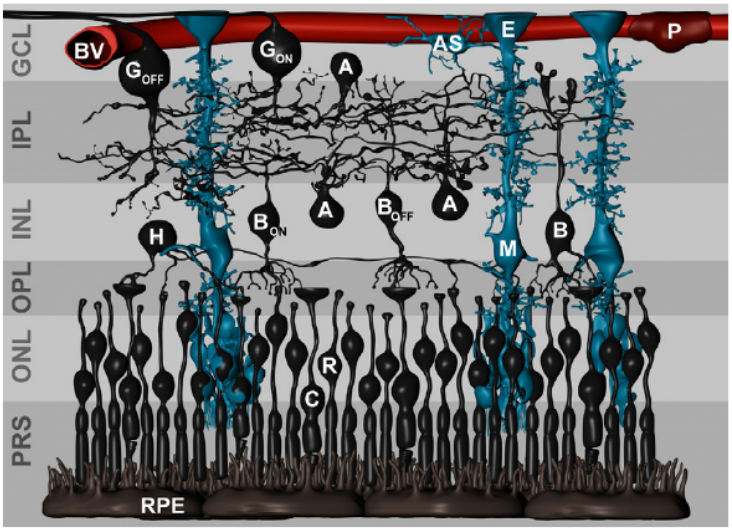

Figura 9 Organización de la retina de vertebrados. La retina neural está compuesta por capas las cuales contienen predominantemente los somas celulares (la capa nuclear externa [ONL] con los somas de las células fotorreceptoras: conos [C] y varas [R]; la capa nuclear interna [INL] con los somas de las células bipolares [B], horizontales [H], amacrinas [A] y de células de Müller [M]; la capa de las células ganglionares [GCL] con los somas de las células ganglionares [G]) y sus sinapsis (en la capa plexiforme externa [OPL] y en la capa plexiforme interna [IPL]) (Bringmann and Wiedemann 2009).

Las CGM juegan un papel crítico en la regulación del volumen del espacio extracelular, la homeostasis de iones y agua en la retina (Tout, Chan-Ling et al. 1993, Bringmann, Pannicke et al. 2006), el mantenimiento de la barrera sanguínea-retinal (Tout, Chan-Ling et al. 1993, Choi and Kim 2008) y la regulación del flujo sanguíneo retinal (Metea and Newman 2006).

Las CGM modulan directamente e indirectamente la excitabilidad y transmisión neuronal, vía la liberación de gliotransmisores y otras sustancias neuroactivas (Newman 2004), por el reciclamiento de neurotransmisores, y la liberación de precursores de neurotransmisores a las neuronas.

El glutamato es el principal neurotransmisor excitador en la retina (Thoreson and Witkovsky 1999), y es usado en la transmisión retinal de señales visuales por células fotorreceptoras, bipolares y ganglionares (Massey and Miller 1987, Massey and Miller 1990). En la retina externa, el glutamato es liberado continuamente de células fotorreceptoras en la obscuridad, esta liberación es modulada por la luz.

Se ha calculado que la concentración intracelular de glutamato en CGM es

de 0.5mM/s si no ocurre la metabolización del glutamato (Barbour, Magnus et al. 1993).

Las CGM y los astrocitos remueven la mayoría del glutamato de los sitios extracelulares al menos en la retina interna.

Las CGM circundan dos sinapsis, las establecidas entre las células bipolares y el fotorreceptor, y las formadas entre células ganglionares y las mencionadas células bipolares (Bringmann, Pannicke et al. 2006).

La eliminación del glutamato sináptico por las CGM es requerida para la prevención de neurotoxicidad; un mal funcionamiento del transporte del glutamato en CGM resulta en el incremento de los niveles extracelulares de glutamato que pueden ser tóxicos para las neurona a través de una sobre estimulación de los receptores ionotrópicos de glutamato (Choi 1988).

El principal transportador de glutamato en CGM es GLAST (Otori, Shimada et al. 1994, Derouiche and Rauen 1995). En adición a GLAST, se ha descrito la presencia de otros EAATs en CGM en varias especies, GLT-1, EAAC1, EAAT4 y EAAT5.

La expresión y la actividad de GLAST en CGM esta regulada por la disponibilidad del sustrato, principalmente esta mediada por vías de señalización intracelulares. La activación de receptores de glutamato en CGM resulta en un incremento del Ca^{2+} citosólico y la activación de PKC (Lopez-Colome, Ortega et al. 1993), la activación de PKC incrementa la captura de glutamato por fosforilación e incremento en la expresión de proteínas transportadoras (Gonzalez, Lopez-Colom et al. 1999).

En desordenes oftálmicos como glaucoma, isquemia, diabetes, y degeneración fotorreceptora inherente se han visto implicados niveles elevados de glutamato extracelular en la pérdida neuronal patofisiológica (Bringmann, Pannicke et al. 2006).

Transducción de señales

La expresión transducción de señales hizo su primera aparición en la literatura biológica en los 70s y apareció por primera vez en el titulo de un

articulo científico en 1972. El termino se hizo famoso gracias a un importante resumen de Martin Rodbell, premio Nobel en medicina y fisiología en 1994 por el descubrimiento de las proteínas G y su papel en la transducción de señales en las células, publicado en 1980 (Rodbell 1980). Para el año 2000, el 12% de los artículos que mencionan el termino célula también usan la expresión transducción de señales.

- **mTOR**

La proteína blanco de rapamicina de mamíferos (mTOR) es una enzima que integra varias vías de señalización para controlar el ciclo celular y la proliferación, es la principal proteína reguladora de la síntesis de proteínas (Proud 2007). La desregulación de mTOR esta implicada en un amplio rango de enfermedades humanas, incluyendo canceres y condiciones cardiovasculares.

mTOR es una serina/treonina cinasa que fosforila un rango amplio de proteínas, como la fosfatasa 2A, el factor de elongación 3 y Huntingtina. mTOR forma un core catalítico con dos complejos diferentes mTOR complejo 1 (mTORC1) y el complejo 2 de mTOR (mTORC2). Cada complejo de mTOR contiene compañeros únicos y compartidos, cada uno de los complejos contiene a mTOR, mLST8/G L y a deptor. En ambos complejos mLST8/G L se une al dominio cinasa de mTOR, aunque aparenta ser más crítico para el ensamblaje y señalización de mTORC2. En ambos complejos deptor funciona como un inhibidor. Sin embargo, otras proteínas permiten distinguir a los dos complejos por solo formar parte de uno de ellos. Exclusivamente mTORC1 contiene a raptor y a PRAS40. Raptor funciona como una proteína de andamiaje que une a la cinasa mTOR con los sustratos de mTORC1 para promover la señalización de mTORC1. PRAS40 tiene una capacidad regulatoria controversial, la cual no esta completamente definida, actúa como un inhibidor de mTORC1 o compitiendo con el substrato, o ambos. Por lo que existe un desacuerdo, entre si PRAS40 representa una proteína que forma parte del complejo de mTORC1 o si es un substrato que interactúa. En contraste, exclusivamente

mTORC2 contiene a rictor (compañero de mTOR insensible a rapamicina), a mSin1 y a PRR5/protor. Rictor y mSin1 promueven el ensamblaje y la señalización de mTORC2, mientras que se desconoce la función de PRR5/protor.

Una exposición aguda a rapamicina inhibe a mTORC1 pero no a mTORC2. La vía canónica que lleva a la activación de mTOR con la fosforilación de la serina 2448 de esta proteína, incluye la cinasa de fosfatidil inositol 3 (PI3-K), la cual produce PIP3, que ancla a la membrana celular a la cinasa dependiente de fosfoinositidos (PDK1) y a la proteína cinasa B (PKB). PKB es activada a través de una secuencia de fosforilaciones por PDK1 y PDK2. PKB activa fosforila y activa a mTOR en el residuo serina 2448 (Foster and Fingar 2010).

El complejo 1 de mTOR fosforilado tiene como blancos a varios componentes de la traducción como a la cinasa de la proteína ribosomal S6 de 70 KDa ($p70^{S6K}$), la cual actúa sobre otros componentes que regulan la traducción como la cinasa del factor de elongación 2 eucariótico (eEF2K) y el factor de elongación eucariótico 1A entre otras proteínas.

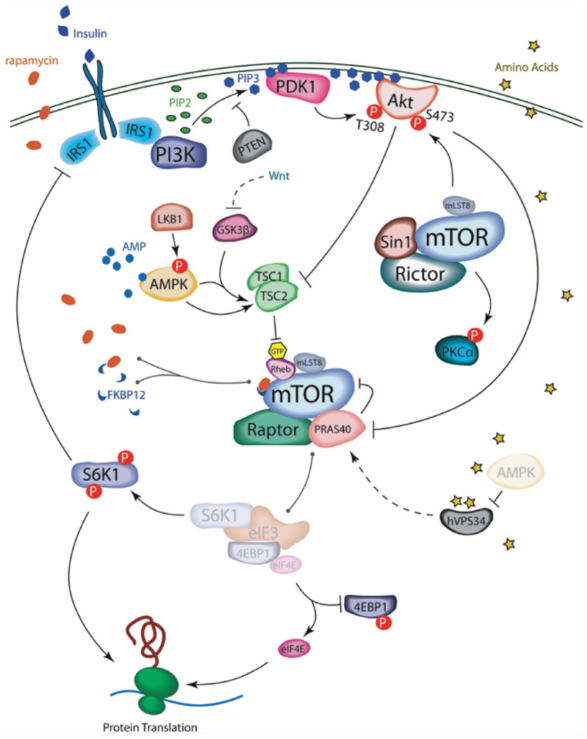

Figura 10 Vía de activación de mTOR y de sus proteínas blanco (modificado de Qian y Kun-Liang, 2007).

ANTECEDENTES

Está ampliamente demostrado que los receptores ionotrópicos de glutamato forman canales iónicos que se abren por ligando y permiten el influjo de iones, y que la permeabilidad a diferentes cationes está comprometida por las subunidades que lo forman (Hollmann and Heinemann 1994). Sabemos, además, que este influjo de iones es capaz de activar diversas vías de señalización.

Los transportadores de glutamato/aspartato acoplan el transporte del glutamato al transporte de Na^+ y de K^+. Los transportadores de glutamato EAAC y GLT tienen la siguiente estequiometria: una molécula de glutamato es tomada junto a tres Na^+ y un H^+ en intercambio por un K^+ (Danbolt 2001). Por lo que es posible que los transportadores se comporten como receptores iónicos, pero además de permitir el influjo de iones y de por este medio activar diversas vías de señalización también acoplar esto con el transporte del ligando.

González y Ortega en el 2000 reportaron que el glutamato regula la actividad de su captura en CGB, al caracterizar este efecto se demostró que aspartato, así como DL-treo-β-hidroxi-aspartato (THA) y aspartato-β-hidroxamato (ABH) (análogos transportables) mimetizan este efecto, en cambio KA, AMPA, NMDA, PDG, quisqualato, t-ACPD y DL-AP4 (agonistas selectivos de receptores ionotrópicos y metabotrópicos del glutamato) no modifican la captura del glutamato.

Después utilizaron estaurosporina (inhibidor de PKC) y demostraron que este fármaco no solo revierte el efecto del glutamato sino que también incrementa la captura basal.

Por lo que ellos concluyen que el glutamato regula su captura y esto es por un mecanismo independiente de los receptores, y que probablemente esta regulación esta ligada a los transportadores de glutamato.

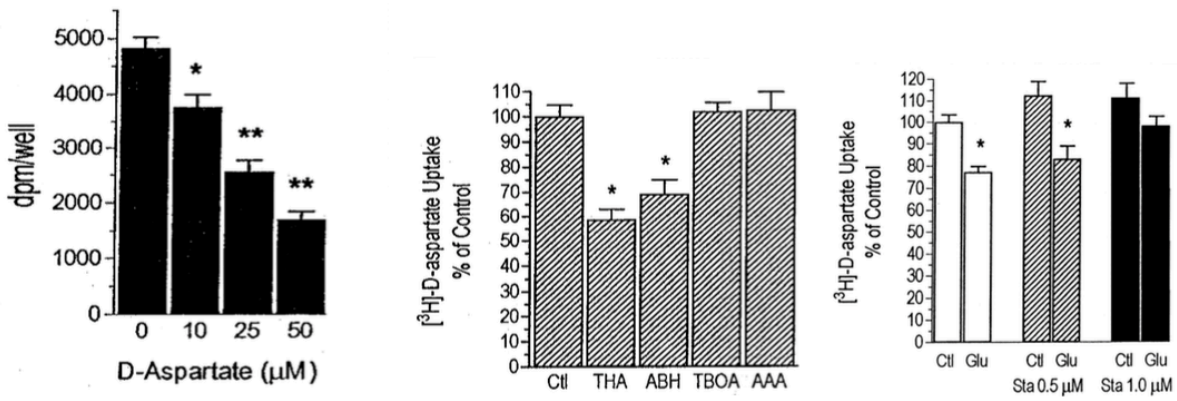

Figura 11 Efecto de diferentes sustratos en la actividad de la captura de glutamato en CGB. (A) CGB se incubaron por 10 min en presencia de 0.1 µCi de D-aspartato marcado-^{3}H más 0, 10, 25 y 50 µM de D-aspartato no marcado, después la radioactividad se determino en el contador de centelleo. (B)CGB se incubaron por 60 min con diferentes sustratos (THA, aspartato β- hidroxamato, TBOA, AAA)todos a una concentración de 1mM. Las monocapas se lavaron con D- aspartato marcado-^{3}H. (C)CGB se expusieron a las concentraciones indicadas de estaurosporina por 45 min antes de la adición de 1mM de glutamato. La incubación continuo por 1h después las monocapas se lavaron con D-aspartato marcado-^{3}H. (González y Ortega, 2000).

Abe y Saito en el 2001 observaron que la exposición de astrocitos a glutamato (100- 1000µM) resulta en un incremento en la fosforilación de p44/p42 MAPK (ERK 1/2) de una manera dependiente del tiempo y la dosis.

Esta fosforilación no fue mimetizada por agonistas de los receptores de glutamato, ni fue bloqueada por antagonistas de receptores de glutamato. En contraste, fue mimetizada por D- y L- aspartato y por inhibidores transportables de la captura de glutamato.

Los autores concluyen que la cascada MEK/ERK es activada por un mecanismo relacionado con los transportadores del glutamato y proponen que los transportadores de glutamato funcionan como receptores que transmiten señales del glutamato extracelular a mensajeros intracelulares.

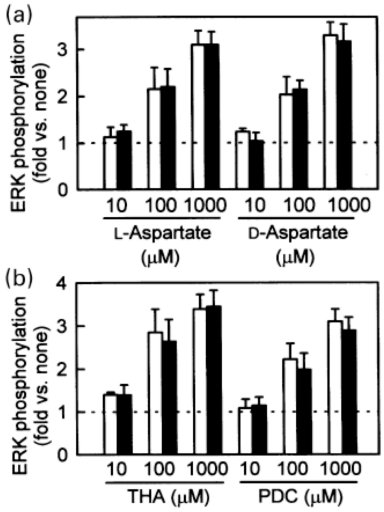

Figura 12 Efectos del aspartato e inhibidores de la captura de glutamato en la fosforilación de ERK 1/2 en cultivos de astrocitos corticales. Las células se expusieron a (a) L- y D-aspartato (b) a THA y PDC por 45 min, y los extractos celulares fueron sometidos a un análisis por Western Blot (Abe and Saito 2001).

De manera análoga Zepeda y colaboradores observaron una fosforilación de mTOR en el residuo Ser 2448 dependiente de GLAST en CGB. Como ya se mencionó, mTOR participa en los procesos de traducción, y representa un punto de control traduccional clave. Con la ayuda de herramientas farmacológicas demostraron que el efecto del glutamato es mediado a través de receptores ionotrópicos y metabotrópicos del glutamato, y de manera interesante, el sistema transportador de glutamato también se ve involucrado en ese fenómeno.

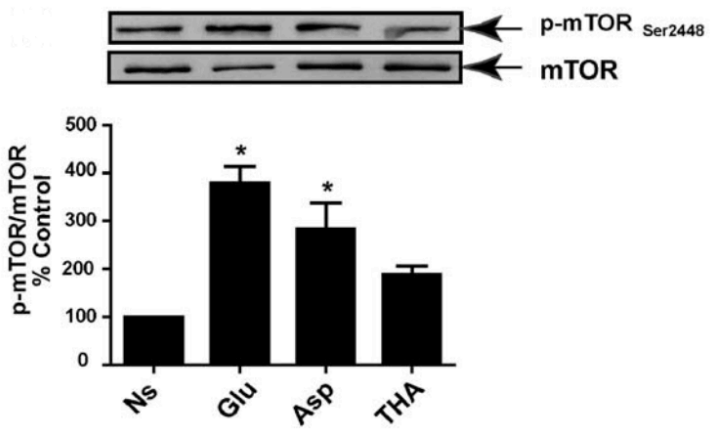

Figura 13 Perfil farmacológico de la fosforilación de mTOR inducida por glutamato. Monocapas de CGB fueron expuestas por 30 min a glutamato (1mM), aspartato (1mM) o THA (100μM) (Zepeda, Barrera et al. 2009).

Además de lo anterior, el grupo de Gegelashvili en el 2007 y el grupo de Hampson en el 2009 demostraron que los transportadores de glutamato y la ATPasa de Na^+, K^+ son parte del mismo complejo molecular y operan como una unidad funcional para regular la neurotransmisión glutamatérgica lo cual muestra un acople metabólico de los transportadores de glutamato, sugiriendo que los transportadores de glutamato pueden actuar como moléculas señalizadoras (Gegelashvili, Rodriguez-Kern et al. 2007, Rose, Koo et al. 2009).

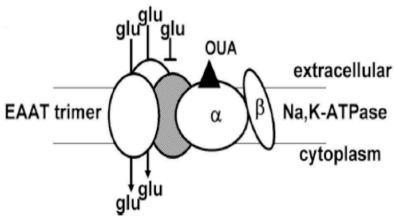

Figura 14 Modelo hipotético de juxtaposición del transportador de glutamato con la ATPasa de Na^+, K^+. Solo una de las subunidades en la estructura tetramérica del transportador esta asociada con la ATPasa de Na^+, K^+ (Rose, Koo et al. 2009).

Por lo anterior nos dimos a la tarea de dilucidar el papel de GLAST como transductor de señales, y durante la maestría demostramos que la actividad de GLAST inducida por glutamato, aspartato y por bloqueadores transportables de los EAATs, repercute en la fosforilación de la cinasa mTOR en su residuo Serina 2448; la cual es mediada por la activación de la vía canónica de mTOR, PI3K/PKB.

Con los resultados de la maestría se propuso el siguiente modelo:

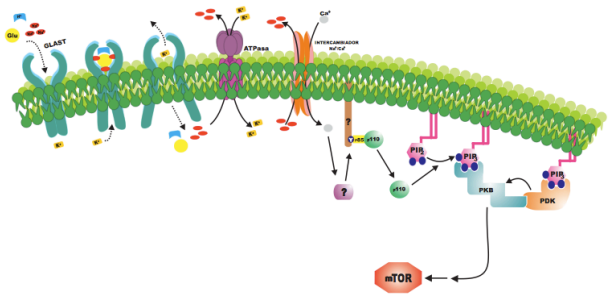

Figura 15 Cascada de señalización activada por GLAST de *Gallus gallus (Martinez-Lozada Zila Tesis Maestría Cinvestav DBGM)*

JUSTIFICACION

El análisis de la participación de los transportadores de glutamato dependientes de Na^+ como moléculas señalizadoras permitirá establecer un vinculo directo entre la remoción del glutamato y los cambios generados en las células gliales por la neurotransmisión glutamatérgica.

OBJETIVO GENERAL

Determinar la participación de los transportadores de glutamato dependientes de Na^+ en la señalización mediada por glutamato.

OBJETIVOS PARTICULARES

- Demostrar la participación de los intercambiadores Na^+/Ca^{2+} en la señalización mediada por GLAST utilizando el inhibidor especifico KB-R7943
- Con el uso de antagonistas de los receptores glutamatérgicos, descartar su participación en la fosforilación de mTOR mediada por GLAST
- Demostrar la participación de cinasas de tirosina dependientes de Ca^{2+}, en la señalización activada por el transportador de glutamato/aspartato
- Evaluar la activación de la proteína 4EBP1 blanco de mTOR, dependiente de la actividad de GLAST
- Descartar la participación de los canales de Ca^{2+} dependientes de voltaje tipo L en el influjo de Ca^{2+} dependiente de GLAST
- Determinar el efecto de la activación de GLAST en la unión del factor transcripcional AP-1 al DNA en CGB y CGM
- Analizar si la señalización glutamatérgica repercute en regulación transcripcional en células gliales de Müller
- Evaluar el efecto de la inhibición de la ATPasa de Na+/K+ y del intercambiador Na^+/Ca^{2+} en la captura de glutamato
- Obtener cultivos primarios de oligodendrocitos de rata
- Demostrar la expresión de los subtipos de transportadores de glutamato (EAATs) en oligodendrocitos
- Analizar el efecto de la actividad de los EAATs en la maduración de los oligodendrocitos

- Evaluar el influjo de Ca^{2+} en oligodendrocitos dependiente de la actividad de los transportadores de glutamato
- Evaluar la activación (fosforilación) de la proteína cinasa dependiente de Ca^{2+}/Calmodulina II β (CaMKIIβ) mediada por la estimulación glutamatérgica vía sus transportadores
- Analizar la participación de CaMKIIβ en la maduración de los oligodendrocitos inducida por los EAATs
- Evaluar el efecto de la sobreexpresión de las mutantes de CaMKIIβ (WT, AllA y AllD) en la morfología de los oligodendrocitos
- Analizar la fosforilación de CaMKIIβ en muestras de individuos fallecidos con esclerosis múltiple

MATERIALES Y METODOS

Materiales

- Los reactivos utilizados para el cultivo de CGM se obtuvieron de GE Healthcare.
- Los reactivos para el cultivo primario de CGB se obtuvieron de Invitrogen (Gaithersburg, MD).
- El ácido glutámico, ácido D-aspártico, AMPA, ácido kaínico y NMDA se obtuvieron de Tocris-Cookson (St. Louis, MO, USA).
- Los inhibidores y bloqueadores Wortmanina, amilorida [3,5-diamino-6-cloro-N-(diamino-metilen)pirazina-2-carboxamida], PP2 {4-amino-5-(4-clorofenil)-7-(dimetiletil)pirazol[3,4-d]pirimidina}, W7 [N-(6-aminohexil)-5-cloro-1-naftalensulfonamida], CNQX (6-cyano-7-nitorquinoxalina-2,3-dione), LAP5 (L-(+)-2-Amino-5-acido-fosfonopentanoico); CPCCOEt (7-(hidroximino)ciclopropa[β]cromen-1a-carboxilato etil ester), CPPG ((RS)-a-ciclopropil-4-fosfonofenilglicina), genisteina, TBOA (acido DL-threo-β-benziloxiaspartico), THA (L-treo-hidroxi-aspartato), A23187 (5-9metilamino)-2-({(2R,3R,6S,8S,9P,11R)-3,9,11-trimetil-8-[(1S)-1-metil-2-oxo-2-(1,3-benzoxazole-4-acido carboxílico), KB-R7943 (2-[2-[4-(4-Nitrobenziloxi)-fenil]-etil]-iso-tioreamesilato), se obtuvieron de Tocris-Cookson (St. Louis, MO, USA).
- Los inhibidores PDC (ácido L-trans-pirrolidina-2,4-dicarboxilico), T3MG [acido-(±)-threo-3-metilglutamico] y otros reactivos no especificados se obtuvieron de Sigma-Aldrich (St. Louis, MO, USA).
- Los inhibidores de proteasas PMSF (Fluoruro de fenilmetil-sulfonilo), leupeptina y aprotinina de Roche Molecular Biochemicals (Indianapolisis, IN).
- Los reactivos para quimioluminiscencia de Amersham (Little Chalfront, Buckinghamshire, UK).

- Los radioligandos [^{3}H]-D-Aspartato, $^{45}Ca^{2+}$ y [α^{32}P]dATP de Pelkin Elmer (Boston, MA, USA).
- El kit Vivo/Muerto Viabilidad/Citotoxicidad para células de mamífero de Invitrogen (Gaithersburg, MD).

Anticuerpos

Los sobrenadantes de células cultivadas de hibridoma clona A2B5 (ATCC, Manassas, VA) se usaron para el cultivo de oligodendrocitos por inmuno-lavado. Los anticuerpos anti-GLAST, anti-GLT1, anti-EAAC1 (Abcam, Cambridge, MA) se usaron para Inmunodetección en fase sólida así como para inmunocitoquímica. Los anticuerpos Anti-CaMKII, anti-pCaMKII $T^{286/287}$ (Cell Signaling Technology, Danvers, MA), anti-pCaMKIIβ S^{371} (generados, caracterizados y donados por el Doctor Kim), anti-GAPDH (EMD Millipore, Billerica, MA), anti-pmTOR Ser^{2448} (Cell Signalling Techonology, Beverly, MA, USA), anti-mTOR (05-235 de Cell Signalling Techonology, Beverly, MA, USA), anti-p-p60^{Src} Y^{527} (Abcam, Cambridge, MA), anti-p4EBP1 T^{70} (Santa Cruz Biotech, CA, USA), anticuerpo monoclonal anti-Actina (donados amablemente por el Dr. Manuel Hernández del Cinvestav-IPN, México) y anticuerpos secundarios acoplados a peroxidasa de rábano (HRP)(Vector Laboratories, Burlingame, CA y/o Amersham Bioscience, Buckinghamshire, UK) se usaron para ensayos de inmunodetección en fase sólida. Los sobrenadantes de células cultivadas de hibridoma clona O4 (donados por el Doctor Pfeiffer), y los anticuerpos anti-MBP (EMD Millipore, Billerica, MA), y los anticuerpos secundarios conjugados con Alexa 488- o Alexa-564 (Life Technologies, Grand Island, NY) se usaron para inmunocitoquímica.

Animales

Para los cultivos celulares de CGB y de CGM se utilizaron embriones de pollo, los cuales fueron donados por Laboratorios Avimex S.A. de C.V. México, D.F. y se mantuvieron a 37°C hasta su uso.

Para los cultivos de oligodendrocitos se utilizaron ratas Sprague-Dawley obtenidas de Laboratorios Harlan, Indianapolis, IN, EUA.

Todos los experimentos se llevaron de acuerdo a las normas internacionales sobre el uso ético de animales.

Cultivo celulares y tratamiento

- **Glía de Bergmann**

El cultivo primario de CGB se preparo de acuerdo a lo descrito previamente por Ortega y colaboradores (Ortega, Eshhar et al. 1991). Embriones de pollo de 14 días se decapitaron y se realizó la extracción de los cerebelos, los cuales se disectaron en medio Pucks, se cortaron los cerebelos con una navaja de disección por 5 minutos, y se pasaron a una solución de medio Pucks con Tripsina y DNasa en la cual se dejaron reposar 15 minutos en la incubadora a 37°C y con una saturación de 5% de CO_2 y se decantaron. La pastilla se pasó a una solución de medio Optimem con 10% de suero fetal bovino (SFB) y DNasa, en esta solución se homogenizaron mecánicamente pasando por una aguja. El homogenizado se dejó sedimentar durante 10 minutos a 37°C para eliminar residuos de tejido y agregados celulares. El sobrenadante se paso a otro tubo y se centrifugo a 3,000 rpm durante 10 minutos. El pellet se resuspendió en medio Optimem con 3% de SFB y 50 µg/mL de gentamicina. Las células se incubaron a 37°C en 5% de CO_2 y se usaron hasta que alcanzaron una confluencia de 80-100% (4 a 6 días).

- **Glía de Müller**

El cultivo primario de CGM se preparó de acuerdo a lo descrito previamente por López-Colomé y colaboradores (Lopez-Colome and Romo-de-Vivar 1991). Brevemente, se prepararon a partir de la retina de embriones de pollo de 7 días. Las células se sembraron en multipozos de 6 o de 24 celdas de plástico en medio Optimem con 4% de SFB, 2mM de glutamina y gentamicina (50 µg/mL) y se usaron en el día 10 a 12 de cultivo *in-vitro*.

- **Oligodendrocitos**

Progenitores de oligodendrocitos de rata se aislaron de cerebros de ratas Sprague-Dawley de 3 días posnatales (P3) a través de un inmuno-lavado (Barres, Hart et al. 1992, Lafrenaye and Fuss 2010). Ratas de P3 se pesaron y se decapitaron y se realizo la extracción de los cerebros, a los cuales se les removieron las meninges y se disectaron en 10mL de medio Hanks se cortaron con una navaja de disección, y se le añadió tripsina y DNasa I incubándose por 15 min a 37°C. Después de la incubación se inactivo la tripsina y la DNasa I al agregar medio DMEM con 10% de SFB 1% de antibióticos. Las células se centrifugaron a 12,000 rpm durante 3 min y la pastilla celular se aspiro con agujas de 16g y de 22g, y esta suspensión celular se sembró en las cajas de inmuno-lavado incubándose a 37°C durante 30 min. Después se descarto el medio y las placas se lavaron 2 veces con PBS 1X y después 2 veces con 10 mL de medio DMEM con 10% de SFB y 1% de antibióticos, las células colectas después de estos lavados se centrifugaron y la pastilla celular se resuspendió para después sembrarse en una placa de bacterias 10 min a 37°C. Las células no unidas (progenitores de oligodendrocitos) se colectaron, centrifugaron y cuantificaron utilizando una cámara de New Bauer; para los ensayos de nucleofección de plásmidos se usaron directamente, para los otros ensayos se sembraron en placas de cultivo a una densidad de $1X10^6$

células por pozo (mp6) o en cubreobjetos preparados con fibronectina (10 µg/mL) a una densidad de 2-2.5X10^4 células por cubreobjetos o pozo (mp24). Los progenitores de oligodendrocitos sembrados se cultivaron en medio de diferenciación (medio DMEM que contenía 40 ng/mL de Tri-yodo-tironina; T3, y suplemento N2) y se dejaron diferenciar por 48 horas. Bajo estas condiciones, la mayoría de las células presentaban características de oligodendrocitos post-migratorios, pre-mielinizantes ya que expresaban el antígeno O4 (Sommer and Schachner 1982, Warrington, Barbarese et al. 1993).

- **Células inmortalizadas de oligodendrocitos de ratón**

La línea celular CIMO se cultivo en medio DMEM con 5% de SFB y 1 µg/mL de interferón γ y se crecieron a 33°C. Estas células se utilizaron en los experimentos de nucleofección de plásmidos.

Protocolo de estimulación

Los cultivos de CGB y de CGM se mantuvieron en una solución de ensayo (25mM HEPES, 130mM NaCl, 5.4mM KCl, 0.8mM $MgCl_2$, 1mM Na_2HPO_4, 33.3mM Glucosa, 1.8mM $CaCl_2$ y el pH ajustado a 7.4) con 0.5% de BSA durante 30 minutos. Para los cursos temporales se aplicaron estímulos de glutamato (1mM), y D-aspartato (1mM) durante 5, 10, 15, 30 y 60 minutos. Para los ensayos de dosis-respuesta se expusieron los cultivos a concentraciones crecientes de glutamato y/o D-aspartato durante un periodo de 15 minutos. Para los ensayos de inmunodetección en fase sólida se realizaron diferentes tratamientos utilizando las dosis y tiempo en donde se observó la máxima respuesta al realizar los cursos temporales y los experimentos de dosis-respuesta. Los inhibidores se agregaron 30 minutos antes de los agonistas, según se indica en cada figura.

Los oligodendrocitos fueron analizados directamente después de las 48 horas de diferenciación o tratados como se indica en cada figura con

glutamato, D-Aspartato, y/o el bloqueador de los transportadores de glutamato, TBOA, el inhibidor no transportable selectivo para GLT-1, ácido dihidrokainato (DHK), el inhibidor selectivo para el transportador GLAST, UCPH-101, el inhibidor de CaMKII, KN-93, o su derivado inactivo, KN-92. En el caso de tratamientos duales, los inhibidores se agregaron 30 minutos antes de la aplicación de glutamato o D-aspartato. Los oligodendrocitos se analizaron 6 horas después de la adicción de glutamato o D-aspartato al menos que en la figura se especifique de manera diferente.

Todos los experimentos se realizaron al menos por triplicado en donde cada experimento fue independiente, entendiéndose por independiente, un experimento en el cual las células se aislaron de diferente grupo de cerebros (oligodendrocitos), cerebelos (CGB) o retinas (CGM) y que se trataron por separado de los otros experimentos independientes.

Captura de [^{3}H]-D-Aspartato

La captura de D-Aspartato marcado con ^{3}H (usado como análogo no metabolizable del glutamato) se realizo como se describió previamente por Ruiz y Ortega (Ruiz and Ortega 1995). A las células sembradas en multipozos de 24 se les retiro el medio cambiándolo por solución de ensayo y se preincubarón 30 minutos a 37°C. Después se incubaron con los ligandos correspondientes por el tiempo indicado en cada figura. Después la solución de ensayo se reemplazo por una solución de ensayo que contenía [3H]-D-Aspartato (0.4 µCi/mL) y se incubaron por 30 minutos. Después el medio se removió por aspiración rápida con vacío y las células se lavaron 3 veces con solución de ensayo fría y se solubilizaron con 0.1 M NaOH. Se tomo una alícuota de la suspensión celular y se utilizó para determinar la concentración de proteínas por el método de Bradford y al resto se le agrego 2 mL de líquido de centelleo y 10µL de ácido acético y se conto en un contador de centelleo.

Ensayos de influjo de Calcio

- **$^{45}Ca^{2+}$ en CGB y CGM**

Monocapas confluentes de CGM y CGB sembradas en pozos de 24 se lavaron tres veces para remover las células no adheridas con 0.5 mL de solución de ensayo. El influjo inducido por glutamato o D-Aspartato se inició en el tiempo cero por la adición de 0.5 mL de solución de ensayo, conteniendo glutamato o D-Aspartato a la concentración deseada. Cuando se probaron los inhibidores, se adicionaron 30 minutos antes de empezar con los ensayos de influjo de $^{45}Ca^{2+}$. La reacción se detuvo por aspiración del medio radioactivo y el lavado de cada pozo por 15 segundos con 0.5 mL de la solución A fría. Las células de los pozos se expusieron por dos horas a 37°C a 250 µL de NaOH 0.1 M y se les agregó 50 µL de ácido acético y 5 mL de solución de centelleo. Y se detecto la radioactividad en un contador de centelleo Beckmann 7800LS. Los experimentos se realizaron al menos tres veces con cuatro repeticiones cada uno.

- **Fura-2 AM en oligodendrocitos**

La concentración intracelular de calcio en los oligodendrocitos se determino como se describió previamente por el grupo de Tsien (Grynkiewicz, Poenie et al. 1985). A los oligodendrocitos se les agregó el éster fura-2 AM (2.5 µM) y ácido plurónico F-127 (0.01%) en medio de diferenciación por 30 minutos a 37°C. Después las células se lavaron y se incubaron en medio de diferenciación por otros 30 minutos a 37°C. Las mediciones radiométricas de calcio se hicieron a una longitud de onda de 340 y 380 nm de excitación y a 510-520 nm de emisión en células cultivadas en medio de diferenciación usando un microscopio Zeiss Observer.Z1 en combinación con un programa de software Axio VisionRel 4.8. Las mediciones se tomaron de al menos nueve células por tratamiento y experimento y de tres experimentos independientes (en total 27 células por tratamiento) antes y después de la aplicación de los compuestos indicados en cada figura. Para calibrar la concentración intracelular de

calcio libre (en nM) se utilizo una curva de calibración (Kit de Calibración de calcio, Life Technologies, Grand Island, NY).

Viabilidad celular

Para determinar si los estímulos de Glutamato, D-Aspartato y el inhibidor MK-801 afectaban la viabilidad de los oligodendrocitos, la viabilidad celular se midió con ayuda del kit Vivo/Muerto Viabilidad/Citotoxicidad para células de mamífero. Los oligodendrocitos se sembraron en cubreobjetos preparados con fibronectina (10 μg/mL) y a estos se les agrego directamente una solución de 2 μM de Calceina-AM y 4 μM de homodímero de Etidio-1, dejándose reaccionar por 10 min, después de este tiempo se llevaron al microscopio y se tomaron imágenes de 4 campos por cada cubreobjetos y 3 cubreobjetos por cada tratamiento con un objetivo 10 X. Las células positivas para Calceina-AM (vivas-verdes) y las células positivas para el homodímero de Etidio-1 (muertas-rojas) se contaron en con el contador de células del programa Image J.

Reacción en cadena de la polimerasa en tiempo real (RT-PCR)

Para determinar los niveles de expresión relativos de RNAm, se realizo una RT-PCR cuantitativa en un sistema de detección CFX96 RT-PCR usando iQ SYBR Green Supermix y la secuencia de pares de primers específicos que se muestra en la tabla I. Las condiciones de reacción de la PCR fueron: 95°C por 3 minutos, seguida de 40 ciclos de 95°C por 15 segundos, 58°C por 30 segundos, y 95°C por 10 segundos. Para comparar los niveles de expresión de los diferentes genes, se determinaron los valores de R_0 como lo describió Perison y colaboradores (2003). Para determinar los niveles de expresión relativos, se utilizo el método de $\Delta\Delta C_T$ (Livak and Schmittgen 2001).

Ensayos de Cambio en la Movilidad Electroforética (EMSA)

Después del periodo de estimulación, a las células se les cambio la solución de ensayo por medio de cultivo completo por una hora y se prepararon los extractos nucleares. Todos los amortiguadores utilizados contenían una mezcla de inhibidores de proteasas para evitar la proteólisis de los factores de transcripción. La concentración de proteínas se determino usando el método de Bradford. 20 μg de extractos nucleares de células control o tratadas se incubaron con 500 ng de poli[(dI-dC)] como competidor no especifico y con 1ng de oligonucleótidos de doble cadena de AP-1 (SV40) marcados en el extremo con [^{32}P] a 4°C. La mezcla de reacción se incubó durante 20 minutos a 4°C, y las proteínas se separaron por electroforesis en SDS-PAGE (geles al 6%) con un amortiguador de baja fuerza iónica 0.5X TBE. Los geles se secaron con vacío y se expusieron a una placa auto radiográfica durante toda la noche.

Extractos nucleares

Los extractos totales de las CGB y CGM se obtuvieron cosechando las células por raspado con 1mL de solución amortiguadora Tris-Dulbeco pH 8.0 con PMSF, y se centrifugaron a 13,000 rpm por 3 min, la pastilla se resuspendió en solución amortiguadora A (1M Hepes pH 7.9, 1M KCl, 50mM EDTA, 10mM EGTA, 100mM DTT, 100 mM PMSF, Aprotinina y Leupeptina), y se incubo en este buffer 20 min, después se agrego 10% NP-40 y se agitaron en vortex 10 seg para romper la membrana citoplasmática. Después de centrifugaron 1 min a 10,000 rpm a 4°C. La pastilla se resuspendió en solución amortiguadora C (1M Hepes pH 7.9, 4M NaCl, 50mM EDTA, 10mM EGTA, 100mM DTT, 100 mM PMSF, Aprotinina y Leupeptina) y se homogenizaron en el vortex a 4°C de 30 a 45min. Por ultimo se centrifugaron 5 min a 9,000 rpm a 4°C. Y se hicieron alícuotas del sobrenadante, los extractos nucleares obtenidos se les determino la concentración de proteínas.

Extractos totales

Los extractos totales de las CGB y CGM se obtuvieron cosechando las células por raspado con 1mL de solución salina de fosfatos (PBS) con inhibidores de fosfatasas (10 mM K_2HPO_4, 150mM NaCl, 2mM Na_3VO_4, 25mM NaF, 10mM Na_3MoO_4) y centrifugando 5 minutos a 13,000 rpm a 4°C. La pastilla se resuspendió en solución de lisis RIPA (1mM EGTA, 1mM EDTA pH 8.0, 10mM TRIS-HCl pH 7.5, 158mM NaCl, 2mM Na_3VO_4, 25mM NaF, 10mM Na_3MoO_4, 1µg/mL Leupeptina, 1 µg/mL aprotinina, 1mM PMSF) y se solubilizaron por agitación durante una hora a 4°C en un agitador por vibración. Los oligodendrocitos se homogenizaron agregando directamente en la caja de cultivo 500 µL de solución de lisis (150 mM NaCl, 10 mM KCl, 20 mM HEPES [pH 7.0], 1mM $MgCl_2$, 20% glicerol, y 1% Triton X-100) a la cual se le agrego 10 µL/mL del coctel de inhibidores de proteasas y fosfatasas (Thermo Scientific, Rockford, IL). A los extractos totales obtenidos se les determino la concentración de proteínas.

Determinación de proteínas

La estimación de proteínas contenidas en los extractos totales y/o nucleares se llevo a cabo utilizando el método de Bradford y como estándar se utilizo una solución de 1 µg/µL de γ-globulina (Bradford 1976).

Inmunodetección en fase sólida

Los extractos totales normalizados por el contenido de proteína se desnaturalizaron y diluyeron 1:3 en buffer de muestra (187.5 mM Tris-HCl pH6.8, 6% dodecil sulfato de sodio (SDS), 30% glicerol, 5% ß-mercapto etanol, 0.03% azul de bromofenol, 2mM DTT Ditiotreitol) y se hirvieron en baño maría durante 5 minutos. Los extractos así preparados se analizaron por electroforesis en geles de poliacrilamida al 6-10% en presencia de dodecil fosfato de sodio (SDS-PAGE) y se transfirieron a una membrana de nitrocelulosa en cámara húmeda (Bio-Rad). Los blots se tiñeron con rojo de Ponceau para confirmar que el contenido de proteína fuera igual en todos los carriles. Las membranas se destiñeron dando dos lavados con agua biodestilada y un tercero con PBS. Los sitios irrelevantes se cubrieron por incubación de las membranas durante una hora a temperatura ambiente con solución de bloqueo: TBS (0.2 M Tris-HCl y 1.36 M NaCl), 5% de leche en polvo semidescremada y 0.1% Tween 20. Después de un breve lavado con TBS-T las membranas se incubaron con el anticuerpo primario indicado en cada figura a una dilución de 1:1000 en solución de anticuerpos (TBS, 0.25% BSA, 0.1% Tween-20 y 0.01% Timerosal) durante toda la noche a 4°C. Las membranas se lavaron tres veces con solución TBS/Tween en un agitador orbital y se incubaron durante 2 horas con anticuerpo secundario acoplado a peroxidasa de rábano en una dilución 1:4000 a temperatura ambiente. Las membranas así tratadas se lavaron 2 veces con TBS/Tween. Después de lavar las membranas, se adicionaron a las membranas el reactivo de quimioluminicencia Amersham como sustrato de la peroxidasa de rábano, la cual cataliza la oxidación de luminol en presencia de peróxido de hidrógeno emitiendo luz. Las bandas relevantes se detectaron por auto radiografía y se examinó la intensidad de la señal. Se realizaron los análisis

densitométricos con ayuda del programa ID Image Analysis Software (Kodak Coorporation, USA) y los datos se analizaron con el Software GraphPad, Prism (San Diego, CA, USA).

Eliminación de los anticuerpos de las membranas

Las membranas se incubaron con solución de eliminación (Glicina 0.1M pH 2.3) por una hora a temperatura ambiente y se lavaron tres veces durante cinco minutos con TBS/Tween. Se bloquearon dos horas en TBS conteniendo 5% de leche semidescremada y 0.1% de Tween-20. Las membranas se incubaron toda la noche con anticuerpo primario diluido 1:1000 en solución de anticuerpos, seguido de tres lavados por cinco minutos en TBS. El anticuerpo secundario en una dilución 1:4000 se incubó por dos horas a temperatura ambiente seguido por tres lavados con TBS/Tween por cinco minutos. Se reveló con equipo de quimioluminiscencia. Se realizaron los análisis densitométricos con ayuda del programa ID Image Analysis Software (Kodak Coorporation, USA) y los datos se analizaron con el Software GraphPad, Prism (San Diego, CA, USA).

Inmunoprecipitación

Perlas de G agarosa se incubaron con los anticuerpos primarios para inmunoprecipitación, según se indique en cada figura, y se pusieron a acoplar en PBS 1X estéril en agitación a 4°C durante 3-4 horas. Pasado este tiempo, a los complejos perlas G – anticuerpos se les agregaron 100-500 µg de extractos totales de proteína y se aforaron a 300 µL con PBS estéril y se agitaron toda la noche a 4°C. Después se centrifugaron a 13,000 rpm durante 10min, se decanto el sobrenadante y se dejaron secar 5 minutos a temperatura ambiente. Al precipitado se le agregó 20 µL de solución amortiguadora de muestra y se hirvieron durante 5 minutos. De esto se cargaron 15 µL en geles de poliacrilamida al 6-10% en presencia de

dodecil fosfato de sodio (SDS-PAGE) y se continuo con el procedimiento como se describe en la sección de inmunodetección en fase sólida.

Inmunocitoquímica

Para la inmunocitoquímica se usaron los sobrenadantes de los hibridomas clona O4, las células se fijaron en PBS con 4% de paraformaldehido, los sitios de unión no específicos se bloquearon con medio DMEM 10% SFB, y las células se incubaron con el sobrenadante O4 durante toda la noche (diluido 1:1 en DMEM con 10% SFB). Para la detección inmunocitoquímica de GLAST, GLT-1, EAAC1 o MBP las células se fijaron en PBS con 4% de paraformaldehído y después se permeabilizaron con PBS que contenía 5% de Tritón X-100 y 0.4 M sacarosa. Subsecuentemente las células se incubaron durante 30 minutos en medio DMEM 10% SFB y después durante toda la noche con anticuerpos anti-GLAST, anti-GLT1, anti-EAAC1 (Abcam, Cambridge, MA) o con anti-MBP (SWI99; Covance, Princeton, NJ). Los anticuerpos primarios se detectaron con anticuerpos secundarios acoplados a Alexa-488 o Alexa-564 (Life Technologies, Grand Island, NY) y los núcleos se contra tiñeron con Hoechst 33342 (EMD Millipore, Billirecica, MA).

Silenciamiento de genes mediante transfección de siRNAs

Oligodendrocitos diferenciados se transfectaron con ON-TARGET plus siRNA SMARTpools dirigidos contra *Glast, Glt-1* o *Eaac1* de rata (Thermo Fisher Scientific, Pittsburg, PA) usando Lipofectamina 2000 (Life Technologies, Grand Island, NY). Como control se utilizo una mezcla de ON-TARGET plus non-targeting siRNA pool (Thermo Fisher Scientific, Pittsburg, PA). El medio de transfección que contenía los complejos siRNAs – lipofectamina se dejo durante tres horas y después se remplazo con medio de diferenciación libre de suero, en el cual se cultivaron los oligodendrocitos por otras 72 horas. El silenciamiento de la expresión de

los genes se determinó por ensayos de qRT-PCR y por Inmunodetección en fase solida.

Análisis de la morfología de los procesos de los oligodendrocitos

La morfología de los oligodendrocitos se analizó y cuantificó como lo describió previamente Dennis y colaboradores (Dennis, White et al. 2008). Los oligodendrocitos se inmunotiñeron usando los sobrenadantes de los hibridomas cepa O4, y se tomaron imagines de aproximadamente 30 células por cada tratamiento en cada experimento (n≥3; al menos 90 células por cada condición) usando un microscopio invertido de fluorescencia Olympus BX51 (Olympus America, Center Valley, PA). Las células se escogieron de todos los campos del cubreobjetos empezando a escanear de la esquina izquierda superior y terminando en la esquina derecha inferior. Solo se seleccionaron para el análisis células que presentaron características de oligodendrocitos sanos (basándonos en la tinción de su núcleo y en la apariencia de su membrana) y aislados. El software IP Lab imaging (BD Bioscience Bioimaging, Rockville, MD) se uso para determinar el área de los procesos de los oligodendrocitos (área total de los procesos de los oligodendrocitos teñidos positivamente con O4 menos el área del soma). Para las barras de error, se utilizo como 100% el valor promedio del área de los procesos de las células cultivadas en condiciones control. Para obtener las imágenes representativas que se muestran en las figuras se utilizo un microscopio de escaneo de laser confocal (Zeiss LSM 510 META NLO; Carl Zeiss Microscopy, LLC, Thornwood, NY). Las imágenes representan proyecciones máximas de dos dimensiones de planos de 0.5 μm de secciones ópticas.

Conteo de células

Para determinar el numero de células inmunopositivas a MBP, se tomaron cuatro campos por cubreobjetos con un objetivo 20X usando un microscopio de fluorescencia Olympus BX51 equipado con una cámara Olympus DP72 CCD (Olympus America, Center Valley, PA). Se analizaron tres cubreobjetos por condición por cada experimento independiente. Los oligodendrocitos que mostraron tinciones positivas para núcleos con Hoechst 33342 y para MBP se contaron utilizando la herramienta para contar células del paquete de software ImageJ.

Análisis estadístico

Los datos se expresaron como el promedio ± el error estándar. Se realizo un análisis de varianza de una cola (ANOVA) para determinar las diferencias significativas entre condiciones. Cuando se compararon dos o mas grupos de datos compuestos por valores variables, se utilizo una prueba de t-Student de dos colas o un ANOVA con una prueba Krustal-Wallis combinada con una prueba de Dunn's post hoc o de Student-Newman-Keuls. Cuando se compararon un grupo control contra diferentes grupos experimentales se utilizo un ANOVA con una prueba de Dunnett's post hoc. Para el análisis estadístico, los datos se analizaron utilizando el Software GraphPad (GraphPad Software, La Jolla, CA).

Tabla I. Secuencias de Oligonucleótidos utilizados

Gen	Primer		Secuencia
Glast	Sentido	qRT-PCR	5'-AGCCTGGGGTGTCTTCCACCA-3'
	Antisentido	qRT-PCR	5'-ACCACAGCCTTGCACTTCAGTGTCT-3'
Glt-1	Sentido	qRT-PCR	5'-TGGCGGCTCCCATCCACCCT-3'
	Antisentido	qRT-PCR	5'-GGCGGCCGCTGGCTTTAGCA-3'
Eaac1	Sentido	qRT-PCR	5'-GCCCACGAGCTCGGGATGCG-3'
	Antisentido	qRT-PCR	5'-CACGATGCCCAGTACCACGGC-3'
Ppia	Sentido	qRT-PCR	5'-GGAGACGAACCTGTAG- GACG-3'
	Antisentido	qRT-PCR	5'-GATGCTCTTTCCTCCTGTGC-3'
Pgk1	Sentido	qRT-PCR	5'-ATGCAAAGACTGGCCAA GCTAC-3'
	Antisentido	qRT-PCR	5'-AGCCACAGCCTCAGCATATTTC-3'
AP-1 (SV40)	Sentido	EMSA	5'-CTAGTTCCGGCTGAGTCATCAAGC-3'

RESULTADOS

I. La proteína p60^{Src} es necesaria para la fosforilación de mTOR inducida por GLAST

Los resultados mencionados anteriormente en antecedentes demostraron que GLAST puede activar una vía de señalización que recae en un aumento en la fosforilación de mTOR, se demostró también que PI3K y Akt forman parte de la vía de señalización. Sin embargo, para la activación de la cinasa PI3K es necesaria la unión de la subunidad p85 de esta proteína a un residuo de tirosina fosforilado, por lo cual, pre-incubamos los cultivos de CGB y CGM con genisteina (25 μM), un inhibidor no selectivo de cinasas de tirosina (Fig 1A) o con PP2, un inhibidor selectivo de la cinasa de tirosinas no receptora p60^{Src} (Fig 1B y 1C), en presencia y/o ausencia del estimulo D-Aspartato (1mM) y medimos la fosforilación de mTOR. Como se muestra en la figura los inhibidores de las cinasas de tirosina anulan el efecto del Aspartato en los dos modelos. Para confirmar la participación de la cinasa p60^{Src} se trataron las CGM con D-Asp en presencia y/o ausencia de genisteina o W7, antagonista de calmodulina como control positivo, ya que la participación de esta cinasa en la activación de Src ya se ha reportado; y se midieron los niveles de fosforilación de Src en tirosina 527, es necesario que se defosforile la cinasa Src en este sitio para que pueda ser activada. Como se muestra en la figura 1D el tratamiento con D-Asp reduce la fosforilación de Src en Tirosina 527, es decir D-Asp activa a la cinasa Src, mientras que el tratamiento con genisteina y con W7 bloquean la activación de esta cinasa.

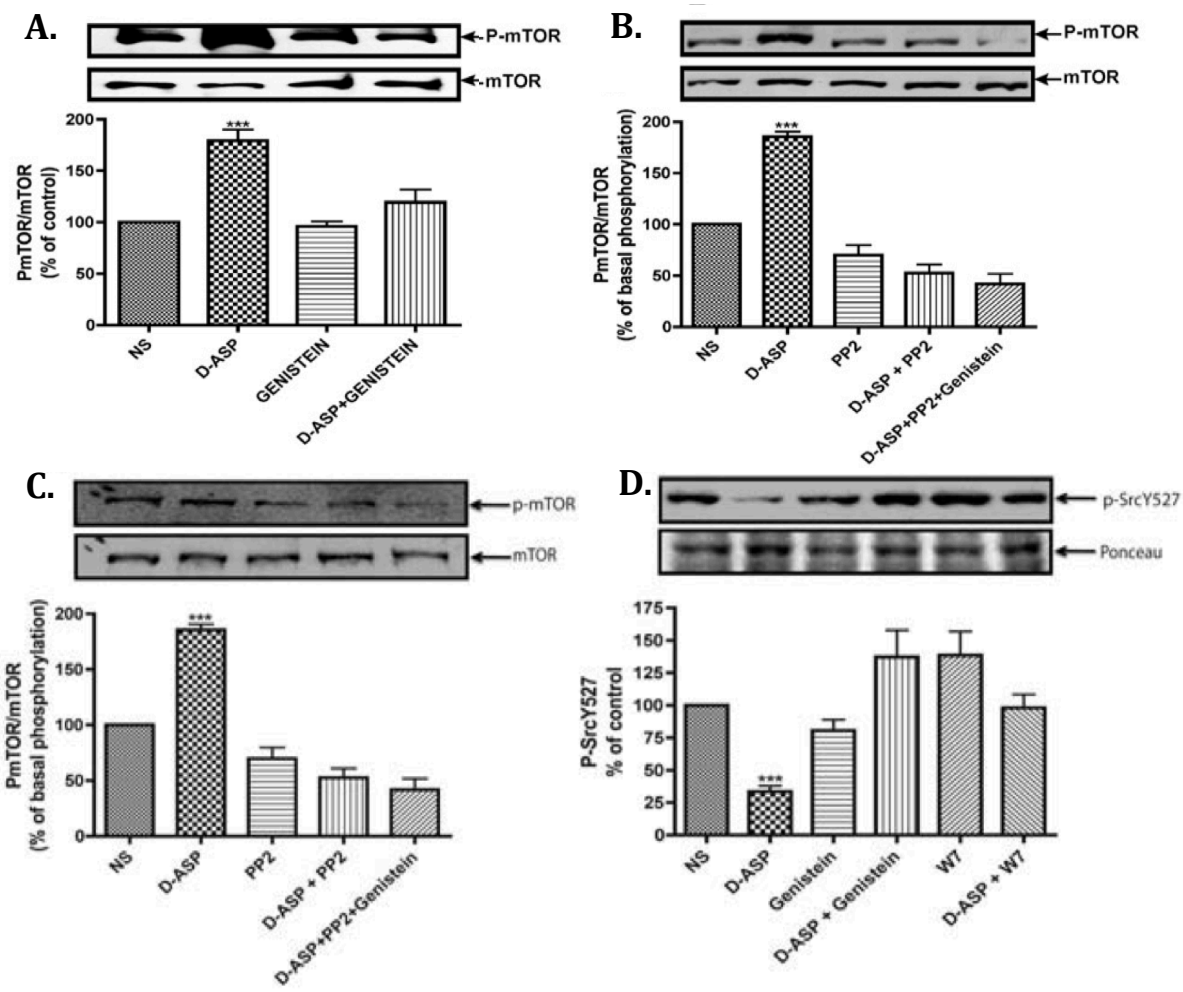

Figura 1R. D-Aspartato induce la fosforilación de mTOR de manera dependiente de Src.

Cultivos primarios de CGB (Panel A y B) y de CGM (Panel C) fueron pre incubadas 30 min con el inhibidor no selectivo de cinasas de tirosina, Genisteina 25 µM, con el inhibidor de $p60^{Src}$, PP2 10 nM, o un pre-tratamiento de ambos inhibidores juntos, en presencia y/o ausencia de un tratamiento de 15 min con Aspartato 1mM. Los niveles de totales y de fosforilación de mTOR en Serina 2448 se analizaron por inmunodetección en fase solida según se describe en la sección de materiales y métodos. (Panel D) Los niveles de fosforilación de $p60^{Src}$ se midieron en CGM después del tratamiento de 15 minutos con Asp 1mM en presencia y/o ausencia de W7 (25 µM) o genisteina (25 µM). Los niveles de fosforilación de $p60^{Src}$ fueron analizados por inmunodetección en fase solida, la tinción con rojo de Ponceau se utilizo como control de carga. Los resultados son el promedio ± E.E. de al menos tres experimentos independientes. En cada panel se muestra una autoradiografía representativa. Los análisis estadísticos se realizaron comparando con las células no tratadas usando un ANOVA no paramétrico de una vía (con una prueba Kruskal-Wallis) y una prueba Dunn's post-hoc (***P<0.001)

II. GLAST es responsable de la activación de mTOR inducida por D-Aspartato

El glutamato puede activar vías de señalización al activar a sus receptores y/o transportadores, su agonista D-Aspartato activa a los transportadores sin tener ningún efecto en sus receptores, sin embargo para corroborar que los efectos en la fosforilación de mTOR era mediada por GLAST y no por los receptores glutamatérgicos se utilizaron antagonistas de los receptores iGluRs y mGluRs. CGB fueron tratadas con Aspartato 1mM durante 15 min en presencia o ausencia del antagonista de los receptores AMPA/KA, DNQX 50 μM; del antagonista de los receptores NMDA, LAP5 10 μM; de los antagonistas de los mGluRs del grupo I, CPCCOEt 100 μM; y grupo II/III, CPPG 300 μM; como se muestra en las figuras 2A y 2B la inhibición de los receptores glutamatérgicos no tiene ningún efecto en la fosforilación de mTOR inducida por GLAST en CGB.

Cultivos primarios de CGM fueron incubadas con glutamato (1 mM, 15 min) y con los agonistas de los receptores iGluRs, AMPA (1 mM, 15 min), KA (1mM, 15 min), NMDA en presencia de glicina (1mM/10μM, 15 min) y del análogo D-Asp (1mM, 15 min), como se observa en la figura 2C, el Glu y el D-Asp aumentan significativamente la activación de mTOR y aunque la activación de los receptores AMPA y KA presentan la tendencia de incrementar la fosforilación de mTOR en Ser2448, esta no es significativa, con lo cual se demuestra que la fosforilación de mTOR inducida por Glu es principalmente llevada a cabo por GLAST en CGM. Para corroborar lo anterior CGM se trataron con antagonistas de los receptores de glutamato, de los receptores del tipo AMPA/KA, CNQX (50μM) (Figura 2D), del tipo NMDA, MK-801 (5μM) y LAP5 (10μM) (Figura 2E), antagonistas de mGluRs (Figura 2F) del grupo I CPCCOEt (100μM), del grupo II/III CPPG (300μM) en presencia y/o ausencia de D-Asp. Como se muestra en la figura 2 (C-F) la activación de mTOR inducida por D-Asp es independiente de la activación de los receptores de glutamato.

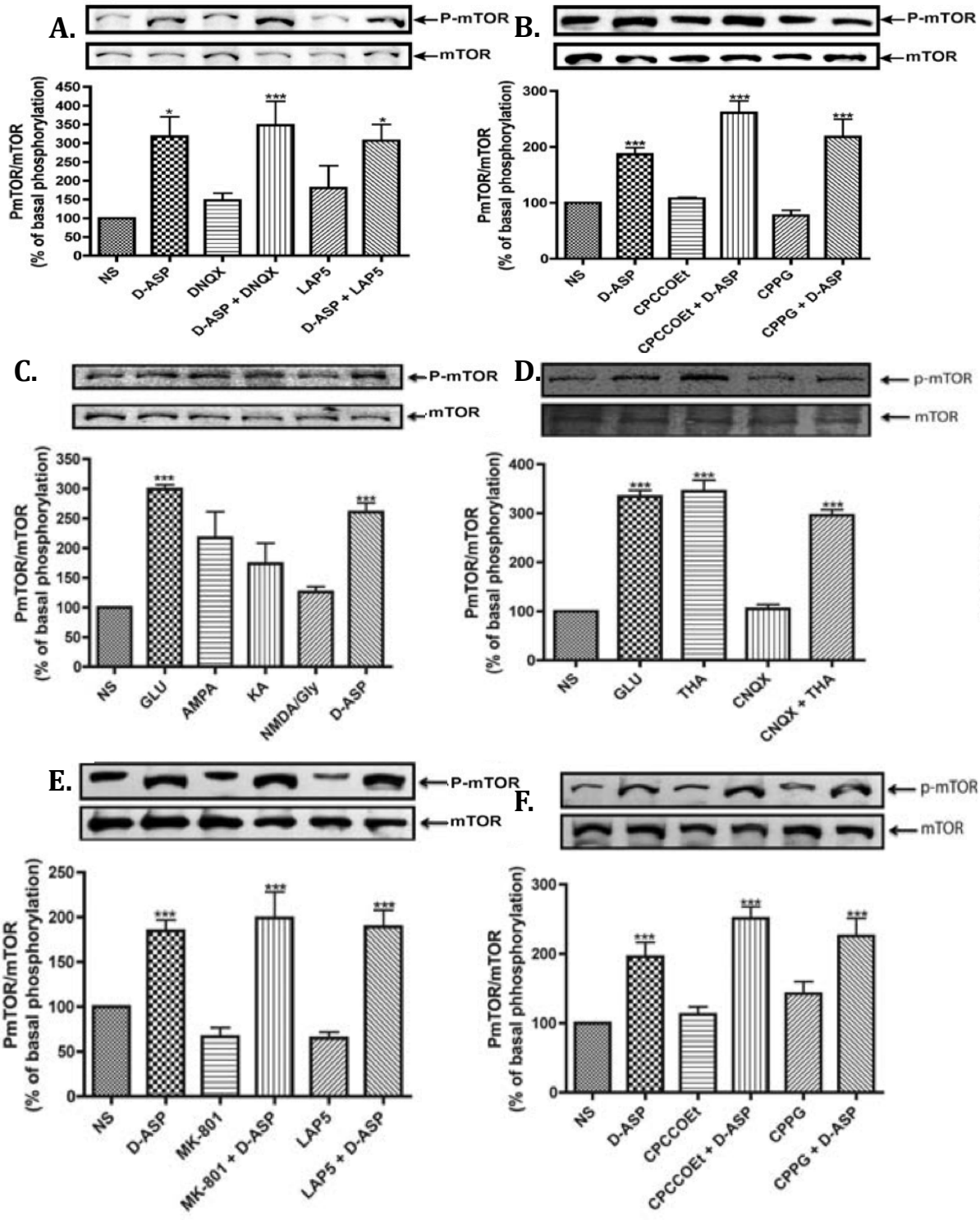

Figura 2R. La activación de mTOR inducida por Aspartato es independiente de los receptores glutamatérgicos.

(A y B) Cultivos primarios de CGB fueron tratadas con D-Asp (1mM, 15 min) en presencia y/o ausencia de antagonistas de los receptores ionotrópicos (Panel A) y metabotrópicos (Panel B) de glutamato, de los receptores AMPA, DNQX (50 μM); de los receptores NMDA, LAP5 (10 μM); de los mGluRs de grupo I, CPCCOEt (100 μM); de los mGluRs de los grupos II/III, CPPG (300 μM), los antagonistas se agregaron 30 min antes del Aspartato. (C) CGM fueron incubadas por 15 minutos con el vehículo (NS), glutamato (1mM) o con los análogos de glutamato AMPA (1mM), KA (1mM), NMDA (1mM) con glicina (10μM), y con aspartato (1mM). (D) Monocapas de CGM se incubaron 15 min con Glutamato (1mM), el bloqueador transportable de los EAATs, THA (100 μM), el antagonista de los receptores

AMPA/KA, CNQX (50 μM) y con THA en presencia de CNQX, en este caso el CNQX se agrego 30 min antes del tratamiento con THA. (E y F) Cultivos de CGM fueron pre incubados durante 30 min con los antagonistas de los receptores NMDA (panel E), MK-801 (5μM) y LAP5 (10 μM); y con los antagonistas de los mGluRs (panel F) del grupo I, CPCOOEt (100 μM) y de los grupos II/III, CPPG (300 μM), después del cual se incubaron con aspartato durante 15 min (1mM). Los niveles de totales y de fosforilación de mTOR en Serina 2448 se analizaron por inmunodetección en fase solida según se describe en la sección de materiales y métodos. Los resultados son el promedio ± E.E. de al menos tres experimentos independientes. En cada panel se muestra una autoradiografía representativa. Los análisis estadísticos se realizaron comparando con las células no tratadas usando un ANOVA no paramétrico de una vía (con una prueba Kruskal-Wallis) y una prueba Dunn's post-hoc (*P<0.05, ***P<0.001)

Con los resultados anteriores se demostró que la activación de mTOR depende de los transportadores de glutamato, sin embargo no descartamos a los otros EAATs. Ruiz y Ortega en 1995 demostraron que en las CGB la captura de glutamato dependiente de Na^+ es llevada a cabo únicamente por GLAST, pero en las CGM se recientemente se reporto la expresión de EAAT4 (Fyk-Kolodziej, Qin et al. 2004), por lo cual decidimos evaluar la participación de este transportador en la activación de mTOR. Con este fin CGM fueron tratadas con D-Asp (1mM, 15 min) en presencia y/o ausencia del bloqueador especifico de los transportadores EAAT4, T3MG (200μM, 30 min), DMSO se utilizo como control ya que fue el vehículo en el que se preparo el T3MG. Como se observa en la figura 3A, los transportadores EAAT4 no participan en la fosforilación de mTOR inducida por D-Asp.

Como se menciona en la sección de antecedentes, la activación de GLAST conlleva a un influjo de iones Calcio, el cual a su vez permite la activación de una tirosin cinasa que repercute en la señalización a través de la cascada PI3K/Akt/mTOR. Con esto en mente se determino si la inhibición de los transportadores EAAT4 afectaba los influjos de calcio inducidos por D-Asp, como se muestra en la figura 3B los influjos de Calcio activados por D-Asp son independientes de EAAT4.

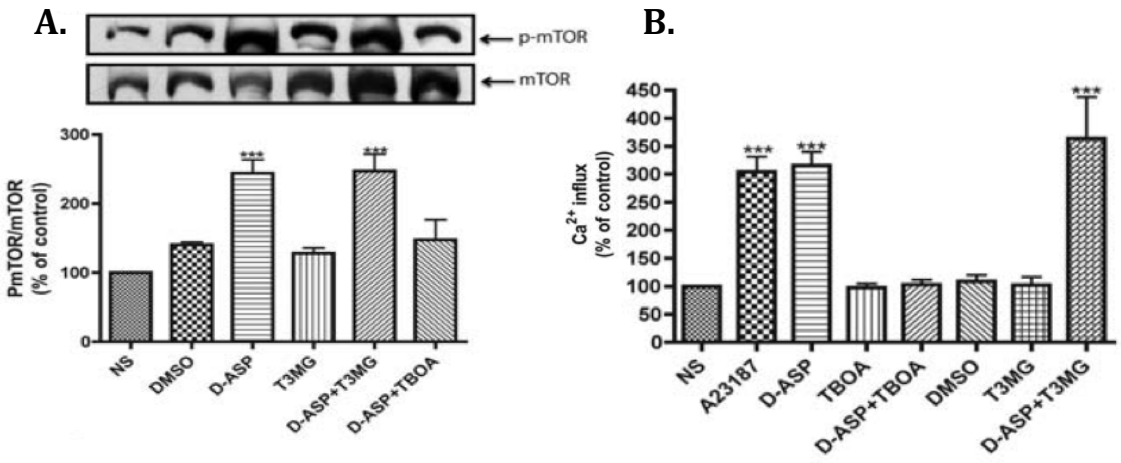

Figura 3R. Los efectos del D-Asp en CGM son independientes de los transportadores EAAT4.

(A) CGM se trataron durante 30 min con el bloqueador de EAAT4, T3MG (200µM) o con el bloqueador no especifico de los EAATs, TBOA (100µM) antes de la adición de D-Asp (1mM, 15 min), DMSO (0.01%) se uso como control del vehículo. Los niveles totales de mTOR y sus niveles de fosforilación en Ser2448, se determinaron por inmunodetección en fase solida. Se muestra una autoradiografía representativa de al menos tres experimentos independientes. (B) Cultivos primarios de CGM se incubaron con TBOA o con el bloqueador de EAAT-4, T3MG por 30 min antes del tratamiento con D-Asp (1mM, 3 min), y después de midió la captura de $^{45}Ca^{2+}$. El ionóforo de Calcio, A23187 (10µM) se uso como control positivo. La captura de $^{45}Ca^{2+}$ fue de 3 min. Los valores representan el promedio ± el E.E. de al menos tres experimentos independientes realizados cada uno por triplicado. Los análisis estadísticos se realizaron comparando con las células no tratadas usando un ANOVA no paramétrico de una vía (con una prueba Kruskal-Wallis) y una prueba Dunn's post-hoc (***P<0.001)

III. La activación de mTOR inducida por GLAST tiene como consecuencia la fosforilación del blanco de mTOR, 4EBP1

Con los resultados anteriores sabemos que GLAST induce la fosforilación de mTOR en Ser2448, pero para corroborar si esta fosforilación tiene un impacto en los blancos de mTOR, decidimos analizar la fosforilación de 4EBP1 en Treonina 70 en los dos modelos celulares. Como se muestra en la figura 4, los tratamientos que activan a GLAST, D-Aspartato y THA aumentan la fosforilación de 4EBP1 en Treonina 70, mientras que la inhibición de mTOR con rapamicina bloquea el efecto, demostrando que GLAST activa a mTOR que a su vez actúa fosforilando a sus blancos como 4EBP1.

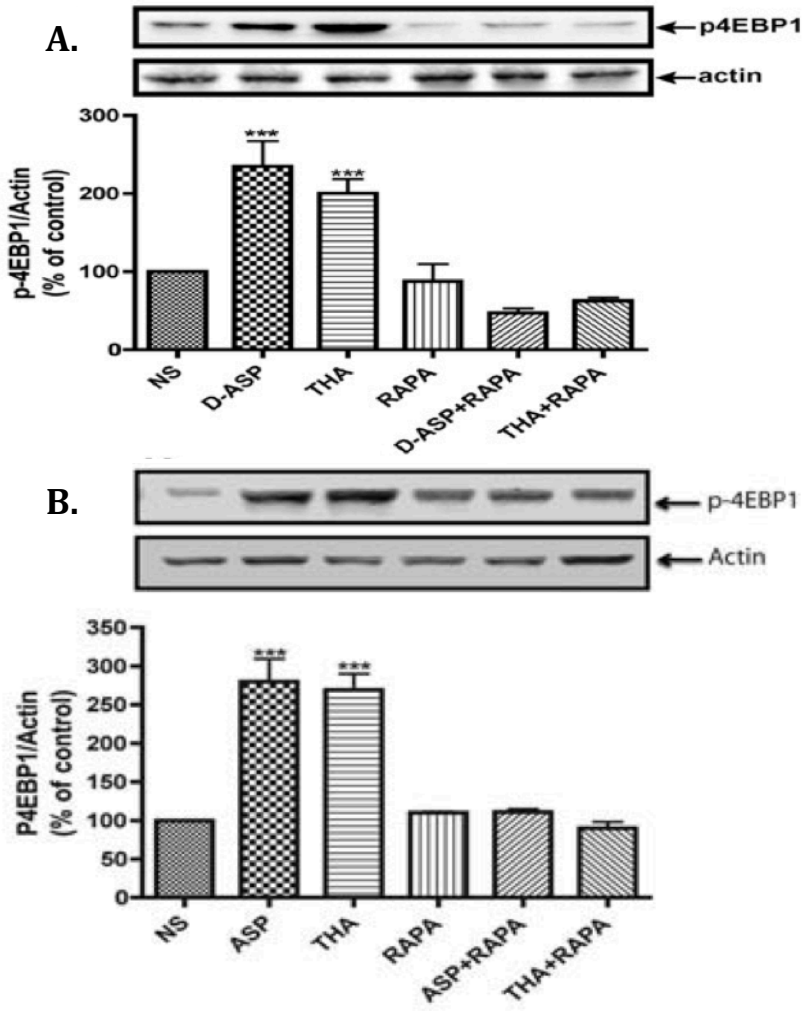

Figura 4R. La activación de mTOR mediada por GLAST repercute en la fosforilación de su blanco 4EBP1.

CGB (Panel A) o CGM (Panel B) fueron tratadas con D-Asp 1mM o THA 100 µM por 15 min, en presencia y/o ausencia del inhibidor de mTORC1 Rapamicina 100 nM, cuando se utilizo rapamicina esta se agrego 30 min antes de los estímulos. Los niveles de 4EBP1 fosforilado en Thr 70 se detectaron por inmunodetección en fase solida. Los niveles de actina se utilizaron como control de carga. Los datos se expresaron como el promedio ± el E.E. de al menos tres experimentos independientes. Se muestra una autoradiografía representativa. Se realizaron análisis estadísticos comparando con células no estimuladas, usando un ANOVA de una vía no paramétrico (prueba de Kruskal-Wallis) y una prueba post-hoc de Dunn (***P<0.001)

IV. Los influjos de Calcio inducidos por GLAST son llevados a cabo por el intercambiador Na^+/Ca^{2+}

Ahora que sabemos que GLAST señaliza, que esta señalización repercute en la activación de la vía PI3K/Akt/mTOR y que para iniciar esta cascada

es necesario un influjo de iones Ca^{2+} quisimos dilucidar la vía de entrada de este Ca^{2+}. Debido a que el transporte de glutamato conlleva un influjo de Na^{+} y de que en células gliales se ha reportado la expresión de los intercambiadores de Na^{+}/Ca^{2+} se podría pensar que estos intercambiadores son los responsables del influjo de Ca^{2+} observado al estimular a GLAST. Para demostrar eso utilizamos el inhibidor especifico del modo reverso (salida de Na^{+}, entrada de Ca^{2+}) de los intercambiadores Na^{+}/Ca^{2+}, KB-R7943 y se midió el influjo de $^{45}Ca^{2+}$ en CGB y CGM. Como se muestra en la figura 5 A y B, el influjo de Calcio activado por D-Asp es inhibido en presencia de KB-R7943. También observamos que para que GLAST active la cascada de señalización que lleva a la fosforilación de mTOR es necesario el influjo de iones Ca^{2+} a través de los intercambiadores Na^{+}/Ca^{2+} (Figura 5C).

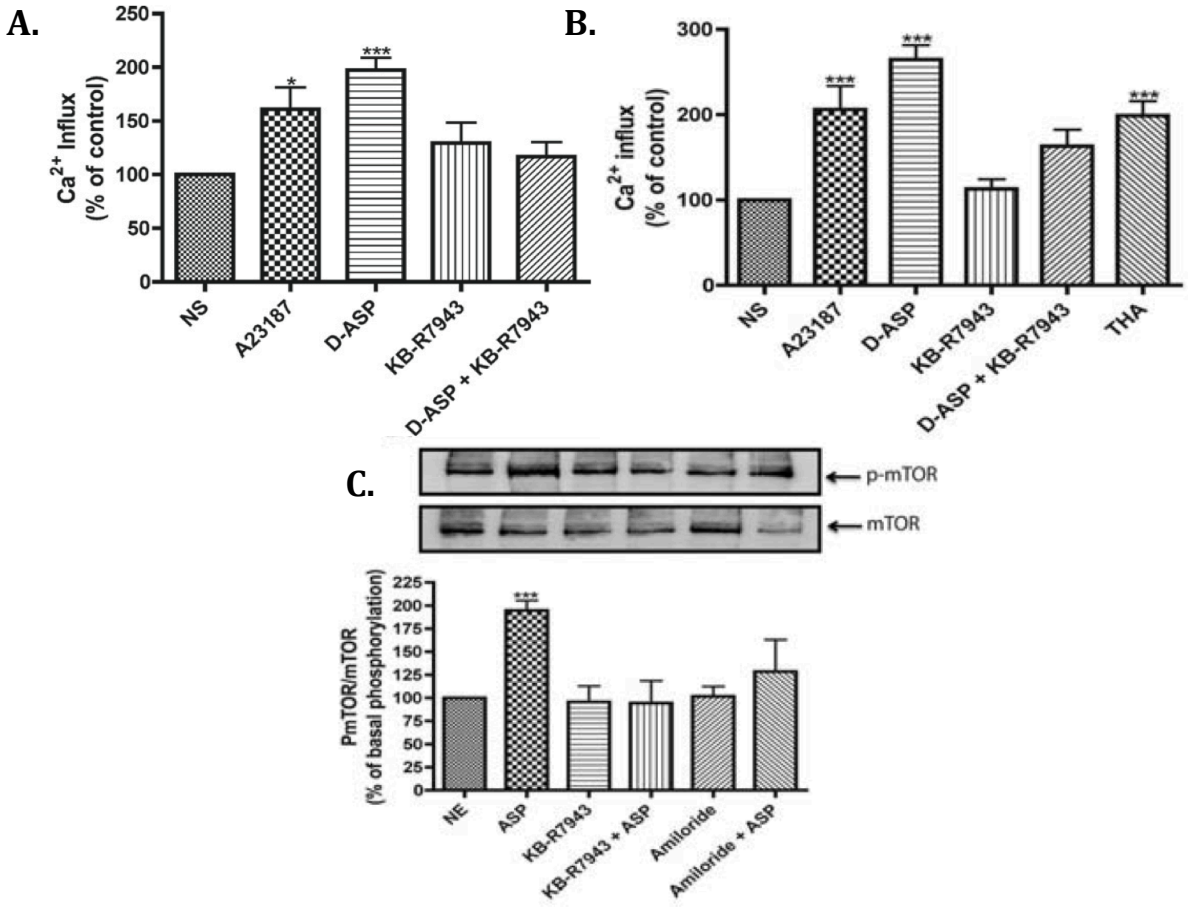

Figura 5R. La activación de GLAST induce un influjo de iones calcio mediado por NCX.

Monocapas confluentes de CGB (panel A) y de CGM (panel B) fueron pre-incubadas con el bloqueador de los intercambiadores Na+/Ca2+, KB-R7943 15 µM durante 30 min, y después incubadas por 3min con D-Asp en presencia del $^{45}Ca^{2+}$. El ionóforo de Ca^{2+} A23187 10 µM se uso como control positivo. Los datos se expresaron como el promedio ± el E.E. de al menos tres experimentos independientes realizados cada uno en cuadriplicado. Se realizaron análisis estadísticos comparando con células no estimuladas, usando un ANOVA de una vía no paramétrico (prueba de Kruskal-Wallis) y una prueba post-hoc de Dunn (*P<0.05, ***P<0.001).
(panel C) CGM se estimularon con D-Asp (1mM, 15 min) en presencio o ausencia del bloqueadores de los intercambiadores Na+/Ca2+, KB-R7943 15 µM el cual se agrego 30 min antes del tratamiento con Asp. Los resultados son el promedio ± el E.E. de al menos tres experimentos independientes. Se muestra una autoradiografía representativa. Se realizaron análisis estadísticos comparando con células no estimuladas, usando un ANOVA de una vía no paramétrico (prueba de Kruskal-Wallis) y una prueba post-hoc de Dunn (***P<0.001).

Con el fin de eliminar la participación de los canales de Ca2+ dependientes de voltaje (VGCC) de tipo L, cultivos primarios de CGM se pre-incubaron con Nifedipina 10 µM y se analizo el efecto de D-Asp en estas condiciones. Como se muestra en la figura 6, la pre-incubación con Nifedipina no modifica el influjo de Ca^{2+} dependiente de D-Asp.

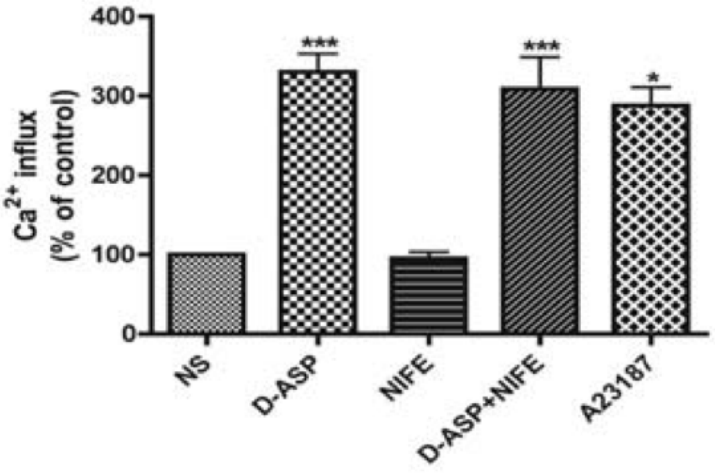

Figura 6R. El influjo de calcio inducido por GLAST es independiente de los canales de calcio dependientes de voltaje tipo L.

CGM fueron pre-incubadas con el inhibidor de los canales VGCC tipo L, nifedipina (10 mM, 30 min), después las células se trataron con D-Asp (1mM, 3 min). El ionóforo de Ca^{2+}, A23187 10 µM se uso como control positivo. Los datos se expresaron como el promedio ± el E.E. de al menos tres experimentos independientes realizados cada uno en cuadriplicado. Se realizaron análisis estadísticos comparando con células no estimuladas, usando un ANOVA de una vía no paramétrico (prueba de Kruskal-Wallis) y una prueba post-hoc de Dunn (*P<0.05, ***P<0.001).

V. La activación de GLAST induce una regulación transcripcional mediante el factor de transcripción AP-1

Los resultados obtenidos demostraron que el transportador de glutamato GLAST es capaz de inducir influjos de Calcio a través del intercambiador Na^+/Ca^{2+}, el incremento en las concentraciones intracelulares de Calcio lleva a la activación de la vía de señalización PI3K/PKB/mTOR, la cual regula la traducción en CGB y en CGM. Sin embargo en estos dos modelos, se ha demostrado que el glutamato también puede regular la transcripción (Lopez-Bayghen, Espinoza-Rojo et al. 2003, Lopez-Bayghen and Ortega 2004). Para mostrar si la regulación transcripcional dependiente de glutamato es mediada únicamente por los receptores glutamatérgicos o si también participan los transportadores de glutamato CGB y CGM fueron tratadas con D-Asp y se midió la actividad de un factor de transcripción el cual ya se ha demostrado que es regulado por glutamato en estas células, el factor transcripcional AP-1 (REF). Como se observa en las figuras 7A y 7B el tratamiento con D-Asp y THA incrementa la unión de AP-1 a su secuencia consenso, mientras que al bloquear al GLAST con TBOA esta unión se interrumpe. También se observo que el intercambiador Na^+/Ca^{2+} y la calmodulina son mediadores del efecto que tiene GLAST sobre el factor transcripcional AP-1, ya que al inhibir a estas proteínas con KB-R7943 y W7 respectivamente, se abate el efecto de D-Asp (Figura 7C). Demostrando así que GLAST regula también a nivel transcripcional.

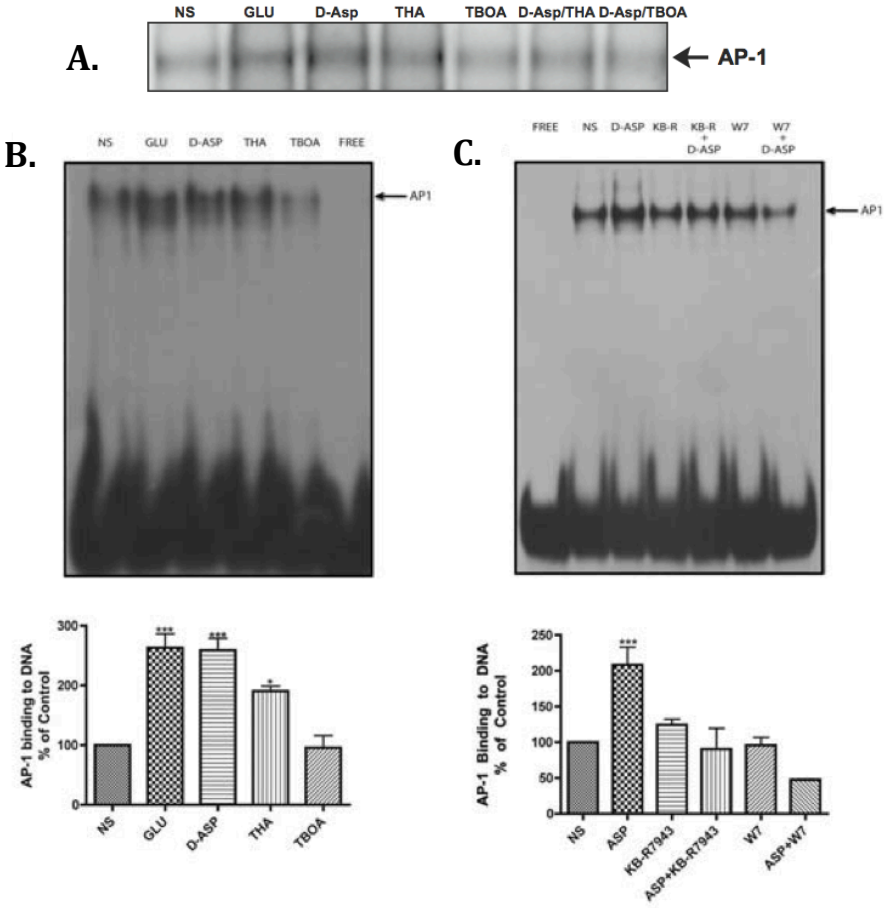

Figura 7R. La actividad de GLAST induce una regulación transcripcional a través de la unión de AP-1 al DNA.

Extractos nucleares se obtuvieron de CGB (panel A) o de CGM (paneles B y C) tratadas con Glutamato, 1mM, D-Asp 1mM, THA 100 µM, TBOA 100 µM, D-Asp mas THA o D-Asp mas TBOA. (Panel C) extractos nucleares de CGM fueron preparados de células pre-incubadas por 30 min con el inhibidor del intercambiador Na+/Ca2+, KB-R7943 15 µM, y con el antagonista de calmodulina, W7 25 µM, después las células se trataron con D-Asp (1mM, 90min), se analizo la unión del factor transcripcional AP-1 a su secuencia consenso. Los resultados son el promedio ± E.E. de al menos tres experimentos independientes. Se realizaron análisis estadísticos comparando con células no estimuladas, usando un ANOVA de una vía no paramétrico (prueba de Kruskal-Wallis) y una prueba post-hoc de Dunn (***P<0.001).

Con los resultados anteriores proponemos el siguiente modelo:

El glutamato es transportado a la células de glía de Bergmann y de Müller por el transportador GLAST, esto provoca un aumento en las concentraciones intracelulares de Na^+, que activan el modo reverso del intercambiador de Na^+/Ca^{2+} el cual toma los iones Na^+ y los exporta permitiendo la entrada de iones Ca^{2+} aumentando las concentraciones intracelulares de este ion. El aumento de calcio intracelular por un lado

activa a Src^{p60} que a su vez activa la vía de señalización PI3K/PKB/mTOR que repercute en la fosforilación de 4EBP1 y de S6K regulando la síntesis de proteínas; y por el otro lado junto a calmodulina se une a CaMKII y la activa induciendo la señalización mediada por Raf/ERK/RSK1^{p90}/CREB que modifica la unión de AP-1 al DNA regulando de esta forma la transcripción (ver modelo en figura 8).

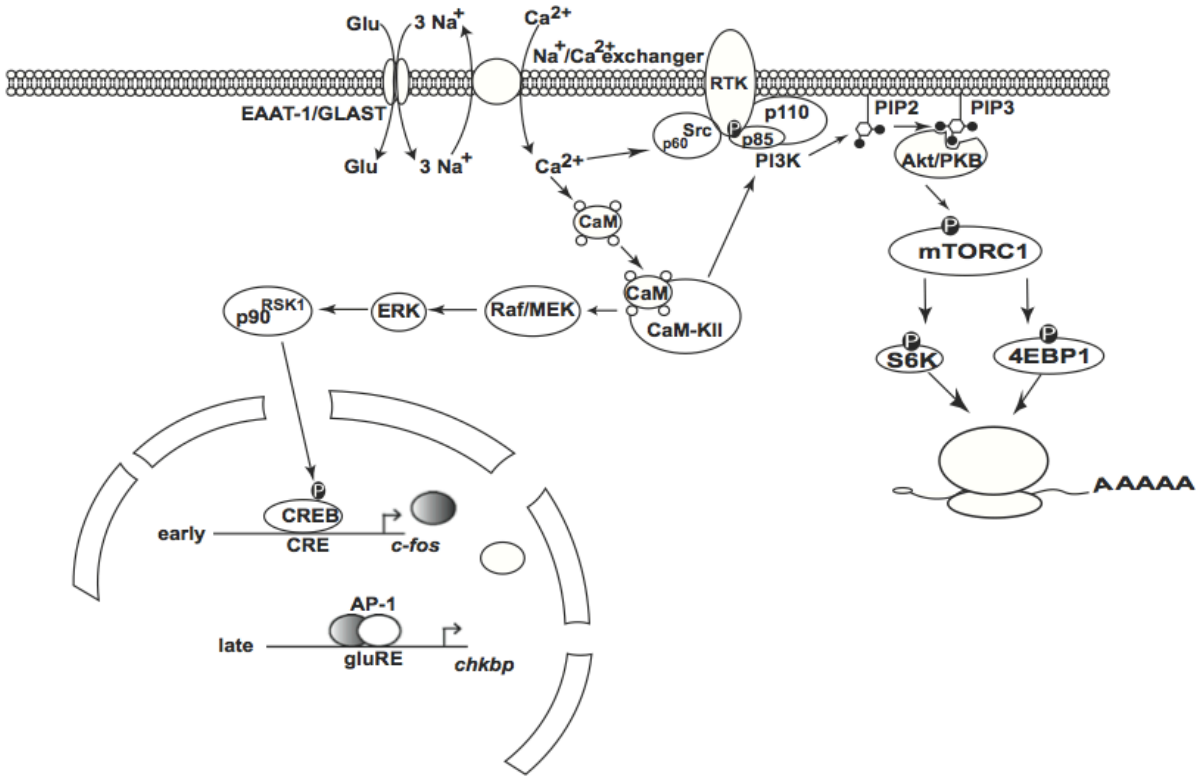

Figura 8R. Modelo de la señalización mediada por EAAT-1/GLAST en cultivos primarios de CGB y CGM.

VI. La actividad de GLAST es regulada por proteínas que transportan Na^+

Ya que se demostró que GLAST es una molécula señalizadora es importante conocer como se regula este transportador. Como se comento, el transporte de glutamato es electrogénico, es decir, para que el glutamato se transporte es necesario el importe de tres iones Na^+ y de un protón, y el exporte de un ion K^+, por lo cual es plausible pensar las concentraciones intracelulares de Na^+ pueden modificar la actividad de GLAST. Para probar esta hipótesis, utilizamos cultivos primarios de CGB los cuales incubamos con inhibidores de las proteínas transportadoras de Na^+ expresadas principalmente en células gliales y que se ha reportado su participación en la transmisión glutamatérgica (Gegelashvili, Rodriguez-Kern et al. 2007, Rose, Koo et al. 2009, Martinez-Lozada, Hernandez-Kelly et al. 2011); el inhibidor de la ATPasa de Na^+/K^+, Ouabaina y el inhibidor del intercambiador Na^+/Ca^{2+}, KB-R7943; como se demostró que Src^{p60} y mTOR son proteínas que se encuentran rio debajo de GLAST también utilizamos los inhibidores de estas proteínas, PP2 y rapamicina respectivamente y medimos la actividad de GLAST. Como se muestra en la figura 9A, los inhibidores de las proteínas transportadoras de Na^+, ATPasa de Na^+/K^+ y del intercambiador Na^+/Ca^{2+} disminuyen la captura de glutamato, mientras que la inhibición de Src^{p60} y de mTOR no afectan la captura mediada por GLAST, eliminando la posibilidad de una asa de retroalimentación negativa. Se observo que la inhibición de la actividad de GLAST mediada por la ATPasa de Na^+/K^+ es dependiente de la dosis utilizada (Figura 9B), mientras que la del intercambiador Na^+/Ca^{2+} es independiente, teniendo su máximo efecto a una dosis de 150 nM (Figura 9C).

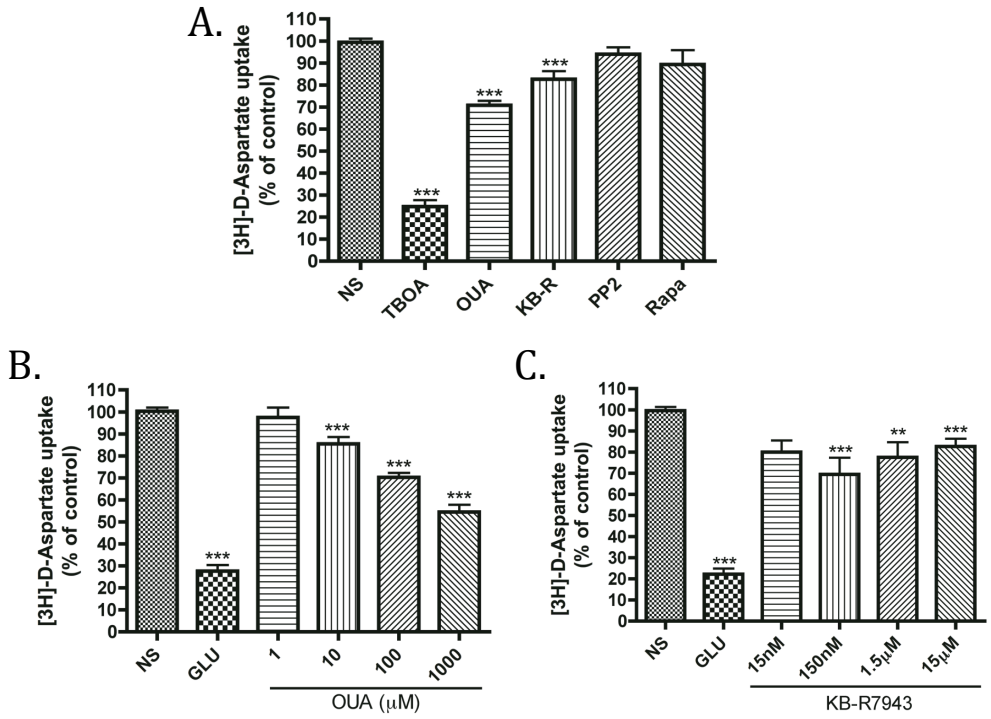

Figura 9R. La actividad de GLAST es regulada por la ATPasa de Na^+/K^+ y por el NCX.

(A) Monocapas confluentes de CGB fueron incubadas por 30 min con diferentes bloqueadores: El bloqueador de los transportadores de glutamato, TBOA (100 μM) como control positivo, el inhibidor de la ATPasa de Na^+/K^+, Ouabaina (100 μM), el inhibidor de los intercambiadores Na^+/Ca^{2+}, KB-R7943 (15 μM), el inhibidor de Src^{p60}, PP2 (10 nM) y el inhibidor de mTOR, rapamicina (100 nM). Después de los 30 min de incubación con los inhibidores las monocapas de CGB se lavaron e inmediatamente se realizo la captura de [3H]-D-Asp (0.4 μCi/mL) por 30 min. (B y C) CGB se incubaron por 30 min con concentraciones crecientes de Ouabaina en el panel B o con KB-R7943 en el panel C. La captura de aspartato se realizo por 30 min como en el panel A. Los valores representan el promedio ± el E.E. de al menos tres experimentos independientes realizados cada uno por cuadriplicado. Los datos se compararon usando una prueba de t de Student (**P<0.01 ***P<0.001)

Ya que la regulación de GLAST mediada por la ATPasa de Na^+/K^+ y por el intercambiador Na^+/Ca^{2+} podría ser por el mismo mecanismo, la acumulación de Na^+ intracelular, decidimos analizar si la inhibición de estas proteínas tenia efectos aditivos o sinérgicos. Como se muestra en la figura 10R el tratamiento con Ouabaina inhibe la captura de glutamato 30%, mientras que el tratamiento con KB-R7943 la inhibe 15%, al colocar juntos los dos inhibidores la disminución en la captura es del 55% demostrando que tienen efecto sinérgico. Esto sugiere que ambos fármacos inhiben la captura por el mismo mecanismo. Nosotros sugerimos

que es a través de la acumulación de las concentraciones intracelulares de Na^+ sin embargo es necesario hacer mas experimentos para demostrar esto.

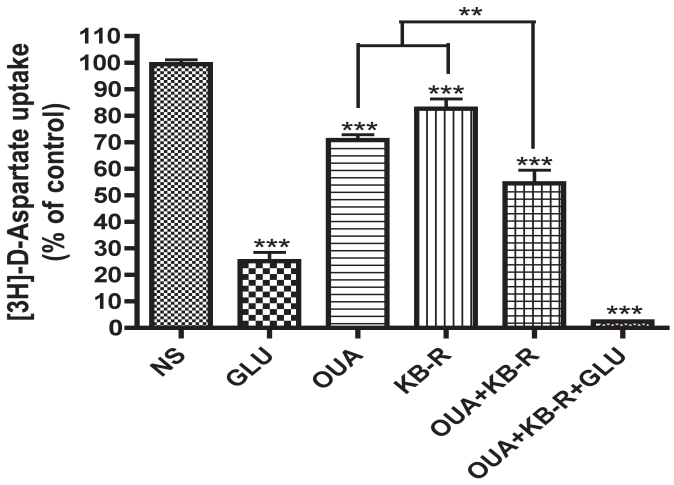

Figura 10R. La actividad de GLAST es regulada por la ATPasa de Na^+/K^+ y por el NCX a través del mismo mecanismo.

Monocapas confluentes de CGB fueron incubadas por 30 min con el inhibidor de la ATPasa de Na^+/K^+, Ouabaina (100 µM) y/o con el inhibidor de los intercambiadores Na^+/Ca^{2+}, KB-R7943 (15 µM), como control positivo se utilizo Glutamato 1mM y la pre incubación de este en presencia de los dos inhibidores. Después de los 30 min de incubación con los inhibidores las monocapas de CGB se lavaron e inmediatamente después se realizo la captura de [3H]-D-Asp (0.4 µCi/mL) por 30 min. Los valores representan el promedio ± el E.E. de al menos tres experimentos independientes realizados cada uno por cuadriplicado. Los datos se compararon usando una prueba de t de Student (***P<0.001).

Con los resultados anteriores demostramos que GLAST es un transductor de señales, sin embargo nos quedan dos preguntas, 1. ¿La señalización mediada por GLAST es un evento exclusivo de las células de glía radial? 2. ¿GLAST es el único transportar de glutamato que puede actuar como molécula señalizadora? Para contestar estas preguntas cambiamos de modelo de estudio a otro tipo de macroglía, los oligodendrocitos. El cultivo primario de oligodendrocitos de rata es un buen modelo para el estudio de la señalización glutamatérgica ya que se ha demostrado que el glutamato participa en la biología de las células mielinizantes del SNC.

VII. Los oligodendrocitos expresan transportadores de Glutamato

Debido a que la expresión de los transportadores de glutamato ha sido debatida en la literatura dependiendo del modelo de oligodendrocitos utilizados y de la etapa de maduración de estos, primeramente decidimos analizar por RT-PCR cuantitativa la expresión de los transportadores de glutamato, como se muestra en la figura 11R (A), la expresión relativa de los RNA mensajeros de los transportadores de glutamato indica que el transportador Glast/Eaat1 es el mas expresado, seguido por el transportador Glt-1/Eaat2 y el transportador de glutamato con menos expresión en estas células es Eaac1/Eaat3, ya que los niveles de RNA mensajero no siempre correlacionan con los niveles de proteína se corroboraron los resultados obtenidos por inmunodetección en fase solida y por inmunofluorescencia Fig 11R (B y C), se observa que los transportadores de glutamato se expresan no únicamente en el soma celular sino que también en los procesos de los oligodendrocitos.

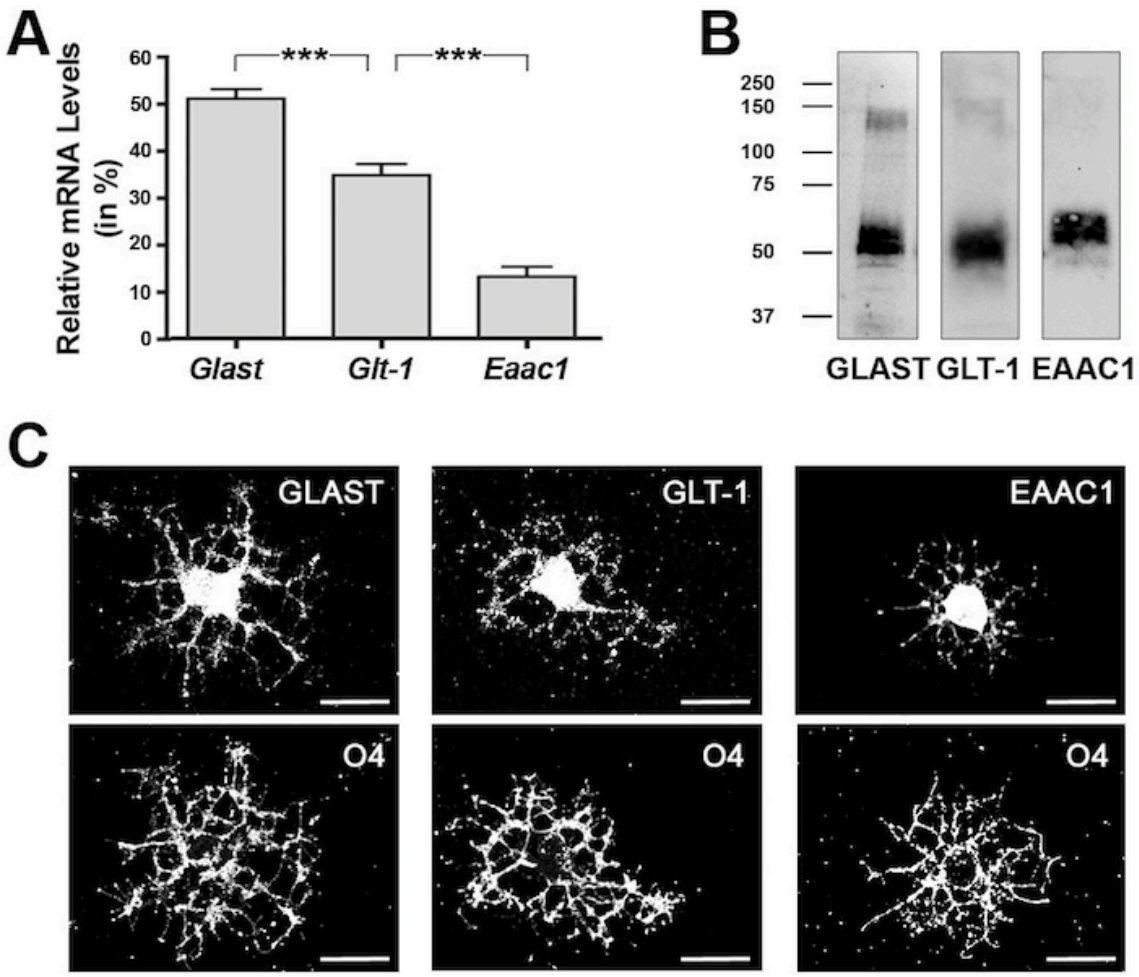

Figura 11R. Los transportadores de glutamato GLAST, GLT-1 y EAAC1 se expresan en oligodendrocitos.

A) Los niveles relativos de RNAm de los transportadores de glutamato dependientes de Na^+ se determinaron por qRT-PCR. Los niveles totales de RNAm de los transportadores de glutamato (Glast+Glt1+Eaac1) se consideraron como el 100% y los valores específicos de cada RNAm se ajustaron de acuerdo al valor de 100%. Los valores representan el promedio ± el E.E. de 3 experimentos independientes ***P≤0.001. B) En la figura se muestra una auto radiografía representativa que muestra la expresión de los transportadores de glutamato. Los números a la izquierda de la figura indican los pesos moleculares en KDa. C) Imagines representativas de oligodendrocitos teñidos con un doble marcaje usando los anticuerpos anti-GLAST, anti-GLT1, anti-EAAC1 en conjunto con el sobrenadante del hibridoma O4. Barra de Escala: 20 μm.

VIII. La activación de los transportadores de Glutamato promueve la diferenciación morfológica de los oligodendrocitos sin modificar la expresión de MBP

Se ha reportado la participación del glutamato en la maduración de los oligodendrocitos, por lo que la siguiente pregunta que nos hicimos fue, ¿Los transportadores de glutamato regulan la maduración de los oligodendrocitos?

Como se menciono en la introducción la diferenciación de los oligodendrocitos involucra cambios morfológicos, de células bipolares, los precursores de los oligodendrocitos a células con una estructura compleja y amplios procesos y finalmente a células mielinizantes (ver Figura 7). Por lo que para resolver la pregunta anterior utilizamos inmunofluorescencia y medimos el índice de los procesos de los oligodendrocitos para analizar si el glutamato tiene un efecto en la diferenciación morfológica de estos.

Para cuantificar el crecimiento de los procesos utilizamos una medida del área de la red de procesos, como lo indica la siguiente formula:

Área de los procesos= Área total de la célula – Área del cuerpo celular

Como se muestra en la figura 12R el tratamiento con glutamato incrementa el área de los procesos de los oligodendrocitos, este incremento fue bloqueado por el pre-tratamiento con TBOA, el inhibidor de los transportadores de glutamato (panel B), y fue mimetizado por Aspartato (panel D). Se observo que el aumento en el área de los procesos de los oligodendrocitos era evidente desde las 2 horas (panel C).

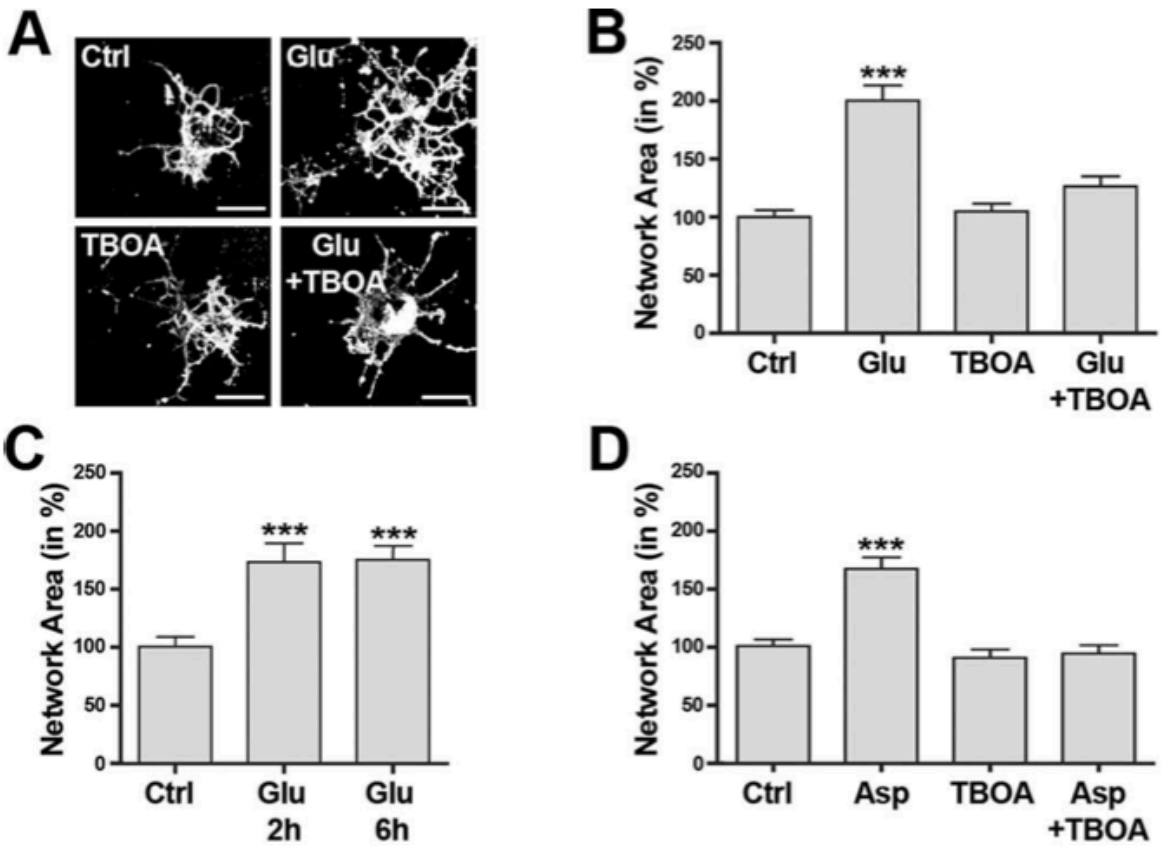

Figura 12R. La activación de los transportadores de Glutamato promueve la diferenciación de los aspectos morfológicos de los oligodendrocitos.

A-D Oligodendrocitos fueron tratados con Glu (100 μM) por 6 horas, excepto en el caso que se menciona lo contrario (Panel C), como se indica en cada figura los oligodendrocitos fueron tratados con L-Glu (100μM), el inhibidor no transportable del transporte de Glu dependiente de Na^+, TBOA (100μM) y D-Aspartato (100μM) o sin tratarse controles (Ctrl). En el panel A se muestran imágenes representativas de oligodendrocitos diferenciados inmunoteñidos con el sobrenadante del hibridoma O4. Barras de escala equivalentes a 20μM. B-D: Las graficas de barras representan un análisis cuantitativo del área de los procesos de los oligodendrocitos (Como en Dennis et al., 2008). Los datos representan el promedio ± el E.E. de 3 experimentos independientes (***P≤0.001 comparados con el control, ANOVA).

Con estos resultados demostramos que los transportadores de glutamato promueven la diferenciación morfológica de los oligodendrocitos, sin embargo, la diferenciación de los oligodendrocitos también conlleva cambios en el perfil global de proteínas que expresan estas células.

Una de las proteínas que empieza a expresarse al diferenciarse los oligodendrocitos es la MBP, por lo que decidimos analizar la expresión de esta proteína usando inmunofluorescencia en oligodendrocitos tratados con Glu, D-Asp y TBOA.

Como se observa en la figura 13R no hay diferencias estadísticamente significativas con los diferentes tratamientos, demostrando que la activación de los transportadores solo regula la diferenciación de los oligodendrocitos al modificar aspectos morfológicos sin alterar la expresión de MBP.

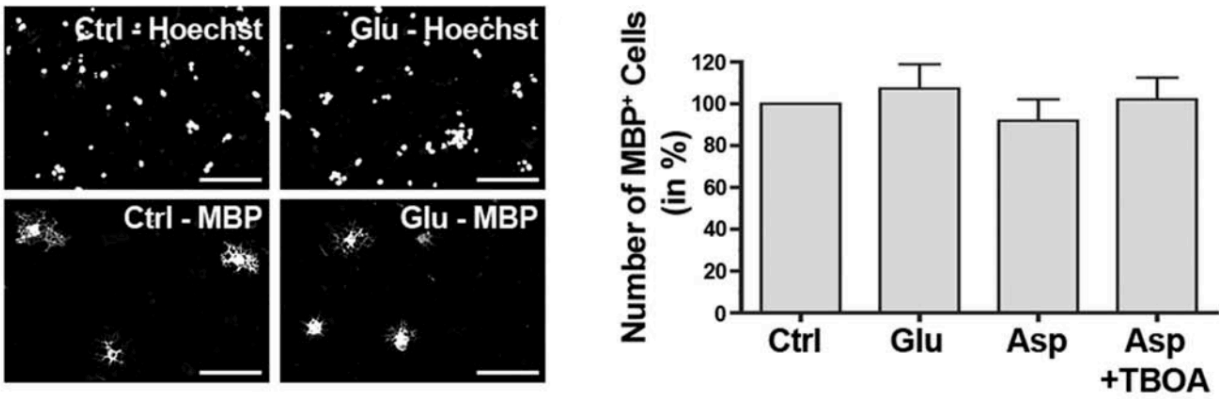

Figura 13R. La activación de los transportadores de Glutamato no promueve cambios en la expresión de MBP en los oligodendrocitos.

En el panel izquierdo se muestran imágenes representativas de oligodendrocitos diferenciados teñidos con un anticuerpo especifico para MBP así como con Hoechst 33342 (Hoechst) para visualizar los núcleos. Las barras de escala representan 100 µM. La grafica de barras representa el numero de células inmunopositivas a MBP normalizadas con el numero de núcleos positivos a Hoechst. Los datos representan el promedio ± el E.E. de 3 experimentos independientes. El ANOVA no revelo diferencias estadísticamente significativas ($P \leq 0.05$).

IX. Todos los transportadores de glutamato expresados en oligodendrocitos actúan como moléculas señalizadoras

Una vez que conocíamos que el Glu a través de la activación de los EAATs, regula la diferenciación de los oligodendrocitos, quisimos resolver la segunda pregunta que teníamos, ¿GLAST es el único transportar de glutamato que puede actuar como molécula señalizadora?. Para resolver esto, utilizamos RNA pequeños interferentes (siRNAs) para inhibir la expresión de los RNAm de los diferentes transportadores de Glu expresados en los oligodendrocitos (GLAST, GLT-1 y EAAC-1).

Como se observa en la figura 14R panel A y B, estos siRNAs demostraron disminuir al menos un 70% la expresión a nivel proteico del transportador de Glu para el cual estaban diseñados sin afectar la expresión de otro EAAT. En el panel C se observa que al inhibir la expresión de Glast y de Glt-1 se elimino el efecto del Glu en la área de los procesos de los oligodendrocitos. Al comparar EAAC-1, el transportador de Glu menos expresado en estas células (Fig 11R), con GLAST o GLT-1, el siRNA para Eaac-1 solo atenuó parcialmente el efecto de Glu (siCtrl+Glu: 157±7%, siEaac1+Glu: 136±6%, P=0.007, ANOVA).

Estos resultados sugieren que incluso una ligera disminución en la expresión de los transportadores de Glu dependientes de Na^+ en los oligodendrocitos puede reducir el efecto del Glu en la maduración de los oligodendrocitos .

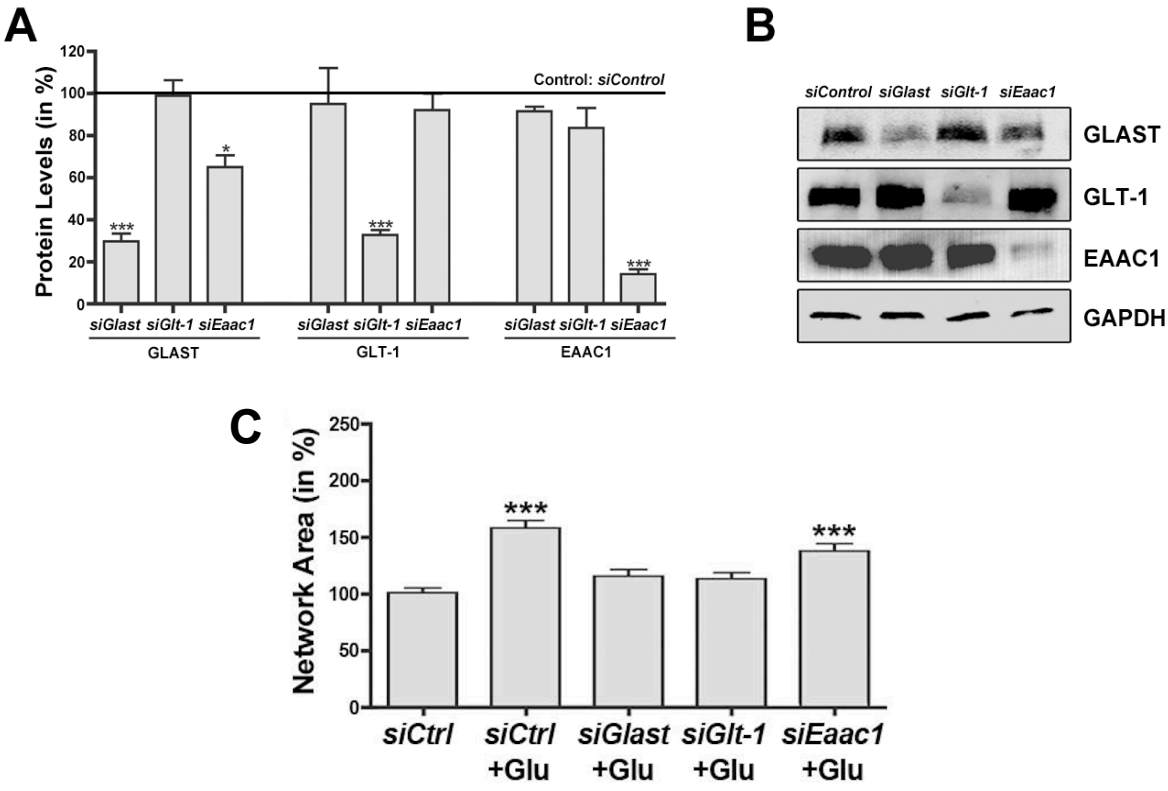

Figura 14R. Todos los transportadores de glutamato participan en la diferenciación de los oligodendrocitos.

A y B) Oligodendrocitos fueron transfectados con siRNAs específicos para cada transportador de Glu expresado en estas células, Glast, Glt-1 y Eaac1 como se describe en la sección de métodos y se observaron los niveles proteicos de los tres transportadores expresados. Para normalizar se utilizo GAPDH. En el panel A se observa una grafica de barras que representa un análisis cuantitativo de los niveles de proteína en porcentaje de los diferentes transportadores de Glu expresados en los oligodendrocitos obtenidos a partir de inmunodetecciones en fase solida como la mostrada en el panel B. C) Se observa una grafica de barras en la cual se muestran las áreas de los procesos de los oligodendrocitos después de un tratamiento con Glu 100 µM a oligodendrocitos previamente transfectados con siRNAs control o con los siRNAs específicos para los transportadores de Glu, según se indica en cada barra. Los datos representan el promedio ± el E.E. de 3 experimentos independientes (***P≤0.001, *P≤0.01 comparados con el control, ANOVA).

X. La activación de los transportadores de Glu incrementa los niveles intracelulares de calcio en los oligodendrocitos

Ya que sabemos que los transportadores de Glu promueven la maduración morfológica de los oligodendrocitos, nos preguntamos los eventos rio abajo involucrados en este proceso. Para esto decidimos enfocarnos en eventos mediados por Ca^{2+}, ya que demostramos que en CGB y CGM los transportadores de Glu pueden activar el modo reverso de NCX, por lo que decidimos medir los niveles de Ca2+ intracelular después de la activación de los transportadores de Glu por D-Aspartato.

Como se observa en la figura 15R el tratamiento con D-Aspartato 100µM incrementa los niveles intracelulares del calcio empezando por los procesos de los oligodendrocitos hasta difundir al cuerpo celular. El máximo efecto lo encontramos a 1 min 10 segundos, regresando a sus niveles basales a 1 min 30 segundos. El efecto fue dependiente de la dosis de D-Aspartato aplicada. Cuando se aplico el tratamiento de D-Aspartato en un medio sin Ca^{2+} extracelular se abatió el efecto, demostrando que el incremento en Ca^{2+} proviene de un influjo de Ca^{2+} y no de una liberación de fuentes de almacenamiento de Ca^{2+} intracelulares.

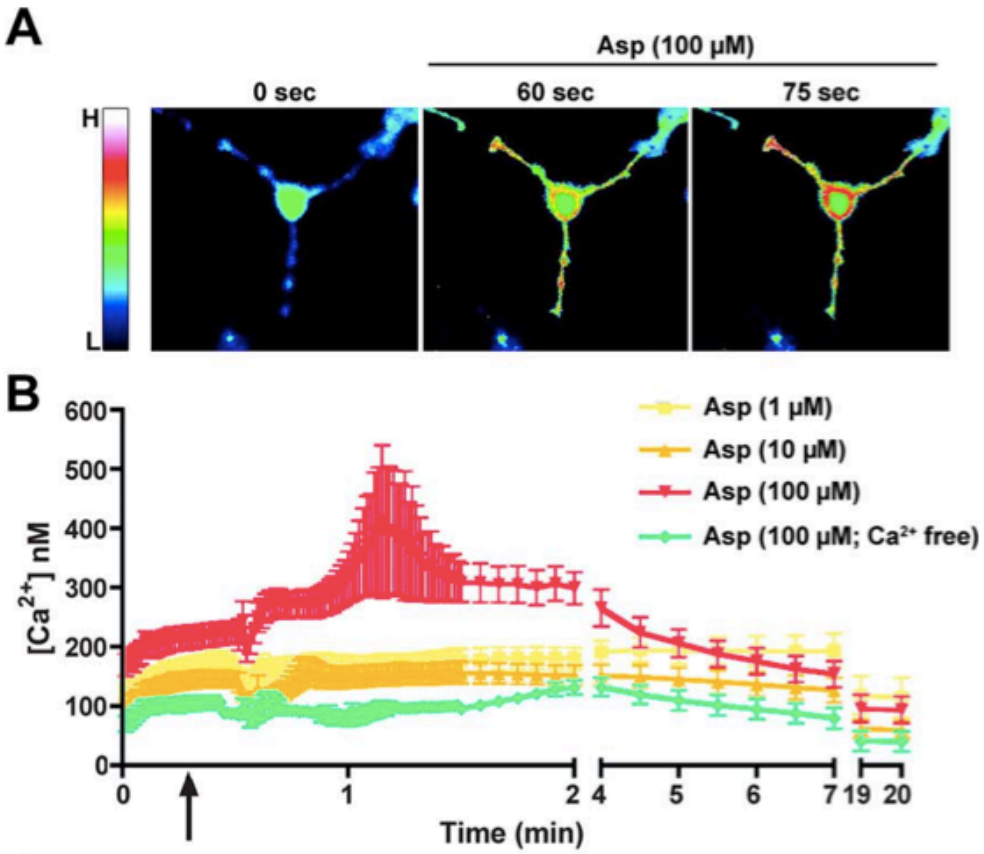

Figura 15R. La activación de los transportadores de Glutamato incrementa los niveles intracelulares de Calcio en los oligodendrocitos.

A) Se muestra una imagen de color representativa de mediciones de fluorescencia con fura-2AM después de que oligodendrocitos fueron tratados con D-Aspartato 100µM. La barra de la izquierda representa una escala de color relativo indicando niveles de calcio bajos (L) y altos (H). B) Curso temporal de los cambios en las concentraciones de calcio intracelular libre [Ca^{2+}] durante tratamientos con diferentes concentraciones de D-Aspartato según se indica en cada línea. El inicio del tratamiento se indica con la flecha. La grafica representa el promedio ± E.E. de al menos tres experimentos independientes realizado cada uno por triplicado.

Para corroborar la participación de los transportadores de Glu se midieron los niveles intracelulares de Ca^{2+} en oligodendrocitos tratados con D-Aspartato en presencia del bloqueador de los EAATs no transportable, TBOA 100 µM (Figura 16R panel A). TBOA bloquea completamente el efecto del D-Aspartato demostrando que los transportadores de Glu son los responsables del incremento en las concentraciones intracelulares de Ca^{2+}.

Para dilucidar la participación independiente de los transportadores de Glu en el influjo de Ca^{2+} se utilizaron inhibidores específicos para los dos transportadores que habían mostrado mayor contribución en la diferenciación morfológica de los oligodendrocitos (Figura 14R panel C), dihidrokainato (DHK) 100μM para inhibir a GLT-1 (Arriza, Fairman et al. 1994) y UCPH-101 10μM para bloquear a GLAST (Erichsen, Huynh et al. 2010, Abrahamsen, Schneider et al. 2013).

Como se muestra en la Figura 16R panel B el aumento del calcio intracelular dependiente de D-Aspartato fue bloqueado completamente con DHK, mientras que UCPH-101 disminuye el influjo de calcio solo parcialmente, sin embargo al medir la captura de [3H]-D-Aspartato en oligodendrocitos en presencia de los inhibidores específicos se observo que ambos transportadores GLAST y GLT-1, participan de manera equivalente en la captura de Glu, por lo que se puede especular que mas transportadores GLT-1 se encuentran acoplados al NCX favoreciendo el influjo de calcio.

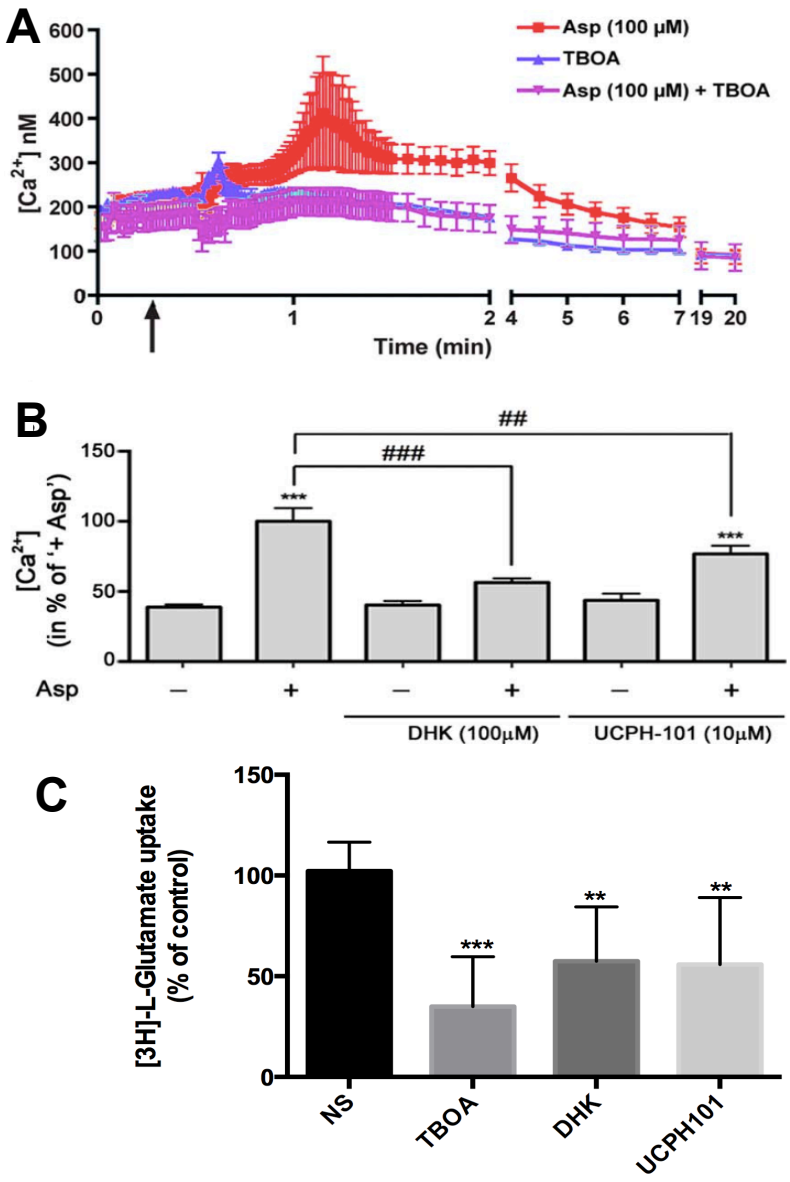

Figura 16R. Los transportadores de glu, GLAST y GLT-1 incrementan los niveles intracelulares de calcio en los oligodendrocitos.

A y B) Curso temporal de los cambios en las concentraciones intracelulares de Ca2+ libre durante los tratamientos indicados según la línea D-Aspartato 100µM, TBOA 100 µM o ambos (Panel A), el inicio del tratamiento se indica con la flecha; o en el panel B, D-Aspartato 100µM en presencia o ausencia de los bloqueadores de GLT-1, DHK y de GLAST, UCPH-101, el valor promedio para células tratadas con D-Aspartato (+Asp) se designo como 100% y los valores remanentes se calcularon basándose en este. Los tratamientos se indican en el eje de las X. La grafica representa el promedio ± E.E. de al menos tres experimentos independientes realizado cada uno por triplicado (***P≤0.001 al compararse con células control [no tratadas], ###P≤0.001 y ##P≤0.01 al compararse con células tratadas con D-Aspartato [+Asp], ANOVA) Panel C: Oligodendrocitos se pre-incubaron durante 30 min con los inhibidores no transportables de los EAATs, TBOA 100µM bloquea todos los EAATs, DHK 100µM bloquea GLT-1, y UCPH-101 10µM bloquea GLAST. Después se realizo la captura de [3H]-D- Aspartato por 30 min. Los datos están expresados como el promedio ± E.E. de al menos 3 experimentos independientes, realizados cada uno por cuadriplicado; se realizo un t-test de Student's con una comparación múltiple de Dunnett para analizar los datos (***P<0.001, **P<0.05)

XI. CaMKIIβ participa en la diferenciación morfológica de los oligodendrocitos inducida por Glu

Los resultados anteriores demuestran que la activación de los transportadores de Glu dependientes de Na^+ promueven un incremento transitorio en los niveles intracelulares de Ca^{2+} a través de un influjo de Ca^{2+} desde el ambiente extracelular. Recientemente se demostró que la proteína CaMKIIβ, una proteína responsable de censar el Ca^{2+}, regula la maduración de los oligodendrocitos y la mielinizacion del SNC a través de su dominio de unión/estabilización del citoesqueleto de actina (Waggener, Dupree et al. 2013). Por lo decidimos analizar la posibilidad de que CaMKIIβ este involucrada en los efectos de la activación de los transportadores de Glu que encontramos. Por lo que analizamos el efecto de pre-incubar oligodendrocitos con KN-93 un inhibidor de CaMKIIβ permeable a la membrana plasmática (Sumi, Kiuchi et al. 1991, Lin and Redmond 2008) y con KN-92 un derivado de KN-93 inactivo. Como se observa en la figura 17R la pre-incubación con KN-93 inhibe el efecto de Glu en la diferenciación morfológica de los oligodendrocitos, mientras que su forma inactiva no modifica el efecto del Glu.

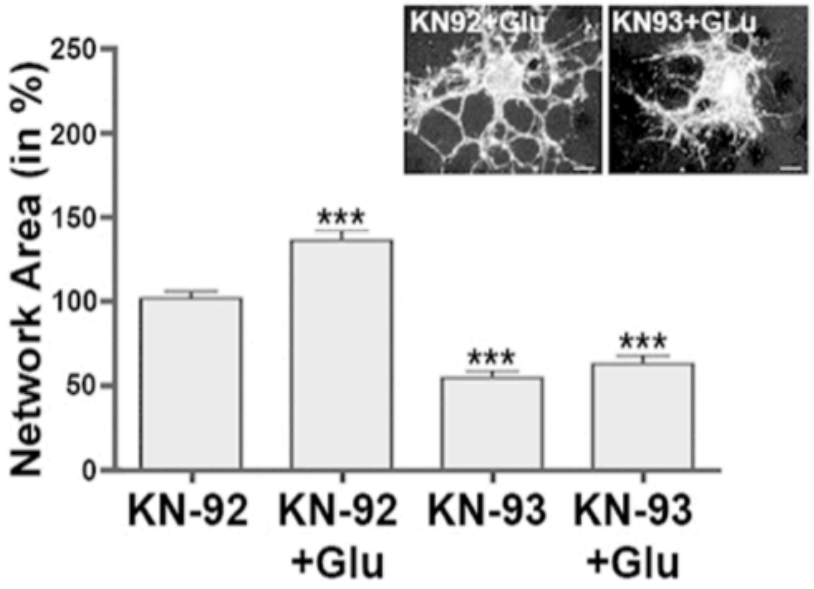

Figura 17R. CaMKIIβ participa en la diferenciación morfológica de los oligodendrocitos inducida por Glu.

Grafica de barras que muestra un análisis cuantitativo del área de los procesos de los oligodendrocitos. Células fueron pre-tratadas con el inhibidor farmacológico KN-93 o su derivado inactivo KN-92 y después incubados en presencia (+Glu) o ausencia de Glu 100μM. Los valores promedio para las células control (pre-tratadas con KN-92 e incubadas en ausencia de Glu) se asignaron como el 100% y los valores experimentales en las otras condiciones se determinaron tomando en cuenta el 100%. Los datos representan el promedio ± E.E. (***P≤0.001, ANOVA). El inserto muestra imágenes representativas de oligodendrocitos tratados con KN-92 con Glu (izquierda) o con KN-93 y Glu (derecha) e inmunoteñidos con el sobrenadante del hibridoma O4. Barra de Escala: 5 μm.

XII. La activación de los transportadores de Glu promueve la fosforilación de CaMKIIβ

Después decidimos analizar la activación de CaMKIIβ dependiente de Glu, para lo cual analizamos la fosforilación de su dominio regulatorio de autofosforilación $T^{286/7}$ y en el dominio de unión/estabilización a actina S^{371} (Okamoto, Narayanan et al. 2007, Lin and Redmond 2008).

Como se observa en la figura 18R, el tratamiento con Glu aumenta significativamente la fosforilación de CaMKIIβ en el residuo S^{371}. El efecto de Glu fue dependiente del tiempo y transitoria, siendo significativa a los 30 min y hasta las 4 horas, mientras que no se encontró un aumento en la fosforilación en el residuo $T^{286/7}$ después de 15-60 min de tratamiento con Glu, tampoco se observaron cambios en los niveles totales de CaMKIIβ.

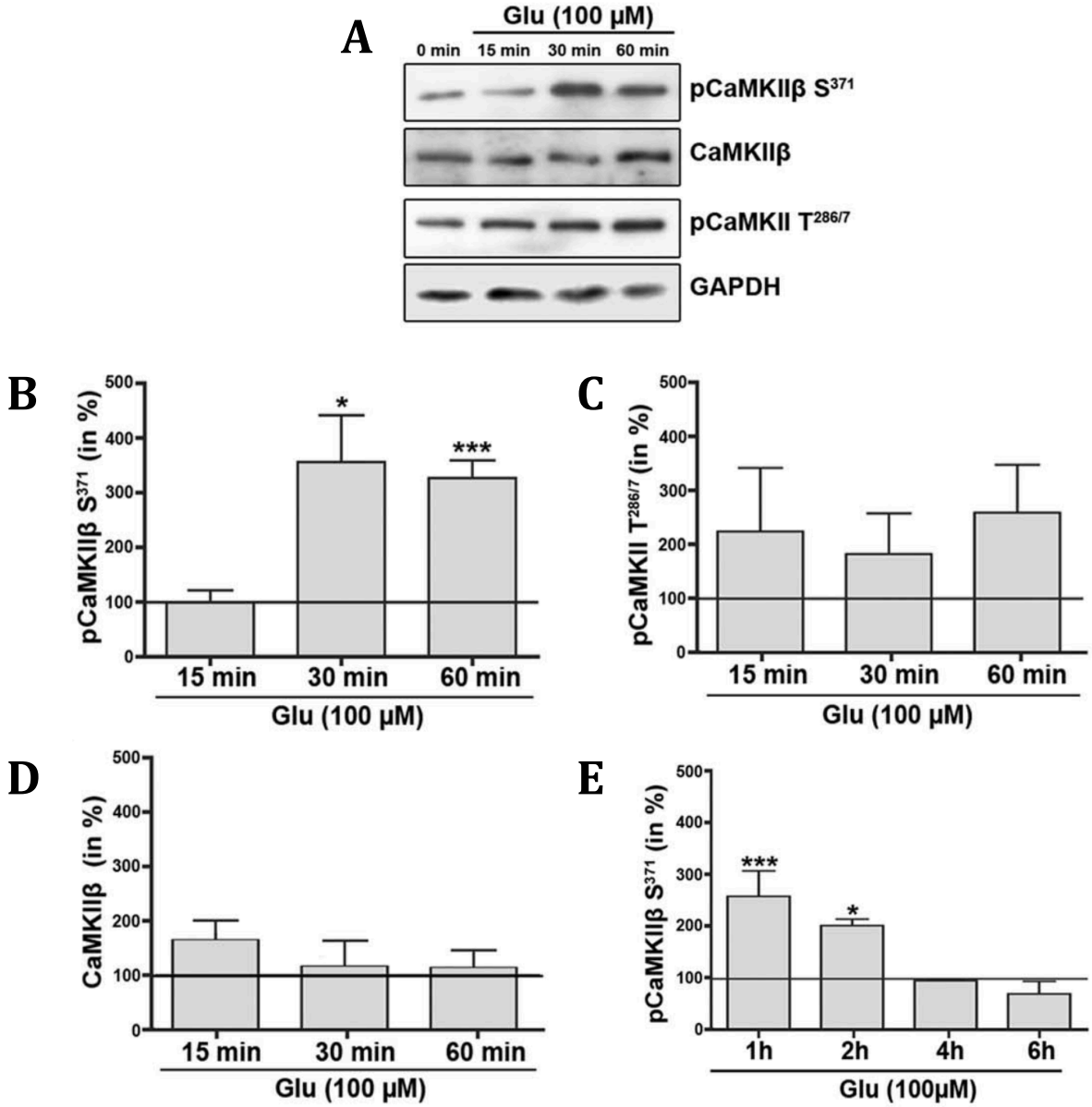

Figura 18R. La activación de los transportadores de Glu promueve la fosforilación de CaMKIIβ Ser^{371}.

A) Se muestra una autoradiografía representativa de la fosforilación de CaMKIIβ (pCaMKIIβ S371, pCaMKIIβ T286/7) o de los niveles totales de CaMKIIβ. Los niveles proteicos de GAPDH se utilizaron para normalizar. B-E) Graficas de barras en los que se muestran los niveles de CaMKIIβ fosforilado en S^{371} (B y E), fosforilado en T$^{286/7}$ (C) o los niveles totales de CaMKIIβ (D). Los valores promedio de los oligodendrocitos no tratados se fijaron en 100% (línea horizontal) y se utilizaron para calcular el porcentaje de los oligodendrocitos tratados. Los datos representan el promedio ± E.E. de al menos tres experimentos independientes (***P≤0.001, *P≤0.05 al compararse con el control, ANOVA).

La fosforilación de CaMKIIβ en el residuo S^{371} inducida por Glu fue bloqueada con TBOA (Figura 19R Panel A). Para analizar la contribución individual de cada transportador de Glu en el aumento de los niveles de fosforilación de CaMKIIβ en S^{371}, oligodendrocitos se transfectaron con siRNAs específicos para Glast, Glt-1 o Eaac1, como se observo con los siRNAs en la morfología de los oligodendrocitos (Figura 14R Panel C), el silenciamiento de Glast y de Glt-1 elimina el efecto del Glu en la fosforilación de CaMKIIβ S^{371}, mientras que el silenciamiento de Eaac1 tiene un efecto menos pronunciado (Figura 19R Panel B).

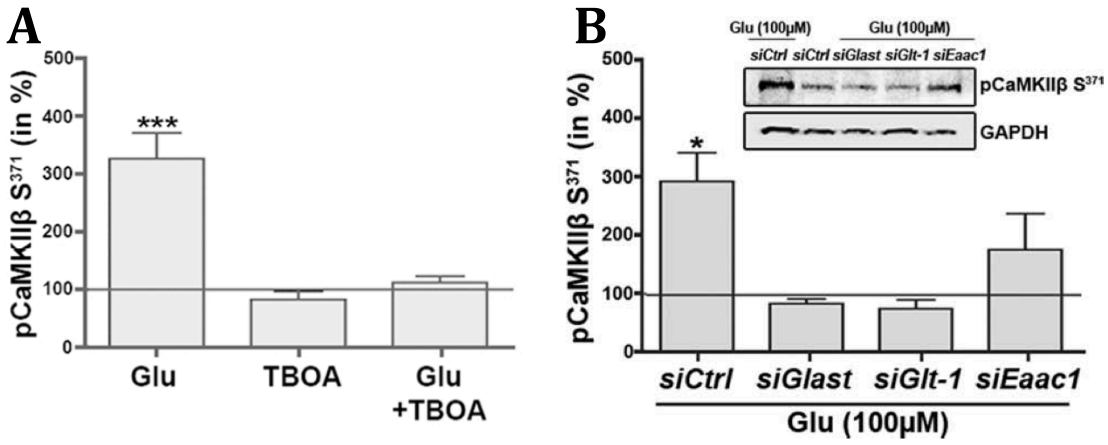

Figura 19R. La activación de GLAST y GLT-1 promueve la fosforilación de CaMKIIβ Ser^{371}.

Graficas de barras en los que se muestran los niveles de CaMKIIβ fosforilado en S^{371} tratados con Glu en presencia o ausencia de TBOA 100μM (Panel A) o de los siRNAs específicos para Glast, Glt-1 y Eaac1 (Panel B). Los valores promedio de los oligodendrocitos no tratados se fijaron en 100% (línea horizontal) y se utilizaron para calcular el porcentaje de los oligodendrocitos tratados. En el inserto del panel B se muestra una autoradiografía representativa en el que se muestra la fosforilación de CaMKIIβ S371 una vez que oligodendrocitos transfectados con siRNAs fueron tratados con Glu. Los niveles de GAPDH se utilizaron para normalizar. Los datos representan el promedio ± E.E. de al menos tres experimentos independientes (***P≤0.001, *P≤0.05 al compararse con el control, ANOVA).

XIII. La fosforilación de CaMKIIβ Ser^{371} regula la asociación de CaMKIIβ con los filamentos de actina

Nuestros datos demuestran que el Glu activa a los transportadores de Glu expresados en los oligodendrocitos, los cuales median un incremento transitorio de Ca^{2+} intracelular, promueven una fosforilación transitoria en el dominio de unión/estabilización de actina de CaMKIIβ y provocando la maduración morfológica de los oligodendrocitos. Nuestros datos arrojan la posibilidad de que la fosforilación de CaMKIIβ mediada por los transportadores de Glu afecte los procesos de los oligodendrocitos al cambiar la asociación de CaMKIIβ con los filamentos de actina. Para probar esta hipótesis, utilizamos proteínas de fusión de CaMKIIβ mutantes acopladas a la proteína verde fluorescente (GFP), las formas mutantes de CaMKIIβ se generaron al cambiar todos los residuos de serinas/treoninas en el dominio de unión/estabilización a actina por Alaninas para mimetizar un estado no fosforilable (eGFP-$CaMKII\beta^{all\ A}$) o cambiadas por Aspartato para mimetizar un estado fosforilado (eGFP-$CaMKII\beta^{all\ D}$), además de una proteína de fusión de eGFP con la proteína CaMKIIβ wild type (eGFP-$CaMKII\beta^{WT}$) y de una CaMKIIβ en la que la lisina del residuo 43 fue cambiada por arginina, esta mutación afecta la unión de ATP por lo que inactiva la actividad cinasa catalítica de CaMKIIβ pero no su unión a actina (Okamoto et al., 2007). Para validad el mecanismo propuesto en el cual la fosforilación de CaMKIIβ S^{371} regula su interacción con actina, realizamos ensayos de nucleofeccion en una línea celular de oligodendrocitos llamada CIMO. Como se muestra en la figura 20R, la forma no fosforilable eGFP-$CaMKII\beta^{all\ A}$ y eGFP-$CaMKII\beta^{WT}$ colocalizan con los filamentos de actina, mientras que la forma fosforilable eGFP-$CaMKII\beta^{all\ D}$ mostro una colocalizacion muy baja con los filamentos de actina similar al control eGFP, con una distribución difusa a través de todo el citoplasma.

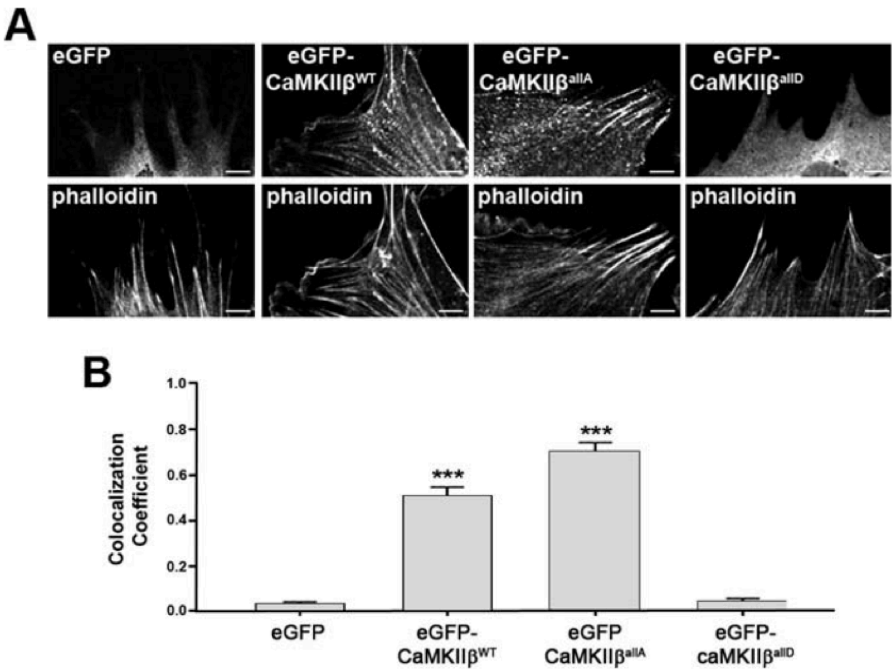

Figura 20R. La fosforilación de CaMKIIβ Ser^{371} regula la asociación de CaMKII con los filamentos de actina.

A) Se muestra una imagen representativa de células CIMO nucleotransfectadas con plásmidos que codifican para las proteínas de fusión eGFP – CaMKIIβ (Wild type o las formas mutantes según se indica) y teñidas con faloidina para visualizar los filamentos de actina. Barras de escala: 5μM. B) Grafica de barras en la que se muestran los niveles de localización de las proteínas de fusión GFP – CaMKIIβ y faloidina. Los datos representan el promedio ± E.E. de al menos tres experimentos independientes (***P≤0.001 al compararse con el control eGFP, ANOVA).

Estos resultados demuestran que la forma no fosforilada de CaMKIIβ se une a los filamentos de actina, mientras que la fosforilación de CaMKIIβ en su dominio de unión/estabilización a actina desestabiliza esta interacción, una vez conociendo esto, decidimos evaluar el papel de la fosforilación de CaMKIIβ en su dominio de unión/estabilización a actina en el efecto del Glu, con este fin se evaluó el efecto de la sobreexpresión de las CaMKIIβ mutantes en la área de los procesos de los oligodendrocitos. Como se observa en la figura 21R la expresión de la CaMKIIβ no fosforilable (eGFP-CaMKIIβ^{AllA}) o de la que mimetiza el estado fosforilado (eGFP- CaMKIIβ^{AllD}) bloquean el efecto del Glu en la maduración morfológica de los oligodendrocitos, lo cual no se observo al sobreexpresar la forma silvestre (eGFP- CaMKIIβ^{WT}). CaMKIIβ que mimetiza el estado fosforilado, no solo inhibe el efecto del Glu, sino que además atenúa la diferenciación morfológica basal de los oligodendrocitos.

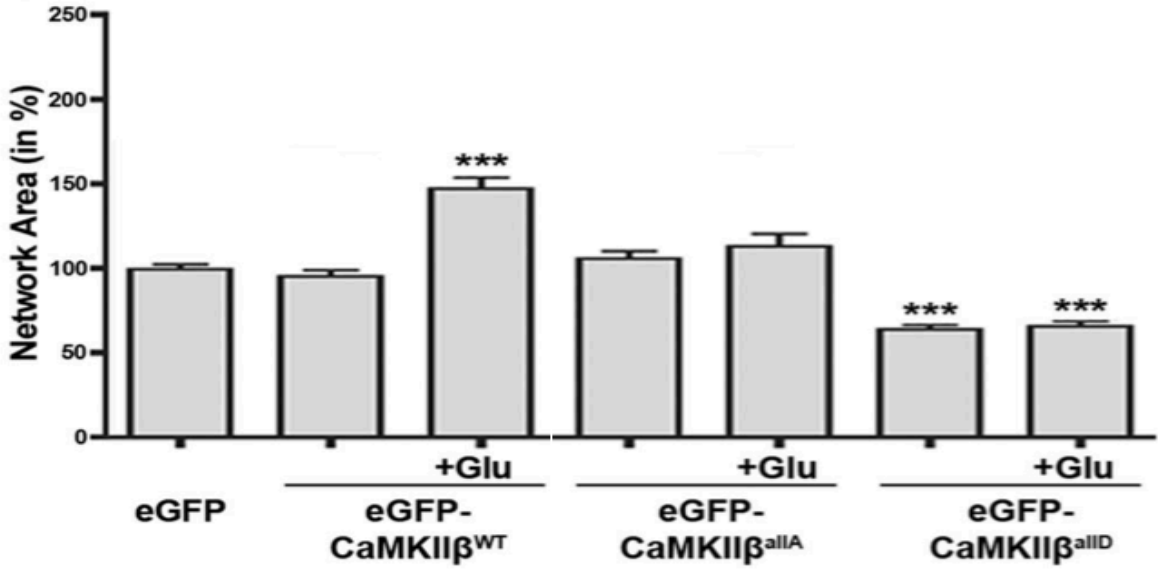

Figura 21R. La fosforilación de CaMKIIβ Ser^{371} regula la diferenciación de los oligodendrocitos por Glu.

Grafica de barras en la que se muestra un análisis cuantitativo del área de los procesos de los oligodendrocitos. Las células fueron nucleofectadas según se indica en cada barra y después incubadas en presencia o ausencia de Glu 100μM. Los valores de células control (nucleofectadas con un plasmido que codifica para eGFP e incubadas en ausencia de Glu) se fijaron como 100% y a partir de este valor se calcularon los datos con los valores experimentales de las otras nucleofecciones. Los datos representan el promedio ± E.E. de al menos tres experimentos independientes (***P≤0.001 al compararse con el control, ANOVA).

Los resultados anteriores sugieren que es necesario una fosforilación transitoria del dominio de unión/estabilización a actina de CaMKIIβ, para llevar a un desacople transitorio de CaMKIIβ con los filamentos de actina para permitir la maduración de los aspectos morfológicos de los oligodendrocitos inducida por la activación de los transportadores de Glu. Con los resultados anteriores proponemos el siguiente modelo:

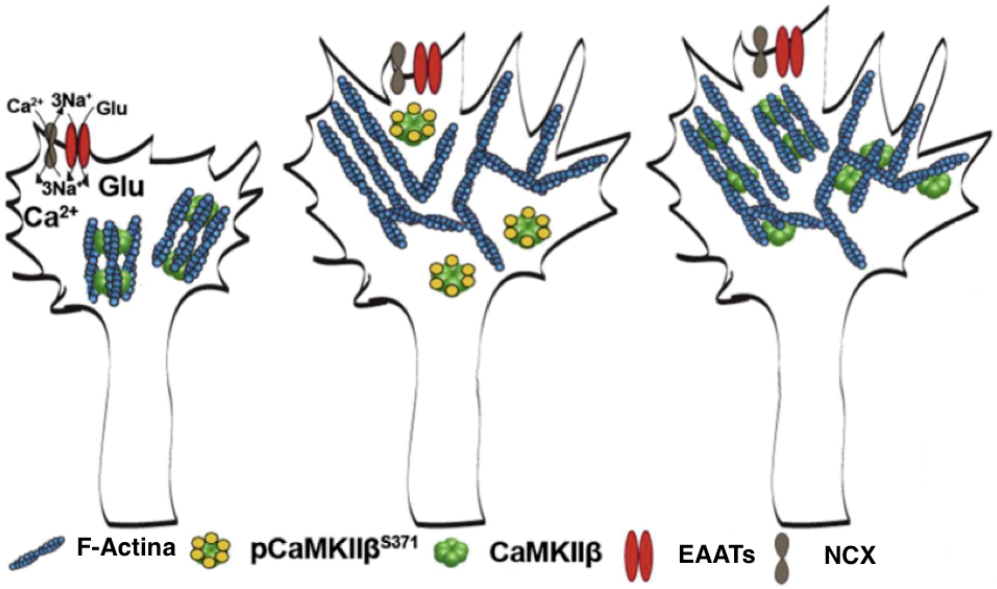

Figura 22R. Modelo de la diferenciación morfológica de los oligodendrocitos inducida por la activación de los EAATs.

En condiciones basales, CaMKIIβ se encuentra asociada al citoesqueleto de actina. Cuando Glu es liberado de, por ejemplo, axones no mielinizados (Etxeberria A et al., 2010, Kukley M et al., 2007) activa a los transportadores de Glu dependientes de Na^+ presentes en los oligodendrocitos, el transporte de Glu con lleva un incremento en las concentraciones intracelulares de Na^+ que activan el modo reverso del NCX, teniendo como resultado un incremento en el Ca^{2+} intracelular.

Este incremento en el Ca^{2+} intracelular lleva a la fosforilación del dominio de unión/estabilización de actina de CaMKIIβ (incluyendo el residuo S^{371}), esta fosforilación inactiva la unión de CaMKIIβ a los filamentos de actina por lo que se separa del citoesqueleto de actina. Esta inactivación transitoria de la unión de CaMKIIβ a actina abre una ventana temporal durante la cual ocurren eventos de remodelamiento del citoesqueleto de actina y se favorece la polimerización de actina (Okamoto, Narayanan et al. 2007). Esta fase dinámica es seguida por una fase de estabilización del citoesqueleto, activada por la unión de CaMKIIβ a los filamentos de actina debido a su defosforilación. Por lo tanto, los ciclos de activación-inactivación de la actividad de unión a actina de CaMKIIβ promueven la maduración morfológica de los oligodendrocitos.

XIV. En esclerosis múltiple hay una desregulación del dominio de unión/estabilización a actina de CaMKIIβ

En la enfermedad de esclerosis múltiple (MS), la principal enfermedad desmielinizante humana, la diferenciación de los oligodendrocitos se encuentra bloqueada, lo cual sea considerado como una de las principales causas de una ineficiente remielinizacion y reparación, debido a los resultados MS múltiple se ha perdido el balance entre los ciclos de activación-inactivación del dominio de unión a actina de CaMKIIβ.

Para corroborar esta hipótesis evaluamos el estado de fosforilación del dominio de unión/estabilización a actina de CaMKIIβ en muestras de individuos fallecidos que padecían la enfermedad de MS.

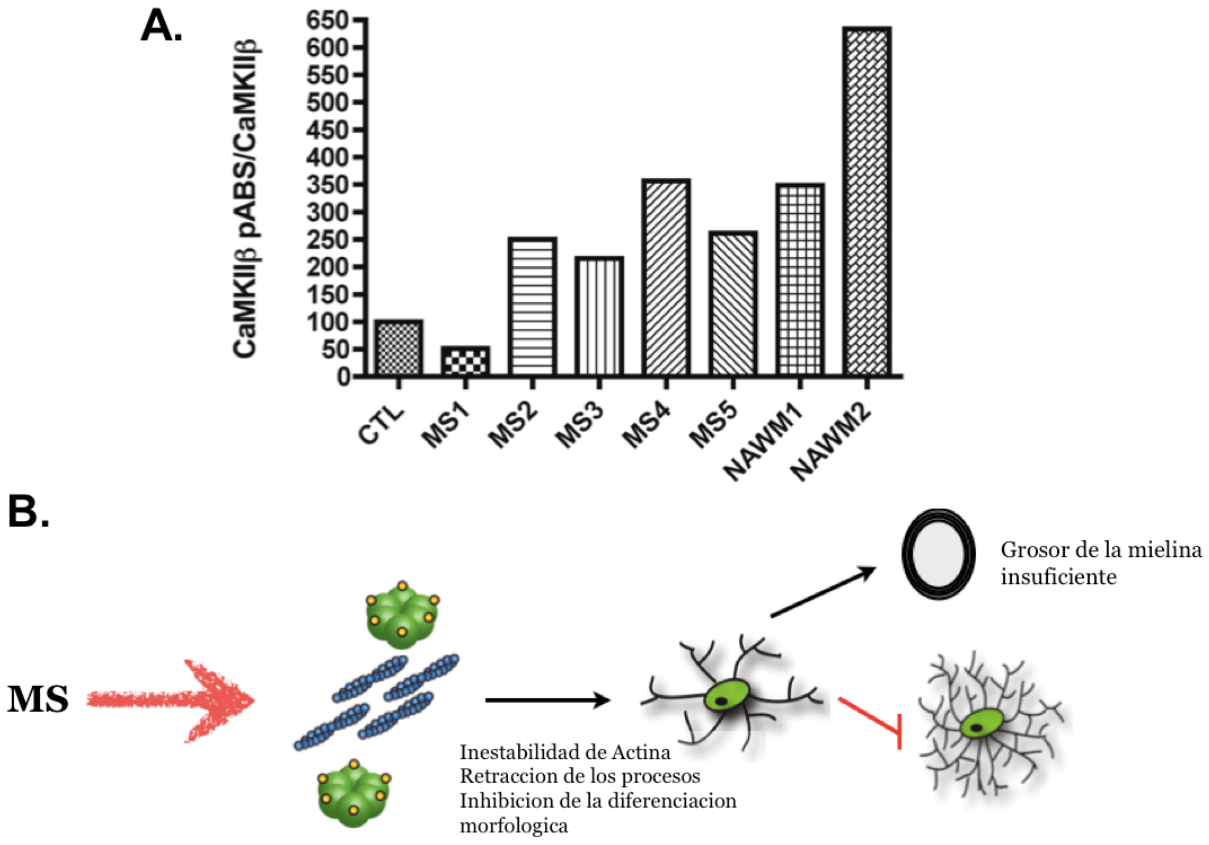

Figura 23R. En esclerosis múltiple hay una desregulación del dominio de unión/estabilización a actina de CaMKIIβ.

A) Se analizaron los niveles de fosforilación del dominio de unión/estabilización a actina de la proteína CaMKIIβ en muestras obtenidas a partir de individuos fallecidos que presentaban la enfermedad de MS (MS1-5 y NAWM1 y 2) y sin MS (CTL). Los niveles totales de CaMKIIβ se utilizaron para normalizar. B) Modelo de la participación de CaMKIIβ de oligodendrocitos en MS.

En la figura 23R panel A observamos que las muestras provenientes de individuos con MS presentan un incremento en la fosforilación de CaMKIIβ en su dominio de unión/ estabilización a actina, lo cual sugiere que en la enfermedad de MS la actividad de unión a actina de CaMKIIβ se encuentra en un estado inactivo, esto repercute en una inestabilidad del citoesqueleto de actina, en la retracción de los procesos de los oligodendrocitos, como se observo en la figura 21R con eGFP-CaMKIIβ^{AllD}, y en la inhibición de la diferenciación morfológica de los oligodendrocitos, por lo tanto en MS hay una disminución en el grosor de la mielina y se encuentran oligodendrocitos inmaduros (Fig 23R Panel B).

DISCUSION

El glutamato es el principal neurotransmisor excitador del SNC, este neurotransmisor transmite una amplia variedad de cascadas de señalización, por mucho tiempo se creyó que el glutamato únicamente ejercía sus funciones a través de la activación de sus receptores ionotrópicos y metabotrópicos, sin embargo gracias a que los antagonistas de los receptores glutamatérgicos no eran capaces de bloquear todos los efectos inducidos por glutamato (Duan, Anderson et al. 1999, Gonzalez and Ortega 2000, Abe and Saito 2001) se empezó a poner mas detalle en la actividad de los transportadores de glutamato y se empezó a sugerir que estos podría actuar como receptores al inducir cascadas de señalización rio abajo.

El trabajo detallado aquí demostró que los transportadores no solo tienen capacidad de señalizar, sino que además su señalización puede repercutir en procesos tan importantes para la célula como traducción y transcripción.

Regular el repertorio de proteínas de una célula es un mecanismo fundamental para darle una identidad propia a cada célula dependiendo su localización, función y etapa, por lo cual es de suma importancia mantener la expresión de proteínas bien regulado. Los mecanismos de regulación los encontramos en la transcripción y en la traducción. Nuestros resultados demuestran que los transportadores de glutamato son capaces de regular estos dos procesos en células de glía radial (CGB y CGM). A nivel traduccional, se demostró que los transportadores de glutamato activan el modo reverso del NCX permitiendo un influjo de calcio y la consecuente activación de la vía de PI3K/Akt/mTOR, esta vía repercute en la activación de $p70^{S6K}$ así como en la fosforilación de 4EBP-1, siendo ambas proteínas reguladores positivos de la síntesis de proteínas. A nivel transcripcional, se observo que el transporte de glutamato mediante GLAST activa el modo reverso del NCX activando a CaMKII, esta cinasa activa la vía de Raf/ERK/$p90^{RSK1}$, la proteína $p90^{RSK}$ viaja entonces al núcleo en donde fosforila al factor transcripcional CREB, permitiendo la transcripción de

sus genes blancos, entre los que se encuentra c-fos, el factor transcripcional AP-1, formado por c-fos y c-jun, puede entonces regular la transcripción de sus genes blanco (Ver Figura 8R).

Además de regular el repertorio de proteínas también es importante regular la morfología de las células, ya que gran parte de la función de las células depende de su morfología. Nuestros resultados demostraron que los transportadores de glutamato regulan la morfológica de los oligodendrocitos, al transportarse el glutamato por medio de GLAST y GLT-1 se incrementan las concentraciones intracelulares de Na^+ lo cual activa el modo reverso del NCX, lo que conlleva un influjo de Ca^{2+}, el Ca^{2+} se une a CaMKIIβ e induce su auto-fosforilación en el domino de unión/estabilización a actina, al fosforilarse esta cinasa se separa de los filamentos de actina permitiendo el re-arreglo del citoesqueleto de actina y el remodelamiento morfológico de los oligodendrocitos (Ver Figura 22R).

Como se ha mencionado, es necesario que los transportadores de glutamato activen el modo reverso del NCX para que se activen cascadas de señalización rio abajo, como se observa en las figuras 9R y 10R KB-R7943, un inhibidor especifico del modo reverso del NCX disminuye significativamente la captura de glutamato, lo cual sugiere fuertemente un acople funcional entre los transportadores de glutamato y el NCX. Sin embargo, sabemos que los transportadores de glutamato se encuentran acoplados a la ATPasa de Na^+/K^+, y que el Na^+ (Gegelashvili, Rodriguez-Kern et al. 2007, Rose, Koo et al. 2009, Bauer, Jackson et al. 2012) transportado junto el glutamato puede ser exportado por la acción de esta bomba, con lo cual uno se podría preguntar que oportunidad tiene el NCX de encontrar concentraciones elevadas de Na^+ para activar su modo reverso?, esto es posible tomando en cuenta dos puntos, el primero es que se ha reportado un acople funcional entre los transportadores de glutamato y el NCX (Rojas, Colina et al. 2007, Martinez-Lozada, Hernandez-Kelly et al. 2011, Magi, Lariccia et al. 2012, Maria Lopez-Colome, Martinez-Lozada et al. 2012), así como una interacción física entre ellos (Magi, Lariccia et al. 2012, Magi, Arcangeli et al. 2013), esto permite que el influjo

de Na^+ mediado por los EAATs sea rápidamente censado por los NCX; segundo, las moléculas de EAATs son muy abundantes, por ejemplo, sea reportado que la concentración de GLT1 en el hipocampo es de 12,000 moléculas por μm^3 de tejido, además se ha estimado que GLT-1 abarca el 2% de la proteína total del cerebro, mientras que en las CGB la densidad de GLAST es de 18,000 moléculas por μm^3 de tejido (Danbolt 2001). Además se ha demostrado que el silenciamiento del NCX3 detiene la diferenciación de los oligodendrocitos (Boscia, D'Avanzo et al. 2012), lo cual favorece el modelo de la diferenciación de los oligodendrocitos mediada por los transportadores de glutamato (Figura 22R).

Se ha observado una conexión entre una remoción deficiente de glutamato con isquemia, esclerosis lateral amiotrófica, Alzheimer, epilepsia, intoxicaciones, encefalopatía hepática, lesión cerebral traumática, entre otras (Danbolt 2001), sin embargo nuestros resultados sugieren que en los desordenes neurológicos y psiquiátricos que se ha observado un mal funcionamiento de los transportadores de glutamato pueden estar ocasionados no únicamente por la falta de remoción del glutamato, sino que además por la inactivación de las vías de señalización rio abajo de los transportadores glutamatérgicos. En esclerosis múltiple, por ejemplo, se ha considerado que una de las principales causas de deficiente mielinización y reparación de la red de mielina, es el bloqueo de la diferenciación de los oligodendrocitos (Chan, Lin et al. 1987, Kuhlmann, Miron et al. 2008, Fancy, Kotter et al. 2010, Kremer, Aktas et al. 2011), y como nuestros resultados mostraron, la diferenciación de los oligodendrocitos es activada por las vías de señalización rio abajo de la captura del glutamato.

Cual podría ser la relevancia de una cascada de señalización activada por transportadores de glutamato en células que expresan receptores glutamatérgicos funcionales? Aunque al momento no tenemos una respuesta precisa a esa pregunta, podemos sugerir tres explicaciones: primera, no todas las señales intracelulares activadas por Glutamato son desencadenadas por la actividad de los receptores glutamatérgicos, por ejemplo, en rebanadas de cerebelo de ratones se ha demostrado que

Glutamato induce una corriente entrante de Na^+ la cual es insensible a CNQX, pero inhibida por TBOA (Kirischuk, Kettenmann et al. 2007). Segunda, la señalización mediada por los transportadores de glutamato tiene cinéticas de inactivación mas lentas que las de los receptores, esto sugiere que esta relacionadas a respuestas bioquímicas sostenidas involucradas en la expresión de proteínas que participan en el acoplamiento neurona/glía, como por ejemplo de la ATPasa de Na+/K+ que permite que las células gliales remuevan eficientemente el glutamato del espacio sináptico, la enzima glutamina sintetasa, y los transportadores de aminoácidos neutros (SNATs) o los transportadores de monocarboxilatos que permiten la lanzadera de lactato astrocito/neurona (Pellerin, Bouzier-Sore et al. 2007). La tercera posibilidad, es que la distribución diferencial dependiente de actividad de los transportadores y receptores glutamatérgicos en dominios membranales resistentes a detergentes (balsas lipídicas) y la inclusión o no de compañeros de señalización selectivos constituya la base molecular de la existencia de transducción de señales mediada por los transportadores (Butchbach, Tian et al. 2004, Gonzalez, Susarla et al. 2007, Hou, Huang et al. 2008).

Tradicionalmente las células gliales han sido rezagadas a un papel de soporte, como elementos pasivos, sin embargo lentamente ha sido aceptado que las células gliales participan activamente en la transmisión excitadora, por ejemplo, a través del ciclo glutamato/glutamina (Shank and Campbell 1984), además de que las neuronas presentan una dependencia energética de las células gliales fenómeno explicado por la lanzadera lactato astrocito/neurona (Pellerin, Bouzier-Sore et al. 2007); nuestros resultados arrojan nueva evidencia de la importancia de las células gliales en la neurotransmisión glutamatérgica, ya que recordemos que el 80% de la remoción del glutamato es llevado a cabo en las células gliales, este proceso además de capturar el glutamato para prevenir procesos de excitotoxicidad y de reciclar el neurotransmisor, también activa cascadas de señalización que permiten regular la expresión de proteínas en las células gliales para hacer mas eficiente la neurotransmisión glutamatérgica.

En resumen, demostramos que el transporte de glutamato en CGB y CGM esta vinculado a la activación de cascadas de señalización que regulan la expresión de genes, mientras que en oligodendrocitos esta acoplado a la regulación del citoesqueleto de actina y por consiguiente de la maduración morfológica de los oligodendrocitos. En la siguiente figura se muestran un resumen de nuestros resultados.

GLIA RADIAL (CGB y CGM)

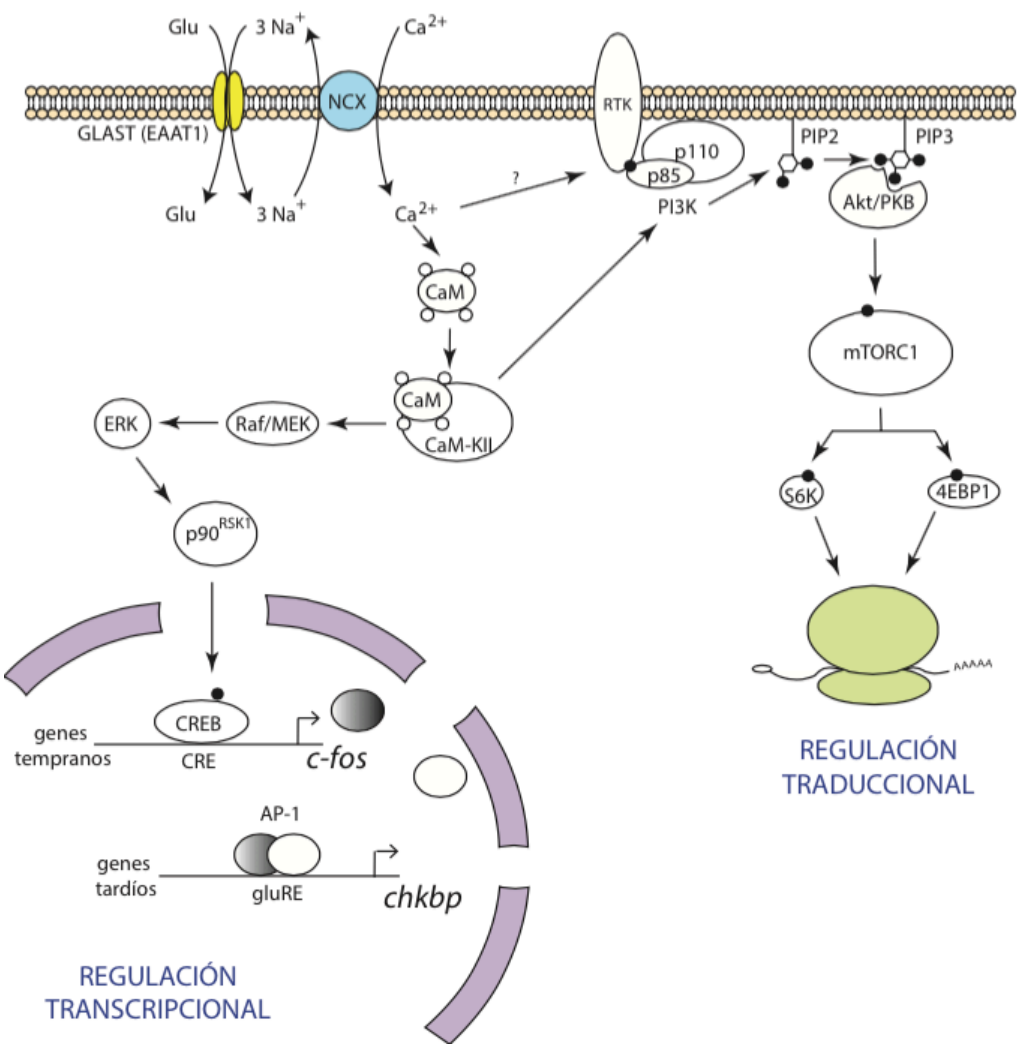

REGULACIÓN TRANSCRIPCIONAL

REGULACIÓN TRADUCCIONAL

OLIGODENDROCITOS

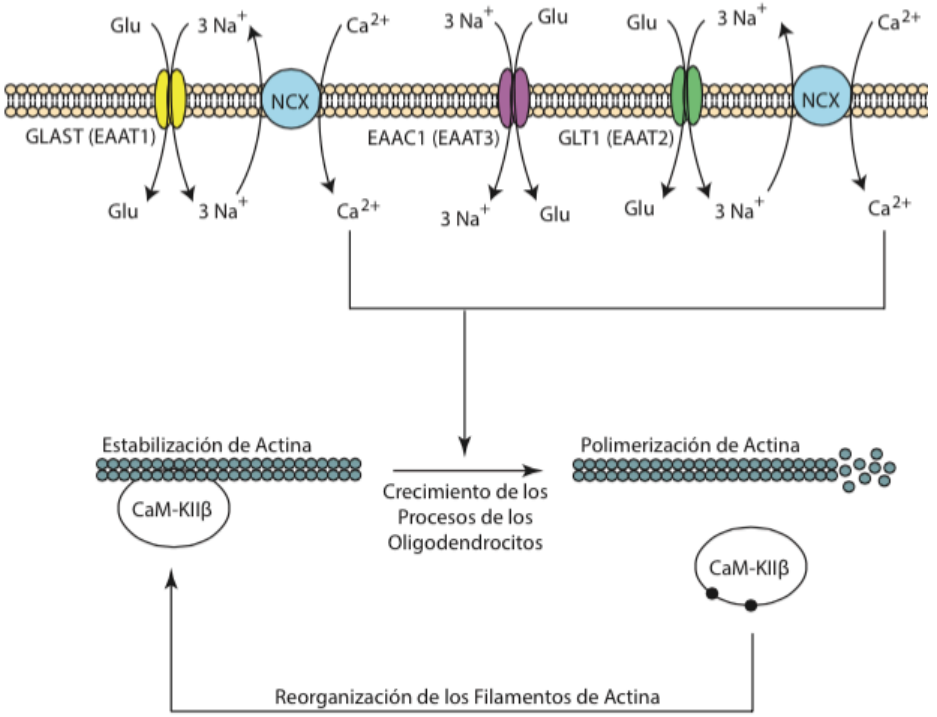

REGULACIÓN MORFOLÓGICA

CONCLUSIONES

Utilizando como modelo las células gliales de Bergmann y las células gliales de Müller, hemos sido capaces de observar la activación de mTOR, regulador clave de la traducción, mediada por la actividad de captura del Glutamato. Además en este mismo escenario, también se regula el repertorio de proteínas de las células de glía radial a nivel transcripcional, al activarse la vía de MAPK/RSK/ CREB/AP-1.

Por otro lado al utilizar como modelo oligodendrocitos fuimos capaces de demostrar que la remoción del glutamato, mediada por los transportadores GLAST y GLT-1, induce la maduración morfológica de los oligodendrocitos, al fosforilarse el dominio de unión/estabilización a actina de CaMKIIβ.

Estos resultados demuestran que el Glutamato además de ejercer sus funciones a través de la activación de sus receptores, también induce la activación de cascadas de señalización mediante los trasportadores de Glutamato.

Nuestros resultados además recalcan la importancia de las células gliales en la neurotransmisión glutamatérgica, ya que la gran mayoría de la remoción del Glutamato es llevada a cabo por estas células.

BIBLIOGRAFÍA

Abe, K. and H. Saito (2001). "Possible linkage between glutamate transporter and mitogen-activated protein kinase cascade in cultured rat cortical astrocytes." J Neurochem **76**(1): 217-223.

Abrahamsen, B., N. Schneider, M. N. Erichsen, T. H. Huynh, C. Fahlke, L. Bunch and A. A. Jensen (2013). "Allosteric modulation of an excitatory amino acid transporter: the subtype-selective inhibitor UCPH-101 exerts sustained inhibition of EAAT1 through an intramonomeric site in the trimerization domain." J Neurosci **33**(3): 1068-1087.

Arriza, J. L., W. A. Fairman, J. I. Wadiche, G. H. Murdoch, M. P. Kavanaugh and S. G. Amara (1994). "Functional comparisons of three glutamate transporter subtypes cloned from human motor cortex." J Neurosci **14**(9): 5559-5569.

Attwell, D. and S. B. Laughlin (2001). "An energy budget for signaling in the grey matter of the brain." J Cereb Blood Flow Metab **21**(10): 1133-1145.

Avossa, D. and S. E. Pfeiffer (1993). "Transient reversion of O4+ GalC-oligodendrocyte progenitor development in response to the phorbol ester TPA." J Neurosci Res **34**(1): 113-128.

Balcar, V. J. and G. A. Johnston (1972). "The structural specificity of the high affinity uptake of L-glutamate and L-aspartate by rat brain slices." J Neurochem **19**(11): 2657-2666.

Balkrishna, S., A. Broer, A. Kingsland and S. Broer (2010). "Rapid downregulation of the rat glutamine transporter SNAT3 by a caveolin-dependent trafficking mechanism in Xenopus laevis oocytes." Am J Physiol Cell Physiol **299**(5): C1047-1057.

Bansal, R. and S. E. Pfeiffer (1992). "Novel stage in the oligodendrocyte lineage defined by reactivity of progenitors with R-mAb prior to O1 anti-galactocerebroside." J Neurosci Res **32**(3): 309-316.

Bansal, R., A. E. Warrington, A. L. Gard, B. Ranscht and S. E. Pfeiffer (1989). "Multiple and novel specificities of monoclonal antibodies O1, O4, and R-mAb used in the analysis of oligodendrocyte development." J Neurosci Res **24**(4): 548-557.

Barbour, B., H. Brew and D. Attwell (1988). "Electrogenic glutamate uptake in glial cells is activated by intracellular potassium." Nature **335**(6189): 433-435.

Barbour, B., C. Magnus, M. Szatkowski, P. T. Gray and D. Attwell (1993). "Changes in NAD(P)H fluorescence and membrane current produced by glutamate uptake into salamander Muller cells." J Physiol **466**: 573-597.

Barres, B. A., I. K. Hart, H. S. Coles, J. F. Burne, J. T. Voyvodic, W. D. Richardson and M. C. Raff (1992). "Cell death and control of cell survival in the oligodendrocyte lineage." Cell **70**(1): 31-46.

Barres, B. A., M. A. Lazar and M. C. Raff (1994). "A novel role for thyroid hormone, glucocorticoids and retinoic acid in timing oligodendrocyte development." Development **120**(5): 1097-1108.

Bauer, D. E., J. G. Jackson, E. N. Genda, M. M. Montoya, M. Yudkoff and M. B. Robinson (2012). "The glutamate transporter, GLAST, participates in a macromolecular complex that supports glutamate metabolism." Neurochem Int **61**(4): 566-574.

Baumann, N. and D. Pham-Dinh (2001). "Biology of oligodendrocyte and myelin in the mammalian central nervous system." Physiol Rev **81**(2): 871-927.
Belvindrah, R., P. Nalbant, S. Ding, C. Wu, G. M. Bokoch and U. Muller (2006). "Integrin-linked kinase regulates Bergmann glial differentiation during cerebellar development." Mol Cell Neurosci **33**(2): 109-125.
Ben Achour, S. and O. Pascual (2010). "Glia: the many ways to modulate synaptic plasticity." Neurochem Int **57**(4): 440-445.
Benjamin, A. M. and J. H. Quastel (1976). "Cerebral uptakes and exchange diffusion in vitro of L- and D-glutamates." J Neurochem **26**(3): 431-441.
Bondy, S. C. and D. K. Lee (1993). "Oxidative stress induced by glutamate receptor agonists." Brain Res **610**(2): 229-233.
Bonfanti, L. and P. Peretto (2007). "Radial glial origin of the adult neural stem cells in the subventricular zone." Prog Neurobiol **83**(1): 24-36.
Boscia, F., C. D'Avanzo, A. Pannaccione, A. Secondo, A. Casamassa, L. Formisano, N. Guida, S. Sokolow, A. Herchuelz and L. Annunziato (2012). "Silencing or knocking out the Na(+)/Ca(2+) exchanger-3 (NCX3) impairs oligodendrocyte differentiation." Cell Death Differ **19**(4): 562-572.
Bradford, M. M. (1976). "A rapid and sensitive method for the quantitation of microgram quantities of protein utilizing the principle of protein-dye binding." Anal Biochem **72**: 248-254.
Bradl, M. and H. Lassmann (2010). "Oligodendrocytes: biology and pathology." Acta Neuropathol **119**(1): 37-53.
Bringmann, A., T. Pannicke, J. Grosche, M. Francke, P. Wiedemann, S. N. Skatchkov, N. N. Osborne and A. Reichenbach (2006). "Muller cells in the healthy and diseased retina." Prog Retin Eye Res **25**(4): 397-424.
Bringmann, A. and P. Wiedemann (2009). "Involvement of Muller glial cells in epiretinal membrane formation." Graefes Arch Clin Exp Ophthalmol **247**(7): 865-883.
Butchbach, M. E., G. Tian, H. Guo and C. L. Lin (2004). "Association of excitatory amino acid transporters, especially EAAT2, with cholesterol-rich lipid raft microdomains: importance for excitatory amino acid transporter localization and function." J Biol Chem **279**(33): 34388-34396.
Chan, Y. L., A. Lin, J. McNally, D. Peleg, O. Meyuhas and I. G. Wool (1987). "The primary structure of rat ribosomal protein L19. A determination from the sequence of nucleotides in a cDNA and from the sequence of amino acids in the protein." J Biol Chem **262**(3): 1111-1115.
Chaudhry, F. A., K. P. Lehre, M. van Lookeren Campagne, O. P. Ottersen, N. C. Danbolt and J. Storm-Mathisen (1995). "Glutamate transporters in glial plasma membranes: highly differentiated localizations revealed by quantitative ultrastructural immunocytochemistry." Neuron **15**(3): 711-720.
Chaudhry, F. A., R. J. Reimer and R. H. Edwards (2002). "The glutamine commute: take the N line and transfer to the A." J Cell Biol **157**(3): 349-355.
Chittajallu, R., S. P. Braithwaite, V. R. Clarke and J. M. Henley (1999). "Kainate receptors: subunits, synaptic localization and function." Trends Pharmacol Sci **20**(1): 26-35.

Choi, D. W. (1988). "Glutamate neurotoxicity and diseases of the nervous system." Neuron **1**(8): 623-634.
Choi, Y. K. and K. W. Kim (2008). "Blood-neural barrier: its diversity and coordinated cell-to-cell communication." BMB Rep **41**(5): 345-352.
Cox, D. W., M. H. Headley and J. C. Watkins (1977). "Actions of L- and D-homocysteate in rat CNS: a correlation between low-affinity uptake and the time courses of excitation by microelectrophoretically applied L-glutamate analogues." J Neurochem **29**(3): 579-588.
Cui, W., N. D. Allen, M. Skynner, B. Gusterson and A. J. Clark (2001). "Inducible ablation of astrocytes shows that these cells are required for neuronal survival in the adult brain." Glia **34**(4): 272-282.
Danbolt, N. C. (2001). "Glutamate uptake." Prog Neurobiol **65**(1): 1-105.
Dennis, J., M. A. White, A. D. Forrest, L. M. Yuelling, L. Nogaroli, F. S. Afshari, M. A. Fox and B. Fuss (2008). "Phosphodiesterase-Ialpha/autotaxin's MORFO domain regulates oligodendroglial process network formation and focal adhesion organization." Mol Cell Neurosci **37**(2): 412-424.
Derouiche, A. and T. Rauen (1995). "Coincidence of L-glutamate/L-aspartate transporter (GLAST) and glutamine synthetase (GS) immunoreactions in retinal glia: evidence for coupling of GLAST and GS in transmitter clearance." J Neurosci Res **42**(1): 131-143.
Duan, S., C. M. Anderson, B. A. Stein and R. A. Swanson (1999). "Glutamate induces rapid upregulation of astrocyte glutamate transport and cell-surface expression of GLAST." J Neurosci **19**(23): 10193-10200.
Erichsen, M. N., T. H. Huynh, B. Abrahamsen, J. F. Bastlund, C. Bundgaard, O. Monrad, A. Bekker-Jensen, C. W. Nielsen, K. Frydenvang, A. A. Jensen and L. Bunch (2010). "Structure-activity relationship study of first selective inhibitor of excitatory amino acid transporter subtype 1: 2-Amino-4-(4-methoxyphenyl)-7-(naphthalen-1-yl)-5-oxo-5,6,7,8-tetrahydro-4H-chrom ene-3-carbonitrile (UCPH-101)." J Med Chem **53**(19): 7180-7191.
Fancy, S. P., M. R. Kotter, E. P. Harrington, J. K. Huang, C. Zhao, D. H. Rowitch and R. J. Franklin (2010). "Overcoming remyelination failure in multiple sclerosis and other myelin disorders." Exp Neurol **225**(1): 18-23.
Foster, K. G. and D. C. Fingar (2010). "Mammalian target of rapamycin (mTOR): conducting the cellular signaling symphony." J Biol Chem **285**(19): 14071-14077.
Franco, P. G., L. Silvestroff, E. F. Soto and J. M. Pasquini (2008). "Thyroid hormones promote differentiation of oligodendrocyte progenitor cells and improve remyelination after cuprizone-induced demyelination." Exp Neurol **212**(2): 458-467.
Fyk-Kolodziej, B., P. Qin, A. Dzhagaryan and R. G. Pourcho (2004). "Differential cellular and subcellular distribution of glutamate transporters in the cat retina." Vis Neurosci **21**(4): 551-565.
Gegelashvili, G. and A. Schousboe (1998). "Cellular distribution and kinetic properties of high-affinity glutamate transporters." Brain Res Bull **45**(3): 233-238.
Gegelashvili, M., A. Rodriguez-Kern, L. Sung, K. Shimamoto and G. Gegelashvili (2007). "Glutamate transporter GLAST/EAAT1 directs cell surface expression of FXYD2/gamma subunit of Na, K-ATPase in human fetal astrocytes." Neurochem Int **50**(7-8): 916-920.

Gonzalez, M. I., A. M. Lopez-Colom and A. Ortega (1999). "Sodium-dependent glutamate transport in Muller glial cells: regulation by phorbol esters." Brain Res **831**(1-2): 140-145.
Gonzalez, M. I. and A. Ortega (2000). "Regulation of high-affinity glutamate uptake activity in Bergmann glia cells by glutamate." Brain Res **866**(1-2): 73-81.
Gonzalez, M. I. and M. B. Robinson (2004). "Neurotransmitter transporters: why dance with so many partners?" Curr Opin Pharmacol **4**(1): 30-35.
Gonzalez, M. I., B. T. Susarla, K. M. Fournier, A. L. Sheldon and M. B. Robinson (2007). "Constitutive endocytosis and recycling of the neuronal glutamate transporter, excitatory amino acid carrier 1." J Neurochem **103**(5): 1917-1931.
Grosche, J., H. Kettenmann and A. Reichenbach (2002). "Bergmann glial cells form distinct morphological structures to interact with cerebellar neurons." J Neurosci Res **68**(2): 138-149.
Grynkiewicz, G., M. Poenie and R. Y. Tsien (1985). "A new generation of Ca2+ indicators with greatly improved fluorescence properties." J Biol Chem **260**(6): 3440-3450.
Guerrini, L., F. Blasi and S. Denis-Donini (1995). "Synaptic activation of NF-kappa B by glutamate in cerebellar granule neurons in vitro." Proc Natl Acad Sci U S A **92**(20): 9077-9081.
Guillet, B., S. Lortet, F. Masmejean, D. Samuel, A. Nieoullon and P. Pisano (2002). "Developmental expression and activity of high affinity glutamate transporters in rat cortical primary cultures." Neurochem Int **40**(7): 661-671.
Guillet, B. A., L. J. Velly, B. Canolle, F. M. Masmejean, A. L. Nieoullon and P. Pisano (2005). "Differential regulation by protein kinases of activity and cell surface expression of glutamate transporters in neuron-enriched cultures." Neurochem Int **46**(4): 337-346.
Hatten, M. E. (1999). "Central nervous system neuronal migration." Annu Rev Neurosci **22**: 511-539.
Haugeto, O., K. Ullensvang, L. M. Levy, F. A. Chaudhry, T. Honore, M. Nielsen, K. P. Lehre and N. C. Danbolt (1996). "Brain glutamate transporter proteins form homomultimers." J Biol Chem **271**(44): 27715-27722.
Headley, P. M. and S. Grillner (1990). "Excitatory amino acids and synaptic transmission: the evidence for a physiological function." Trends Pharmacol Sci **11**(5): 205-211.
Hollmann, M. and S. Heinemann (1994). "Cloned glutamate receptors." Annu Rev Neurosci **17**: 31-108.
Hou, Q., Y. Huang, S. Amato, S. H. Snyder, R. L. Huganir and H. Y. Man (2008). "Regulation of AMPA receptor localization in lipid rafts." Mol Cell Neurosci **38**(2): 213-223.
Jiang, J. and S. G. Amara (2011). "New views of glutamate transporter structure and function: advances and challenges." Neuropharmacology **60**(1): 172-181.
Jin, R., S. K. Singh, S. Gu, H. Furukawa, A. I. Sobolevsky, J. Zhou, Y. Jin and E. Gouaux (2009). "Crystal structure and association behaviour of the GluR2 amino-terminal domain." EMBO J **28**(12): 1812-1823.

Kandel, E. R., J. H. Schwartz and T. M. Jessell (2000). Principles of neural science. New York ; London, McGraw-Hill, Health Professions Division.
Kanner, B. I. and I. Sharon (1978). "Active transport of L-glutamate by membrane vesicles isolated from rat brain." Biochemistry **17**(19): 3949-3953.
Kew, J. N. and J. A. Kemp (2005). "Ionotropic and metabotropic glutamate receptor structure and pharmacology." Psychopharmacology (Berl) **179**(1): 4-29.
Kirischuk, S., H. Kettenmann and A. Verkhratsky (2007). "Membrane currents and cytoplasmic sodium transients generated by glutamate transport in Bergmann glial cells." Pflugers Arch **454**(2): 245-252.
Koirala, S. and G. Corfas (2010). "Identification of novel glial genes by single-cell transcriptional profiling of Bergmann glial cells from mouse cerebellum." PLoS One **5**(2): e9198.
Kremer, D., O. Aktas, H. P. Hartung and P. Kury (2011). "The complex world of oligodendroglial differentiation inhibitors." Ann Neurol **69**(4): 602-618.
Kuhlmann, T., V. Miron, Q. Cui, C. Wegner, J. Antel and W. Bruck (2008). "Differentiation block of oligodendroglial progenitor cells as a cause for remyelination failure in chronic multiple sclerosis." Brain **131**(Pt 7): 1749-1758.
Kwak, S. and J. H. Weiss (2006). "Calcium-permeable AMPA channels in neurodegenerative disease and ischemia." Curr Opin Neurobiol **16**(3): 281-287.
Lafrenaye, A. D. and B. Fuss (2010). "Focal adhesion kinase can play unique and opposing roles in regulating the morphology of differentiating oligodendrocytes." J Neurochem **115**(1): 269-282.
Lehre, K. P. and N. C. Danbolt (1998). "The number of glutamate transporter subtype molecules at glutamatergic synapses: chemical and stereological quantification in young adult rat brain." J Neurosci **18**(21): 8751-8757.
Lin, Y. C. and L. Redmond (2008). "CaMKIIbeta binding to stable F-actin in vivo regulates F-actin filament stability." Proc Natl Acad Sci U S A **105**(41): 15791-15796.
Liu, B., M. Liao, J. G. Mielke, K. Ning, Y. Chen, L. Li, Y. H. El-Hayek, E. Gomez, R. S. Zukin, M. G. Fehlings and Q. Wan (2006). "Ischemic insults direct glutamate receptor subunit 2-lacking AMPA receptors to synaptic sites." J Neurosci **26**(20): 5309-5319.
Livak, K. J. and T. D. Schmittgen (2001). "Analysis of relative gene expression data using real-time quantitative PCR and the 2(-Delta Delta C(T)) Method." Methods **25**(4): 402-408.
Lopez-Bayghen, E., M. Espinoza-Rojo and A. Ortega (2003). "Glutamate down-regulates GLAST expression through AMPA receptors in Bergmann glial cells." Brain Res Mol Brain Res **115**(1): 1-9.
Lopez-Bayghen, E. and A. Ortega (2004). "Glutamate-dependent transcriptional regulation of GLAST: role of PKC." J Neurochem **91**(1): 200-209.
Lopez-Bayghen, E. and A. Ortega (2010). "[Glial cells and synaptic activity: translational control of metabolic coupling]." Rev Neurol **50**(10): 607-615.

Lopez-Colome, A. M., A. Ortega and M. Romo-de-Vivar (1993). "Excitatory amino acid-induced phosphoinositide hydrolysis in Muller glia." Glia **9**(2): 127-135.
Lopez-Colome, A. M. and M. Romo-de-Vivar (1991). "Excitatory amino acid receptors in primary cultures of glial cells from the retina." Glia **4**(5): 431-439.
MacDonald, M. J. and L. A. Fahien (2000). "Glutamate is not a messenger in insulin secretion." J Biol Chem **275**(44): 34025-34027.
Madden, D. R. (2002). "The structure and function of glutamate receptor ion channels." Nat Rev Neurosci **3**(2): 91-101.
Magi, S., S. Arcangeli, P. Castaldo, A. A. Nasti, L. Berrino, E. Piegari, R. Bernardini, S. Amoroso and V. Lariccia (2013). "Glutamate-induced ATP synthesis: relationship between plasma membrane Na+/Ca2+ exchanger and excitatory amino acid transporters in brain and heart cell models." Mol Pharmacol **84**(4): 603-614.
Magi, S., V. Lariccia, P. Castaldo, S. Arcangeli, A. A. Nasti, A. Giordano and S. Amoroso (2012). "Physical and functional interaction of NCX1 and EAAC1 transporters leading to glutamate-enhanced ATP production in brain mitochondria." PLoS One **7**(3): e34015.
Malatesta, P., I. Appolloni and F. Calzolari (2008). "Radial glia and neural stem cells." Cell Tissue Res **331**(1): 165-178.
Maria Lopez-Colome, A., Z. Martinez-Lozada, A. M. Guillem, E. Lopez and A. Ortega (2012). "Glutamate transporter-dependent mTOR phosphorylation in Muller glia cells." ASN Neuro **4**(5).
Martinez-Lozada, Z., L. C. Hernandez-Kelly, J. Aguilera, E. Lopez-Bayghen and A. Ortega (2011). "Signaling through EAAT-1/GLAST in cultured Bergmann glia cells." Neurochem Int **59**(6): 871-879.
Massey, S. C. and R. F. Miller (1987). "Excitatory amino acid receptors of rod- and cone-driven horizontal cells in the rabbit retina." J Neurophysiol **57**(3): 645-659.
Massey, S. C. and R. F. Miller (1990). "N-methyl-D-aspartate receptors of ganglion cells in rabbit retina." J Neurophysiol **63**(1): 16-30.
Mathews, C. K., K. E. Van Holde and K. G. Ahern (2000). Biochemistry. San Francisco, Calif. ; Harlow, Benjamin Cummings.
McLennan, H. and H. V. Wheal (1976). "The interaction of glutamic and aspartic acids with excitatory amino acid receptors in the mammalian central nervous system." Can J Physiol Pharmacol **54**(1): 70-72.
Metea, M. R. and E. A. Newman (2006). "Glial cells dilate and constrict blood vessels: a mechanism of neurovascular coupling." J Neurosci **26**(11): 2862-2870.
Moepps, B. and L. Fagni (2003). "Mont Sainte-Odile: a sanctuary for GPCRs. Confidence on signal transduction of G-protein-couple receptors." EMBO Rep **4**(3): 237-243.
Nakanishi, S., Y. Nakajima, M. Masu, Y. Ueda, K. Nakahara, D. Watanabe, S. Yamaguchi, S. Kawabata and M. Okada (1998). "Glutamate receptors: brain function and signal transduction." Brain Res Brain Res Rev **26**(2-3): 230-235.
Newman, E. A. (2001). "Propagation of intercellular calcium waves in retinal astrocytes and Muller cells." J Neurosci **21**(7): 2215-2223.

Newman, E. A. (2004). "Glial modulation of synaptic transmission in the retina." Glia **47**(3): 268-274.
Nimmerjahn, A., E. A. Mukamel and M. J. Schnitzer (2009). "Motor behavior activates Bergmann glial networks." Neuron **62**(3): 400-412.
Nissen-Meyer, L. S., M. C. Popescu, H. Hamdani el and F. A. Chaudhry (2011). "Protein kinase C-mediated phosphorylation of a single serine residue on the rat glial glutamine transporter SN1 governs its membrane trafficking." J Neurosci **31**(17): 6565-6575.
Niswender, C. M. and P. J. Conn (2010). "Metabotropic glutamate receptors: physiology, pharmacology, and disease." Annu Rev Pharmacol Toxicol **50**: 295-322.
Novelli, A., J. A. Reilly, P. G. Lysko and R. C. Henneberry (1988). "Glutamate becomes neurotoxic via the N-methyl-D-aspartate receptor when intracellular energy levels are reduced." Brain Res **451**(1-2): 205-212.
O'Shea, R. D., M. V. Fodera, K. Aprico, Y. Dehnes, N. C. Danbolt, D. Crawford and P. M. Beart (2002). "Evaluation of drugs acting at glutamate transporters in organotypic hippocampal cultures: new evidence on substrates and blockers in excitotoxicity." Neurochem Res **27**(1-2): 5-13.
Okamoto, K., R. Narayanan, S. H. Lee, K. Murata and Y. Hayashi (2007). "The role of CaMKII as an F-actin-bundling protein crucial for maintenance of dendritic spine structure." Proc Natl Acad Sci U S A **104**(15): 6418-6423.
Olney, J. W. (1969). "Brain lesions, obesity, and other disturbances in mice treated with monosodium glutamate." Science **164**(880): 719-721.
Ortega, A., N. Eshhar and V. I. Teichberg (1991). "Properties of kainate receptor/channels on cultured Bergmann glia." Neuroscience **41**(2-3): 335-349.
Otori, Y., S. Shimada, K. Tanaka, I. Ishimoto, Y. Tano and M. Tohyama (1994). "Marked increase in glutamate-aspartate transporter (GLAST/GluT-1) mRNA following transient retinal ischemia." Brain Res Mol Brain Res **27**(2): 310-314.
Ozawa, S., H. Kamiya and K. Tsuzuki (1998). "Glutamate receptors in the mammalian central nervous system." Prog Neurobiol **54**(5): 581-618.
Peghini, P., J. Janzen and W. Stoffel (1997). "Glutamate transporter EAAC-1-deficient mice develop dicarboxylic aminoaciduria and behavioral abnormalities but no neurodegeneration." EMBO J **16**(13): 3822-3832.
Pellerin, L., A. K. Bouzier-Sore, A. Aubert, S. Serres, M. Merle, R. Costalat and P. J. Magistretti (2007). "Activity-dependent regulation of energy metabolism by astrocytes: an update." Glia **55**(12): 1251-1262.
Pellerin, L. and P. J. Magistretti (1994). "Glutamate uptake into astrocytes stimulates aerobic glycolysis: a mechanism coupling neuronal activity to glucose utilization." Proc Natl Acad Sci U S A **91**(22): 10625-10629.
Pellerin, L. and P. J. Magistretti (1997). "Glutamate uptake stimulates Na+,K+-ATPase activity in astrocytes via activation of a distinct subunit highly sensitive to ouabain." J Neurochem **69**(5): 2132-2137.
Proud, C. G. (2007). "Cell signaling. mTOR, unleashed." Science **318**(5852): 926-927.
Raff, M. C., E. R. Abney, J. Cohen, R. Lindsay and M. Noble (1983). "Two types of astrocytes in cultures of developing rat white matter: differences

in morphology, surface gangliosides, and growth characteristics." J Neurosci **3**(6): 1289-1300.
Raff, M. C., E. R. Abney and R. H. Miller (1984). "Two glial cell lineages diverge prenatally in rat optic nerve." Dev Biol **106**(1): 53-60.
Rana, R. S. and L. E. Hokin (1990). "Role of phosphoinositides in transmembrane signaling." Physiol Rev **70**(1): 115-164.
Reichenbach, A., A. Siegel, M. Rickmann, J. R. Wolff, D. Noone and S. R. Robinson (1995). "Distribution of Bergmann glial somata and processes: implications for function." J Hirnforsch **36**(4): 509-517.
Ribeiro, F. M., M. Paquet, S. P. Cregan and S. S. Ferguson (2010). "Group I metabotropic glutamate receptor signalling and its implication in neurological disease." CNS Neurol Disord Drug Targets **9**(5): 574-595.
Robinson, M. B. and L. A. Dowd (1997). "Heterogeneity and functional properties of subtypes of sodium-dependent glutamate transporters in the mammalian central nervous system." Adv Pharmacol **37**: 69-115.
Rodbell, M. (1980). "The role of hormone receptors and GTP-regulatory proteins in membrane transduction." Nature **284**(5751): 17-22.
Rojas, H., C. Colina, M. Ramos, G. Benaim, E. H. Jaffe, C. Caputo and R. DiPolo (2007). "Na+ entry via glutamate transporter activates the reverse Na+/Ca2+ exchange and triggers Ca(i)2+-induced Ca2+ release in rat cerebellar Type-1 astrocytes." J Neurochem **100**(5): 1188-1202.
Rose, E. M., J. C. Koo, J. E. Antflick, S. M. Ahmed, S. Angers and D. R. Hampson (2009). "Glutamate transporter coupling to Na,K-ATPase." J Neurosci **29**(25): 8143-8155.
Roskoski, R., Jr. (1979). "Net uptake of aspartate by a high-affinity rat cortical synaptosomal transport system." Brain Res **160**(1): 85-93.
Ruiz, M. and A. Ortega (1995). "Characterization of an Na(+)-dependent glutamate/aspartate transporter from cultured Bergmann glia." Neuroreport **6**(15): 2041-2044.
Saglietti, L., C. Dequidt, K. Kamieniarz, M. C. Rousset, P. Valnegri, O. Thoumine, F. Beretta, L. Fagni, D. Choquet, C. Sala, M. Sheng and M. Passafaro (2007). "Extracellular interactions between GluR2 and N-cadherin in spine regulation." Neuron **54**(3): 461-477.
Santos, S. D., A. L. Carvalho, M. V. Caldeira and C. B. Duarte (2009). "Regulation of AMPA receptors and synaptic plasticity." Neuroscience **158**(1): 105-125.
Sarantis, M. and D. Attwell (1990). "Glutamate uptake in mammalian retinal glia is voltage- and potassium-dependent." Brain Res **516**(2): 322-325.
Schousboe, A. and L. Hertz (1981). "Role of astroglial cells in glutamate homeostasis." Adv Biochem Psychopharmacol **27**: 103-113.
Shank, R. P. and G. L. Campbell (1984). "Alpha-ketoglutarate and malate uptake and metabolism by synaptosomes: further evidence for an astrocyte-to-neuron metabolic shuttle." J Neurochem **42**(4): 1153-1161.
Slemmer, J. E., C. I. De Zeeuw and J. T. Weber (2005). "Don't get too excited: mechanisms of glutamate-mediated Purkinje cell death." Prog Brain Res **148**: 367-390.
Smith, C. U. M. (2002). Elements of molecular neurobiology. Chichester, Wiley.

Sommer, I. and M. Schachner (1982). "Cell that are O4 antigen-positive and O1 antigen-negative differentiate into O1 antigen-positive oligodendrocytes." Neurosci Lett **29**(2): 183-188.
Sottile, V., M. Li and P. J. Scotting (2006). "Stem cell marker expression in the Bergmann glia population of the adult mouse brain." Brain Res **1099**(1): 8-17.
Sumi, M., K. Kiuchi, T. Ishikawa, A. Ishii, M. Hagiwara, T. Nagatsu and H. Hidaka (1991). "The newly synthesized selective Ca2+/calmodulin dependent protein kinase II inhibitor KN-93 reduces dopamine contents in PC12h cells." Biochem Biophys Res Commun **181**(3): 968-975.
Szatkowski, M., B. Barbour and D. Attwell (1991). "The potassium-dependence of excitatory amino acid transport: resolution of a paradox." Brain Res **555**(2): 343-345.
Tanaka, K., K. Watase, T. Manabe, K. Yamada, M. Watanabe, K. Takahashi, H. Iwama, T. Nishikawa, N. Ichihara, T. Kikuchi, S. Okuyama, N. Kawashima, S. Hori, M. Takimoto and K. Wada (1997). "Epilepsy and exacerbation of brain injury in mice lacking the glutamate transporter GLT-1." Science **276**(5319): 1699-1702.
Thomas, G. M. and R. L. Huganir (2004). "MAPK cascade signalling and synaptic plasticity." Nat Rev Neurosci **5**(3): 173-183.
Thoreson, W. B. and P. Witkovsky (1999). "Glutamate receptors and circuits in the vertebrate retina." Prog Retin Eye Res **18**(6): 765-810.
Tout, S., T. Chan-Ling, H. Hollander and J. Stone (1993). "The role of Muller cells in the formation of the blood-retinal barrier." Neuroscience **55**(1): 291-301.
Wadiche, J. I., J. L. Arriza, S. G. Amara and M. P. Kavanaugh (1995). "Kinetics of a human glutamate transporter." Neuron **14**(5): 1019-1027.
Wadiche, J. I. and M. P. Kavanaugh (1998). "Macroscopic and microscopic properties of a cloned glutamate transporter/chloride channel." J Neurosci **18**(19): 7650-7661.
Waggener, C. T., J. L. Dupree, Y. Elgersma and B. Fuss (2013). "CaMKIIbeta regulates oligodendrocyte maturation and CNS myelination." J Neurosci **33**(25): 10453-10458.
Wang, H., B. Gong, K. I. Vadakkan, H. Toyoda, B. K. Kaang and M. Zhuo (2007). "Genetic evidence for adenylyl cyclase 1 as a target for preventing neuronal excitotoxicity mediated by N-methyl-D-aspartate receptors." J Biol Chem **282**(2): 1507-1517.
Warrington, A. E., E. Barbarese and S. E. Pfeiffer (1993). "Differential myelinogenic capacity of specific developmental stages of the oligodendrocyte lineage upon transplantation into hypomyelinating hosts." J Neurosci Res **34**(1): 1-13.
Warrington, A. E. and S. E. Pfeiffer (1992). "Proliferation and differentiation of O4+ oligodendrocytes in postnatal rat cerebellum: analysis in unfixed tissue slices using anti-glycolipid antibodies." J Neurosci Res **33**(2): 338-353.
Watase, K., K. Hashimoto, M. Kano, K. Yamada, M. Watanabe, Y. Inoue, S. Okuyama, T. Sakagawa, S. Ogawa, N. Kawashima, S. Hori, M. Takimoto, K. Wada and K. Tanaka (1998). "Motor discoordination and increased

susceptibility to cerebellar injury in GLAST mutant mice." Eur J Neurosci **10**(3): 976-988.
Watkins, J. C. and R. H. Evans (1981). "Excitatory amino acid transmitters." Annu Rev Pharmacol Toxicol **21**: 165-204.
Willard, S. S. and S. Koochekpour (2013). "Glutamate, glutamate receptors, and downstream signaling pathways." Int J Biol Sci **9**(9): 948-959.
Witcher, M. R., S. A. Kirov and K. M. Harris (2007). "Plasticity of perisynaptic astroglia during synaptogenesis in the mature rat hippocampus." Glia **55**(1): 13-23.
Zepeda, R. C., I. Barrera, F. Castelan, E. Suarez-Pozos, Y. Melgarejo, E. Gonzalez-Mejia, L. C. Hernandez-Kelly, E. Lopez-Bayghen, J. Aguilera and A. Ortega (2009). "Glutamate-dependent phosphorylation of the mammalian target of rapamycin (mTOR) in Bergmann glial cells." Neurochem Int **55**(5): 282-287.

ANEXOS

1. Signaling through EAAT-1/GLAST in cultured Bergmann glia cells. Zila Martinez-Lozada, Luisa C. Hernandez-Kelly, Jose Aguilera, Esther Lopez-Bayghen, Arturo Ortega. Neurochem Int. 2011 Nov; 59(6): 871-9.
2. Glutamate transporter-dependent mTOR phosphorylation in Müller glia cells. Lopez-Colome M, Martinez-Lozada Z, Guillem AM, Lopez E, Ortega A. ASN Neuro. 2012 Aug 16; 4(5).
3. GLAST/EAAT1-induced glutamine release via SNAT3 in Bergmann glial cells: evidence of a functional and physical coupling. Martínez-Lozada Z, Guillem AM, Flores-Méndez M, Hernández-Kelly LC, Vela C, Meza E, Zepeda RC, Caba M, Rodríguez A, Ortega A. J Neurochem. 2013 May;125(4):545-54
4. Glutamate-dependent translational control in cultured Bergmann glia cells: eIF2α phosphorylation. Flores-Méndez MA, Martínez-Lozada Z, Monroy HC, Hernández-Kelly LC, Barrera I, Ortega A. Neurochem Res. 2013 Jul;38(7):1324-32.
5. GLAST/EAAT1 regulation in cultured Bergmann glia cells: role of the NO/cGMP signaling pathway. Balderas A, Guillem AM, Martínez-Lozada Z, Hernández-Kelly LC, Aguilera J, Ortega A. Neurochem Int. 2014 Jul;73:139-45.
6. Activation of sodium-dependent glutamate transporters regulates the morphological aspects of oligodendrocyte maturation via signaling through calcium/calmodulin-dependent kinase IIβ's actin-binding/-stabilizing domain. Martinez-Lozada Z, Waggener CT, Kim K, Zou S, Knapp PE, Hayashi Y, Ortega A, Fuss B. Glia. 2014 Sep;62(9):1543-58.
7. Glutamate-dependent translational control through ribosomal protein S6 phosphorylation in cultured Bergmann glial cells. Marco Flores-Mendez, Miguel Escalante-Lopez, Zila Martinez-Lozada, Luisa C Hernandez-Kelly, Mustapha Najimi, Ettiene Sokal, Arturo Ortega. Neurochemical Research, 2015. NERE-D-14-00555R1

Neurochemistry International 59 (2011) 871–879

Contents lists available at SciVerse ScienceDirect

Neurochemistry International

journal homepage: www.elsevier.com/locate/nci

Signaling through EAAT-1/GLAST in cultured Bergmann glia cells

Zila Martínez-Lozada [a], Luisa C. Hernández-Kelly [a,b], José Aguilera [b], Esther López-Bayghen [a], Arturo Ortega [a,*]

[a] Departamento de Genética y Biología Molecular, Centro de Investigación y de Estudios Avanzados del Instituto Politécnico Nacional, Apartado Postal 14-740, México DF 07000, Mexico
[b] Institut de Neurosciénces i Departament de Bioquímica i Biología Molecular, Universitat Autònoma de Barcelona, Cerdanyola del Vallès, Barcelona, Spain

ARTICLE INFO

Article history:
Received 15 February 2011
Received in revised form 26 July 2011
Accepted 29 July 2011
Available online 10 August 2011

Keywords:
Glutamate transporters
Bergmann glia
mTOR
Transcription regulation
Translational control

ABSTRACT

Glutamate, the major excitatory amino acid, activates a wide variety of signal transduction cascades. Synaptic plasticity relies on activity-dependent differential protein expression. Ionotropic and metabotropic glutamate receptors have been critically involved in long-term synaptic changes, although recent findings suggest that the electrogenic Na^+-dependent glutamate transporters, responsible of its removal from the synaptic cleft, participate in glutamate-induced signaling. Transporter proteins are expressed in neurons and glia cells albeit most of the glutamate uptake occurs in the glial compartment. Within the cerebellum, Bergmann glial cells are close to glutamatergic synapses and participate actively in the recycling of glutamate through the glutamate/glutamine shuttle. In this context, we decided to investigate a plausible role of Bergmann glia glutamate transporters as signaling entities. To this end, primary cultures of chick cerebellar Bergmann glial cells were exposed to D-aspartate (D-Asp) and other transporter ligands and the serine 2448 phosphorylation pattern of the master regulator of protein synthesis, namely the mammalian target of rapamycin (mTOR), determined. An increase in mTOR phosphorylation and activity was detected. The signaling cascade included Ca^{2+} influx, activation of the phosphatidylinositol 3-kinase and protein kinase B. Furthermore, transporter signaling resulted also in an increase in activator protein-1 (AP-1) binding to DNA and the up-regulation of the transcription of an AP-1 driven gene construct. These results add a novel mediator of the glutamate effects at the translational and transcriptional levels and further strengthen the notion of the critical involvement of glia cells in synaptic function.

1. Introduction

Excitatory neurotransmission in the vertebrate central nervous system (CNS) is mediated largely by glutamate (Glu). Two main subtypes of Glu receptors have been defined: ionotropic (iGluRs) and metabotropic receptors (mGluRs). Three iGluRs exist: *N*-methyl-D-aspartate (NMDA), α-amino-3-hydroxy-5-methyl-4-isoaxazolepropionate (AMPA) and kainate (KA) receptors (Hollmann and Heinemann, 1994). Metabotropic receptors are divided in terms of sequence similarity, signal transduction mechanisms and pharmacology in three groups. Group I receptors are coupled to the stimulation of phospholipase C with the consequent release of intracellular Ca^{2+}, while Groups II and III are coupled to the inhibition of adenylate cyclase. These three groups are activated preferentially by (RS)-3,5-dihydroxyphenylglycine (DHPG) for Group I, (S)-4-carboxy-3-hydroxyphenylglycine (S)-4C3HPG activates Group II while L-(+)-2-amino-4-phosphonobutyric acid (L-AP4) acts upon Group III (Coutinho and Knopfel, 2002).

Bergmann glia cells (BGCs) are the most abundant glia cells in the cerebellum, comprising more than 90% of the cerebellar glia. These cells span the entire cerebellar molecular layer and encapsulate neuronal somata, dendrites and axons. BGC are involved in neurotransmitter uptake, K^+ homeostasis and pH regulation due to the expression of a battery of receptors and transporters (Lopez-Bayghen et al., 2007). In terms of glutamatergic transmission, BGC are in a very short proximity to the parallel fiber-Purkinje cell synapses, and are involved in the Glu/glutamine shuttle that assures the Glu supply to the presynaptic terminals. In this sense, BGC respond to glutamatergic stimulation, as we have been able to characterize over the years (Barrera et al., 2010).

Activity-dependent gene expression regulation stabilizes the synaptic changes that underlie the late phase of long-term potentiation (Pittenger and Kandel, 1998). Transcription and translation are essential for long-term memory (Hu et al., 2006). While most studies have focused in gene expression regulation at the transcriptional level, regulation of protein synthesis has a crucial role in synaptic plasticity (Cammalleri et al., 2003). Translational

* Corresponding author. Address: Departamento de Genética y Biología Molecular, Cinvestav-IPN, Apartado Postal 14-740, México DF 07000, Mexico. Tel.: +52 5 55061 3800x5316; fax: +52 5 55061 3800x5317.
E-mail address: arortega@cinvestav.mx (A. Ortega).

0197-0186/$ - see front matter © 2011 Elsevier B.V. All rights reserved.
doi:10.1016/j.neuint.2011.07.015

control offers the possibility of a rapid response to external stimulus without mRNA synthesis and transport. Therefore, immediacy is the most conspicuous advantage of translational over transcriptional control.

The mammalian target of rapamycin (mTOR) is a master regulator of protein synthesis (Proud, 2007). It is a multi-domain serine/threonine kinase that phosphorylates a wide array of proteins like phosphatase 2A and Huntingtin. It forms the catalytic core of two different complexes, mTOR complex 1 (mTORC1) and mTOR complex 2 (mTORC2). During acute exposure, rapamycin inhibits mTORC1 but not mTORC2. In a rather simplified scenario, mTORC1 mediates the mTOR effects that are rapamycin-sensitive. The canonical pathway that leads to mTOR serine 2448 phosphorylation and thus activation, includes phosphatidylinositol 3-kinase (PI3-K), which produces phosphatidylinositol 3,4,5-triphosphate (PIP3), that anchors phosphoinositide-dependent kinase 1 (PDK1) and protein kinase B (PKB) to the cell membrane (Sabatini, 2006). PKB is activated through a sequential phosphorylation cascade by PDK1 and a PDK2 activity that now it has been shown to correspond to mTORC2 (Bayascas and Alessi, 2005). Phosphorylated PKB activates mTORC1 that acts upon several translation components like eukaryotic initiation factor 4E binding protein-1 (4EBP1) and the 70 kDa S6 ribosomal kinase ($p70^{S6K}$) increasing protein synthesis (Bayascas and Alessi, 2005; Foster and Fingar, 2010).

Glu is removed from the synaptic cleft by a family of electrogenic sodium-dependent transporters expressed in neurons and glia cells (Danbolt, 2001). Five subtypes of transporters named excitatory amino acids transporters 1–5 (EAAT-1–5) have been characterized. The glial transporters EAAT-1 (GLAST) and EAAT-2 (GLT-1) account for more than 80% of the Glu uptake activity in the brain (Eulenburg and Gomeza, 2010; Swanson, 2005). Within BGC, EAAT-1/GLAST is the predominant transporter (Maragakis et al., 2004). Evidences suggest that Glu transporters might also participate in the signaling transactions triggered by this amino acid. In fact, Glu regulates the uptake process in a receptor-independent manner (Gonzalez and Ortega, 2000). More recently, it has also been reported that EAAT-1 is coupled to the Na^+/K^+ ATPase (Gegelashvili et al., 2007; Rose et al., 2009). To provide further evidence for a role of EAAT-1/GLAST in Glu signaling, in the present contribution we challenged the plausible participation of Glu transporters in gene expression regulation. We show here that Glu uptake is linked to an increase in the translation process and that it is also coupled to the transcriptional activation of an AP-1 driven construct. These results are discussed in terms of the physiological significance of an alternative signaling entity to Glu receptors and the identity of the genes regulated. A preliminary description of a D-Asp-dependent mTOR phosphorylation was reported earlier (Zepeda et al., 2009).

2. Materials and methods

2.1. Materials

Tissue culture reagents were obtained from GE Healthcare (Carlsbad, CA, USA). A23187 (5-(methylamino)-2-({(2*R*,3*R*,6*S*,8*S*,9*R*,11*R*)-3,9,11-trimethyl-8-[(1*S*)-1-methyl-2-oxo-2-(1*H*-pyrrol-2-yl) ethyl]-1,7-dioxaspiro[5.5] undec-2-yl}methyl)-1,3-benzoxazole-4-carboxylic acid), Wortmannin, Amiloride (3,5-diamino-6-chloro-*N*-(diaminomethylene)pyrazine-2-carboxamide), KB-R7943 (2-[2-[4-(4-Nitrobenzyloxy)phenyl]ethyl]isothioureamesylate), DL-TBOA (DL-threo-β-Benzyloxyaspartic acid), THA (threo β–hydroxyaspartate), DNQX (6,7-Dinitroquinoxaline-2,3-dione), LAP5 (L-(+)-2-Amino-5-phosphonopentanoic acid); CPCCOEt (7-(hydroxyimino)cyclopropa[b]chromen-1a-carboxylate ethyl ester), CPPG ((RS)-α-cyclopropyl-4-phosphonophenylglycine), PP2 (4-amino-5-(4-chlorophenyl)-7-(dimethylethyl)pyrazolo[3,4-*d*]pyrimidine, genistein and D-aspartate (D-Asp) and Glu were all obtained from Tocris-Cookson (St. Louis, MO, USA). PDC (L-trans-Pyrrolidine-2,4-dicarboxylic acid) was purchased to Sigma–Aldrich (St. Louis, MO, USA); ^{45}Ca was from Perkin Elmer (Boston, MA, USA). Polyclonal anti-phospho-mTOR (Ser 2448) and anti mTOR antibodies (05–235) were purchased from Cell Signaling Technology (Beverly, MA, USA). Polyclonal phospho-4EBP1 (Thr 70) was purchased from Santa Cruz Biotech, (Santa Cruz, CA, USA, sc-18092-R). Monoclonal anti-actin antibodies were kindly donated by Prof. Manuel Hernández (Cinvestav-IPN). Horseradish peroxidase-linked anti-rabbit and anti-mouse antibodies, and the enhanced chemiluminescence reagent (ECL), were obtained from Amersham Biosciences (Buckinghamshire, UK). All other chemicals were purchased from Sigma (St. Louis, MO, USA).

2.2. Cell culture and stimulation protocol

Primary cultures of cerebellar BGC were prepared from 14-day-old chick embryos as previously described (Ortega et al., 1991). Cells were plated in 6 or 24-well plastic culture dishes in DMEM containing 10% fetal bovine serum, 2 mM glutamine, and gentamicin (50 μg/ml) and used on the 4th to 7th day after culture. Before any treatment, confluent monolayers were switched to non-serum DMEM media containing 0.5% bovine serum albumin (BSA) for 30 min and then treated as indicated. Inhibitors were added 30 min before agonists. The cells were treated with Glu analogues added to culture medium for the indicated time periods; after that, in the case of transfected cells, the medium was replaced with DMEM/0.5% albumin.

2.3. SDS–PAGE and Western blots

Cells from confluent monolayers were harvested with phosphate-buffer saline (PBS) (10 mM K_2HPO_4/KH_2PO_4, 150 mM NaCl, pH 7.4) containing phosphatase inhibitors (10 mM NaF, 1 mM Na_2MoO_4 and 1 mM Na_3VO_4). The cells were lysed with RIPA buffer (50 mM Tris–HCl, 1 mM EDTA, 150 mM NaCl, 1 mM phenylmethylsufonyl fluoride, 1 mg/ml aprotinin, 1 mg/ml leupeptin, 1% NP-40, 0.25% sodium deoxycholate, 10 mM NaF, 1 mM Na_2MoO_4 and 1 mM Na_3VO_4 pH 7.4). Cell lysates were denaturized in Laemmli's sample buffer, and equal amount of proteins (100 μg as determined by the Bradford method) were resolved through a 6% SDS–PAGE and then electroblotted to nitrocellulose membranes. Blots were stained with Ponceau S stain to confirm that protein content was equal in all lanes. Membranes were soaked in PBS to remove the Ponceau S and incubated in TBS containing 5% dried skimmed milk and 0.1% Tween 20 for 60 min to block the excess of non-specific protein binding sites. Membranes were then incubated overnight at 4 °C with the particular primary antibodies indicated in each figure, followed by secondary antibodies. Immunoreactive polypeptides were detected by chemiluminescence and exposed to X-ray films. Densitometry analyses were performed and data analyzed with Prism GraphPad Software (San Diego, CA, USA).

2.4. $^{45}Ca^{2+}$ Influx

Confluent BGC monolayers seeded in 24-well plates were washed three times to remove all non-adhering cells with 0.5 ml aliquots of solution A containing 25 mM HEPES-Tris, 130 mM NaCl, 5.4 mM KCl, 1.8 mM $CaCl_2$. 0.8 mM $MgCl_2$, 33.3 mM glucose and 1 mM NaH_2PO_4 at pH 7.4. The Glu or D-Asp-induced influx of $^{45}Ca^{2+}$ ions was initiated at $t = 0$ by the addition of 0.5 ml solution A containing 1.5 μCi/ml solution A, Glu or Asp at the specified con-

centration. When inhibitors or modulators were tested, they were added 30 min prior to the beginning of the $^{45}Ca^{2+}$ influx assay. The reaction was stopped by aspirating the radioactive medium and washing each well within 15 s with 0.5 ml aliquots of an ice-cold solution A. The cells in the wells were then exposed for 2 h at 37 °C to 0.5 ml NaOH and an aliquot of that solution counted in a Beckmann 7800LS scintillation counter in the presence of a scintillation cocktail. Experiments were carried out at least three times in quadruplicates.

2.5. Electrophoretic mobility shift assays

Nuclear extracts were prepared as described previously (Lopez-Bayghen et al., 1996). All buffers contained a protease inhibitors cocktail to prevent nuclear factor proteolysis. Protein concentration was measured by the Bradford method (Bradford, 1976). Nuclear extracts (approximately 7.5 μg) from control or agonist-treated BGC were incubated on ice with 1 μg of poly [(dI–dC)] as a non-specific competitor (GE Healthcare) and 1 μg of [^{32}P]-end labeled double stranded oligonucleotide *chAP-1* 5′*AAGCTTGATCTGA CATCAGCTT*3′ (Aguirre et al., 2000). The reaction mixtures were incubated for 20 min on ice, electrophoresed in 8% polyacrylamide gels using a low ionic strength 0.5X TBE buffer. The gels were dried and exposed to an autoradiographic film.

2.6. Transient transfections and CAT assays

The TRE–CAT plasmid contains five copies of AP-1 site cloned in front of the thymidine kinase promoter and the CAT reporter gene. Transient transfections and CAT assays were performed in 60%

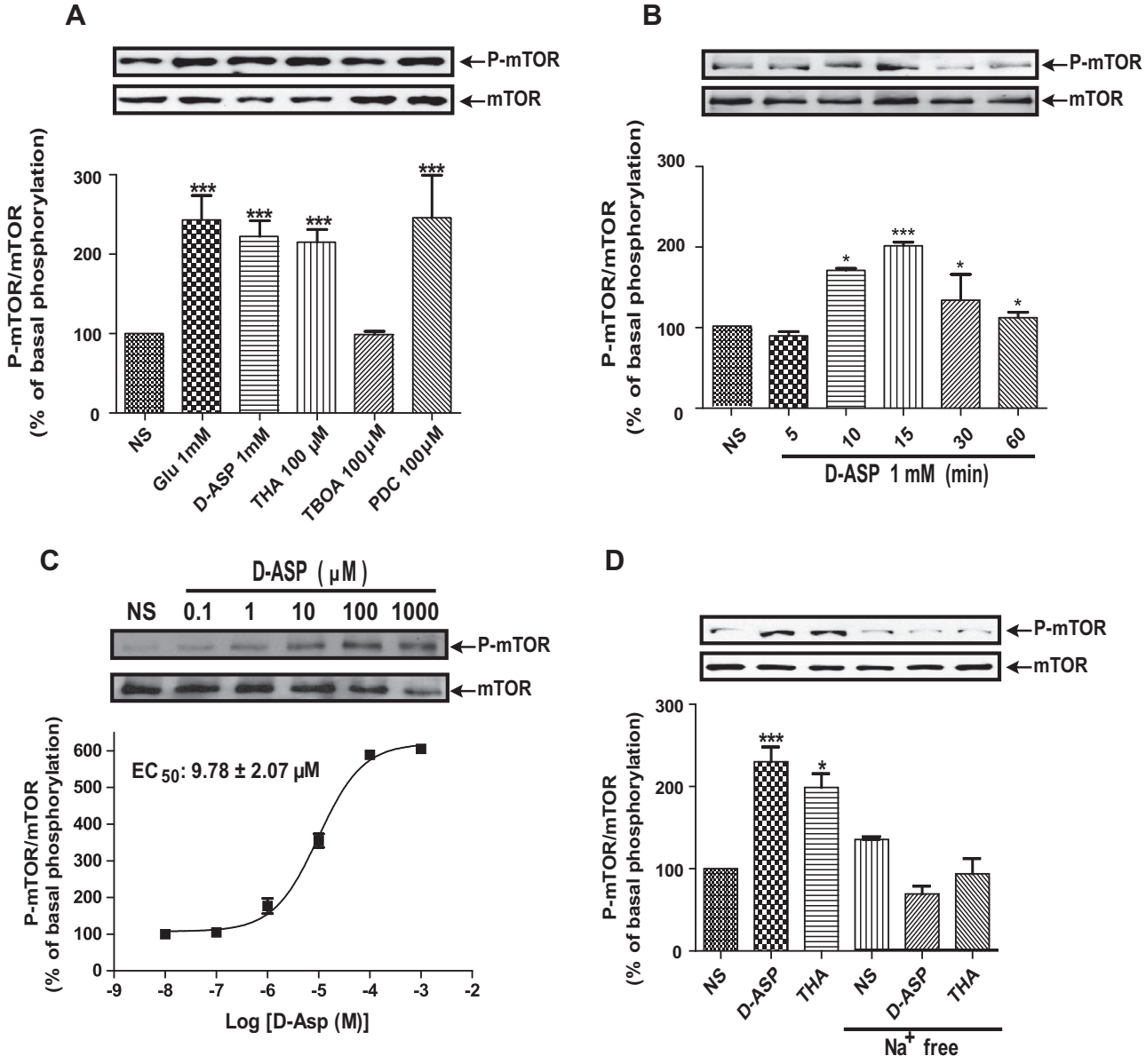

Fig. 1. D-Asp induces mTOR Ser 2448 phosphorylation in cultured Bergmann glia cells. Panel A: Confluent BGC monolayers were exposed for 15 min to the indicated concentrations of the transporter ligands and the levels of Ser 2448 phosphorylated mTOR and total mTOR were detected via Western blots as described under Section 2. Panel B: Cultured BGC were treated with 1 mM D-Asp for the indicated time periods; phospho-mTOR and total mTOR were detected as in panel A. Panel C: Cells were exposed for 15 min to increasing D-Asp concentrations. The EC_{50} was calculated after the densitometric analysis with the Prism program (GraphPad). Panel D: BGC cultures were treated for 15 min with either 1 mM D-Asp or 100 μM THA in complete or sodium-free assay buffer. Results are presented as mean values +/− standard error of at least three independent experiments. In each panel, a representative Western blot is shown. Statistical analysis was performed comparing against data from non-stimulated cells using a non-parametric one-way ANOVA (Kruskal–Wallis test) and Dunn's pos hoc test ($^{*}p < 0.05$, $^{***}p < 0.001$).

confluent BGC cultures using calcium phosphate protocol with 6 μg of p435kbpCAT reporter plasmid or 1 μg of the TRE–CAT construct. Under such conditions, the transfection efficacy was approximately 50% determined in every cell batch by an internal transfection control (β-gal). Treatment with D-Asp was performed 16 h post-transfection with indicated concentrations. Protein lysates were obtained as follows: cells were harvested in TEN buffer (40 mM Tris–HCl pH 8.0, 1 mM EDTA, 15 mM NaCl), lysed by three freeze–thaw cycles in 0.25 M Tris–HCl pH 8.0 and centrifuged at 12,000*g* for 3 min. Equal amounts of protein lysates (approximately 80 μg) were incubated with 0.25 μCi of [^{14}C]-chloramphenicol (50 mCi/mmol, GE Healthcare) and 0.8 mM Acetyl-CoA (Sigma) at 37 °C. Acetylated forms were separated by thin-layer chromatography and quantified using a Typhoon Optical Scanner (Molecular Dynamics, GE Healthcare). CAT activities were expressed as the acetylated fraction corrected for the activity in the pCAT-BASIC vector and are expressed as relative activities to non-treated control cell lysates.

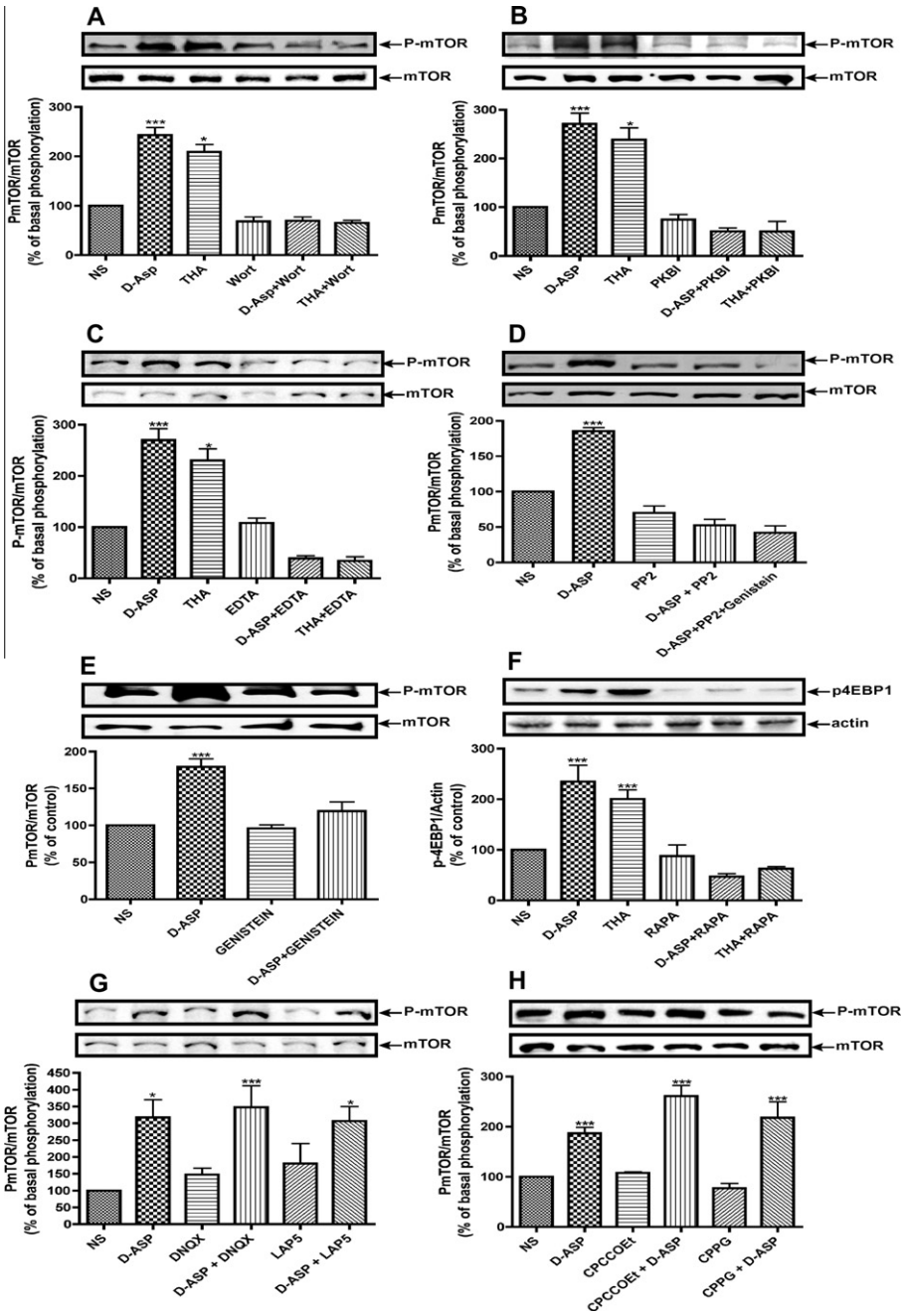

Fig. 2. D-Asp induced mTOR phosphorylation is PI3-K/Src and Ca^{2+} dependent. In all panels, Bergmann glia cultures were pre-exposed to normal medium or medium supplemented with the indicated inhibitor for 30 min and then to 1 mM D-Asp or 100 μM THA for 15 min, phosphorylated mTOR was detected as in Fig. 1. Panel A: 10 nM Wortmannin (Wort). Panel B: 100 nM PKB inhibitor IV (PKBI-IV). Panel C: Cells treated with 1 mM D-Asp or 100 μM THA in a Ca^{2+}-free medium (EDTA 500 μM). Panel D: 10 nM PP2, in the absence or presence of the tyrosine kinase inhibitor Genistein (25 μM). Panel E: 25 μM Genistein. Panel F: levels of Thr 70 phosphorylated 4EBP1 were detected after treatment with 1 mM D-Asp or 100 μM THA in the presence or absence of 100 nM Rapamicin (RAPA) for 30 min; actin was used as a loading control. Panel G: AMPA receptor antagonist DNQX (50 μM) and the NMDA receptor antagonist LAP5 (10 μM) and Panel H: metabotropic Glu receptors antagonists, for group I CPCCOEt (100 μM) and for group II/III CPPG (300 μM). All were added 30 min prior to D-Asp (1 mM, 15 min) treatment. All results are the mean values +/− the standard error of at least three independent experiments. In each case, a representative Western blot is shown. Statistical analysis was performed comparing against data obtained from non-stimulated cells using a non-parametric one-way ANOVA (Kruskal–Wallis test) and Dunn's pos hoc test ($^{*}p < 0.05$, $^{***}p < 0.001$).

2.7. Statistical analysis

Data are expressed as the mean (average) ± standard error (S.E.). A one-way analysis of variance (ANOVA) was performed to determine significant differences between conditions. When this analysis indicated significance (at the 0.05 level), post hoc Student–Newman–Keuls test analysis was used to determine which conditions were significantly different from each other with the Prism software.

3. Results

3.1. D-Aspartate induces mTOR phosphorylation in Bergmann glial cells

Translational control is the fine-tuning process of gene expression regulation. Our preliminary findings regarding Glu-dependent mTOR phosphorylation in BGC, and particularly, the fact that D-Asp treatment mimicked this effect (Zepeda et al., 2009), prompted us to characterize it. As depicted in panel A of Fig. 1, exposure of the cultured cells for 15 min to a fixed 1 mM concentration of either Glu or D-Asp, results in an increase in Ser 2448 mTOR phosphorylation. Note that this effect is reproduced by the transportable inhibitors THA and PDC but not by the non-transportable blocker TBOA, all used at a 100 μM concentration. It should also be noted that [^{3}H] D-Asp is preferred to measure Glu uptake activity in cellular systems since it is not a substrate of glutamine synthase and by these means it is not released from the cells (Gadea et al., 2004; Lau et al., 2010).

We decided to establish the time-dependence of the D-Asp effect. To this end, we exposed BGC to 1 mM D-Asp for different time periods. As clearly shown in panel B of Fig. 1, mTOR phosphorylation is maximal after a 15 min treatment. When the cells were treated with increasing D-Asp concentrations, a clear dose-dependency was found in an apparent EC_{50} of 9.78 μM (Fig. 1, panel C). Note that this value is only indicative of a transporter-mediated effect, since it does not consider the amplification inherent to any signaling cascade (Kholodenko, 2006). As Glu uptake is a Na^+-dependent process, we decided to remove Na^+ from the extracellular medium and replace it with choline chloride, and as depicted in panel D of Fig. 1, this replacement prevents D-Asp and THA effects (Fig. 1, panel D).

3.2. Signaling involved in D-Asp-mediated Ser 2448 mTOR phosphorylation and activation

To delineate the signaling cascade triggered by EAAT-1/GLAST, the sole Glu transporter expressed in cultured chick BGC (Ruiz and Ortega, 1995), we evaluated the involvement of PI-3K. This kinase is upstream of mTORC1 in several systems (Bayascas and Alessi, 2005). As expected, pretreatment of BGC monolayers with the PI-3K inhibitor wortmannin, prevented mTOR phosphorylation. (Fig. 2, panel A). Phosphorylated membrane phosphoinositides become docking sites of proteins with a pleckstrin homology domain (PH), like protein kinase B (PKB). With the use of a selective PKB inhibitor, PKB inhibitor IV (PKBI-IV), we could establish its involvement in EAAT-1/GLAST-dependent mTOR phosphorylation (Fig. 2 panel B). PI-3K activation requires its anchoring to phosphotyrosine residues and the dissociation of its catalytic subunit (p110), therefore EAAT-1/GLAST signaling necessarily leads to the activation of a tyrosine kinase (Vanhaesebroeck et al., 2010). In this context, we have previously characterized a Glu-dependent activation of the non-receptor focal adhesion kinase pp125^{FAK} in this cellular system (Millan et al., 2001; Millan et al., 2004). Such activation requires Ca^{2+} influx and the activity of the non-receptor tyrosine kinase p60^{src}, thus we decided to explore if EAAT-1/GLAST-induced mTOR phosphorylation depends on these two phenomena. To this end, confluent BGC cultures were

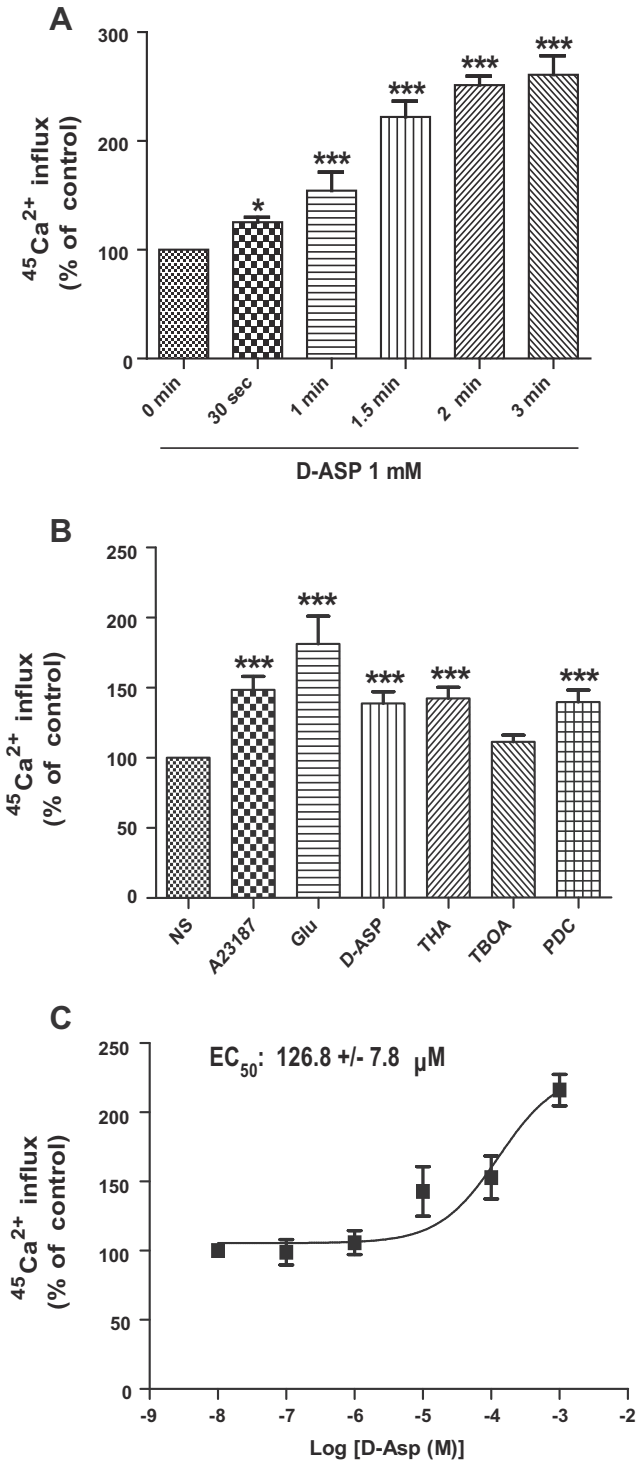

Fig. 3. D-Asp increases Ca^{2+} influx in a time and dose-dependent fashion. Panel A: Cells were incubated with 1 mM of D-Asp and the uptake performed for the indicated time periods (0, 0.5, 1, 1.5, 2 and 3 min). Panel B: $^{45}Ca^{2+}$ influx was assayed in Bergmann glia cells treated with 1 mM of Glu, 1 mM of D-Asp, 100 μM of THA, 100 μM of TBOA or 100 μM of PDC. The Ca^{2+}ionophore A23187 (10 μM) was used as a positive control. Panel C: Monolayers were incubated with increasing D-Asp concentrations (0–1 mM); in all cases, uptake time was 3 min. Graphs represent the mean values +/− standard error from at least three independent experiments in quadruplicate. Statistical analysis was performed comparing against data from non-stimulated cells using a non-parametric one-way ANOVA (Kruskal–Wallis test) and Dunn's pos hoc test (*$p < 0.05$, ***$p < 0.001$).

pre-incubated in a Ca^{2+}-free medium, supplemented with 500 μM EDTA. As shown in panel C of Fig. 2, removal of Ca^{2+} from the extracellular media prevents mTOR phosphorylation. Moreover, the $p60^{src}$ inhibitor PP2 (10 nM) prevents the D-Asp effect (Fig. 2, panel D). As expected, genistein, another tyrosine kinase inhibitor (25 μM) also prevents mTOR phosphorylation (Fig. 2, panel E). Next, in order to provide an evidence of mTORC1 activation, we examined the phosphorylation of one of its substrates, 4EBP1; the results are depicted in panel F of Fig. 2. A robust increase in Thr 70 4EBP1 phosphorylation is obtained after a 15 min exposure to D-Asp or THA. The effect is prevented by 100 nM rapamycin, demonstrating the involvement of mTORC1.

To rule out the participation of Glu receptors in the D-Asp effect, mTOR phosphorylation assays were performed in the presence of the ionotropic and metabotropic Glu receptors antagonists DNQX, LAP5, CPCCOEt and CPPG (AMPA, NMDA, group I mGluR and group II/III mGlu receptors antagonists, respectively). Neither of these antagonists prevented the D-Asp effect (Fig. 2, panels G and H), supporting the notion of an EAAT-1/GLAST mediated signaling that modulates mRNA translation.

3.3. D-Asp-induced $^{45}Ca^{2+}$ influx

The sensitivity of mTOR phosphorylation to the removal of extracellular Ca^{2+} (Fig. 2, panel C), prompted us to characterize a plausible D-Asp-induced $^{45}Ca^{2+}$ influx. Confluent BGC monolayers were exposed for different time periods to a 1 mM D-Asp solution that contained 0.4 μCi/ml of $^{45}Ca^{2+}$. As clearly shown in panel A of Fig. 3, a time-dependent $^{45}Ca^{2+}$ influx is present upon D-Asp exposure. The effect is reproduced by a Ca^{2+} ionophore, A23187 used at a 10 μM concentration, THA (100 μM) and by PDC (100 μM) another transportable inhibitor, that does not interact with Glu receptors (Amin and Pearce, 1997). Note that the non-transportable blocker TBOA fails to elicit a significant Ca^{2+} influx (Fig. 3, panel B). The dose-dependency of the Ca^{2+} influx is shown in panel C of Fig. 3, an apparent EC_{50} of 126.8 μM was obtained, indicative of a ligand–transporter interaction. In order to demonstrate that indeed, EAAT-1/GLAST triggers the Ca^{2+} influx, NaCl was replaced by choline chloride; as depicted in Fig. 4 (panel A), this is sufficient to prevent the Ca^{2+} influx. Moreover, TBOA also blocks D-Asp or THA dependent Ca^{2+} entry (Fig. 4, panel B).

Next, we decided to explore the origin of the Ca^{2+} influx. We hypothesized that the increase in intracellular Na^+ levels due to the Glu transport would lead to the activation of the Na^+/Ca^{2+} exchanger. Two blockers of the Na^+/Ca^{2+} exchanger, Amiloride (10 μM) (Knox and Ajao, 1994) and KB-R7943 (15 μM) (Elias et al., 2001) were used to challenge this possibility. The results shown in Fig. 4C indicate that amiloride reduced to non-significative levels the D-Asp induced $^{45}Ca^{2+}$ influx, whereas the more selective Na^+/Ca^{2+} exchanger blocker KB-R7943, completely abolished

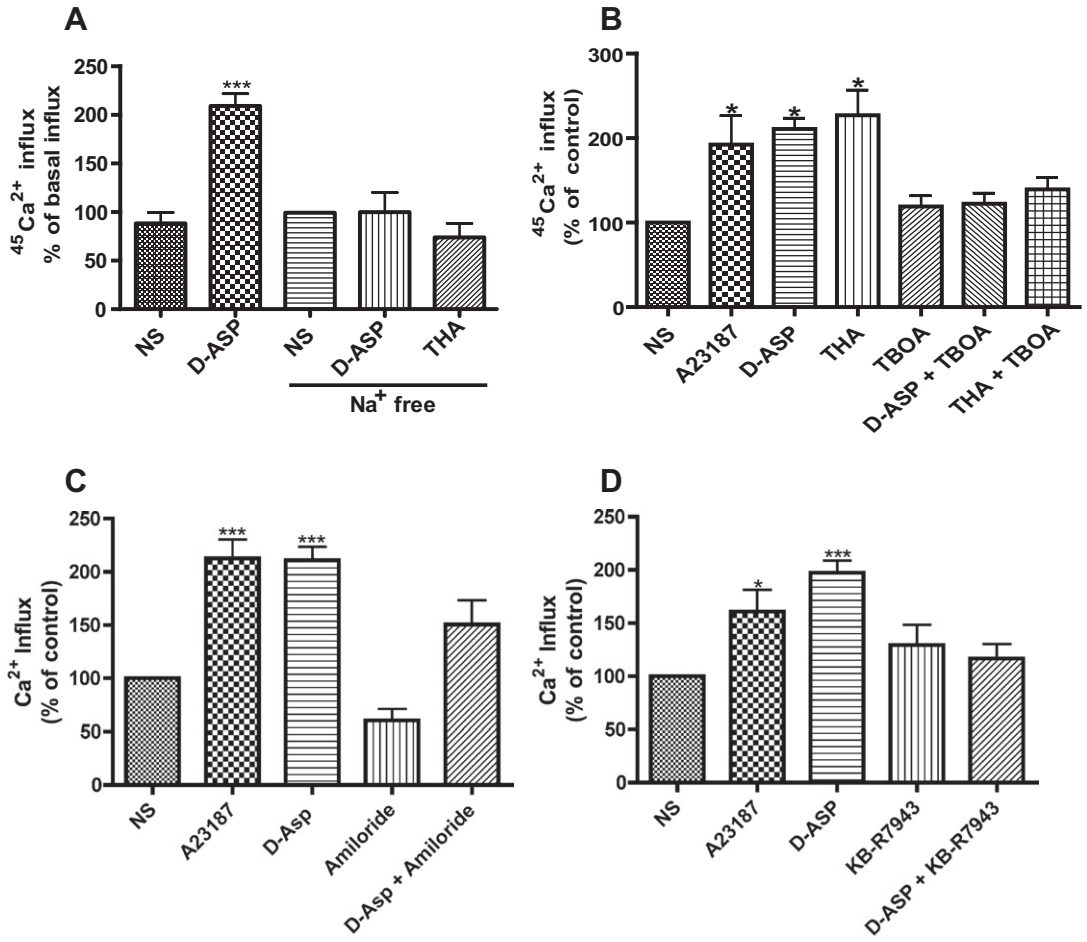

Fig. 4. D-Asp induced $^{45}Ca^{2+}$influx is EAAT-1/GLAST-dependent and involves Na^+/Ca^{2+} exchanger. Panel A: Cells were incubated with 1 mM D-Asp and 100 μM THA in regular or sodium-free assay buffer. The uptake time was 3 min. Panel B: BGC were pre-exposed for 30 min 100 μM to the non-transportable blocker, TBOA and then to 1 mM of D-Asp or 100 μM of THA. The uptake time was 3 min. Confluent BGC monolayers were pre-exposed for 30 min to the Na^+/Ca^{2+} exchanger blockers Amiloride 10 μM (Panel C) or KB-R7943 15 μM (Panel D). In all cases, $^{45}Ca^{2+}$influx was measured as in Fig. 3. Mean values +/− standard error from at least three independent experiments in triplicates. Statistical analysis: non-parametric one-way ANOVA (Kruskal–Wallis test) and Dunn's pos hoc test ($^*p < 0.05$, $^{***}p < 0.001$) against data from non-stimulated controls.

the D-Asp response (Fig. 4, panel D). Therefore one can be confident that the co-transport of Glu and Na^+ leads to the activation of the Na^+/Ca^{2+} exchanger.

3.4. D-Asp-dependent transcriptional regulation

Thus far, the results described suggest that EAAT-1/GLAST signaling is linked to translational control through mTORC1. Nevertheless, it has also been demonstrated that Glu participates in transcriptional control (Lopez-Bayghen and Ortega, 2010; Wang et al., 2007). With this in mind, we explored if the transporter is also linked to transcriptional regulation in BGC. Our first approach consisted to investigate if D-Asp or THA augmented the DNA binding activity of ubiquitous transcription factors, like Fos or Jun. Using an AP-1 sequence present in a BGC expressed gene, the chick kainate binding protein (*chkbp*) (Aguirre et al., 2000), we detected a significant enhancement of the AP-1 DNA binding activity in nuclear extracts prepared form Glu, D-Asp, THA or D-Asp + THA treated cells (Fig. 5, panel A). Note that TBOA prevents this increase and that the signal obtained after the exposure to D-Asp + THA is less prominent than the one obtained when the cells were exposed to either D-Asp or THA, suggesting that both ligands activate a common signaling pathway. The biochemical significance of the latter results, were demonstrated by gene reporter assays, BGC were transfected with an AP-1 responsive construct (TRE–CAT). A dose-dependent increase in the transcriptional activity of the reporter gene was found in the presence of D-Asp (Fig. 5, panel B). Taken together the results presented here demonstrate that the clearance of Glu from the synaptic space initiates a signal transduction cascade that presumably modifies the glial protein repertoire by regulation of the translation and transcription profiles.

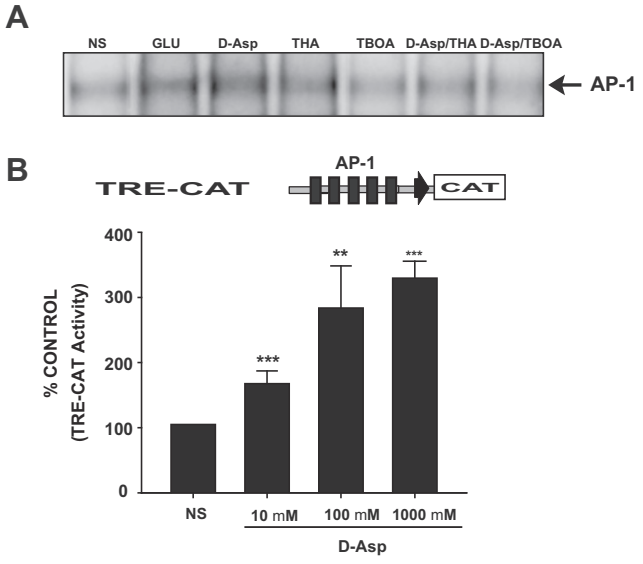

Fig. 5. D-Asp stimulation increases AP-1 DNA binding activity and up regulates an AP-1 driven construct. Panel A: Nuclear extracts were obtained from BGC treated with 1 mM Glu, 1 mM D-Asp, 100 μM THA, 100 μM TBOA, 1 mM D-Asp plus 100 μM THA or 1 mM D-Asp plus 100 μM TBOA. Gel shift assays were performed using a ^{32}P end-labeled probe (*chkbp* promoter AP-1 site, nt 337–329). A typical autoradiogram at least of three experiments is shown. Panel B: The TRE–CAT construct was transfected in BGC monolayers; 16 h post-transfection cells were exposed to the indicated D-Asp concentrations for 30 min. The transcriptional activity was determined as described under Section 2. Results are the mean value +/− the standard error of the mean of at least six independent experiments. Statistical analysis was performed comparing against non-stimulated cell using a non-parametric one-way ANOVA (Kruskal–Wallis test) and Dunn's pos hoc test ($^*p < 0.05$, $^{***}p < 0.001$).

4. Discussion

Neurotransmitter uptake is one of the most important aspects of synaptic transmission, it fact, the existence of a specific uptake system is one of the requisites that any neuroactive substance has to cover to be considered a neurotransmitter. It has been assumed that its physiological role is mainly restricted to the recycling of the neurotransmitter (Holz and Fisher, 2006). Dysfunction of the various transporter systems result in a plethora of neurological and psychiatry disorders ranging from epilepsy to depression (Kanner, 2011; Wankerl et al., 2010). Glu transporters are not the exemption and have also been described to actively participate in the homeostasis of glutamatergic transmission (Danbolt, 2001).

Glial Glu uptake and its rapid transformation into glutamine to complete the Glu/glutamine shuttle provided a biochemical framework for the involvement of these cells in glutamatergic neurotransmission (Shank and Campbell, 1984). Thereafter, the expression and characterization of glia neurotransmitter receptors paved the way into the concept of the tripartite synapse (Araque et al., 1999) and more recently the involvement of the extracellular matrix in synaptic signaling has postulated the so called tetrapartite synapse (Dityatev and Rusakov, 2011). In this context, glia cells associated to glutamatergic synapses respond to synaptic activity via receptors through the generation of Ca^{2+} waves (Muller et al., 1996) and via transporters by the Glu/glutamine shuttle and its associated inward Na^+ current (Owe et al., 2006). Of particular interest, has been glial gene expression regulation by Glu (Balazs, 2006; Gallo and Ghiani, 2000; Lopez-Bayghen and Ortega, 2010; Lopez-Bayghen et al., 2007). During our studies on the involvement of mTOR in Glu-dependent translational control in cultured BGC, we realized that part of the response was not sensitive to Glu receptors antagonists and decided to explore whether EAAT-1/GLAST, the unique Glu transporter present in these cells, was involved. A D-Asp mediated mTOR phosphorylation was found although not characterized at that time (Zepeda et al., 2009).

In an effort to fully understand these findings and to link a transporter-inward Na^+ current to a lasting response, we analyzed D-Asp-dependent translational and transcriptional regulation. We chose mTOR as an index of translational control and AP-1 DNA binding and gene reporter assays as a demonstration of transcriptional regulation. Both levels of gene expression regulation are affected by EAAT-1/GLAST in a Na^+ and Ca^{2+}-dependent manner involving PI3-K/PKB/mTOR/4EBP1/AP-1 signaling components (Aguirre et al., 2002). One could argue that neither D-Asp nor THA, TBOA or PDC are specific enough to rule out the involvement of other transporters such as GLT-1 (EAAT-2) in the described D-Asp effects. This suggestion is unlikely since BGC harbor exclusively EAAT-1/GLAST and the reported IC_{50} for dihidrokainate, a specific GLT-1 blocker is >3 mM (Ruiz and Ortega, 1995).

What could be the physiological relevance of a transporter-mediated signaling cascade in cells that express functional Glu receptors? It is difficult to have a precise answer to this question at this moment. Nevertheless, it is important to mention that exposure of mouse cerebellar slices to Glu induces inward Na^+ currents accompanied by an increase in intracellular Na^+ concentration that is marginally sensitive to CNQX but inhibited by TBOA. Furthermore, the same scenario is present upon electrical stimulation of the parallel fibers (Kirischuk et al., 2007). It is tempting to speculate that the signaling triggered by the transporters, having slower inactivation kinetics (Bazille et al., 2005) are linked to sustained biochemical responses involved in the expression of polypeptides that participate in neuron/glia coupling, such as the Na^+/K^+ ATPase that allows glia cells to clear efficiently the synaptic space. In support of this idea, is the fact that EAAT-1/GLAST associates with this plasma membrane ATPase and even, operates as an unit (Rose

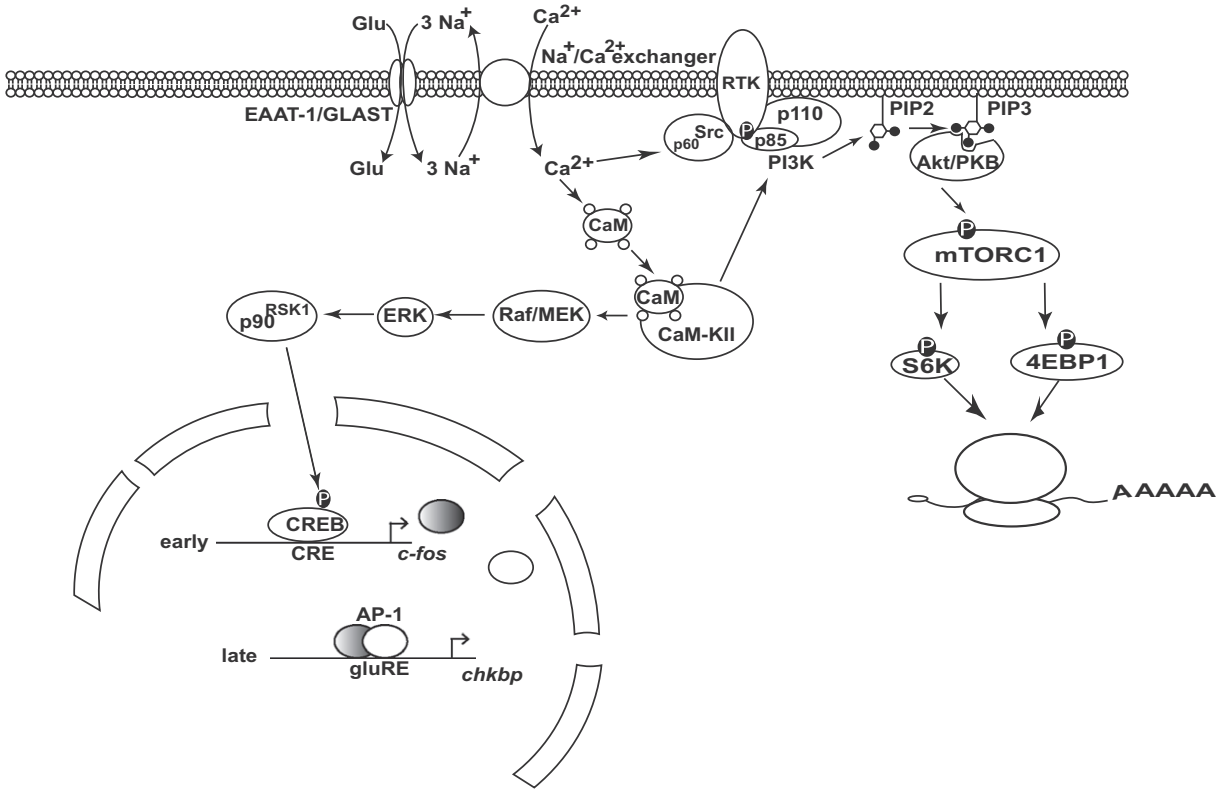

Fig. 6. Current model for EAAT-1/GLAST signaling in cultured Bergmann glia cells. Glu clearance leads to Na^+ influx, which activates the Na^+/Ca^{2+} exchanger resulting in an increase in intracellular Ca^{2+} levels, leading to the activation of a tyrosine kinase receptor (RTK) and resulting in the docking of PI3-K and $p60^{src}$. Phosphorylated phosphatidyl inositol (PIP2) recruits pleckstrin-motif containing proteins like PKB that phosphorylates mTOR, with the eventual $p70^{S6K}$ (Gonzalez-Mejia et al., 2006) and 4EBP-1 phosphorylation increasing protein synthesis. Alternatively, increased Ca^{2+} intracellular levels augments AP-1 DNA binding and this leads to the transcriptional activity of a TRE–CAT, most possibly through a Ca^{2+}/calmodulin (CaM)/Extracellular regulated kinase (ERK)/$p90^{RSK}$/CREB cascade (Aguirre et al., 2002).

et al., 2009). Other glia proteins, which expression might be regulated through the activity of the transporters are those that participate either in the Glu/glutamine shuttle like glutamine synthetase (GS) and the sodium-coupled neutral amino acid transporters (SNAT) or in the astrocyte/neuron lactate shuttle like the monocarboxylate transporters (Pellerin et al., 2007). Work currently in progress in our lab is aimed in this direction.

In conclusion, Glu transactions in glia cells are mediated through Glu receptors and transporters. From a biochemical perspective, the specificity of the cascades has started to be elucidated. A model of our present findings is depicted in Fig. 6.

Acknowledgements

This work was supported by Grants from Conacyt-Mexico (79502 and 123625) and Fundación Pandea-Mexico to A.O. Z.M.-L. is supported by Conacyt-Mexico fellowship. The technical assistance of Luis Cid and Blanca Ibarra is acknowledged.

Appendix A. Supplementary data

Supplementary data associated with this article can be found, in the online version, at doi:10.1016/j.neuint.2011.07.015.

References

Aguirre, A., Lopez-Bayghen, E., Ortega, A., 2002. Glutamate-dependent transcriptional regulation of the chkbp gene: signaling mechanisms. J. Neurosci. Res. 70, 117–127.

Aguirre, A., Lopez, T., Lopez-Bayghen, E., Ortega, A., 2000. Glutamate regulates kainate-binding protein expression in cultured chick Bergmann glia through an activator protein-1 binding site. J. Biol. Chem. 275, 39246–39253.

Amin, N., Pearce, B., 1997. Glutamate toxicity in neuron-enriched and neuron-astrocyte co-cultures: effect of the glutamate uptake inhibitor L-trans-pyrrolidine-2,4-dicarboxylate. Neurochem. Int. 30, 271–276.

Araque, A., Parpura, V., Sanzgiri, R.P., Haydon, P.G., 1999. Tripartite synapses: glia, the unacknowledged partner. Trends Neurosci. 22, 208–215.

Balazs, R., 2006. Trophic effect of glutamate. Curr. Top Med. Chem. 6, 961–968.

Barrera, I., Flores-Mendez, M., Hernandez-Kelly, L.C., Cid, L., Huerta, M., Zinker, S., Lopez-Bayghen, E., Aguilera, J., Ortega, A., 2010. Glutamate regulates eEF1A phosphorylation and ribosomal transit time in Bergmann glial cells. Neurochem. Int. 57, 795–803.

Bayascas, J.R., Alessi, D.R., 2005. Regulation of Akt/PKB Ser473 phosphorylation. Mol. Cell 18, 143–145.

Bazille, C., Megarbane, B., Bensimhon, D., Lavergne-Slove, A., Baglin, A.C., Loirat, P., Woimant, F., Mikol, J., Gray, F., 2005. Brain damage after heat stroke. J. Neuropathol. Exp. Neurol. 64, 970–975.

Bradford, M.M., 1976. A rapid and sensitive method for the quantitation of microgram quantities of protein utilizing the principle of protein-dye binding. Anal. Biochem. 72, 248–254.

Cammalleri, M., Lutjens, R., Berton, F., King, A.R., Simpson, C., Francesconi, W., Sanna, P.P., 2003. Time-restricted role for dendritic activation of the mTOR-p70S6K pathway in the induction of late-phase long-term potentiation in the CA1. Proc. Natl. Acad. Sci. USA 100, 14368–14373.

Coutinho, V., Knopfel, T., 2002. Metabotropic glutamate receptors: electrical and chemical signaling properties. Neuroscientist 8, 551–561.

Danbolt, N.C., 2001. Glutamate uptake. Prog. Neurobiol. 65, 1–105.

Dityatev, A., Rusakov, D.A., 2011. Molecular signals of plasticity at the tetrapartite synapse. Curr. Opin. Neurobiol. 21, 353–359.

Elias, C.L., Lukas, A., Shurraw, S., Scott, J., Omelchenko, A., Gross, G.J., Hnatowich, M., Hryshko, L.V., 2001. Inhibition of Na+/Ca2+ exchange by KB-R7943: transport mode selectivity and antiarrhythmic consequences. Am. J. Physiol. Heart Circ. Physiol. 281, H1334–H1345.

Eulenburg, V., Gomeza, J., 2010. Neurotransmitter transporters expressed in glial cells as regulators of synapse function. Brain Res. Rev. 63, 103–112.

Foster, K.G., Fingar, D.C., 2010. Mammalian target of rapamycin (mTOR): conducting the cellular signaling symphony. J. Biol. Chem. 285, 14071–14077.

Gadea, A., Lopez, E., Lopez-Colome, A.M., 2004. Glutamate-induced inhibition of D-aspartate uptake in Muller glia from the retina. Neurochem. Res. 29, 295–304.

Gallo, V., Ghiani, C.A., 2000. Glutamate receptors in glia: new cells, new inputs and new functions. Trends Pharmacol. Sci. 21, 252–258.

Gegelashvili, M., Rodriguez-Kern, A., Sung, L., Shimamoto, K., Gegelashvili, G., 2007. Glutamate transporter GLAST/EAAT1 directs cell surface expression of FXYD2/

gamma subunit of Na, K-ATPase in human fetal astrocytes. Neurochem. Int. 50, 916–920.
Gonzalez-Mejia, M.E., Morales, M., Hernandez-Kelly, L.C., Zepeda, R.C., Bernabe, A., Ortega, A., 2006. Glutamate-dependent translational regulation in cultured Bergmann glia cells: involvement of p70S6K. Neuroscience 141, 1389–1398.
Gonzalez, M.I., Ortega, A., 2000. Regulation of high-affinity glutamate uptake activity in Bergmann glia cells by glutamate. Brain Res. 866, 73–81.
Holz, R.W., Fisher, S.K., 2006. Synaptic transmission and cellular signaling: an overview. In: Siegel, G., Wayne, A.R., Brady, S., Price, D. (Eds.), Basic Neurochemistry: Molecular, Cellular and Medical Aspects. Elsevier Academic Press, Canada, pp. 167–181.
Hollmann, M., Heinemann, S., 1994. Cloned glutamate receptors. Annu. Rev. Neurosci. 17, 31–108.
Hu, D., Serrano, F., Oury, T.D., Klann, E., 2006. Aging-dependent alterations in synaptic plasticity and memory in mice that overexpress extracellular superoxide dismutase. J. Neurosci. 26, 3933–3941.
Kanner, A.M., 2011. Depression and epilepsy: a bidirectional relation? Epilepsia 52 (Suppl. 1), 21–27.
Kholodenko, B.N., 2006. Cell-signalling dynamics in time and space. Nat. Rev. Mol. Cell Biol. 7, 165–176.
Kirischuk, S., Kettenmann, H., Verkhratsky, A., 2007. Membrane currents and cytoplasmic sodium transients generated by glutamate transport in Bergmann glial cells. Pflugers Arch. 454, 245–252.
Knox, A.J., Ajao, P., 1994. The effect of inhibitors of Na/H exchange and Na/Ca exchange on airway smooth muscle contractility. Pulm. Pharmacol. 7, 99–102.
Lau, C.L., Beart, P.M., O'Shea, R.D., 2010. Transportable and non-transportable inhibitors of L-glutamate uptake produce astrocytic stellation and increase EAAT2 cell surface expression. Neurochem. Res. 35, 735–742.
Lopez-Bayghen, E., Ortega, A., 2010. Glial cells and synaptic activity: translational control of metabolic coupling. Rev. Neurol. 50, 607–615.
Lopez-Bayghen, E., Rosas, S., Castelan, F., Ortega, A., 2007. Cerebellar Bergmann glia: an important model to study neuron-glia interactions. Neuron. Glia Biol. 3, 155–167.
Lopez-Bayghen, E., Vega, A., Cadena, A., Granados, S.E., Jave, L.F., Gariglio, P., Alvarez-Salas, L.M., 1996. Transcriptional analysis of the 5'-noncoding region of the human involucrin gene. J. Biol. Chem. 271, 512–520.
Maragakis, N.J., Dietrich, J., Wong, V., Xue, H., Mayer-Proschel, M., Rao, M.S., Rothstein, J.D., 2004. Glutamate transporter expression and function in human glial progenitors. Glia 45, 133–143.
Millan, A., Aguilar, P., Mendez, J.A., Arias-Montano, J.A., Ortega, A., 2001. Glutamate activates PP125(FAK) through AMPA/kainate receptors in Bergmann glia. J. Neurosci. Res. 66, 723–729.
Millan, A., Arias-Montano, J.A., Mendez, J.A., Hernandez-Kelly, L.C., Ortega, A., 2004. Alpha-amino-3-hydroxy-5-methyl-4-isoxazolepropionic acid receptors signaling complexes in Bergmann glia. J. Neurosci. Res. 78, 56–63.
Muller, T., Moller, T., Neuhaus, J., Kettenmann, H., 1996. Electrical coupling among Bergmann glial cells and its modulation by glutamate receptor activation. Glia 17, 274–284.
Ortega, A., Eshhar, N., Teichberg, V.I., 1991. Properties of kainate receptor/channels on cultured Bergmann glia. Neuroscience 41, 335–349.
Owe, S.G., Marcaggi, P., Attwell, D., 2006. The ionic stoichiometry of the GLAST glutamate transporter in salamander retinal glia. J. Physiol. 577, 591–599.
Pellerin, L., Bouzier-Sore, A.K., Aubert, A., Serres, S., Merle, M., Costalat, R., Magistretti, P.J., 2007. Activity-dependent regulation of energy metabolism by astrocytes: an update. Glia 55, 1251–1262.
Pittenger, C., Kandel, E., 1998. A genetic switch for long-term memory. C. R. Acad. Sci. III 321, 91–96.
Proud, C.G., 2007. Cell signaling. mTOR, unleashed. Science 318, 926–927.
Rose, E.M., Koo, J.C., Antflick, J.E., Ahmed, S.M., Angers, S., Hampson, D.R., 2009. Glutamate transporter coupling to Na, K-ATPase. J. Neurosci. 29, 8143–8155.
Ruiz, M., Ortega, A., 1995. Characterization of an Na(+)-dependent glutamate/aspartate transporter from cultured Bergmann glia. Neuroreport 6, 2041–2044.
Sabatini, D.M., 2006. MTOR and cancer: insights into a complex relationship. Nat. Rev. Cancer 6, 729–734.
Shank, R.P., Campbell, G.L., 1984. Glutamine, glutamate, and other possible regulators of alpha-ketoglutarate and malate uptake by synaptic terminals. J. Neurochem. 42, 1162–1169.
Swanson, D.B., 2005. Astrocyte neurotransmitter uptake. In: Kettenmann, H., Ransom, B.R. (Eds.), Neuroglia. OUP, Oxford, pp. 346–354.
Vanhaesebroeck, B., Guillermet-Guibert, J., Graupera, M., Bilanges, B., 2010. The emerging mechanisms of isoform-specific PI3K signalling. Nat. Rev. Mol. Cell Biol. 11, 329–341.
Wang, J.Q., Fibuch, E.E., Mao, L., 2007. Regulation of mitogen-activated protein kinases by glutamate receptors. J. Neurochem. 100, 1–11.
Wankerl, M., Wust, S., Otte, C., 2010. Current developments and controversies: does the serotonin transporter gene-linked polymorphic region (5-HTTLPR) modulate the association between stress and depression? Curr. Opin. Psych. 23, 582–587.
Zepeda, R.C., Barrera, I., Castelan, F., Suarez-Pozos, E., Melgarejo, Y., Gonzalez-Mejia, E., Hernandez-Kelly, L.C., Lopez-Bayghen, E., Aguilera, J., Ortega, A., 2009. Glutamate-dependent phosphorylation of the mammalian target of rapamycin (mTOR) in Bergmann glial cells. Neurochem. Int. 55, 282–287.

ASN NEURO RESEARCH ARTICLE

ASN NEURO 4(5):art:e00095.doi:10.1042/AN20120022

Glutamate transporter-dependent mTOR phosphorylation in Müller glia cells

Ana María López-Colomé*, Zila Martínez-Lozada†, Alain M Guillem†, Edith López* and Arturo Ortega†1

*División de Neurociencias, Instituto de Fisiología Celular, Universidad Nacional Autónoma de México, México D.F., México

†Departamento de Genética y Biología Molecular, Centro de Investigación y de Estudios Avanzados del Instituto Politécnico Nacional, Apartado Postal 14-740, México D.F. 07000, México

Cite this article as: López-Colomé AM, Martínez-Lozada Z, Guillem AM, López E and Ortega A (2012) Glutamate transporter-dependent mTOR phosphorylation in Müller glia cells. ASN NEURO 4(5):art:e00095.doi:10.1042/AN20120022

ABSTRACT

Glu (glutamate), the excitatory transmitter at the main signalling pathway in the retina, is critically involved in changes in the protein repertoire through the activation of signalling cascades, which regulate protein synthesis at transcriptional and translational levels. Activity-dependent differential gene expression by Glu is related to the activation of ionotropic and metabotropic Glu receptors; however, recent findings suggest the involvement of Na^+-dependent Glu transporters in this process. Within the retina, Glu uptake is aimed at the replenishment of the releasable pool, and for the prevention of excitotoxicity and is carried mainly by the GLAST/EAAT-1 (Na^+-dependent glutamate/aspartate transporter/excitatory amino acids transporter-1) located in Müller radial glia. Based on the previous work showing the alteration of GLAST expression induced by Glu, the present work investigates the involvement of GLAST signalling in the regulation of protein synthesis in Müller cells. To this end, we explored the effect of D-Asp (D-aspartate) on Ser-2448 mTOR (mammalian target of rapamycin) phosphorylation in primary cultures of chick Müller glia. The results showed that D-Asp transport induces the time- and dose-dependent phosphorylation of mTOR, mimicked by the transportable GLAST inhibitor THA (threo-β-hydroxyaspartate). Signalling leading to mTOR phosphorylation includes Ca^{2+} influx, the activation of $p60^{src}$, phosphatidylinositol 3-kinase, protein kinase B, mTOR and $p70^{S6K}$. Interestingly, GLAST activity promoted AP-1 (activator protein-1) binding to DNA, supporting a function for transporter signalling in retinal long-term responses. These results add a novel receptor-independent pathway for Glu signalling in Müller glia, and further strengthen the critical involvement of these cells in the regulation of glutamatergic transmission in the retina.

Key words: excitatory amino acid, gene expression regulation, signalling.

INTRODUCTION

Glu (glutamate), the main excitatory neurotransmitter in the radial signalling pathway of the vertebrate retina (Massey and Miller, 1990), regulates proliferation, migration and survival of neuronal progenitors and immature neurons (Guerrini et al., 1995). It also plays a key role in the regulation of gene expression required for physiological adaptive processes, including synaptic plasticity (Thomas and Huganir, 2004; Wang et al., 2007).

The ability of Glu to drive a diversity of functions relates to its interaction with a wide variety of receptor subtypes and transporters that act independently or in combination to attain differential responses. Glutamatergic activity is mediated by iGluRs (ionotropic receptors) and mGluRs (G-protein-coupled metabotropic receptors). The superfamily of iGluRs includes the Na^+- or Ca^{2+}-permeable cation channels NMDA (*N*-methyl-D-aspartate), AMPA (α-amino-3-hydroxy-5-methylisoxazole-4-propionic acid) and KA (kainite) receptors. Eight mGluRs, linked to the activation of second messenger cascades, have been identified (Michaelis, 1998), coupled to the stimulation of phospholipase C and the release of intracellular Ca^{2+} (Group I), or to the inhibition of adenylyl cyclase (Groups II and III) (Coutinho and Knopfel, 2002).

Glia cells respond to neurotransmitters through the activation of specific receptors and intracellular pathways,

[1]To whom correspondence should be addressed (email arortega@cinvestav.mx).

Abbreviations: AMPA, α-amino-3-hydroxy-5-methylisoxazole-4-propionic acid; AP-1, activator protein-1, EAAT1-5, excitatory amino acids transporters 1-5; 4E-BP, 4E-binding protein; GLAST, Na^+-dependent glutamate/aspartate transporter; iGluR, ionotropic receptor; KA, kainite; MGC, Müller glia cells; mGluRs, G-protein-coupled metabotropic receptors; mTOR, mammalian target of rapamycin; NMDA, *N*-methyl-D-aspartate; PBS, phosphate-buffer saline; PDC, L-*trans*-pyrrolidine-2,4-dicarboxylic acid; PKB/Akt, protein kinase B; $p70^{S6K}$, 70 kDa S6 ribosomal kinase; RTK, receptor tyrosine kinase; Src, non-receptor tyrosine kinase $p60^{src}$; T3MG, ($\pm$)-threo-3-methylglutamic acid; THA, threo-β-hydroxyaspartate.

which directly or indirectly modify the neuronal activity (Fields and Stevens-Graham, 2002). Among its functions, MGC (Müller glia cells), the main type of retinal glia, are responsible for potassium homoeostasis, lactate supply to neurons, pH regulation and neurotransmitter removal (Hollander et al., 1991; Lopez-Colome and Romo-de-Vivar, 1991; Rauen and Kanner, 1994; Lopez et al., 1997; Bringmann et al., 2009).

Owing to their close apposition to synaptic contacts in both plexiform layers of the retina, MGC are exposed to synaptically released Glu, and are involved in the recycling of Glu through the Glu/glutamine neuron–glia shuttle, which provides Glu supply to the presynaptic terminals. Also along this line, the activation of Glu receptors in Müller cells feeds back on to neurons by triggering the release of neuroactive compounds (Uchihori and Puro, 1993; Lopez-Colome et al., 1995; Lopez et al., 1998; Lopez-Bayghen et al., 2006).

mTOR (mammalian target of rapamycin), now officially known as mechanistic TOR, is a protein kinase involved in the regulation of a wide range of cellular processes including protein synthesis, gene transcription, the cell cycle and autophagy (Proud, 2007; Laplante and Sabatini, 2012), and it has been implicated in cancer and other diseases, as well as in the control of lifespan and aging (Blagosklonny, 2010). mTOR forms the catalytic core of two different complexes: mTOR complex 1 (mTORC1) and mTOR complex 2 (mTORC2) that differ in composition; while complex 1 contains raptor, complex 2 is composed of rictor, Sin1 and protor. Both complexes contain mLST8 (Wang and Proud, 2011). mTORC1 but not mTORC2 is inhibited by a low concentration of the macrolide rapamycin; in an over-simplified scenario, mTORC1 mediates the mTOR effects that are rapamycin-sensitive. An accepted index of mTOR activation is Ser-2448 phosphorylation as the result of a signalling cascade involving PI3K (phosphoinositide 3-kinase), PDK1 (phosphoinositide-dependent kinase 1), mTORC2 and PKB/Akt (protein kinase B), which can phosphorylate mTORC1 (Foster and Fingar, 2010). Phosphorylated mTORC1 acts on $p70^{S6K}$ (70 kDa S6 ribosomal kinase), 4E-BP (4E-binding protein), eEF2K (eukaryotic elongation factor 2 kinase) and eEF1A (eukaryotic elongation factor 1A), increasing translation. It should be noted that $p70^{S6K}$ also phosphorylates mTOR at Ser-2448, which is assumed to be an additional level of mTOR regulation (Rosner and Hengstschlager, 2010).

Glu concentration at the synaptic cleft requires tight regulation in order to avoid excitotoxic neuronal death (Mattson, 2003; Olney, 2003). Such regulation is accomplished through the removal of Glu by a family of Na^+-dependent transporters expressed in neurons and glia (Danbolt, 2001). To date, five subtypes of transporters known as EAAT1–5 (excitatory amino acids transporters 1–5) have been reported. The glia transporters EAAT-1 [GLAST (Na^+-dependent glutamate/aspartate transporter)] and EAAT-2 (GLT-1) are responsible for more than 90% of the Glu uptake in the brain. In the retina, although the expression of EAAT-4 has been reported (Fyk-Kolodziej et al., 2004), GLAST, located in Müller cells, is the predominant transporter responsible for Glu reuptake (Gadea et al., 2004).

Evidence has accumulated suggesting that Glu transporters might be involved in intracellular signalling. In fact, Glu and transportable blockers down-regulate Glu uptake in a receptor-independent manner (Gonzalez and Ortega, 2000; Gadea et al., 2004). Furthermore, the coupling of GLAST/EAAT-1 activity to the Na^+/K^+ ATPase in astrocytes (Gegelashvili et al., 2007; Rose et al., 2009) and to the promotion of mTOR phosphorylation in cerebellar glia (Zepeda et al., 2008) has also been reported.

Dysfunction of EAATs is specifically involved in excitotoxic neuronal death under pathological neurodegenerative conditions and ischaemic stroke injury, characterized by the elevation of extracellular Glu. Hence, the characterization of signalling mechanisms activated by transporter function may provide tools for the modulation of EAAT function under pathological conditions.

In order to provide evidence for GLAST/EAAT-1-mediated Glu signalling in the vertebrate retina, we analysed transporter-dependent mTOR phosphorylation in primary cultures of chick MGC. Our results show that GLAST activity triggers Ca^{2+} influx, and increases mTOR phosphorylation and AP-1 (activator protein-1) DNA-binding activity, suggesting that Glu imbalance could alter the translation of proteins involved in gene regulation in the retina.

MATERIALS AND METHODS

Materials

Tissue culture reagents were obtained from GE Healthcare. Wortmannin, amiloride [3,5-diamino-6-chloro-*N*-(diaminomethylene)pyrazine-2-carboxamide], PP2 {4-amino-5-(4-chlorophenyl)-7-(dimethylethyl)pyrazolo[3,4-*d*]pyrimidine}, W7 [N-(6-aminohexyl)-5-chloro-1-naphthalenesulfonamide], AMPA, KA acid, NMDA, CNQX (6-cyano-7-nitroquinoxaline-2,3-dione), DL-TBOA (DL-threo-b-benzyloxyaspartic acid), THA (threo-β-hydroxyaspartate), D-Asp and Glu were all obtained from Tocris-Cookson. $^{45}Ca^{2+}$ and [α^{32}P]dATP was from PerkinElmer. Polyclonal anti-phospho-mTOR (Ser-2448) and anti-mTOR antibodies (05-235) were purchased from Cell Signalling Technology. Anti-phospho-$p60^{src}$ (Tyr-527) was obtained from Abcam. Horseradish peroxidase-linked anti-rabbit antibodies and the enhanced chemiluminescence reagent (ECL) were obtained from Amersham Biosciences. PDC (L-*trans*-pyrrolidine-2,4-dicarboxylic acid), T3MG [(±)-threo-3-methylglutamic acid] and all other chemicals were purchased from Sigma.

Cell culture and stimulation protocol

Primary cultures of retina MGC were prepared from 7-day-old chick embryos as previously described (Lopez-Colome

et al., 1993). The cells were plated in 6- or 24-well plastic culture dishes in OptiMEM containing 4% foetal bovine serum, 2 mM glutamine and gentamicin (50 μg/ml) and used on the 10th to the 12th day in the culture. Before any treatment, confluent monolayers were serum-deprived with 0.5% bovine serum albumin in OptiMEM for 30 min and then treated as indicated. Inhibitors were included 30 min prior to agonist addition. Glu and its analogues were added to the medium for the indicated time periods; following treatment, the medium was replaced by 0.5% albumin/OptiMEM.

SDS/PAGE and Western blots

Cells from confluent monolayers were harvested in PBS (phosphate-buffered saline) (10 mM K_2HPO_4/KH_2PO_4, 150 mM NaCl, pH 7.4) containing phosphatase inhibitors (10 mM NaF, 1 mM Na_2MoO_4 and 1 mM Na_3VO_4). The cells were lysed with RIPA buffer (50 mM Tris/HCl, 1 mM EDTA, 150 mM NaCl, 1 mM PMSF, 1 mg/ml aprotinin, 1 mg/ml leupeptin, 1% NP-40, 0.25% sodium deoxycolate, 10 mM NaF, 1 mM Na_2MoO_4 and 1 mM Na_3VO_4, pH 7.4). Cell lysates were denatured in Laemmli's buffer, and proteins resolved by SDS/PAGE (6–10% gel) and electroblotted on to nitrocellulose membranes. Blots were stained with Ponceau S to confirm that protein content was equal in all lanes. Membranes were soaked in PBS to remove the Ponceau S and incubated in 50 mM Tris/HCl, pH 7.4, and 150 mM NaCl (TBS) containing 5% dried skimmed milk and 0.1% Tween 20 for 60 min to block the excess of non-specific protein binding sites. The membranes were then incubated overnight at 4°C with the primary antibodies indicated in each Figure, followed by the corresponding secondary antibodies. Immunoreactive polypeptides were detected by chemiluminescence and exposed to X-ray films. Densitometric analyses were performed and data were analysed with Prism from GraphPad Software.

$^{45}Ca^{2+}$ Influx

Confluent MGC monolayers seeded in 24-well plates were washed three times to remove all non-adhering cells with 0.5 ml aliquots of solution A containing 25 mM Hepes/Tris, 130 mM NaCl, 5.4 mM KCl, 1.8 mM $CaCl_2$, 0.8 mM $MgCl_2$, 33.3 mM glucose and 1 mM NaH_2PO_4 at pH 7.4. The Glu- or D-Asp-induced $^{45}Ca^{2+}$ influx was initiated at $t=0$ by the addition of 0.5 ml of solution A containing 1.5 μCi of $^{45}Ca^{2+}$/ml solution A, Glu or D-Asp at a given concentration. When tested, inhibitors or modulators were included 30 min prior to the addition of $^{45}Ca^{2+}$. The reaction was stopped by aspirating the radioactive medium and washing each well within 15 s with 0.5 ml aliquots of an ice-cold solution A. The cells were digested in 0.5 ml of 1 M NaOH for 2 h at 37°C. The radioactivity contained in each fraction was determined using a Beckmann 7800LS scintillation counter in the presence of a scintillation cocktail. All experiments were performed in triplicate.

EMSAs (electrophoretic mobility-shift assays)

After the stimulation period, the cells were shifted to complete culture media for 1 h and nuclear extracts were prepared as described previously (Zepeda et al., 2008). All the buffers contained a protease inhibitor cocktail to prevent nuclear factor proteolysis. Protein concentration was measured using the Bradford method. Nuclear extracts (approximately 20 μg) from control or treated MGC were incubated on ice with 500 ng of poly[(dI-dC)] as non-specific competitor (LG Healthcare) and 1 ng of [^{32}P]-end labelled double-stranded AP-1 (SV40) oligonucleotide: 5′-CTAGTTCC-GGCTGAGTCATCAAGC-3′

The reaction mixtures were incubated for 20 min on ice, and the proteins were separated by electrophoresis in SDS/PAGE (6% gels) in a low ionic strength 0.5X TBE buffer. The gels were vacuum-dried and exposed to an auto-radiographic film overnight.

Statistical analysis

Data are expressed as the mean (average) ± standard error (S.E.). A one-way analysis of variance (ANOVA) (Kruskal–Wallis test) and Dunn's post-hoc test were performed to determine significant differences between conditions with the Prism software.

RESULTS

Glu- and D-Asp-induced mTOR phosphorylation in MGCs

mTOR is a fundamental kinase involved in translational control, the fine-tuning process of gene expression. As Glu is known to modify this process, we investigated a possible Glu transport-mediated change in mTOR phosphorylation pattern in retinal MGC. As depicted in Figure 1(A), inclusion of 1 mM Glu induced a fast time-dependent increase in Ser-2448 mTOR phosphorylation, reaching a maximal value at 15 min. No apparent changes in mTOR levels were observed in this condition. The results presented in Figure 1(B) show that a time-dependent increase in mTOR phosphorylation by Glu was also induced by 1 mM D-Asp. The return of mTOR phosphorylation to basal levels in both conditions suggests a Glu- or D-Asp-dependent $p70^{S6K}$ dephosphorylation that through a feedback loop would decrease mTOR Ser-2448 phosphorylation (Harrington et al., 2004; Um et al., 2004; Rosner and Hengstschlager, 2010).

Exposure of MGC cultures to increasing concentrations of D-Asp for 15 min reveals a clear dose-dependency with an apparent EC_{50} of 15.2 μM (Figure 1C), indicating the specificity of the effect. It should be noted that this value is only indicative of a receptor/transporter-mediated effect,

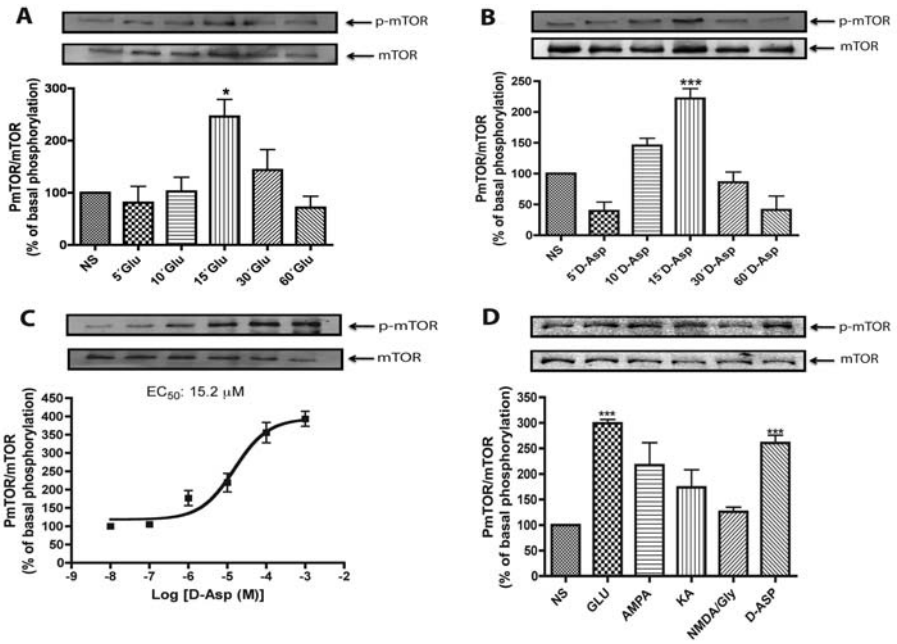

Figure 1 **D-Asp induces Ser-2448 mTOR phosphorylation**

(**A**) MGC were treated with 1 mM Glu for the indicated time periods, and the level of total and Ser-2448 phosphorylated mTOR were analysed by Western blot as described in the Materials and methods section. (**B**) Confluent MGC monolayers were treated with 1 mM D-Asp for the indicated time periods. The level of mTOR phosphorylation was determined as described for (**A**). (**C**) Müller glia cultures were exposed for 15 min to increasing D-Asp concentrations; the EC_{50} was calculated from the densitometric analysis using the Prism program (GraphPad). (**D**) Cells were incubated for 15 min with vehicle (NS), Glu (1 mM) or the Glu analogues AMPA (1 mM), KA (1 mM), NMDA (1 mM) plus 10 μM glycine (NMDA/Gly), and D-Asp (1 mM). The results are presented as the mean ±S.E. of at least three independent experiments. In each panel, a representative Western blot is shown. Statistical analysis was performed comparing against non-stimulated cells using a non-parametric one-way ANOVA (Kruskal–Wallis test) and Dunn's post-hoc test (*$P<0.05$, ***$P<0.001$).

as it does not take into consideration the amplification inherent to signalling cascades (Kholodenko, 2006).

In order to discard the contribution of Glu receptors to the observed effects, the cells were treated with 1 mM of the specific ionotropic receptor agonists: AMPA, KA and NMDA plus glycine (10 μM). A discrete non-significant increase in mTOR phosphorylation by AMPA and KA was detected (Figure 1D), suggesting that the transporter activity is responsible for most, if not all, of the Glu-induced mTOR phosphorylation.

In order to confirm these results, MGC were treated for 30 min, prior to D-Asp or THA addition, with 50 μM of the non-NMDA iGluR antagonist CNQX (Figure 2A), the NMDA receptor antagonist MK-801, the group I mGluR antagonist LAP5, or with CPCCOEt, the group II/III mGluR antagonist (Figures 2B and 2C). The results showed that Glu receptor antagonists failed to block the increase in mTOR phosphorylation induced by D-Asp or THA, further supporting the fact that the effect of Glu on mTOR is mainly transporter-mediated. Moreover, as D-Asp does not activate Glu receptors, the lack of a statistically significant difference between the Glu- and D-Asp-induced effects further indicates that mTOR phosphorylation is transporter-mediated.

GLAST/EAAT-1-dependent mTOR phosphorylation

In order to directly confirm that the D-Asp-induced increase in mTOR phosphorylation relies on GLAST/EEAT-1 transport activity, the effect of transportable and non-transportable GLAST inhibitors was analysed. As shown in Figure 3(A), D-Asp-induced increase in mTOR phosphorylation was mimicked by 100 μM of the transportable inhibitors THA and PDC. In contrast, the non-transportable inhibitor TBOA (100 μM) had no effect. As the expression of EAAT-4 in MGC has been recently reported (Fyk-Kolodziej et al., 2004), we evaluated the involvement of this transporter in mTOR phosphorylation. As clearly shown in Figure 3(B), pretreatment with the specific EAAT-4 blocker T3MG did not alter the D-Asp response, ruling out the participation of EAAT-4.

If, indeed, the effect of D-Asp and THA is mediated by GLAST activity, it should be abolished in the Na^+-free medium. As clearly shown in Figure 3(C), mTOR phosphorylation was completely prevented by substituting choline chloride for NaCl, clearly demonstrating the involvement of Na^+-dependent transport in this process. In order to provide evidence for transporter-mediated mTOR activation, we

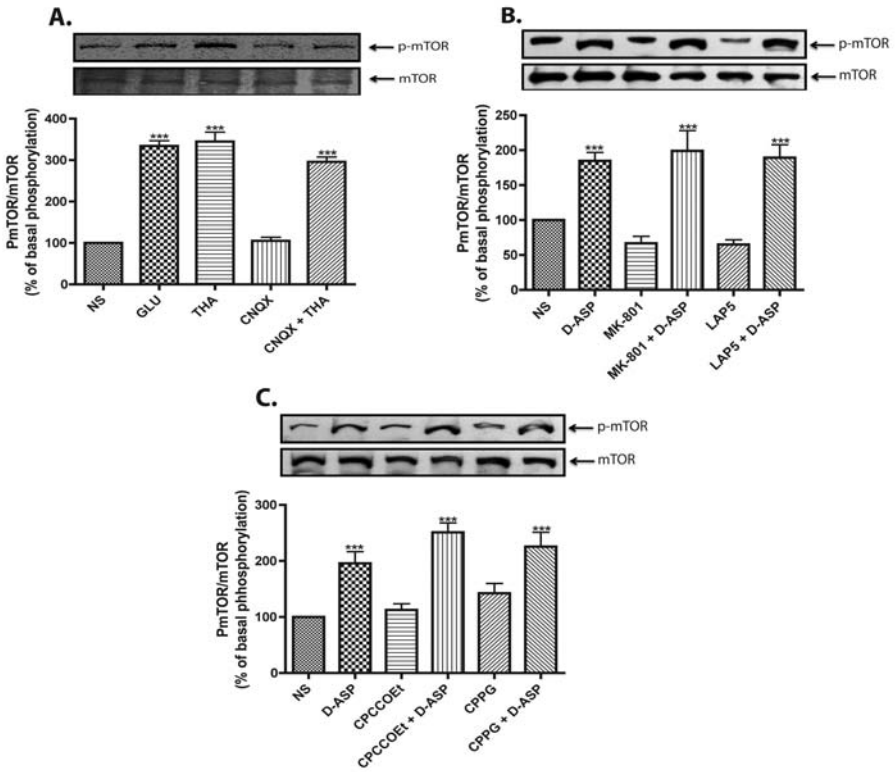

Figure 2 **D-Asp-induced mTOR phosphorylation is GLAST activity-dependent**
In all panels phosphorylated mTOR was detected as described for Figure 1. (**A**) MGC monolayers were incubated for 15 min with Glu (1 mM), THA (100 μM), the AMPA receptor antagonist CNQX (50 μM), and CNQX plus THA, in this case CNQX was added 30 min prior to THA treatment (100 μM, 15 min). MGC cultures were pre-exposed to NMDA receptor antagonists MK-801 (5 μM) or LAP5 (10 μM) (**B**) and to metabotropic Glu receptors antagonists, for group I CPCCOEt (100 μM) and for group II/III CPPG (300 μM) (**C**), 30 min prior to D-Asp treatment (1 mM, 15 min). Data are expressed as the mean ±S.E. of at least three independent experiments. Representative Western blots are shown for each condition. Statistical analysis was performed comparing against non-stimulated cells using a non-parametric one-way ANOVA (Kruskal–Wallis test) and Dunn's post-hoc test (*$P<0.05$, ***$P<0.001$).

explored the phosphorylation of one of its substrates, 4E-BP; the results are shown in Figure 4(D). Exposure of the cultured cells to D-Asp or THA results in a rapamycin-sensitive increase in 4E-BP phosphorylation.

GLAST-induced mTOR phosphorylation is Ca^{2+}-dependent

Intracellular Na^+ increase driven by GLAST may activate Na^+/Ca^{2+} exchange, leading to an increase in intracellular Ca^{2+} concentration. In order to assess the Ca^{2+}-dependence of the GLAST response, the cells were treated with D-Asp or THA in Ca^{2+}-free medium supplemented with 500 μM EDTA. As shown in Figure 4(A), removal of extracellular Ca^{2+} fully prevented the GLAST effect on mTOR phosphorylation. These results demonstrate that GLAST-mediated mTOR phosphorylation requires Ca^{2+} influx. As a possible mechanism linking transporter activity to Ca^{2+} entry, the activation of the Na^+/Ca^{2+} exchanger by GLAST-mediated Na^+ influx was explored using the inhibitors amiloride and KB-R7943. The results in Figure 4(B) show that both compounds prevented D-Asp-induced mTOR phosphorylation. Since calmodulin is the main Ca^{2+} intracellular receptor, its possible participation in GLAST induction of Ca^{2+}-dependent mTOR activation was explored. The results in Figure 4(C) show that 25 μM of the calmodulin antagonist W7 fully prevented the D-Asp response. Collectively, these data indicate that the D-Asp increase in mTOR phosphorylation is achieved through the entry of Na^+ as a result of GLAST activity and the consequent activation of the Na^+/Ca^{2+} exchanger, which, in turn, increases the intracellular Ca^{2+} that binds to calmodulin.

GLAST-induced $^{45}Ca^{2+}$ influx

To further confirm this conclusion, confluent MGC cultures were exposed to a 1 mM D-Asp solution containing 1 μCi/ml $^{45}Ca^{2+}$ for various time periods. As shown in Figure 5(A), D-Asp induced a fast time-dependent influx of $^{45}Ca^{2+}$, which saturated at 3 min. As expected, removal of extracellular Na^+ ions prevents the D-Asp-induced $^{45}Ca^{2+}$ influx (Figure 5B). A fixed 10 μM concentration of the Ca^{2+}ionophore A23187, as well as THA and PDC, also evoked significant entry of the

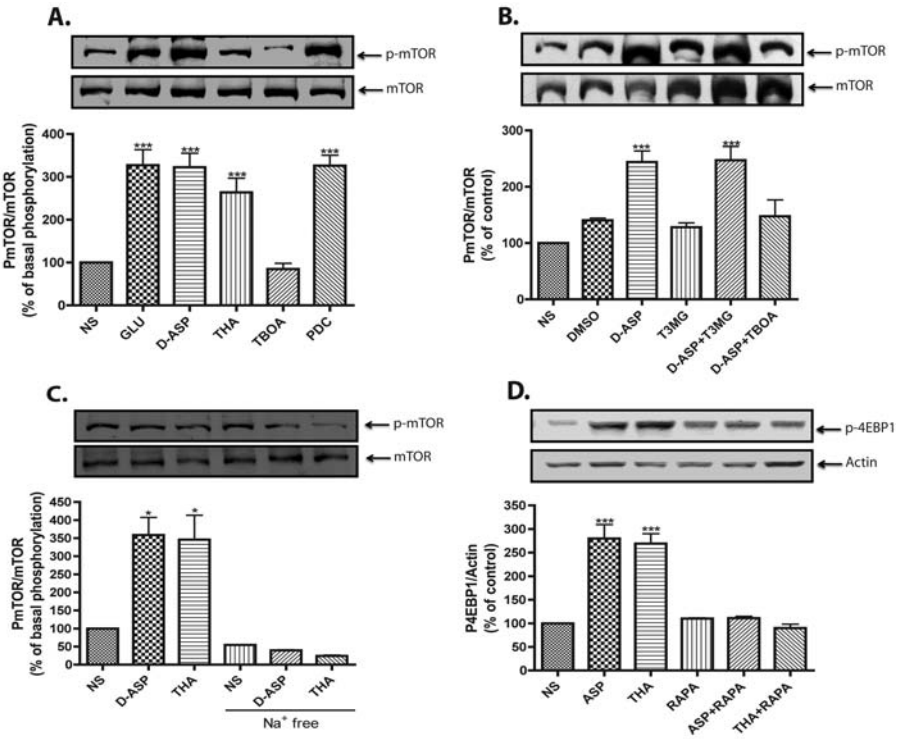

Figure 3 **D-Asp-induced mTOR phosphorylation is transport-dependent event**

(**A**) MGC monolayers were incubated for 15 min with vehicle (NS), Glu (1 mM), D-Asp (1 mM) or EAAT blockers, THA (100 μM), TBOA (100 μM) and PDC (100 μM), and the levels of Ser-2448 phosphorylated mTOR and total mTOR were detected via Western blots. (**B**) Cultured cells were treated with EAAT-4 blocker T3MG (200 μM) or TBOA (100 μM) for 30 min, prior to the addition of 1 mM D-Asp for 15 min, DMSO (0.01%) was used as a vehicle control. (**C**) MGC monolayers were exposed to vehicle (NS), D-Asp (1 mM) or THA (100 μM), in complete or Na^+-free assay buffer and then the phosphorylation of mTOR was analysed. (**D**) Levels of Thr 70 phosphorylated 4E-BP were detected after treatment with 1 mM D-Asp or 100 μM THA in the presence or absence of 100 nM rapamicin (RAPA) for 30 min; actin was used as loading control. Data are expressed as the mean ± S.E. of at least three independent experiments. Representative Western blots are shown for each condition. Statistical analysis was performed comparing against non-stimulated cells using a non-parametric one-way ANOVA (Kruskal–Wallis test) and Dunn's post-hoc test (*$P<0.05$, ***$P<0.001$).

radioactive ion (Figure 5C). In contrast, the non-transportable GLAST inhibitor TBOA did not induce $^{45}Ca^{2+}$ influx (Figure 5D). The EAAT-4 blocker T3MG failed to prevent the D-Asp-evoked response (Figure 5E). Furthermore, the Na^+/Ca^{2+} exchanger specific inhibitor KB-R7943 prevented the D-Asp-triggered increase in $^{45}Ca^{2+}$ influx (Figure 5F), clearly indicating a transporter-induced effect. To rule out the participation of the L-type voltage-gated Ca^{2+} channels (VGCC), confluent MGC cultures were pre-incubated with 10 μM nifedipine and the effect of D-Asp measured. As shown in Figure 5(G), pre-incubation with nifedipine did not modify the D-Asp-dependent Ca^{2+} influx.

Intracellular signalling involved in GLAST-mediated mTOR phosphorylation

To establish the molecular signalling cascade involved in GLAST-mediated mTOR phosphorylation, we first explored the participation of PI3K, known to act upstream of mTOR in several systems. Pretreatment of MGC for 15 min with 10 nM of the PI3K inhibitor wortmannin, completely prevented the increase in mTOR phosphorylation induced by either D-Asp or THA (Figure 6A).

The phosphorylation of membrane phosphatidylinositol at the C3-OH position of the inositol ring by PI3K is known to anchor proteins containing PH (pleckstrin homology) domains (Harrington et al., 2004), such as PKB. The results in Figure 6(B) demonstrate that 100 nM of the PKB inhibitor PKBI-IV was capable of preventing the GLAST-mediated effect, indicating the involvement of PKB, downstream of PI3K, in GLAST-dependent mTOR phosphorylation.

Activation of PI3K involves the docking of the regulatory subunit of PI3K to a phosphorylated tyrosine residue (Vanhaesebroeck and Alessi, 2000). We evaluated the possible involvement of the Src (non-receptor tyrosine kinase $p60^{src}$) in GLAST signalling. As clearly shown in Figure 6(C), MGC pretreatment with 10 nM of the specific Src inhibitor PP2, prevented the D-Asp effect on mTOR. Since Src activation requires Tyr-527 in a dephosphorylated state, we examined the phosphorylation level of this residue in D-Asp-stimulated MGC and showed that, indeed, D-Asp treatment sharply reduced Tyr-527 $p60^{src}$ phosphorylation levels (Figure 6D). This result

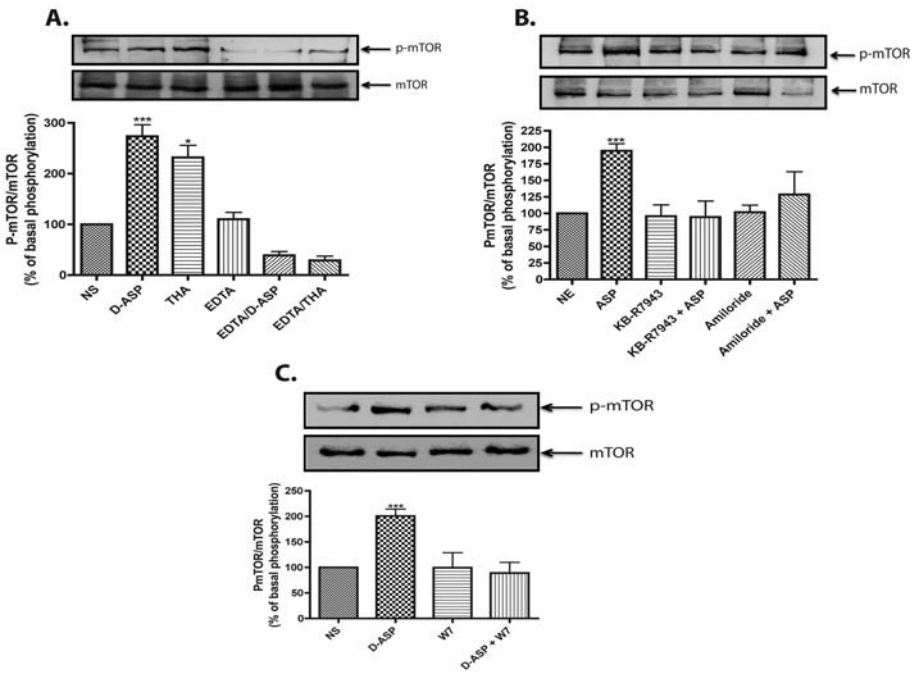

Figure 4 **D-Asp-induced mTOR phosphorylation is a Na^+/Ca^{2+} exchanger-dependent event**
mTOR phosphorylation was detected as for Figure 1. (**A**) Monolayers were incubated in normal or Ca^{2+}-free medium supplemented with EDTA (500 μM, 30 min), and then treated with D-Asp (1 mM) or THA (100 μM) for 15 min. (**B**) MGC were stimulated with D-Asp (1 mM, 15 min) in the presence or absence of the Na^+/Ca^{2+} exchanger inhibitors amiloride (10 μM) or KB-R7943 (15 μM) added 30 min prior to D-Asp treatment. (**C**) MGC monolayers were pretreated (30 min) with the calmodulin antagonist, W7 (25 μM) prior treatment with D-Asp (1 mM, 15 min). The results are the mean ± S.E. of at least three independent experiments. In each panel a representative Western blot is shown. Statistical analysis was performed comparing against non-stimulated cells using a non-parametric one-way ANOVA (Kruskal–Wallis test) and Dunn's post-hoc test (*$P<0.05$, ***$P<0.001$).

suggested the participation of an RTK (receptor tyrosine kinase) upstream of Src in GLAST-mediated mTOR phosphorylation. In order to explore this possibility, the effect of the RTK inhibitor genistein (25 μM) was tested. As expected, genistein was capable of preventing the effect of D-Asp (Figure 6D), suggesting a $p60^{src}$-dependent RTK *trans*-phosphorylation.

GLAST activity signalling-dependent transcriptional control

Glu stimulation has been linked to transcriptional control in glial cells (Lopez-Bayghen et al., 2006). Following the demonstration of GLAST-induced Ca^{2+}-dependent activation of the translation regulator mTOR, the possible induction of gene transcription by this process was analysed. We investigated if GLAST activity induced by D-Asp and THA results in increased DNA binding of the inducible transcription factor AP-1, known to be Ca^{2+}-dependent in MGC (Lopez-Colome et al., 1995). The results presented in Figure 7(A), clearly show that D-Asp as well as Glu and THA increase GLAST-mediated AP-1 DNA-binding activity in Müller cells. In order to explore the participation of Na^+/Ca^{2+} exchanger in transcriptional regulation, the effects of the Na^+/Ca^{2+} exchanger inhibitor (KB-R7943) and of the calmodulin antagonist W7 were determined. The results shown in Figure 7(B) clearly demonstrate that Na^+/Ca^{2+} exchanger and calmodulin participates in the transcriptional regulation mediated by GLAST.

DISCUSSION

Traditionally regarded as supportive and passive elements, glia cells have proven to be critically involved in glutamatergic transmission (Eulenburg and Gomeza, 2010). The participation of glia cells in the control of excitatory transmission through the so-called Glu/glutamine shuttle, which replenishes releasable Glu stores in neurons, has been recognized for more than 25 years (Shank and Campbell, 1984). Furthermore, an energetic neuronal dependence on astrocytes has also been described for glutamatergic synapses (Pellerin, 2008). In spite of the fact that most Glu receptors are expressed in glia cells (D'Antoni et al., 2008), the availability of Glu for inter-neuronal and neuron–glia

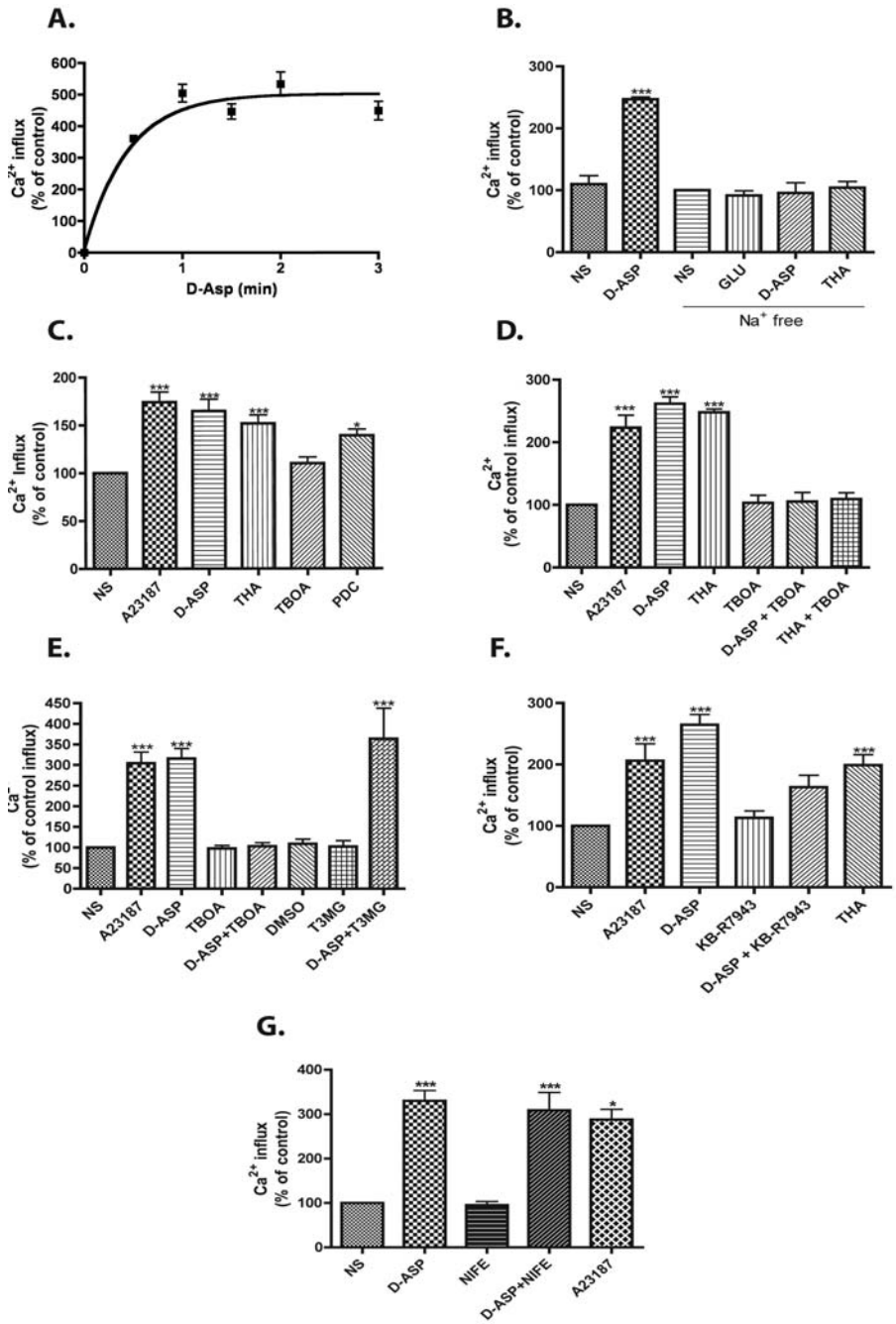

Figure 5 **GLAST activity induces $^{45}Ca^{2+}$ entry**

(**A**) MGC were incubated with 1 mM D-Asp at room temperature, and $^{45}Ca^{2+}$ uptake was measured at the indicated time periods (0, 0.5, 1, 1.5, 2 and 3 min). (**B**) Monolayers were incubated in complete or Na^+-free assay buffer and treatment with Glu (1 mM), D-Asp (1 mM) or THA (100 μM). (**C**) $^{45}Ca^{2+}$ influx was determined in the presence of 1 mM D-Asp, 100 μM THA, 100 μM TBOA or 100 μM PDC. The Ca^{2+} ionophore A23187 (10 μM) was used as a positive control. All drugs were included for 3 min. (**D**) Cells were pre-exposed for 30 min to the non-transportable Glu transport blocker TBOA 100 μM and then to D-Asp 1 mM and THA 100 μM, the influx time was 3 min. (**E**) MGC were incubated with TBOA (100 μM) or EAAT-4 blocker T3MG (200 μM) for 30 min prior the D-Asp treatment and then $^{45}Ca^{2+}$ uptake was measured. (**F**) Monolayers were pre-incubated (30 min) in presence or absence of KB-R7943 (15 μM) and treatment with D-Asp (1 mM). (**G**) MGC were pre-incubated for 30 min with the L-type VGCC blocker nifedipine (NIFE, 10 μM), and then exposed to 1 mM D-Asp. The Ca^{2+} ionophore A23187 10 μM was used as a positive control. The different drugs were present during the 3 min of $^{45}Ca^{2+}$ influx. Values represent the mean ± S.E. of at least three independent experiments performed in triplicate. Statistical analysis was performed comparing against non-stimulated cells using a non-parametric one-way ANOVA (Kruskal–Wallis test) and Dunn's post-hoc test (*$P<0.05$, ***$P<0.001$).

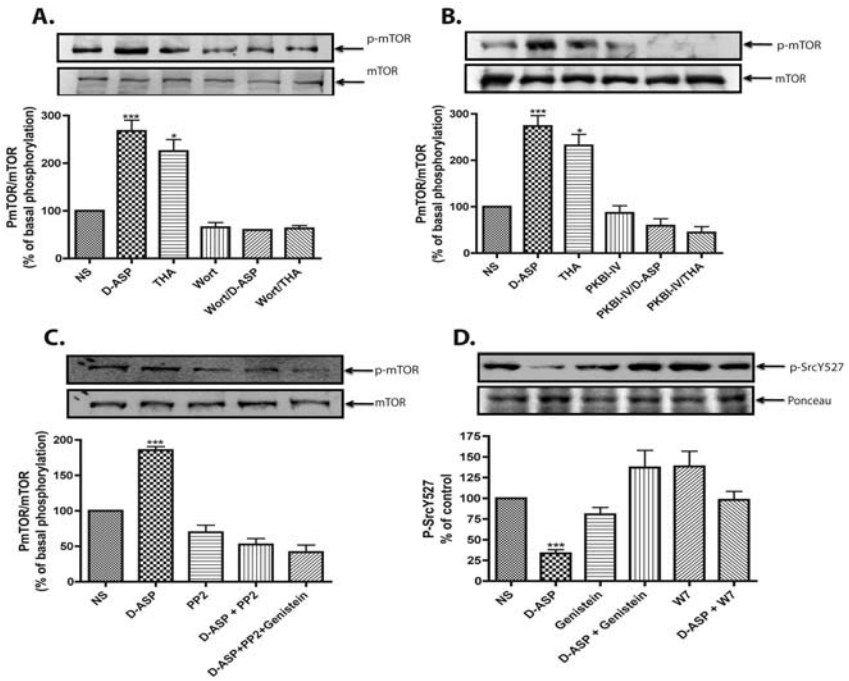

Figure 6 **D-Asp-induced mTOR phosphorylation is a PI3K-PKB/Akt pathway-dependent event**
MGC were pre-incubated for 30 min with 10 nM of the PI3K inhibitor wortmannin (Wort) (**A**), with 100 nM of the PKB inhibitor (PKBI-IV) (**B**), or the $p60^{src}$ inhibitor PP2 (10 nM) in the absence or presence of the RTK inhibitor genistein at 25 μM (**C**); and then treated with D-Asp (1 mM) or THA (100 μM). Levels of mTOR phosphorylation were detected as for Figure 1. (**D**) Levels of Tyr-527 phosphorylated $p60^{src}$ were detected after treatment with 1 mM D-Asp in the presence/absence of W7 (25 μM) or genistein (25 μM). Phospho-$p60^{src}$ levels were analysed by Western blot, Ponceau S was used as a loading control. The results are the mean ±S.E. of at least three independent experiments. In each panel, a representative Western blot is shown. Statistical analysis was performed comparing against non-stimulated cells using a non-parametric one-way ANOVA (Kruskal-Wallis test) and Dunn's post-hoc test (*$P<0.05$, ***$P<0.001$).

interactions relies on an efficient Glu uptake activity. It is therefore conceivable that transporters may contribute to Glu signalling, particularly in glia cells. In this context, we have described the regulation of Glu removal in radial glia cells by a transporter-mediated process involving the regulation of GLAST/EAAT-1 membrane expression (Gonzalez and Ortega, 2000; Gadea et al., 2004). More recently, the group of Hampson have demonstrated a direct coupling of Glu transporters to the Na,K-ATPase in glia cells (Rose et al., 2009). In such a scenario, it is tempting to speculate that intracellular signalling activated by Glu transporters could be linked to the long-term regulation of glia–neuronal reciprocal interactions in excitatory transmission.

The results from this study clearly show that the transport process itself triggers a signal transduction cascade involving the activation of $p60^{src}$, PI3K and PKB (Akt) linked to extracellular Ca^{2+} entry, which leads, not only to the promotion of translation by Ser-2448 phosphorylated mTOR, but also to transcriptional activity mediated by Ca^{2+}-dependent binding of inducible transcription factors, such as the AP-1. In this regard, the activation of CaMKII induces the phosphorylation/activation of RTKs which, in turn, allows PI3K membrane anchoring and activation (Wang and Proud, 2011). We show here, that Ca^{2+} entry promoted by GLAST activity induces a transient mTOR phosphorylation through $p60^{src}$/PI3K/Akt/mTOR/$p70^{S6K}$ signalling. It is quite possible that the Ca^{2+} signal activates phosphatase 2A that would dephosphorylate and inactivate $p70^{S6K}$, thus reducing mTOR Ser-2448 phosphorylation giving up the transient nature of the effect (Nunbhakdi-Craig et al., 2002). Furthermore, as CaMKII has been shown to activate the expression of *c-fos* through the MAPK MEK/ERK cascade in Müller glia, the proposed GLAST signalling cascade is supported by the increase in AP-1 binding (Abe and Saito, 2001; Takeda et al., 2002).

As mTOR has been regarded as a master regulator of protein synthesis (Foster and Fingar, 2010) and AP-1 DNA binding is critical for the transcriptional control of a number of genes (Shaulian, 2010), it is possible that the removal of Glu from the synaptic cleft is linked to gene expression regulation in glia cells. A working hypothesis is that specific genes, such as those coding for the Glu transporters, the Na^+/K^+-ATPase, glutamine synthetase or the neutral amino acid transporters could be the targets of GLAST-dependent gene expression regulation, and could participate actively in glia–neuronal coupling. Work currently in progress in our group is aimed at the identification of these genes. Taking into consideration that mTOR is not only a transducing molecule for mitogenic signals, but also for

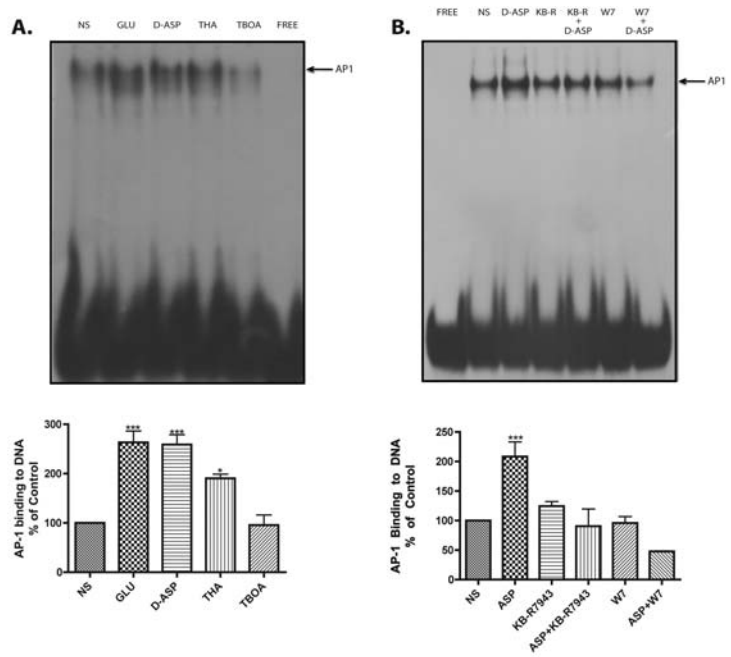

Figure 7 **GLAST activity signals to AP-1 DNA binding**

(**A**) EMSAs. Nuclear extracts were prepared from control or treated cells (Glu, D-Asp, THA or TBOA) and binding to the AP-1 consensus sequence was analysed as described in the Materials and methods section. (**B**) Nuclear extracts were prepared from cells pre-incubated 30 min with Na^+/Ca^{2+} exchanger inhibitor (KB-R7943, 15 μM) and with the calmodulin antagonist (W7, 25 μM), after that treated with D-Asp (1 mM, 90 min) the binding to the AP-1 consensus sequence was analysed. The results are the mean ± S.E. of at least three independent experiments. Statistical analysis was performed comparing against non-stimulated cells using a non-parametric one-way ANOVA (Kruskal–Wallis test) and Dunn's post-hoc test (*$P<0.05$, ***$P<0.001$).

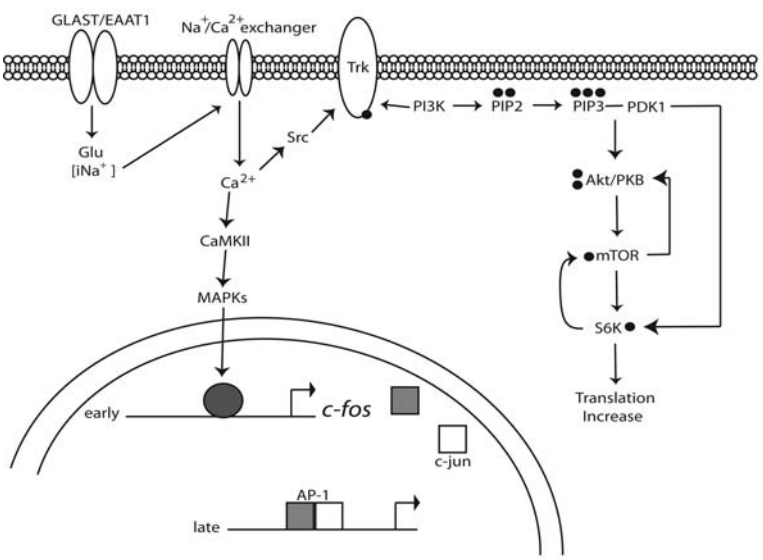

Figure 8 **Current model for GLAST signalling in MGC**

Glu uptake leads to an influx of Na^+ that activates the Na^+/Ca^{2+} exchanger, resulting in a net Ca^{2+} influx. The elevation of intracellular Ca^{2+} leads to the up-regulation of *c-fos* transcription and the promotion of AP-1 DNA-binding activity. On the other hand, Ca^{2+} entry results in $p60^{src}$ Tyr-527 dephosphorylation and Trk transactivation, the recruitment and activation of PI3K and Akt/PKB, which, in turn, results in mTOR phosphorylation and an increase in mRNA translation.

nutrient availability correlated with protein synthesis for housekeeping glial functions, transporter signalling to mTOR and gene expression could play a role in linking these responses (towards cell division).

The functional significance of signalling through the transporters compared with the cascades activated via Glu receptors, and the fact that both would lead to gene expression regulation in glia cells (Lopez-Bayghen et al., 2006), is elusive at this point. Yet, it is conceivable that the difference in the kinetics of activation, favoured by lower affinity of the transporters and their higher density (Danbolt, 2001), is the basis for a transporter-selective response at the level of transcriptional and/or translational control. Yet another possibility is that an activity-dependent differential distribution of transporters and receptors in detergent-resistant membrane domains and the inclusion or not of differential signalling partners constitutes the molecular basis of the existence of transporter-mediated signal transduction (Butchbach et al., 2004; Gonzalez et al., 2007; Hou et al., 2008).

In summary, we demonstrated here that Glu transport in MGC is linked to the activation of signal transduction cascades that lead to gene expression regulation. A description of our present findings is summarized in Figure 8. Our results further strengthen the pivotal role of glia cells in glutamatergic transmission in the retina.

ACKNOWLEDGEMENTS

The technical assistance of Luis Cid and Blanca Ibarra and the critical reading of the paper by Professor Angelina Rodríguez are acknowledged.

FUNDING

This work was supported by the Conacyt-Mexico [grant numbers 79502 and 123625 (to A.O.)], PAPIIT/UNAM [grant number IN201812 (to A.M.L.C.)]. Z.M.-L. and A.M.G. are supported by fellowships from Conacyt-Mexico.

REFERENCES

Abe K, Saito H (2001) Possible linkage between glutamate transporter and mitogen-activated protein kinase cascade in cultured rat cortical astrocytes. J Neurochem 76:217–223.

Blagosklonny MV (2010) Revisiting the antagonistic pleiotropy theory of aging: TOR-driven program and quasi-program. Cell Cycle 9:3151–3156.

Bringmann A, Pannicke T, Biedermann B, Francke M, Iandiev I, Grosche J, Wiedemann P, Albrecht J, Reichenbach A (2009) Role of retinal glial cells in neurotransmitter uptake and metabolism. Neurochem Int 54:143–160.

Butchbach ME, Tian G, Guo H, Lin CL (2004) Association of excitatory amino acid transporters, especially EAAT2, with cholesterol-rich lipid raft microdomains: importance for excitatory amino acid transporter localization and function. J Biol Chem 279:34388–34396.

Coutinho V, Knopfel T (2002) Metabotropic glutamate receptors: electrical and chemical signaling properties. Neuroscientist 8:551–561.

D'Antoni S, Berretta A, Bonaccorso CM, Bruno V, Aronica E, Nicoletti F, Catania MV (2008) Metabotropic glutamate receptors in glial cells. Neurochem Res 33:2436–2443.

Danbolt NC (2001) Glutamate uptake. Prog Neurobiol 65:1–105.

Eulenburg V, Gomeza J (2010) Neurotransmitter transporters expressed in glial cells as regulators of synapse function. Brain Res Rev 63:103–112.

Fields RD, Stevens-Graham B (2002) New insights into neuron–glia communication. Science 298:556–562.

Foster KG, Fingar DC (2010) Mammalian target of rapamycin (mTOR): conducting the cellular signaling symphony. J Biol Chem 285:14071–14077.

Fyk-Kolodziej B, Qin P, Dzhagaryan A, Pourcho RG (2004) Differential cellular and subcellular distribution of glutamate transporters in the cat retina. Vis Neurosci 21:551–565.

Gadea A, Lopez E, Lopez-Colome AM (2004) Glutamate-induced inhibition of D-aspartate uptake in Muller glia from the retina. Neurochem Res 29:295–304.

Gegelashvili M, Rodriguez-Kern A, Sung L, Shimamoto K, Gegelashvili G (2007) Glutamate transporter GLAST/EAAT1 directs cell surface expression of FXYD2/gamma subunit of Na, K-ATPase in human fetal astrocytes. Neurochem Int 50:916–920.

Gonzalez MI, Ortega A (2000) Regulation of high-affinity glutamate uptake activity in Bergmann glia cells by glutamate. Brain Res 866:73–78.

Gonzalez MI, Susarla BT, Fournier KM, Sheldon AL, Robinson MB (2007) Constitutive endocytosis and recycling of the neuronal glutamate transporter, excitatory amino acid carrier 1. J Neurochem 103:1917–1931.

Guerrini L, Blasi F, Denis-Donini S (1995) Synaptic activation of NF-kappa B by glutamate in cerebellar granule neurons *in vitro*. Proc Natl Acad Sci USA 92:9077–9081.

Harrington LS, Findlay GM, Gray A, Tolkacheva T, Wigfield S, Rebholz H, Barnett J, Leslie NR, Cheng S, Shepherd PR, Gout I, Downes CP, Lamb RF (2004) The TSC1-2 tumor suppressor controls insulin-PI3K signaling via regulation of IRS proteins. J Cell Biol 166:213–223.

Hollander H, Makarov F, Dreher Z, van Driel D, Chan-Ling TL, Stone J (1991) Structure of the macroglia of the retina: sharing and division of labour between astrocytes and Muller cells. J Comp Neurol 313:587–603.

Hou Q, Huang Y, Amato S, Snyder SH, Huganir RL, Man HY (2008) Regulation of AMPA receptor localization in lipid rafts. Mol Cell Neurosci 38:213–223.

Kholodenko BN (2006) Cell-signalling dynamics in time and space. Nat Rev Mol Cell Biol 7:165–176.

Laplante M, Sabatini DM (2012) mTOR Signaling. Cold Spring Harb Perspect Biol 4:2

Lopez T, Lopez-Colome AM, Ortega A (1997) NMDA receptors in cultured radial glia. FEBS Lett 405:245–248.

Lopez T, Lopez-Colome AM, Ortega A (1998) Changes in GluR4 expression induced by metabotropic receptor activation in radial glia cultures. Brain Res Mol Brain Res 58:40–46.

Lopez-Bayghen E, Cruz-Solis I, Corona M, Lopez-Colome AM, Ortega A (2006) Glutamate-induced octamer DNA binding and transcriptional control in cultured radial glia cells. J Neurochem 98:851–859.

Lopez-Colome AM, Romo-de-Vivar M (1991) Excitatory amino acid receptors in cultures of glial cells from the retina. Glia 4:431–439.

Lopez-Colome AM, Murbartian J, Ortega A (1995) Excitatory amino acid-induced AP-1 DNA binding activity in Muller glia. J Neurosci Res 41:179-184.

Lopez-Colome AM, Ortega A, Romo-de-Vivar M (1993) Excitatory amino acid-induced phosphoinositide hydrolysis in Muller glia. Glia 9:127–135.

Massey SC, Miller RF (1990) N-methyl-D-aspartate receptors of ganglion cells in rabbit retina. J Neurophysiol 63:16–30.

Mattson MP (2003) Excitotoxic and excitoprotective mechanisms: abundant targets for the prevention and treatment of neurodegenerative disorders. Neuromolecular Med 3:65–94.

Michaelis EK (1998) Molecular biology of glutamate receptors in the central nervous system and their role in excitotoxicity, oxidative stress and aging. Prog Neurobiol 54:369–415.

Nunbhakdi-Craig V, Machleidt T, Ogris E, Bellotto D, White CL, 3rd, Sontag E (2002) Protein phosphatase 2A associates with and regulates atypical PKC and the epithelial tight junction complex. J Cell Biol 158:967–978.

Olney JW (2003) Excitotoxicity, apoptosis and neuropyschiatric disorders. Curr Opin Pharmacol 3:101–109.

Pellerin L (2008) Brain energetics (thought needs food). Curr Opin Clin Nutr Metab Care 11:701–705.

Proud CG (2007) Cell signaling: mTOR, unleashed. Science 318:926–927.

Rauen T, Kanner BI (1994) Localization of the glutamate transporter GLT-1 in rat and macaque monkey retinae. Neurosci Lett 169:137–140.

Rose EM, Koo JC, Antflick JE, Ahmed SM, Angers S, Hampson DR (2009) Glutamate transporter coupling to Na,K-ATPase. J Neurosci 29: 8143–8155.

Rosner M, Hengstschlager M (2010) Evidence for cell cycle-dependent, rapamycin-resistant phosphorylation of ribosomal protein S6 at S240/244. Amino Acids 39:1487–1492.
Shank RP, Campbell GL (1984) Amino acid uptake, content, and metabolism by neuronal and glial enriched cellular fractions from mouse cerebellum. J Neurosci 4:58–69.
Shaulian E (2010) AP-1–The Jun proteins: Oncogenes or tumor suppressors in disguise? Cell Signal 22:894–899.
Takeda M, Takamiya A, Yoshida A, Kiyama H (2002) Extracellular signal-regulated kinase activation predominantly in Muller cells of retina with endotoxin-induced uveitis. Invest Ophthalmol Vis Sci 43:907–911.
Thomas GM, Huganir RL (2004) MAPK cascade signalling and synaptic plasticity. Nat Rev Neurosci 5:173–183.
Uchihori Y, Puro DG (1993) Glutamate as a neuron-to-glial signal for mitogenesis: role of glial N-methyl-D-aspartate receptors. Brain Res 613:212–220.
Um SH, Frigerio F, Watanabe M, Picard F, Joaquin M, Sticker M, Fumagalli S, Allegrini PR, Kozma SC, Auwerx J, Thomas G (2004) Absence of S6K1 protects against age- and diet-induced obesity while enhancing insulin sensitivity. Nature 431:200–205.
Vanhaesebroeck B, Alessi DR (2000) The PI3K-PDK1 connection: more than just a road to PKB. Biochem J 346:561–576.
Wang H, Gong B, Vadakkan KI, Toyoda H, Kaang BK, Zhuo M (2007) Genetic evidence for adenylyl cyclase 1 as a target for preventing neuronal excitotoxicity mediated by N-methyl-D-aspartate receptors. J Biol Chem 282:1507–1517.
Wang X, Proud CG (2011) mTORC1 signaling: what we still don't know. J Mol Cell Biol 3:206–220.
Zepeda RC, Barrera I, Castelan F, Soto-Cid A, Hernandez-Kelly LC, Lopez-Bayghen E, Ortega A (2008) Glutamate-dependent transcriptional regulation in bergmann glia cells: involvement of p38 MAP kinase. Neurochem Res 33:1277–1285.

Received 2 April 2012/27 June 2012; accepted 28 June 2012
Published as Immediate Publication 23 July 2012, doi 10.1042/AN20120022

Journal of Neurochemistry

JOURNAL OF NEUROCHEMISTRY | 2013 | 125 | 545–554 doi: 10.1111/jnc.12211

ORIGINAL ARTICLE

GLAST/EAAT1-induced Glutamine release via SNAT3 in Bergmann glial cells: evidence of a functional and physical coupling

Zila Martínez-Lozada,* Alain M. Guillem,* Marco Flores-Méndez,* Luisa C. Hernández-Kelly,* Carmelita Vela,† Enrique Meza,† Rossana C. Zepeda,† Mario Caba,† Angelina Rodríguez‡ and Arturo Ortega*

*Departamento de Genética y Biología Molecular, Centro de Investigación y de Estudios Avanzados del Instituto Politécnico Nacional, México D.F., México

†Centro de Investigaciones Biomédicas, Universidad Veracruzana, Xalapa, México

‡Facultad de Química, Centro Universitario Cerro de las Campanas, Universidad Autónoma de Querétaro, Querétaro, México

Abstract

Glutamate, the major excitatory transmitter in the vertebrate brain, is removed from the synaptic cleft by a family of sodium-dependent glutamate transporters profusely expressed in glial cells. Once internalized, it is metabolized by glutamine synthetase to glutamine and released to the synaptic space through sodium-dependent neutral amino acid carriers of the N System (SNAT3/slc38a3/SN1, SNAT5/slc38a5/SN2). Glutamine is then taken up by neurons completing the so-called glutamate/glutamine shuttle. Despite of the fact that this coupling was described decades ago, it is only recently that the biochemical framework of this shuttle has begun to be elucidated. Using the established model of cultured cerebellar Bergmann glia cells, we sought to characterize the functional and physical coupling of glutamate uptake and glutamine release. A time-dependent Na^+-dependent glutamate/aspartate transporter/EAAT1-induced System N-mediated glutamine release could be demonstrated. Furthermore, D-aspartate, a specific glutamate transporter ligand, was capable of enhancing the co-immunoprecipitation of Na^+-dependent glutamate/aspartate transporter and Na^+-dependent neutral amino acid transporter 3, whereas glutamine tended to reduce this association. Our results suggest that glial cells surrounding glutamatergic synapses may act as sensors of neuron-derived glutamate through their contribution to the neurotransmitter turnover.

Keywords: Bergmann glia, glutamate transporters, glutamate/glutamine shuttle, glutamine transporters.

J. Neurochem. (2013) **125**, 545–554.

Received June 18, 2012; revised manuscript received October 11, 2012; accepted February 15, 2013.

Address correspondence and reprint requests to Arturo Ortega, Ph.D., Departamento de Genética y Biología Molecular, Cinvestav-IPN, Apartado Postal 14-740, México DF 07000, México.
E-mail: arortega@cinvestav.mx

Abbreviations used: AMPA, α-amino-3-hydroxy-5-methylisoxazole-4-propionate; ANOVA, analysis of variance; BGC, Bergmann glial cells; BSA, bovine serum albumin; DAB, diaminobenzidine; D-Asp, D-Aspartate; DCG-IV, (1R,2R)-3-[(1S)-1-amino-2-hydroxy-2-oxoethyl]cyclopropoane-1,2-dicarboxylic acid; DHPG, (RS)-3,5-dihydroxyphenilglicine; DL-TBOA, DL-threo-b-Benzyloxyaspartic acid; DMEM, Dulbecco's modified Eagle's medium; DNQX, 6,7-Dinitroquinoxaline-2,3-dione; EAAT 1-5, excitatory amino acid transporters; ECL, enhanced chemiluminescence reagent; EDTA, ethylenediaminetetraacetic acid; GLAST, Na^+-dependent glutamate/aspartate transporter; Gln, glutamine; Glt-1, glutamate transporter-1; GS, glutamine synthetase; KA, kainate; KBP, kainate binding protein; L-AP4, L-(+)-2-amino-4-phosphonobutyric acid; L-Glu, L-glutamate; NMDA, N-methyl-D-aspartate; NP-40, Nonidet P-40; PBS, phosphate-buffer saline; PBT, phosphate-buffer saline containing 0.3% Triton; SDS-PAGE, sodium dodedecyl sulfate polyacrylamide gel electrophoresis; SNAT2-3-5, Na^+-dependent neutral amino acid transporter 2-3-5; TBS, Tris-buffered saline; THA, threo-β-hydroxyaspartate; trans-ACPD, (+/-)-1-aminocyclopentane-trans-1,3-dicarboxilic acid.

L-Glutamate (L-Glu) is the major excitatory amino acid neurotransmitter in the vertebrate brain. Membrane-specific L-Glu receptors expressed in neurons and glial cell mediate most, albeit not all, of its effects. Ionotropic receptors of the α-amino-3-hydroxy-5-methylisoxazole-4-propionate (AMPA), N-methyl-D-aspartate (NMDA), and kainate (KA) subtypes are proteins composed of different subunits (Sager *et al.* 2009). Metabotropic Glu receptors have been subdivided in terms of sequence similarity and signaling mechanisms in three groups. Signaling through these receptors is carried out by the phospholipase C and Ca^{2+} for Group I and inhibition of adenylate cyclase for Groups II and III (Wieronska and Pilc 2009).

L-Glu extracellular levels are tightly regulated through its uptake, mostly into glial cells, by a family of Na^+-dependent L-Glu transporters known as excitatory amino acid transporters of which EAAT-1, also known as Na^+-dependent glu/aspartate transporter (GLAST) and EAAT-2 or Glu transporter-1 (Glt-1) are mainly expressed in glia cells (Danbolt 2001). Once this amino acid has been removed, it is rapidly converted to L-glutamine (L-Gln) through the action of Gln synthetase (GS) (Shank and Campbell 1984). Neutral amino acid transporters mediate both the glial release and the neuronal uptake of L-Gln. Several transporter systems have been described for these amino acids, based not only in sequence identity but also on their kinetic properties (Dolinska *et al.* 2000, 2003; Hagglund *et al.* 2011). In general terms, it has been assumed that L-Gln release from astrocytes (Albrecht 1989). One of the transporters that carries out this release is the Na^+-dependent neutral amino acid transporter 3 (SNAT3), a member of System N, a family of L-Gln transporters capable of acting in a reversed fashion (Broer *et al.* 2004). In contrast, neuronal L-Gln uptake has been postulated to be carried out by members of System A transporters (SNAT2) (Jenstad *et al.* 2009), although this proposal has been questioned at least for neocortical neurons (Grewal *et al.* 2009).

Bergmann glial cells (BGC) extend their processes through the molecular layer of the cerebellar cortex surrounding excitatory and inhibitory synapses (Somogyi *et al.* 1990). The tripartite relationship between pre-synapse, post-synapse, and surrounding glia as a source of neuroactive substances like ATP and D-serine has also been acknowledged (Henneberger *et al.* 2010). Therefore, it has been postulated that BGCs are involved in neuronal communication and that they might even constitute a neuronal reservoir (Hansson and Ronnback 1995; Malatesta *et al.* 2003; Anthony *et al.* 2004). When cultured, BGC become an excellent model in which the molecular and cellular basis of glial–neuronal signaling can be analyzed in the context of glutamatergic transmission (Lopez-Bayghen *et al.* 2007). In such preparations, L-Glu acting through its receptors, changes gene expression at the transcriptional and translational levels (Gonzalez-Mejia *et al.* 2006; Rosas *et al.* 2007). In addition, it has become evident that plasma membrane L-Glu transporters are also involved in glutamatergic signaling. For example, it has been demonstrated that L-Glu uptake activity triggers glucose influx (Magistretti 2009) and increases GS activity (Lehmann *et al.* 2009) in astrocytes. Furthermore, in BGC cultures, GLAST/EAAT-1, the sole L-Glu transporter expressed in these cells (Regan *et al.* 2007) is linked to the mammalian target of rapamycin (mTOR) activation and thus protein expression regulation (Martinez-Lozada *et al.* 2011). With these evidences in mind, we decided to explore the putative role of L-Glu transporters in the regulation of L-Gln release. To reach this goal, we first characterized the L-[^{3}H] Gln uptake activity in our culture system and evaluated if GLAST/EAAT-1 substrates such as D-Aspartate (D-Asp) would induce a significant L-Gln release. Once we were able to detect such an effect, we hypothesized that both transporters are present in a macromolecular complex and that D-Asp treatment would be linked to the appearance of such complex. Indeed, we were able to detect a coupling between GLAST and SNAT3.

These results suggest that glia cells associated to glutamatergic synapses behave as L-Glu sensors and that these cells may control, to a greater extent than assumed before, excitatory transmission. Moreover, our findings strengthen the notion of the active participation of glia cells in synaptic transmission.

Materials and methods

Materials

Tissue culture reagents were obtained from GE Healthcare (Carlsbad, CA, USA). DHPG, 6,7-Dinitroquinoxaline-2,3-dione, AMPA, NMDA, DL-threo-b-Benzyloxyaspartic acid, threo-β-hydroxyaspartate and L-Glu were all obtained from Tocris-Cookson (St. Louis, MO USA). KA was obtained from Ocean Produce International (Shelburne, Nova Scotia, Canada). L-[^{3}H] Glutamic acid (specific activity 40 Ci/mmol) and L-[^{3}H] Glutamine (specific activity 50.3 Ci/mmol) were obtained from Perkin Elmer (Waltham, MA, USA). The AG 1X-8 anion exchange resin was purchased from Bio-Rad (Hercules, CA, USA). The antibodies used were anti- SNAT3 (Santa Cruz, CA, USA), anti-calbindin (Sigma-Aldrich, St. Louis, MO, USA), anti-kainate binding protein (KBP), and an anti-peptide (GLIQALVTALGTSSSSAT) GLAST anti-serum (produced and characterized in our laboratories). Specificity of the anti-peptide anti-GLAST antibodies was performed as follows. A 1 : 1000 dilution of the sera was pre-absorbed with 10 and 50 ng of the peptide for 30 min at 4°C and used for Western blot analysis of chick cerebellum and cultured Bergmann glia extracts (see below). Horseradish peroxidase-linked anti-mouse or anti-rabbit antibodies, and the enhanced chemiluminescence reagent, were obtained from Amersham Biosciences (Buckinghamshire, UK). All other chemicals were purchased from Sigma (St. Louis, MO, USA).

Cell culture and stimulation protocol

Primary cultures of cerebellar BGC were prepared from 14-day-old chick embryos as previously described (Ortega *et al.* 1991). Cells were plated in plastic culture dishes in Dulbecco's modified Eagle's medium (DMEM) containing 10% fetal bovine serum, 2 mM Gln, and gentamicin (50 μg/mL) and used on the fourth or fifth day after culture. Before any treatment, confluent monolayers were switched to non-serum DMEM media containing 0.5% bovine serum albumin for 30 min and then treated as indicated. Antagonists or inhibitors were added 30 min before agonists. The cells were treated with the L-Glu analogs added to culture medium for the indicated times; after that, medium was replaced with DMEM/0.5% albumin.

Staining procedures

BGC primary cultures were grown on poly-L-lysine-treated (0.01 mg/mL) glass coverslips following the procedure described above. Cells were fixed by exposure for 10 min to methanol at −20ºC and washed twice with phosphate-buffer saline (PBS) containing 0.5% Triton X-100 (washing solution). Non-specific binding was prevented by incubation with 1% bovine serum albumin in PBS (blocking solution) for 1 h. Cells were exposed 1 h to the primary antibodies anti-SNAT3 in blocking solution at 25°C. Then, cells were washed three times with washing solution and incubated with a 1 : 100 dilution of the fluorescent-labeled secondary antibodies dissolved in blocking solution. After washing out secondary antibody, cell preparations were mounted with Vectashield (Vector Laboratories, Burlingame, CA, USA) and examined with an inverted fluorescence microscope (Zeiss Axioscope 40, Gottingen, Germany).

For immunohistochemistry, P0 chick cerebella was removed and placed immediately in cold PBS. The tissue was washed once in cold PBS to remove blood and placed in 4% paraformaldehyde in PBS (pH 7.4) for one hour. The fixative was changed once and the tissue was left at 4°C during 48 h. The cerebella were cryoprotected successively in 10%, 20%, and 30% sucrose in PBS and sagittally sectioned at 50 μm with a cryostat (Microm International GmbH, Walldorf, Germany). For immunohistochemistry, tissue was washed profusely in PBS to remove excess aldehydes and then incubated 10 min in 1.8% hydrogen peroxide solution to remove endogenous peroxidase activity. Non-specific antibody binding was blocked by incubating the sections in blocking solution (3% goat serum in PBS containing 0.3% Triton, PBT) for 1 h at 25°C. Sections were incubated at 4°C for 48 h with primary antibodies; mouse anti-calbindin (1 : 5000), anti-KBP (1 : 2500), and anti-SNAT3 (1 : 2500) in blocking solution. The sections were washed three times in PB, and placed in biotinylated anti-mouse secondary antibodies (1 : 1000; Vector Laboratories, Inc., Burlingame, CA, USA) for 3 h (for calbindin), anti-rabbit secondary antibodies for KBP, and anti-guinea pig secondary antibodies for SNAT3. A 1 h incubation with the avidin-biotinylated horseradish peroxidase complex (1 : 250; Vector Labs) followed. The antibody-peroxidase complexes were revealed with a solution containing 0.05% diaminobenzidine, nickel sulfate (10 mg/mL; Fisher Scientific, Pittsburg, PA, USA), cobalt chloride (10 mg/mL; Fisher Scientific), and 0.01% hydrogen peroxide, which produced a black–purple precipitate. Sections were mounted onto gelatin-subbed slides, dehydrated, and cleared in Hemo-De (Fisher Scientific); then, cover slips were collocated with Permount. The sections were analyzed in an Olympus BX41 microscope.

L-[^{3}H]Gln Uptake and release

Confluent BGC monolayers seeded in 24-well plates were washed three times to remove all non-adhering cells with 0.5 mL aliquots of solution A containing 25 mM HEPES-Tris, 130 mM NaCl, 5.4 mM KCl, 1.8 mM $CaCl_2$. 0.8 mM $MgCl_2$, 33.3 mM glucose, and 1 mM NaH_2PO_4 at pH 7.4. When indicated, NaCl was replaced by LiCl. The time course of L-[^{3}H] Gln influx was initiated at $t = 0$ by the addition of 0.5 ml solution A containing 0.5 μCi/mL of L-[^{3}H] Gln solution A, 200 μM Gln. The reaction was stopped by aspirating the radioactive medium and washing each well within 15 s with 0.5 mL aliquots of an ice-cold solution A. For the determination of the kinetic parameters, the cold L-Gln concentration was modified to a final 0.5, 3, 5, 7.5, and 10 mM concentration and the uptake time was 30 min. The uptake was stopped as described above. The cells in the wells were then exposed for 2 h at 37°C to 0.5 mL NaOH and an aliquot of that solution counted in a Beckmann 7800LS scintillation counter. A minimum of three experiments in quadruplicates was done for each condition.

For the release experiments, BGC were seeded on 60 mm dishes and loaded for 3 h with 0.5 μCi/mL of L-[^{3}H] Gln in solution A. The medium was replaced every 2 min and a total of 15 fractions were collected. The various stimuli were added in fractions 6-10. The radioactivity associated to each fraction was determined by liquid scintillation counting and expressed as percentage of the total radioactivity in the experiment.

L-[^{3}H] Glutamine metabolism

The extent of L-[^{3}H] Gln remaining after the 3 h loading period and the percentage of L-[^{3}H] Gln released was determined by means of anion exchange separation of L-[^{3}H] Gln, using a AG 1X-8 200/400 resin essentially as described previously (Mongin *et al.* 2011). The system was standardized with L-[^{3}H] Glu and L-[^{3}H] Gln, that were eluted with HCl and H_2O, respectively.

Immunoprecipitation and Western blots

Cells from confluent monolayers were harvested with PBS (10 mM K_2HPO_4/KH_2PO_4, 150 mM NaCl, pH 7.4) containing protease inhibitors (1 mM phenylmethylsufonyl fluoride, 1 mg/mL aprotinin, 1 mg/mL leupeptin). Tissues or cells suspensions were lysed with RIPA buffer (50 mM Tris-HCl, 1 mM ethylenediaminetetraacetic acid, 150 mM NaCl, 1% Nonidet P-40, 0.25% sodium deoxycolate, pH 7.4). Cell lysates were pre-absorbed with 15 μL of protein G coupled to Sepharose 4B for 25 min at 4°C. The cleared lysates (1 mg of protein) were incubated with agarose-coupled anti-GLAST or anti-SNAT3 antibodies for 10 h, 4°C and then immunoblotted.

For Western blots, immunoprecipitates or cell lysates were denaturized in Laemmli's sample buffer, resolved through 10% sodium dodedecyl sulfate polyacrylamide gel electrophoresis and then electroblotted to nitrocellulose membranes. Blots were stained with Ponceau S stain to confirm that protein content was equal in all lanes. Membranes were soaked in PBS to remove the Ponceau S and incubated in Tris-buffered saline containing 5% dried skimmed milk and 0.1% Tween 20 for 60 min to block the excess of non-specific protein binding sites. Membranes were then incubated overnight at

4°C with the particular primary antibodies indicated in each figure, followed by the adequate secondary antibodies. Immunoreactive polypeptides were detected by chemiluminescence and exposed to X-ray films. Densitometric analyses were performed and data analyzed with the Prism, GraphPad Software (San Diego, CA, USA).

Statistical analysis

Data are expressed as the mean values (average) ± the standard error (SE). Statistical analyses were performed with a one-way ANOVA, and Tukey *post hoc* comparisons were considered statistically significant when $p \leq 0.05$.

Results

L-Gln transporter SNAT3 is expressed in cultured chick cerebellar BGC

As a first step in the characterization of a plausible coupling between L-Glu uptake and L-Gln release, we decided to explore the biochemical nature of L-Gln uptake activity in BGC. Taking into consideration that of the L-Gln transporters described thus far in glial cells, the N family is capable to function in a reverse mode, we concentrated in this system and particularly in SNAT3, because it has been described that the highest levels of this transporter are present from post-natal day 7 in the rat cerebella, which corresponds roughly to chick embryonic day 14 (middle stage of cerebellar development) (Boulland *et al.* 2003). To gain insight into SNAT3 expression in BGC, we performed immunolabeling of P0 chick cerebella with an anti-SNAT3 specific antibody along with staining for specific cell markers, calbindin, KBP, and GLAST/EAAT1 to identify the layers of the cerebellar cortex.

It is important to mention that the anti-GLAST/EAAT1 antibody used in this study was generated in our lab against a peptide sequence specific of the chick protein, that it is known to possess a divergent C-terminus from the rat, mouse, and human sequence (Espinoza-Rojo *et al.* 2000). The specificity of this anti serum is presented in Fig. 1a. Pre-absorption of a 1 : 1000 dilution of the antibodies with 50 ng of the peptide prevents completely the recognition of the characteristic 60 kDa band. Figure 1b illustrates the localization of the Purkinje cell bodies and their arborizations after immunolabeling with the Purkinje's cell marker, calbindin. BGC were localized through the use of anti-KBP antibodies, and by GLAST/EAAT1 immunoreactivity. KBP is expressed exclusively in chick cerebellum BGC (Somogyi *et al.* 1990) and GLAST/EAAT1 is the major cerebellar glia transporter (Ottersen *et al.* 1997). SNAT3 immunostaining was abundantly found in the pial border lining the molecular cell layer as well as in Bergmann glia processes, in a similar fashion as KBP labeling, in contrast to calbindin that strongly labels the Purkinje cell soma and arborizations. Note that the pial cerebellar surface corresponds to BGC terminal end-feet (Fig. 1b). Immunofluorescence experiments in our cultured cells demonstrate that SNAT3 is present in cultured BGC both in the cytoplasm and in the plasma membrane (Fig. 1c). Finally, in Fig. 1(d), the 60-kDa immunoreactive band that corresponds to SNAT3 was detected. Taken together, these results show that SNAT3 is present in Bergmann glia both *in situ* as well as in primary cultures.

Characterization of L-[^{3}H]Gln uptake activity in cultured Bergmann glia

To establish a functional coupling between L-Glu uptake and L-Gln release, we measured the kinetic parameters of L-[^{3}H] Gln uptake in our culture system. Since it is known that System N is the only L-Gln uptake system capable to function with Li^+, we decided to use a LiCl-containing solution A. The results are presented in Fig. 2. A time-dependence of L-[^{3}H] Gln accumulation in LiCl-buffer was observed (Fig. 2a). By increasing L-Gln concentrations, we were able to determine the kinetic parameters of L-[^{3}H] Gln uptake. As depicted in Fig. 2b, the Li^+-tolerant component displays a K_M of 2.925 mM and a V_{max} of 1.818 μmol/min*mg. In addition, we made an amino acid competition experiment, we used MeAIB, the specific inhibitor of system A, alanine as a competitor for System Asc, A and N; for system N we used histidine and the mix of leucine and threonine as competitors for systems Asc and L. As shown in Fig. 2c, His reduces approximately 50% of Gln uptake in BGC, which is similar to the amount of uptake that remains in Li^+ containing assay solution. Overall these results suggest that L-Gln transport in BGC is mediated in an approximate 40% by SNAT3.

Functional coupling of GLAST with SNAT3

In BGC, L-Glu uptake is carried out by GLAST/EAAT1 (Ruiz and Ortega 1995) and D-Asp is capable to be transported by this carrier in an electrogenic fashion, with a net Na^+ influx. Under such circumstances, we reasoned that the uptake of L-[^{3}H] Gln, that relies on the Na^+ gradient would have to be inhibited. The results are presented in Fig. 3a, D-Asp at saturating concentrations (60 and 120 μM), prevents L-[^{3}H] Gln uptake. As expected, this effect is dose dependent with an IC_{50} of 0.873 μM (Fig. 3b). It should be noted that this value is only indicative of a specific transporter mediated effect and by no means reflects the affinity of D-Asp toward GLAST/EAAT-1 as established by D-[^{3}H] Asp uptake experiments. It should be noted a common property of any signaling cascade is amplification (Seger and Krebs 1995). These results prompted us to evaluate if the exposure of L-[^{3}H]-Gln-loaded BGC to L-Glu or D-Asp resulted in an increase in the presence of radioactivity in the medium, consequence of a reversed transport of the tracer through SNAT3. Indeed this is the case, as depicted in Fig. 4: L-Glu treatment resulted in an induced L-[^{3}H] Gln release. The identity of the released material as L-[^{3}H] Gln was determined by ion exchange chromatography in a subset of experiments. Each fraction

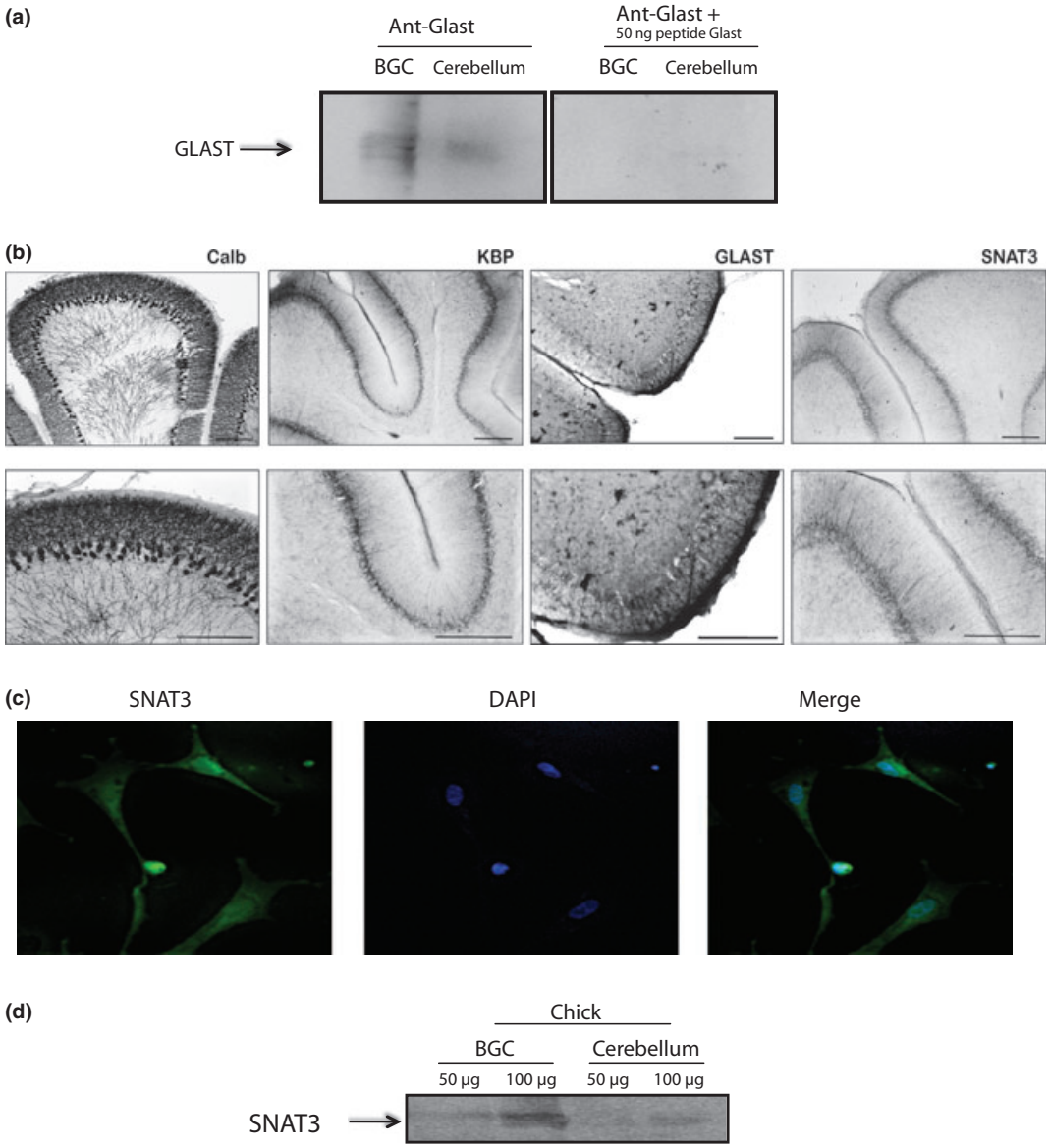

Fig. 1 Na^+-dependent neutral amino acid transporter 3 (SNAT3) expression in Bergmann glia. (a) Specificity of anti Na^+-dependent glutamate/aspartate transporter (GLAST)/EAAT1 anti-peptide antibodies. Total protein extracts from cultured chicken Bergmann glial cells (BGC) (50 µg) and cerebellum (75 µg) were assayed by Western blot with and without pre-absorption with 50 ng of the C-terminus chick GLAST peptide. (b) SNAT3 expression in chick cerebellum. Immunohistochemical characterization of chick cerebellar sections. Calbindin (Calb) labels Purkinje cells; kainate binding protein (KBP) and GLAST/EAAT1 are the BGC markers. Bar size: 50 µm. (c) Cells staining with anti-SNAT3 antibodies in cultured BGC (green). Nuclei were counterstained with DAPI (blue). (d) Total protein extracts from chick BGC cultures and cerebellum were assay by Western blot with anti-SNAT3 antibodies. A representative Western blot is shown.

collected *under the stimulus* (2 mL) of these experiments (three independent release experiments), as well as the final lysate, were added onto an activated 2 ml AG 1X-8 200/400 anion exchange column to separate L-[^{3}H] Gln from its metabolites. The column content was eluted with 2 ml volumes of H_2O, followed by three 2 ml volumes of 0.1 M HCl. Water elution removed uncharged L-[^{3}H] Gln, while subsequent acid elution extracted negatively charged metabolites such as L-Glu, α-ketoglutarate and other tricarboxylic acid intermediates (Mongin *et al.* 2011). The system was standardized with the application of a 150 µL aliquot of 10 µM L-[^{3}H] Glu aliquot and a 150 µL sample of 10 µM L-[^{3}H] Gln, that were eluted with HCl and H_2O, respectively. In all the fractions tested, roughly 70% of the radioactivity passed through the column as the L-[^{3}H] Gln standard. Moreover, this percentage was also found in the final cell

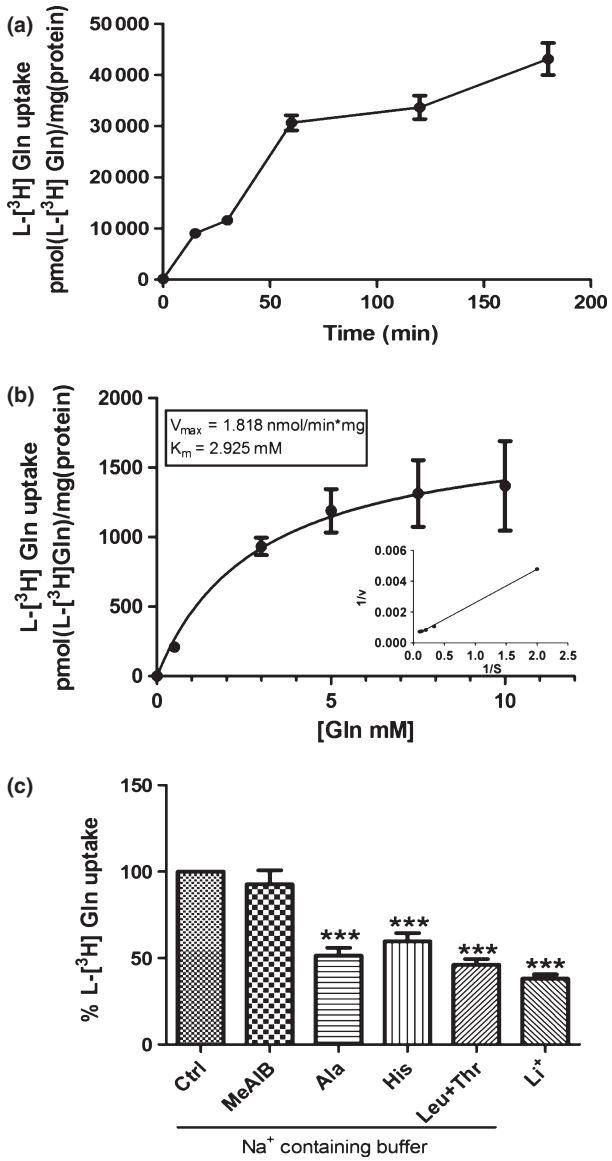

Fig. 2 System N kinetic parameters in cultured Bergmann glial cells (BGC). (a) Time course of L-[^{3}H] Gln uptake in BGC. The uptake was carried out in assay solution in which NaCl was replaced by LiCl (see Methods). A fixed amount of 0.5 μCi/mL L-[^{3}H] Gln, 200 μM L-Gln final concentration was present in the uptake assay for the indicated time periods. (b) L-[^{3}H] Gln uptake assay was performed with increasing L-Gln concentrations (0 mM, 0.5 mM, 3 mM, 5 mM, 7.5 mM, 10 mM). Transport kinetics V_{max} (μmol/min per mg protein) and K_M (mM) were determined by non-linear regression with the Prism 5 software (GraphPad) (c) Effect of different amino acids or the replacement of NaCl by LiCl on L-[^{3}H] Gln uptake in BGC. L-Gln was added at 200 μM concentration, the A-System specific substrate MeAIB was added at a 0.5 mM concentration, while other amino acids were added at a 10 mM concentration. Values represent mean ± SEM of a three independent experiments in quadruplicate, reproduced three times with similar results. Data were compared with non-stimulated of normal solution A by a Student's t-test (*** $p < 0.001$).

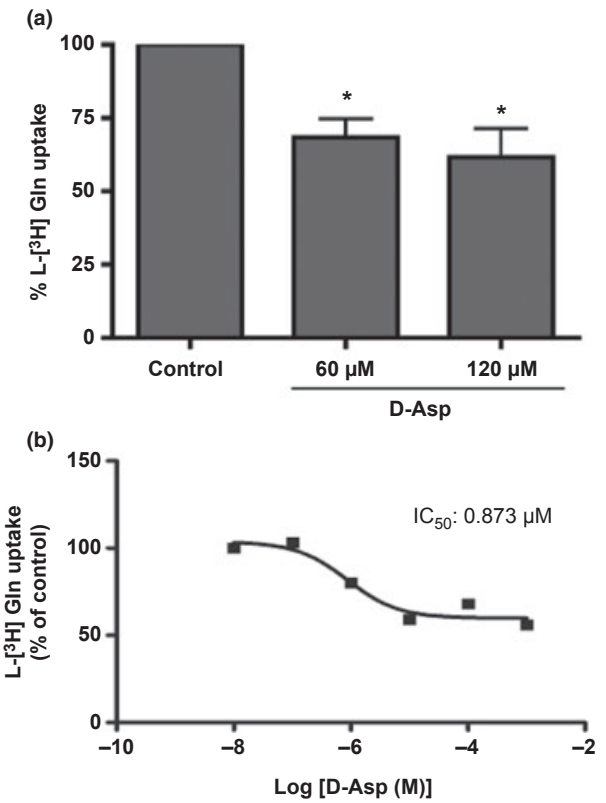

Fig. 3 Effect of D-Aspartate (D-Asp) in L-Gln uptake. (a) Effect of two different D-Asp concentrations (60 and 120 μM) in BGC L-[^{3}H] Gln uptake activity. Data were compared with non-stimulated cultures by a Student's t-test (*$p < 0.05$). (b) IC_{50} calculation of the D-Asp effect on L-[^{3}H] Glu uptake. Results are the mean ± SEM of three independent experiments. GraphPad Prism 5 was used to calculate the IC_{50} value.

extract, suggesting that most of the material released (> 70%) corresponds to L-Gln (Deitmer *et al.* 2003).

Note that exposure to either 50 μM or 1 mM D-Asp, also results in a stimulus-mediated release. In contrast, the AMPA receptors agonist, KA, did not evoke any significant L-[^{3}H] Gln release. These results suggest that L-Glu uptake is likely linked to L-Gln release.

Physical interaction between GLAST and SNAT3

The results described above were suggestive of a plausible physical interaction between GLAST and SNAT3. To test this possibility, we performed immunoprecipitation assays coupled to Western blot identification. The blots presented in Fig. 5a show that immunoprecipitation of BGC lysates with anti-GLAST antibodies and Western blot analysis with anti-SNAT3 antibodies enables us to detect the latter transporter in the immune complexes. As expected, SNAT3 immunoprecipitates contain GLAST. At this point, we decided to explore the possibility that GLAST activity would modulate its interaction with SNAT3. To this end, we exposed

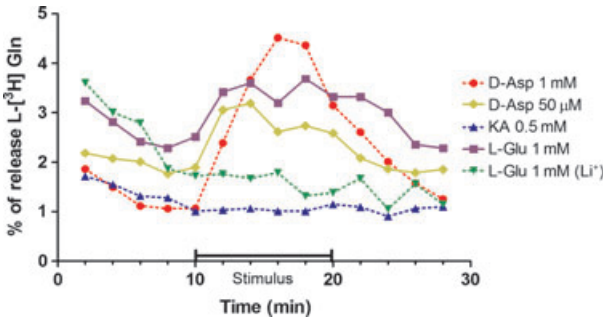

Fig. 4 L-glutamate (L-Glu) induces L-[^{3}H] Gln release from Bergmann glial cells (BGC). Cells were loaded with 0.5 μCi/mL of L-[^{3}H] Gln for 3 h. The media was removed and replaced every 2 min, a total of 15 fractions were collected. Fractions 1–5 and 11–14 contained solution A (see methods section), while in fractions 6–10 the following stimulus were added, D-Aspartate (D-Asp) 1 mM or 50 μM, kainate (KA) 0.5 mM, L-Glu 1 mM in sodium-containing or sodium-free assay buffer. Fraction 15 represents the cell lysates. The radioactivity associated to each fraction was determined by liquid scintillation counting and expressed as percentage of the total radioactivity in the experiment. A typical experiment is shown, reproduced three times with similar results.

confluent BGC cultures to 1 mM L-Glu and/or 2 mM L-Gln. As depicted in Fig. 5b, L-Glu but not L-Gln favor GLAST/SNAT3 physical interaction. We next explored if the transport activity of these two proteins would affect their putative association. To this end, we exposed the cultured cells to 60 μM D-Asp, 200 μM L-Gln, or a combination of both. The results are depicted in Fig. 5c: D-Asp induces GLAST/SNAT3 association (line 2), while L-Gln reduces the D-Asp effect (line 4). Note that 200 μM L-Gln induces a non-significative (compared to control) increase in GLAST/SNAT3 co-immunoprecipitation.

Discussion

Over the last decade, the concept of the tripartite synapse has been widely supported (Araque *et al.* 1999; Volterra and Meldolesi 2005; Halassa *et al.* 2007; Haydon *et al.* 2009). Glia cells express a battery of neurotransmitter receptors and transporters that enable them to respond to neuronal activity. Within glutamatergic synapses, the fundamental role of astrocytes in the recycling of the neurotransmitter has long been acknowledged (Bak *et al.* 2006). The L-Glu/Gln shuttle provides good evidence about the capacity of glial cells to respond to synaptic activity through the modification of their cellular functions such as GS expression and activity (Lehmann *et al.* 2009). Another example of a tight coupling of glia cells to glutamatergic synaptic activity is the astrocyte/neuron lactate shuttle (Magistretti 2009). Furthermore, depolarization of the cerebellar parallel fibers activates Bergmann glial L-Glu receptors and transporters (Balakrishnan and Bellamy 2009).

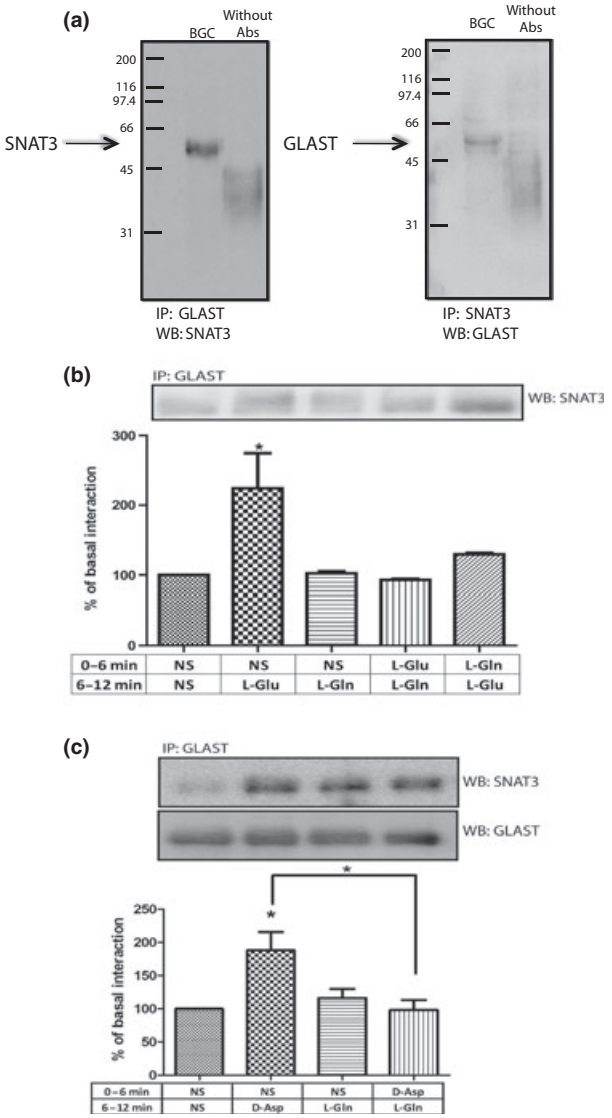

Fig. 5 Na^+-dependent neutral amino acid transporter 3 (SNAT3)/Na^+-dependent glutamate/aspartate transporter (GLAST) interaction in Bergmann glial cells (BGC). (a) BGC extracts were immunoprecipitated with anti-GLAST antibodies and the immunoprecipitate assayed by Western blot analysis with SNAT3 antibodies. The opposite experiment was done, total BGC proteins were immunoprecipitated with anti-SNAT3 and then subject to Western blot analysis with anti-GLAST serum. (b and c) BGC monolayers were exposed to the indicated stimulus; L-glutamate (L-Glu) 1 mM or L-Gln 2 mM (b), D-Asp 60 μM and L-Gln 200 μM (c). Total extracts were inmmunoprecipitated with anti-GLAST and then subjected to Western blot analysis with SNAT3 antibodies. Western blot anti-GLAST was used as loading control. (*$p < 0.05$) by a Student's *t*-test. A typical autoradiogram of three independent experiments is shown.

Using as a model system cultured BGC from chick cerebellum, we characterized several signaling cascades involved in L-Glu-dependent transcriptional regulation (Lopez-Bayghen *et al.* 2007). We have been able to demonstrate

that L-Glu signaling is also supported by the unique L-Glu transporter expressed in these cells, GLAST/EAAT1 (Martinez-Lozada *et al.* 2011). All these findings, as well as the lack of a complete biochemical characterization of the L-Glu/Gln shuttle, led us to explore a plausible interaction between L-Glu uptake and L-Gln release.

The first issue that we had to tackle before any biochemical experiment could even be designed, was the identification of the expression of L-Gln transporters that function in reverse mode within BGC. Since System N members could fulfill this requirement, and SNAT3 expression is prominent in the days just before birth and in the adulthood in the rat, we restricted our approach to SNAT3. However, we must mention that SNAT5 has been shown to be present in rat Bergmann glia cells (Cubelos *et al.* 2005). The results presented in Fig. 1, demonstrate, in the one hand, the specificity of our anti-peptide anti-GLAST/EAAT1 antibodies (Fig. 1a) as well as that SNAT3 is expressed in chick cerebellar BGC, both *in situ* as well as in our culture system. It is important to note the similar labeling of the Bergmann glia processes with anti-GLAST, anti-KBP, and anti-SNAT3 antibodies. Unfortunately, all these antibodies were generated in goat, preventing us to do double immunolabeling experiments. Nevertheless, if one compares the decoration with anti-calbindin antibodies, a Purkinje cells marker, it remains clear that SNAT3 co-localizes with KBP and GLAST.

The fact that the kinetic parameters detected for SNAT3 in our culture system are in the mM range as has been reported for other glia cells, made us confident that indeed, Bergmann glia express SNAT3 transporters. One could argue that several reports settle a K_m value of approximately 1 mM (Kilberg *et al.* 1980; Chaudhry *et al.* 2001; Broer *et al.* 2004) for SNAT3 and that the ones we report here are higher (2.9 mM). It should be noted, however, that the reported constants were obtained in heterologous glial cultures, whereas we use an enriched BGC culture (Ortega *et al.* 1991). Besides, our model system is avian origin in contrast to rodent cells used in the referred studies. Whether the apparent discrepancy is related to the cell population examined or the species used, it is not known at this moment. At this stage, we cannot rule out a plausible involvement of SNAT5 in our measurements of L-[^{3}H] Gln uptake or release. A pertinent observation could also be that if we expect that this carrier would function in a reverse manner, why we would be interested in the characterization of the uptake activity. The answer is simple: it is easier to measure uptake than release, and for kinetic purposes it is valid approach (Broer *et al.* 2004).

In any event, it became important to demonstrate a L-Glu-induced L-Gln release. Given the fact that in our experimental conditions, > 70% of the L-[^{3}H] Gln loaded in the cells remains as L-[^{3}H] Gln as judged by ion exchange chromatography, the experiments described in Fig. 4 show that D-Asp is capable to trigger L-Gln release in a more efficient manner than L-Glu. A plausible explanation to this finding is that L-Glu binds to receptors and transporters, whereas D-Asp would only binds to GLAST/EAAT1. These results strengthen our confidence in the hypothesis of a complex between these transporters. A detectable immunoreactive SNAT3 polypeptide is present in anti-GLAST immunoprecipitates and *vice versa* (Fig. 5a). Whether this is a direct protein–protein interaction between these two transporters, it is not known at this moment, work in progress in our lab is aimed at that direction. In support to our hypothesis, it is important to mention that recently the group of Billups, using electrophysiological recordings, has reported that astrocytes juxtaposed to the glutamatergic calyx of Held synapse in the rat medial nucleus of the trapezoid body release L-Gln as a consequence of L-Glu transport activation (Uwechue *et al.* 2012).

What could it be the purpose of a GLAST/SNAT3 association? One could postulate that in order for SNAT3 to work in reverse mode a significant rise in intracellular Na^+ within the vicinity of the transporter should be taking place. A functional coupling with GLAST would provide that local rise in Na^+ concentration, if this interpretation is correct then, first of all, D-Asp influx should prevent any L-[^{3}H] Gln uptake, and as demonstrated in Fig. 3, this is exactly the case. The fact that this prevention in L-[^{3}H] Gln uptake is dose dependent suggests that this is an specific effect. A valid argument in the interpretation of these results is that the

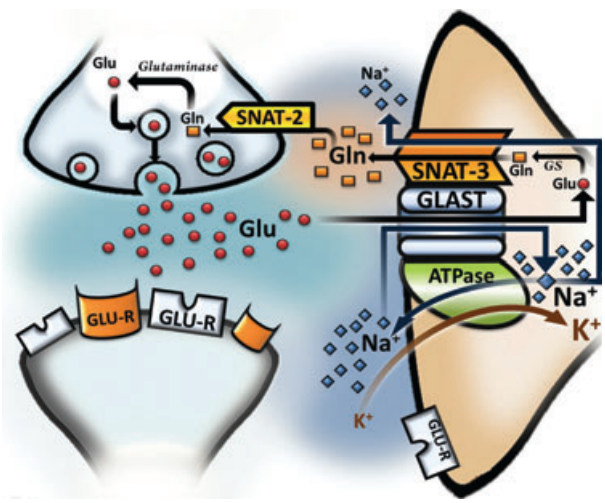

Fig. 6 Schematic representation of the Na^+-dependent glutamate/aspartate transporter (GLAST)/Na^+-dependent neutral amino acid transporter 3 (SNAT3) complex. L-Glu released from the parallel fibers is taken up into Bergmann glia cells through GLAST. The increase in $[Na^+]_i$ favors the operation, in reverse mode, of SNAT3 with the consequent release of L-Gln. Glu, L-glutamate; Gln, glutamine; GLU-R, Glutamate receptors; GLAST, sodium-dependent glutamate/aspartate transporter; SNAT, sodium-dependent neutral amino acid transporter.

reported K_m of BGC GLAST/EAAT1 is 62 μM and the IC_{50} values for the prevention in L-[^{3}H] Gln uptake is of 0.873 μM. A plausible explanation for this apparent discrepancy lies in the signal amplification inherent to cell signaling. For example, in BGC, a 1 mM L-Glu has to be applied to record a Na^+ inward current (Bennay *et al.* 2008), whereas the EC_{50} for L-Glu obtained through Oct-2/DNA binding activity is 164 μM (Mendez *et al.* 2004). Furthermore, it could be expected that D-Asp should increase GLAST/SNAT3 association whereas L-Gln not. Indeed, the results presented in Fig. 5c support this vision. A model of our interpretation of the results is shown in Fig. 6.

Taken together, our results provide a support to the critical involvement of glia cells in the modulation of L-Glu-mediated neurotransmission in what is nowadays known as the tripartite synapse.

Acknowledgements

This study was supported by grants from Conacyt-Mexico to A.O. (79502,188138) and PROMEP/SEP to A.R (UAQ-FOFI2012-FCQ201216). Z.M-L, A.M.G. and M.F-M are supported by Conacyt-Mexico fellowships. The technical assistance of Blanca Ibarra is acknowledged. The authors certify that there is no conflict of interest with any financial organization regarding the material discussed in the manuscript.

References

Albrecht J. (1989) L-glutamate stimulates the efflux of newly taken up glutamine from astroglia but not from synaptosomes of the rat. *Neuropharmacology* **28**, 885–887.

Anthony T. E., Klein C., Fishell G. and Heintz N. (2004) Radial glia serve as neuronal progenitors in all regions of the central nervous system. *Neuron* **41**, 881–890.

Araque A., Parpura V., Sanzgiri R. P. and Haydon P. G. (1999) Tripartite synapses: glia, the unacknowledged partner. *Trends Neurosci.* **22**, 208–215.

Bak L. K., Schousboe A. and Waagepetersen H. S. (2006) The glutamate/GABA-glutamine cycle: aspects of transport, neurotransmitter homeostasis and ammonia transfer. *J. Neurochem.* **98**, 641–653.

Balakrishnan S. and Bellamy T. C. (2009) Depression of parallel and climbing fiber transmission to Bergmann glia is input specific and correlates with increased precision of synaptic transmission. *Glia.* **57**, 393–401.

Bennay M., Langer J., Meier S. D., Kafitz K. W. and Rose C. R. (2008) Sodium signals in cerebellar Purkinje neurons and Bergmann glial cells evoked by glutamatergic synaptic transmission. *Glia.* **56**, 1138–1149.

Boulland J. L., Rafiki A., Levy L. M., Storm-Mathisen J. and Chaudhry F. A. (2003) Highly differential expression of SN1, a bidirectional glutamine transporter, in astroglia and endothelium in the developing rat brain. *Glia.* **41**, 260–275.

Broer A., Deitmer J. W. and Broer S. (2004) Astroglial glutamine transport by system N is upregulated by glutamate. *Glia.* **48**, 298–310.

Chaudhry F. A., Krizaj D., Larsson P., Reimer R. J., Wreden C., Storm-Mathisen J., Copenhagen D., Kavanaugh M. and Edwards R. H. (2001) Coupled and uncoupled proton movement by amino acid transport system. *N. EMBO J.* **20**, 7041–7051.

Cubelos B., Gonzalez-Gonzalez I. M., Gimenez C. and Zafra F. (2005) Amino acid transporter SNAT5 localizes to glial cells in the rat brain. *Glia.* **49**, 230–244.

Danbolt N. C. (2001) Glutamate uptake. *Prog. Neurobiol.* **65**, 1–105.

Deitmer J. W., Broer A. and Broer S. (2003) Glutamine efflux from astrocytes is mediated by multiple pathways. *J. Neurochem.* **87**, 127–135.

Dolinska M., Dybel A. and Albrecht J. (2000) Glutamine transport in C6 glioma cells. *Neurochem. Int.* **37**, 139–146.

Dolinska M., Dybel A., Zablocka B. and Albrecht J. (2003) Glutamine transport in C6 glioma cells shows ASCT2 system characteristics. *Neurochem. Int.* **43**, 501–507.

Espinoza-Rojo M., Lopez-Bayghen E. and Ortega A. (2000) GLAST: gene expression regulation by phorbol esters. *NeuroReport* **11**, 2827–2832.

Gonzalez-Mejia M. E., Morales M., Hernandez-Kelly L. C., Zepeda R. C., Bernabe A. and Ortega A. (2006) Glutamate-dependent translational regulation in cultured Bergmann glia cells: involvement of p70S6K. *Neuroscience* **141**, 1389–1398.

Grewal S., Defamie N., Zhang X., De Gois S., Shawki A., Mackenzie B., Chen C., Varoqui H. and Erickson J. D. (2009) SNAT2 amino acid transporter is regulated by amino acids of the SLC6 gamma-aminobutyric acid transporter subfamily in neocortical neurons and may play no role in delivering glutamine for glutamatergic transmission. *J. Biol. Chem.* **284**, 11224–11236.

Hagglund M. G., Sreedharan S., Nilsson V. C., Shaik J. H., Almkvist I. M., Backlin S., Wrange O. and Fredriksson R. (2011) Identification of SLC38A7 (SNAT7) protein as a glutamine transporter expressed in neurons. *J. Biol. Chem.* **286**, 20500–20511.

Halassa M. M., Fellin T. and Haydon P. G. (2007) The tripartite synapse: roles for gliotransmission in health and disease. *Trends Mol Med.* **13**, 54–63.

Hansson E. and Ronnback L. (1995) Astrocytes in glutamate neurotransmission. *FASEB J.* **9**, 343–350.

Haydon P. G., Blendy J., Moss S. J. and Rob Jackson F. (2009) Astrocytic control of synaptic transmission and plasticity: a target for drugs of abuse? *Neuropharmacology* **56**(Suppl 1), 83–90.

Henneberger C., Papouin T., Oliet S. H. and Rusakov D. A. (2010) Long-term potentiation depends on release of D-serine from astrocytes. *Nature* **463**, 232–236.

Jenstad M., Quazi A. Z., Zilberter M. *et al.* (2009) System A transporter SAT2 mediates replenishment of dendritic glutamate pools controlling retrograde signaling by glutamate. *Cereb. Cortex* **19**, 1092–1106.

Kilberg M. S., Handlogten M. E. and Christensen H. N. (1980) Characteristics of an amino acid transport system in rat liver for glutamine, asparagine, histidine, and closely related analogs. *J. Biol. Chem.* **255**, 4011–4019.

Lehmann C., Bette S. and Engele J. (2009) High extracellular glutamate modulates expression of glutamate transporters and glutamine synthetase in cultured astrocytes. *Brain Res.* **1297**, 1–8.

Lopez-Bayghen E., Rosas S., Castelan F. and Ortega A. (2007) Cerebellar Bergmann glia: an important model to study neuron-glia interactions. *Neuron Glia Biol.* **3**, 155–167.

Magistretti P. J. (2009) Role of glutamate in neuron-glia metabolic coupling. *Am. J. Clin. Nutr.* **90**, 875S–880S.

Malatesta P., Hack M. A., Hartfuss E., Kettenmann H., Klinkert W., Kirchhoff F. and Gotz M. (2003) Neuronal or glial progeny: regional differences in radial glia fate. *Neuron* **37**, 751–764.

Martinez-Lozada Z., Hernandez-Kelly L. C., Aguilera J., Lopez-Bayghen E. and Ortega A. (2011) Signaling through EAAT-1/GLAST in cultured Bergmann glia cells. *Neurochem. Int.* **59**, 871–879.

Mendez J. A., Lopez-Bayghen E., Rojas F., Hernandez M. E. and Ortega A. (2004) Glutamate regulates Oct-2 DNA-binding activity through alpha-amino-3-hydroxy-5-methylisoxazole-4-propionate receptors in cultured chick Bergmann glia cells. *J. Neurochem.* **88**, 835–843.

Mongin A. A., Hyzinski-Garcia M. C., Vincent M. Y. and Keller R. W., Jr (2011) A simple method for measuring intracellular activities of glutamine synthetase and glutaminase in glial cells. *Am. J. Physiol. Cell Physiol.* **301**, C814–822.

Ortega A., Eshhar N. and Teichberg V. I. (1991) Properties of kainate receptor/channels on cultured Bergmann glia. *Neuroscience* **41**, 335–349.

Ottersen O. P., Chaudhry F. A., Danbolt N. C., Laake J. H., Nagelhus E. A., Storm-Mathisen J. and Torp R. (1997) Molecular organization of cerebellar glutamate synapses. *Prog. Brain Res.* **114**, 97–107.

Regan M. R., Huang Y. H., Kim Y. S., Dykes-Hoberg M. I., Jin L., Watkins A. M., Bergles D. E. and Rothstein J. D. (2007) Variations in promoter activity reveal a differential expression and physiology of glutamate transporters by glia in the developing and mature CNS. *J. Neurosci.* **27**, 6607–6619.

Rosas S., Vargas M. A., Lopez-Bayghen E. and Ortega A. (2007) Glutamate-dependent transcriptional regulation of GLAST/EAAT1: a role for YY1. *J. Neurochem.* **101**, 1134–1144.

Ruiz M. and Ortega A. (1995) Characterization of an Na(+)-dependent glutamate/aspartate transporter from cultured Bergmann glia. *NeuroReport* **6**, 2041–2044.

Sager C., Tapken D., Kott S. and Hollmann M. (2009) Functional modulation of AMPA receptors by transmembrane AMPA receptor regulatory proteins. *Neuroscience* **158**, 45–54.

Seger R. and Krebs E. G. (1995) The MAPK signaling cascade. *FASEB J.* **9**, 726–735.

Shank R. P. and Campbell G. L. (1984) Glutamine, glutamate, and other possible regulators of alpha-ketoglutarate and malate uptake by synaptic terminals. *J. Neurochem.* **42**, 1162–1169.

Somogyi P., Eshhar N., Teichberg V. I. and Roberts J. D. (1990) Subcellular localization of a putative kainate receptor in Bergmann glial cells using a monoclonal antibody in the chick and fish cerebellar cortex. *Neuroscience* **35**, 9–30.

Uwechue N. M., Marx M. C., Chevy Q. and Billups B. (2012) Activation of glutamate transport evokes rapid glutamine release from perisynaptic astrocytes. *J. Physiol.* **590**, 2317–2331.

Volterra A. and Meldolesi J. (2005) Astrocytes, from brain glue to communication elements: the revolution continues. *Nat. Rev. Neurosci.* **6**, 626–640.

Wieronska J. M. and Pilc A. (2009) Metabotropic glutamate receptors in the tripartite synapse as a target for new psychotropic drugs. *Neurochem. Int.* **55**, 85–97.

Glutamate-Dependent Translational Control in Cultured Bergmann Glia Cells: eIF2α Phosphorylation

Marco A. Flores-Méndez, Zila Martínez-Lozada, Hugo C. Monroy, Luisa C. Hernández-Kelly, Iliana Barrera & Arturo Ortega

Neurochemical Research

ISSN 0364-3190

Neurochem Res
DOI 10.1007/s11064-013-1024-1

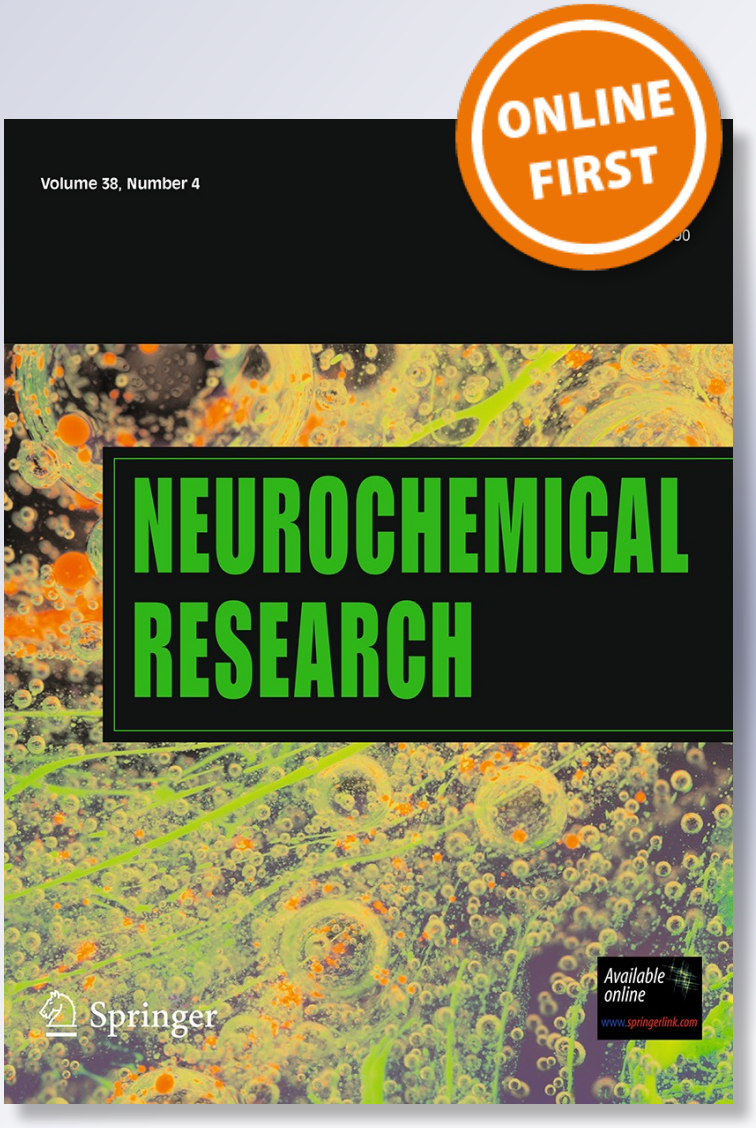

Springer

Neurochem Res
DOI 10.1007/s11064-013-1024-1

ORIGINAL PAPER

Glutamate-Dependent Translational Control in Cultured Bergmann Glia Cells: eIF2α Phosphorylation

Marco A. Flores-Méndez · Zila Martínez-Lozada · Hugo C. Monroy · Luisa C. Hernández-Kelly · Iliana Barrera · Arturo Ortega

Received: 24 December 2012 / Revised: 20 February 2013 / Accepted: 15 March 2013

Abstract Glutamate (Glu), the major excitatory amino acid, activates a wide variety of signal transduction cascades. Synaptic plasticity relies on activity-dependent differential protein expression. Glu receptors have been critically involved in long-term synaptic changes, although recent findings suggest that Na^+-dependent Glu transporters participate in Glu-induced signalling. Within the cerebellum, Bergmann glia cells are in close proximity to glutamatergic synapses and through their receptors and transporters, sense and respond to neuronal glutamatergic activity. Translational control represents the fine-tuning stage of protein expression regulation and Glu modulates this event in glial cells. In this context, we decided to explore the involvement of Glu receptors and transporters in the regulation of the initiation phase of protein synthesis. To this end, Bergmann glia cells were exposed to glutamatergic ligands and the serine 51-phosphorylation pattern of the main regulator of the initiation phase of translation, namely the α subunit of eukaryotic initiation factor 2 (eIF2α), determined. A time and dose-dependent increase in eIF2α phosphorylation was detected. The signalling cascade included Ca^{2+} influx, activation of the Ca^{2+}/calmodulin-dependent protein kinase II and protein kinase C. These results provide an insight into the molecular targets of the Glu effects at the translational level and strengthen the notion of the critical involvement of glia cells in glutamatergic synaptic function.

M. A. Flores-Méndez · Z. Martínez-Lozada · H. C. Monroy · L. C. Hernández-Kelly · I. Barrera · A. Ortega (✉)
Departamento de Genética y Biología Molecular, Centro de Investigación y de Estudios Avanzados del Instituto Politécnico Nacional (Cinvestav-IPN), Apartado Postal 14-740, 07000 Mexico, D.F., Mexico
e-mail: arortega@cinvestav.mx

Keywords Bergmann glia · Eukaryotic initiation factor 2 · Glutamate receptors · Translational control

Introduction

Excitatory neurotransmission in the vertebrate central nervous system (CNS) is mediated largely by glutamate (Glu). Two different subtypes of Glu receptors have been described to be expressed in neurons and glia cells: ionotropic (iGluRs) and metabotropic receptors (mGluRs). Glu analogs that activate these receptors selectively serve to classify them iGluRs are divided into *N*-methyl-D-aspartate (NMDA), α-amino-3-hydroxy-5-methyl-4-isoaxazolepropionate (AMPA) and kainate (KA) receptors [1]. Metabotropic receptors are described in terms of sequence similarity, signal transduction mechanisms and pharmacology. Group I receptors are coupled to the stimulation of phospholipase C with the consequent release of intracellular Ca^{2+}, while Groups II and III are coupled to the inhibition of adenylate cyclase. These three groups are activated preferentially by (RS)-3,5-dihydroxyphenylglycine (DHPG) for Group I, (S)-4-Carboxy-3-hydroxyphenylglycine (S)-4C3HPG activates Group II while L-(+)-2-amino-4-phosphonobutyric acid (L-AP4) acts upon Group III [2].

Astrocytes outnumber neurons in the CNS and despite of this fact, their contribution to brain physiology has been a matter of debate for a number of years. In the last decades, their ability to produce and release neuroactive substances and their proven expression of most of the identified neurotransmitter receptors and transporters have made that this perception gradually changes [3]. An excellent model in which the role of glia cells as partners of neurons can be documented is the primary cultures of chick

Published online: 28 March 2013

cerebellar Bergmann glia cells (BGC). These cells are the most abundant non-neuronal population of the cerebellum, span the molecular layer covering completely excitatory and inhibitory synapses [4]. This characteristic localization is related their involvement in neurotransmitter uptake and turnover, K^+ homeostasis, lactate supply and pH regulation [5]. In terms of glutamatergic transmission, BGC are in a very short proximity to the parallel fiber-Purkinje cell synapses, and participate in the Glu/glutamine shuttle that assures the proper neurotransmitter supply to presynaptic terminals. In this sense, BGC respond to glutamatergic stimulation, as we have been able to characterize over the years [6].

It has long been established that transcription and translation are essential for long-term memory [7]. Activity-dependent gene expression regulation stabilizes the synaptic changes that underlie the late phase of long-term potentiation [8]. In this regard, it should be noted that most studies focused in gene expression regulation are devoted to the study of this process at the transcriptional level. Nevertheless, the rate of protein synthesis has a crucial role in synaptic plasticity [9]. Translational control offers the possibility of a rapid response to external stimulus without mRNA synthesis and transport. Therefore, immediacy is the most conspicuous advantage of translational over transcriptional control.

In eukaryotes, the initiator methionyl-tRNA is conveyed to the ribosome by eukaryotic initiation factor 2 (eIF2) once it has been complexed with GTP by eukaryotic factor 2B (eIF2B) a guanine nucleotide exchange factor. This reaction is inhibited by the phosphorylation of the α subunit of eIF2 on Serine 51 [10]. Although this post-translational modification *per se* does not inhibit the general function of eIF2, it renders the protein unable to recycle due to the tight binding of phospho eIF2α to the regulatory subunits of eIF2B, preventing its nucleotide exchange function and thus, the formation of the ternary complex. Under these conditions, total protein synthesis decrease [11, 12]. In this context, modulating the phosphorylation state of eIF2α has proven to be one of the major ways in which cells regulate the overall rate of protein synthesis. Thus far, there are four known eIF2α kinases: general control non-depressible 2 kinase (GCN2), heme-regulated inhibitor kinase (HRI), double-stranded RNA-dependent protein kinase (PKR) and PKR-like endoplasmic reticulum kinase (PERK) [13].

In the present communication we demonstrate that exposure of cultured chick Bergmann glia cells to Glu is linked to an increase in eIF2α Ser 51 phosphorylation. Apparently, both receptors and transporters are involved in this process and the signalling cascade involves the Ca^{2+}-dependent kinases CaMKII and PKC.

Methods

Materials

Tissue culture reagents were obtained from GE Healthcare (Carlsbad, CA, USA). DL-TBOA (DL-threo-b-Benzyloxyaspartic acid), THA (threo-β-hydroxyaspartate), DNQX (6,7-Dinitroquinoxaline-2,3-dione), LAP5 (L-(+)-2-Amino-5-phosphonopentanoic acid); Asp (D-aspartate), W7 (*N*-(6-Aminohexyl)-5-chloro-1-naphtha lene sulfonamide hydrochloride and Glu were all obtained from Tocris-Cookson (St. Louis, MO USA). Polyclonal anti phospho-eIF2α (Ser 51) and anti eIF2α were purchased from Life Technologies (Mexico City, Mexico). Monoclonal anti-actin antibody was kindly donated by Prof. Manuel Hernández (Cinvestav-IPN). Horseradish peroxidase-linked anti-rabbit antibodies, and the enhanced chemiluminescence reagent (ECL), were obtained from Amersham Biosciences (Buckinghamshire, UK). All other chemicals were purchased from Sigma (St. Louis, MO, USA).

Cell Culture and Stimulation Protocol

Primary cultures of cerebellar BGC were prepared from 14-day-old chick embryos as previously described [14]. Cells were plated in 6-well plastic culture dishes in DMEM containing 10 % fetal bovine serum, 2 mM glutamine, and gentamicin (50 μg/ml) and used on the 4th to 7th day after culture. Before any treatment, confluent monolayers were switched to non-serum DMEM media containing 0.5 % bovine serum albumin (BSA) for 30 min and then treated as indicated. Inhibitors were added 30 min before agonists. The cells were treated with Glu analogues added to culture medium for the indicated time periods; after that the medium was replaced with DMEM/0.5 % albumin.

SDS-PAGE and Western Blots

Cells from confluent monolayers were harvested with phosphate-buffer saline (PBS) (10 mM K_2HPO_4/KH_2PO_4, 150 mM NaCl, pH 7.4) containing phosphatase inhibitors (10 mM NaF, 1 mM Na_2MoO_4 and 1 mM Na_3VO_4). The cells were lysed with RIPA buffer (50 mM Tris–HCl, 1 mM EDTA, 150 mM NaCl, 1 mM phenylmethylsufonyl fluoride, 1 mg/ml aprotinin, 1 mg/ml leupeptin, 1 % NP-40, 0.25 % sodium deoxycholate, 10 mM NaF, 1 mM Na_2MoO_4 and 1 mM Na_3VO_4 pH 7.4). Cell lysates were denaturized in Laemmli's sample buffer, and equal amount of proteins (50 μg as determined by the Bradford method) were resolved through a 15 % SDS-PAGE and then electroblotted to nitrocellulose membranes. Blots were stained with Ponceau S stain to confirm that protein content was

equal in all lanes. Membranes were soaked in PBS to remove the Ponceau S and incubated in TBS containing 5 % dried skimmed milk and 0.1 % Tween 20 for 60 min to block the excess of non-specific protein binding sites. Membranes were then incubated overnight at 4 °C with the particular primary antibodies indicated in each figure, followed by secondary antibodies. Immunoreactive polypeptides were detected by chemiluminescence and exposed to X-ray films. Densitometry analyses were performed and data analyzed with Prism, GraphPad Software (San Diego, CA, USA).

Staining Procedures

Bergmann glia cells primary cultures were grown on poly-L-lysine-treated (0.01 mg/ml) glass coverslips following the procedure described above. Cells were fixed by exposure for 10 min to methanol at −20 °C and washed twice with PBS containing 0.5 % Triton X-100 (washing solution). Non-specific binding was prevented by incubation with 1 % BSA in PBS (blocking solution) for 1 h. Cells were exposed to a 1:50 dilution of the primary antibody anti-phospho-eIF2α in blocking solution overnight to 4 °C. Then, cells were washed three times with washing solution and incubated with a 1:200 dilution of the fluorescent-labeled secondary antibodies dissolved in blocking solution. After washing out secondary antibodies, cell preparations were mounted with Vectashield (Vector Laboratories, Burlingame, CA, USA) and examined with an inverted fluorescence microscope (Zeiss Axioscope 40).

Metabolic Labeling of Proteins

Confluent BGC monolayers were labeled overnight with 1 μCi of L-[^{35}S] Methionine (Amersham Pharmacia Biotech) in methionine-free medium DMEM. After extensive washing, the cells were treated with Asp at selected time points. Cells were washed twice with ice-cold PBS (10 mM K_2HPO_4/KH_2PO_4, 150 mM NaCl, pH 7.4) and lysed with ice-cold RIPA buffer (20 mM Tris–HCl, pH 7.5, 50 mM KCl, 5 mM $MgCl_2$, 400 mM NaCl, 2 mM dithiothreitol, 1 mM aprotinin, 1 mM leupeptin, and 100 μM phenylmethylsulfonyl fluoride, 20 % glycerol, 1 % Triton X-100).

Assessment of Overall Protein Synthesis

To measure overall protein synthesis, an aliquot of the samples (approximately 15 μg of protein) was spotted onto GF/C microfiber filters Glass (Whatman). The filters were air-dried and washed for 10 min in ice-cold 10 % trichloroacetic acid (TCA) followed by three 10-min washes in ice-cold 5 % TCA. The filters were air-dried at room temperature and placed in scintillation vials with 2 ml of scintillation liquid containing 10 μl glacial acetic acid. [^{35}S]-methionine incorporation was determined via liquid scintillation counting (Beckman LS 6000 SC).

Statistical Analysis

Data are expressed as the mean values (average) ± the standard error (S.E.). A nonparametric one-way ANOVA (Kruskal–Wallis test) was performed to determine significant differences between conditions. When these analyses indicated significance (at the 0.05 level), a Dunn's post hoc test was used to determine which conditions were significantly different from each other with Prism, GraphPad Software (San Diego, CA, USA).

Results

Glu Induces eIF2α Phosphorylation in Bergmann Glia Cells

Protein synthesis is probably the most energy-consuming cellular process; therefore it is not surprising that it is temporarily inhibited when specific cellular functions have to be accomplished in order to preserve viability. Cells respond rapidly to external stimuli by modulating global rates of protein synthesis and/or the translational efficiencies of specific mRNAs. In previous reports, we have observed that Glu treatment decreases [^{35}S]-methionine incorporation in BGC in a dose and time-dependent manner [15]. Such treatment leads to the Thr 56 phosphorylation of eEF2 preventing its binding to the ribosomes [16]. Since the initiation phase of the translational process is usually the rate-limiting step, we decided to study Ser-51 eIF2α phosphorylation in BGC. As a first approach, we exposed confluent BGC monolayers to a fixed 1 mM Glu concentration for 10 min and as depicted a clear increase in eIF2α Ser-51 phosphorylation was found (Fig. 1, panel a). As expected, neither the levels of eIF2α nor those of actin changed in Glu-treated cells (Fig. 1, panel a). Note the low level of detection of the anti eIF2α antibodies in the chicken primary cultured cells; therefore we decided to normalize all subsequent gels with actin. Immunochemical evidence of the increase in eIF2α phosphorylation after Glu exposure is presented in Fig. 1 (panel b).

The time-dependence of eIF2α phosphorylation was established, a 5 min Glu treatment is sufficient to increase the phosphorylation signal reaching its maximal levels after 10 min of Glu (Fig. 2, panel a). All subsequent experiments were done after 10 min of glutamatergic stimulation. In order to support a physiological relevance of this phosphorylation, we treated BGC cultures with

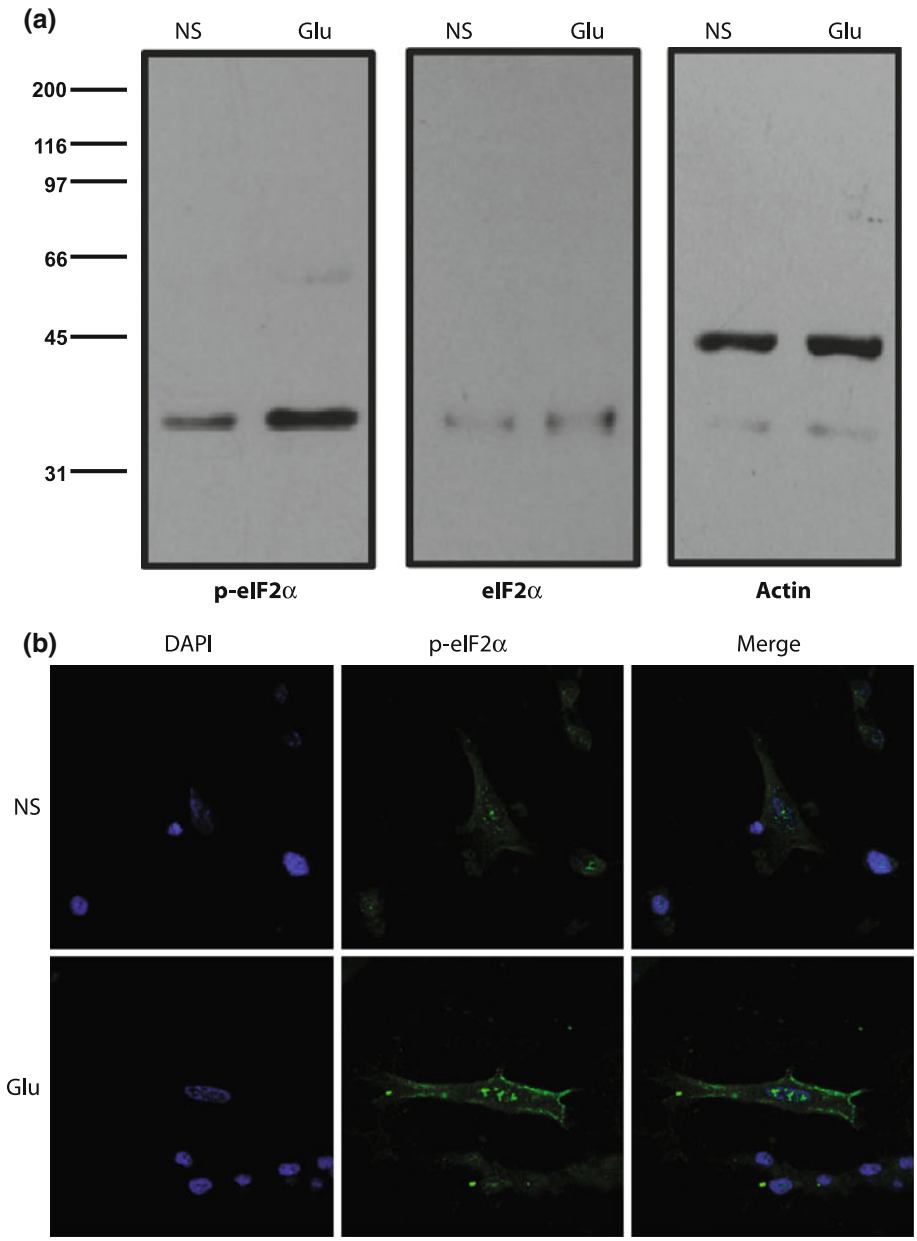

Fig. 1 Glu induces eIF2α phosphorylation in BGC. Confluent BGC monolayers were treated with 1 mM Glu for 10 min. **a** Total protein extracts were subjected to Western blot analysis. The membranes were incubated with a specific antibody that recognizes Ser-51 phosphorylated eIF2α, and an antibody that recognizes total eIF2α. Actin was detected in the same cell extracts as a loading control. **b** Cells were incubated with anti-phospho-eIF2α antibody and immunostained with the antibody that recognizes phosphorylated eIF2α. *NS* non-stimulated. The immunopositive polypeptides were visualized with peroxidase-conjugated goat anti-rabbit IgGs, using ECL kit. An autoradiography of a typical experiment is shown

increasing Glu concentrations and as can be seen in Fig. 2 a clear dose-dependency could be established with an EC_{50} of 11.4 μM, suggesting a receptor-mediated effect (Fig. 2, panel c). Our group, as well as others, have reported that Glu transporters are capable to activate signal transduction cascades [17–19], with this in mind, we decided to investigate whether the activation of the Na^+-dependent Glu transporter expressed in BGC, namely the excitatory amino acid transporter 1 (EAAT-1/GLAST), could be coupled to eIF2α phosphorylation. The results are presented in Fig. 3, exposure of the cultured cells to a 1 mM concentration of D-aspartate (Asp), leads to a time-dependent increase in Ser 51 eIF2α phosphorylation. Note that the maximal phosphorylation is obtained after 15 min, in contrast with the Glu effect that peaks after 10 min. A dose-dependence effect could also be established for Asp with an EC_{50} of 50.2 μM. Furthermore, Asp exposure also regulates [^{35}S]-methionine incorporation into newly synthetized polypeptides (Fig. 3, panel d) in a similar fashion as Glu [15].

Pharmacological Characterization of the Glu-Dependent Ser-51 eIF2α Phosphorylation

Through the use of pharmacological tools, the profile of the Glu response was determined. As shown in Fig. 4, the ionotropic agonist NMDA, as well as the group I mGluRs agonist DHPG and group III mGluRs agonist L-AP4, augments eIF2α phosphorylation. Neither, AMPA nor KA

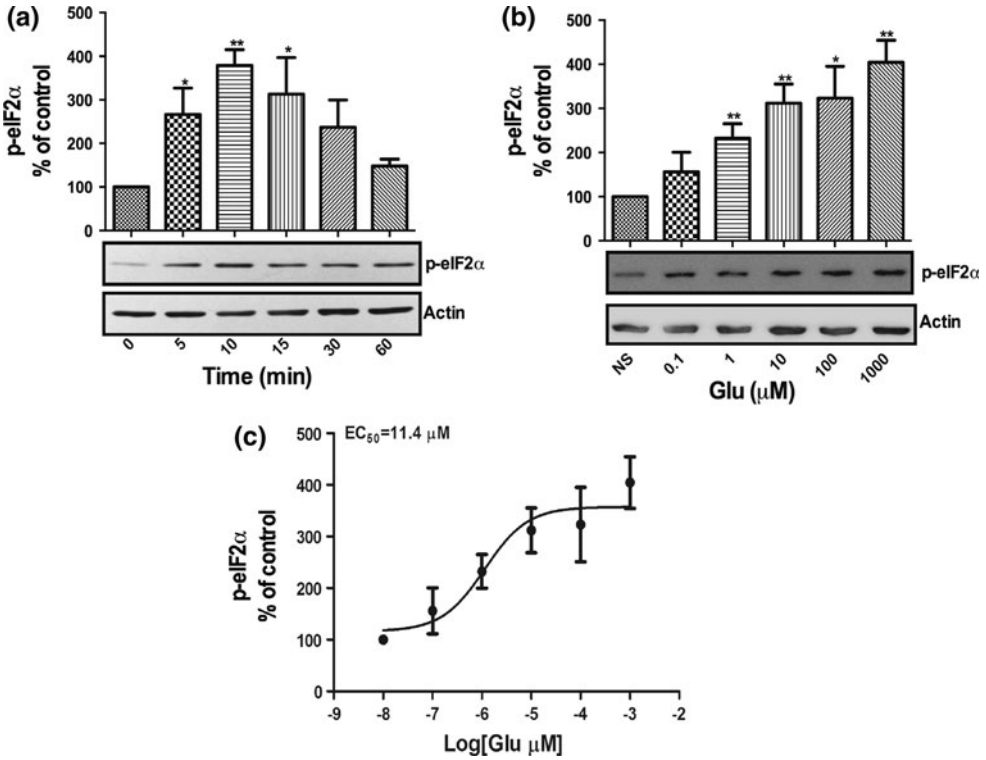

Fig. 2 eIF2α phosphorylation is time and dose-dependent. **a** BGC monolayers were treated for different time periods with a 1 mM Glu concentration. **b** BGC cultures were treated with increasing Glu concentrations for 10 min. The levels of eIF2α phosphorylation were detected via Western blots with anti-phospho eIF2α antibody and were normalized with respect to actin levels. **c** Nonlinear regression of the incubation with increased Glu concentrations for 10 min. Date are expressed as mean ± SE from at least three independent experiments. An autoradiography of a typical experiment is shown. Statistical analysis was performed comparing against data obtained from non-stimulated (NS) cells using non-parametric one-way ANOVA (Kruskal–Wallis test) and Dunn's post hoc test (*$P < 0.05$, **$P < 0.01$)

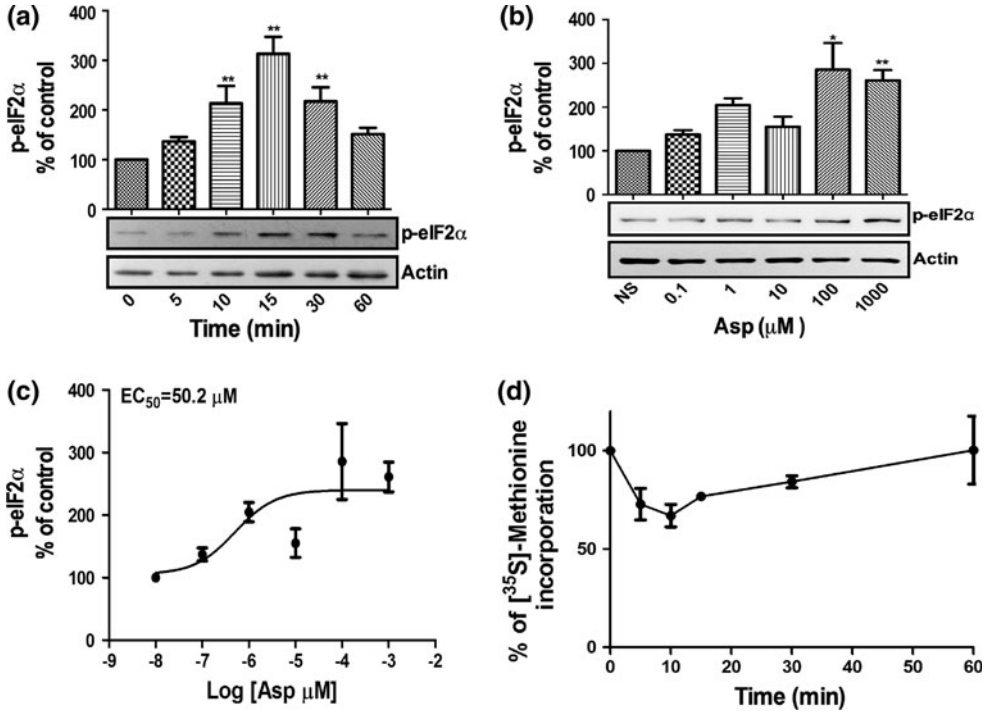

Fig. 3 Asp-dependent eIF2α phosphorylation. **a** BGC monolayers were treated for different time periods with 1 mM Asp concentration. **b** BGC cultures were treated with increasing Asp concentrations for 15 min. The levels of eIF2α phosphorylation were detected via Western blots with anti-phospho eIF2α antibody and were normalized to actin levels. **c** Non-linear regression of the incubation with increased Asp concentrations for 15 min. **d** [^{35}S]-methionine incorporation from BGC monolayers treated for the indicated time periods with 1 mM Asp. Data is expressed as mean ± SE from at least three independent experiments. An autoradiography of a typical experiment is shown. Statistical analysis was performed comparing data of each condition against non-stimulated (NS) cells using a non-parametric one-way ANOVA (Kruskal–Wallis test) and Dunn's post hoc test (*$P < 0.05$, **$P < 0.01$)

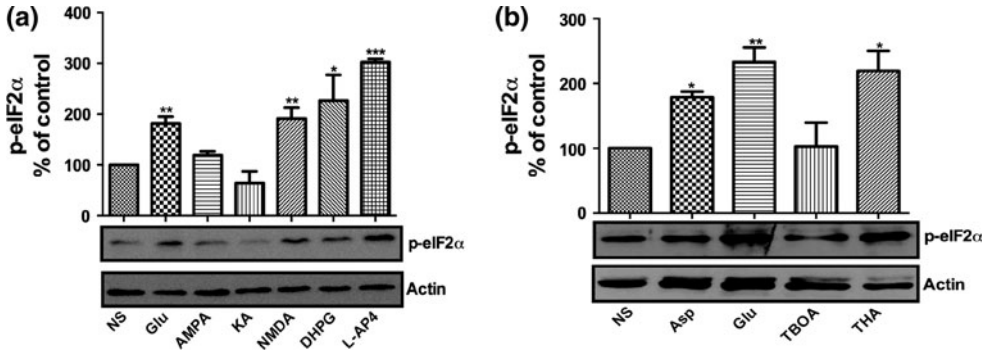

Fig. 4 Pharmacological profile of eIF2α phosphorylation. **a** BGC monolayers were incubated for 10 min with the indicated Glu analogues, 500 μM AMPA, 500 μM KA, 500 μM NMDA plus 10 μM Gly, 25 μM DHPG and 500 μM L-AP4. **b** BGC cultures were incubated with the Glu transporter blockers, THA (100 μM) or with TBOA (100 μM) for 10 min. The levels of eIF2α phosphorylation were detected via Western blots with anti-phospho eIF2α antibody and were normalized to actin levels. Data is expressed as mean ± SE from at least three independent experiments. An autoradiography of a typical experiment is shown. Statistical analysis was performed comparing data of each condition against non-stimulated (NS) using a non-parametric one-way ANOVA (Kruskal–Wallis test) and Dunn's post hoc test (*$P < 0.05$, **$P < 0.01$, ***$P < 0.001$)

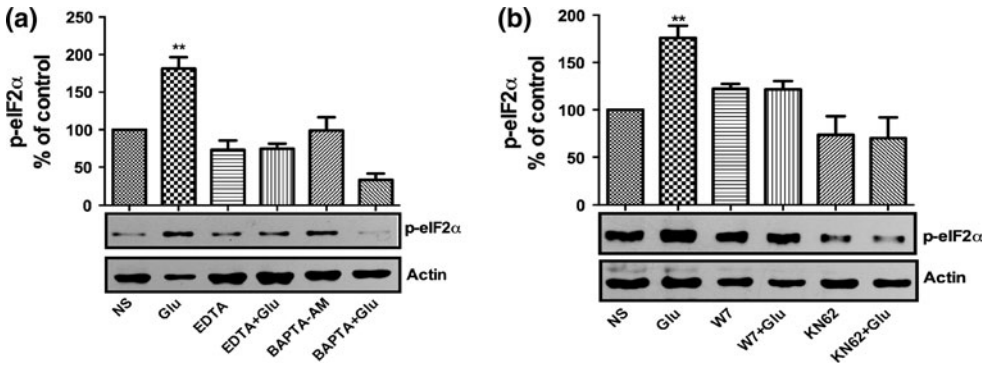

Fig. 5 Involvement of Ca^{2+}in eIF2α phosphorylation. **a** BGC monolayers were treated with 500 μM EDTA and 25 μM BAPTA-AM for 30 min in Ca^{2+}-free assay buffer prior to 1 mM Glu treatment. **b** BGC cultures were incubated with the CaM antagonist W7 (25 μM) or with the CaMKII inhibitor KN-62 (10 μM) for 30 min before 1 mM Glu exposure (10 min). The levels of eIF2α phosphorylation were detected via Western blots with anti-phospho eIF2α antibody and were normalized to actin levels. Data are expressed as mean ± SE from at least three independent experiments. An autoradiography of a typical experiment is shown. Statistical analysis was performed comparing data of each condition against non-stimulated (NS) using a non-parametric one-way ANOVA (Kruskal–Wallis test) and Dunn's post hoc test (**$P < 0.01$)

were capable to mimic the Glu effect (Fig. 4, panel a). We also decided to investigate if the Asp effect was linked to the Na^+ entrance through the Glu transporters. To this end, we exposed the cultured cells to the transportable inhibitor THA as well as to the non-transportable blocker TBOA. The results are presented in Fig. 4 (panel b), of the two inhibitors tested, only THA could reproduce the aspartate effect suggesting that Na^+ influx through the transporter is necessary for the increase in the phosphorylation of eIF2α.

Signalling of the Glu-Mediated eIF2α Phosphorylation

To gain insight into the biochemical pathways that participate in the Glu response, we first decided to interfere with a plausible Glu-dependent increase in intracellular Ca^{2+} levels, since it is known that iGluRs expressed in BGC are permeable to this ion, and that group I mGluRs are coupled to phosphatidylinositol metabolism and the release of the Ca^{2+} from the endoplasmic reticulum. As expected, the removal of Ca^{2+} with EDTA or BAPTA-AM decreased the Glu effect (Fig. 5, panel a). Since the main intracellular Ca^{2+} receptor is calmodulin (CaM), we explored its involvement in the described effect. Pre-incubation with CaM antagonist W7 blocked the eIF2α phosphorylation. In line with these results, when the cells were incubated with the Ca^{2+}/calmodulin dependent protein kinase II (CaMKII) blocker KN-62, the Glu effect was totally prevented (Fig. 5, panel b). Another component of the signal transduction cascade triggered by mGluRs (Group I and Group III), namely the Ca^{2+}/diacylglicerol

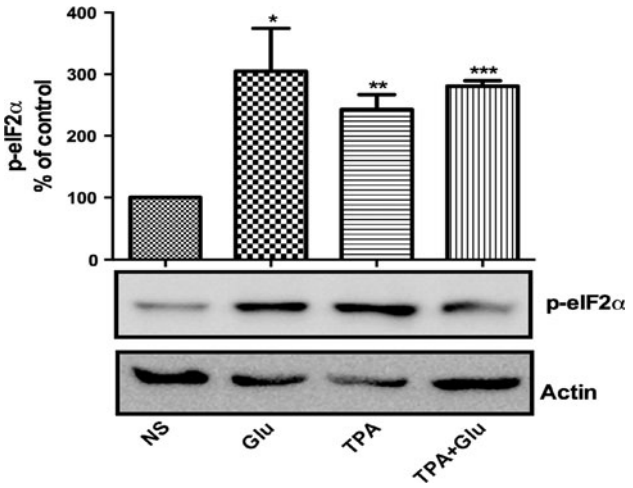

Fig. 6 PKC-dependent eIF2α phosphorylation. BGC monolayers were treated with 100 nM TPA or/and 1 mM Glu for 10 min. The levels of eIF2α phosphorylation were detected via Western blots with anti-phospho eIF2α antibody and normalized to actin levels. Data are expressed as mean ± SE from at least three independent experiments. An autoradiography of a typical experiment is shown. Statistical analysis was performed comparing data of each condition against non-stimulated (NS) using a non-parametric one-way ANOVA (Kruskal–Wallis test) and Dunn's post hoc test ($*P < 0.05$, $**P < 0.01$, $***P < 0.001$)

protein kinase (PKC) was evaluated. Pre-incubation with the PKC activator tetradecanoylphorbol 13-acetate (TPA) increased eIF2α phosphorylation (Fig. 6).

Taken together the described results demonstrate that glial cells might be capable to adjust their proteome in response to Glu by controlling the translational process at the initiation phase.

Discussion

The protein repertoire of a vertebrate cell is in permanent change that reflects the extracellular milieu composition. Within the CNS, these changes in the extracellular media are the basis of intercellular communication not only between neurons but also of their coupling with the brain most abundant cells, glia cells. Glutamatergic synapases are an excellent model in which the involvement of glia cells has long been proven in terms of the neurotransmitter recycling [20] and more recently in metabolic fluxes [21]. Such an interaction is clearly modulated by Glu receptors and transporters that through their signalling properties modify the physiology of neurons and glia cells in the short and long term [22, 23]. One also has to keep in mind that a role for internalized Glu, besides as a precursor of Glutamine and intermediate metabolites has been suggested [3].

Protein synthesis is the most energy consuming cellular process and it is reduced upon stress conditions [13]. Stimulation of ionotropic Glu receptors promotes the inhibition of protein synthesis through Ca^{2+} influx and

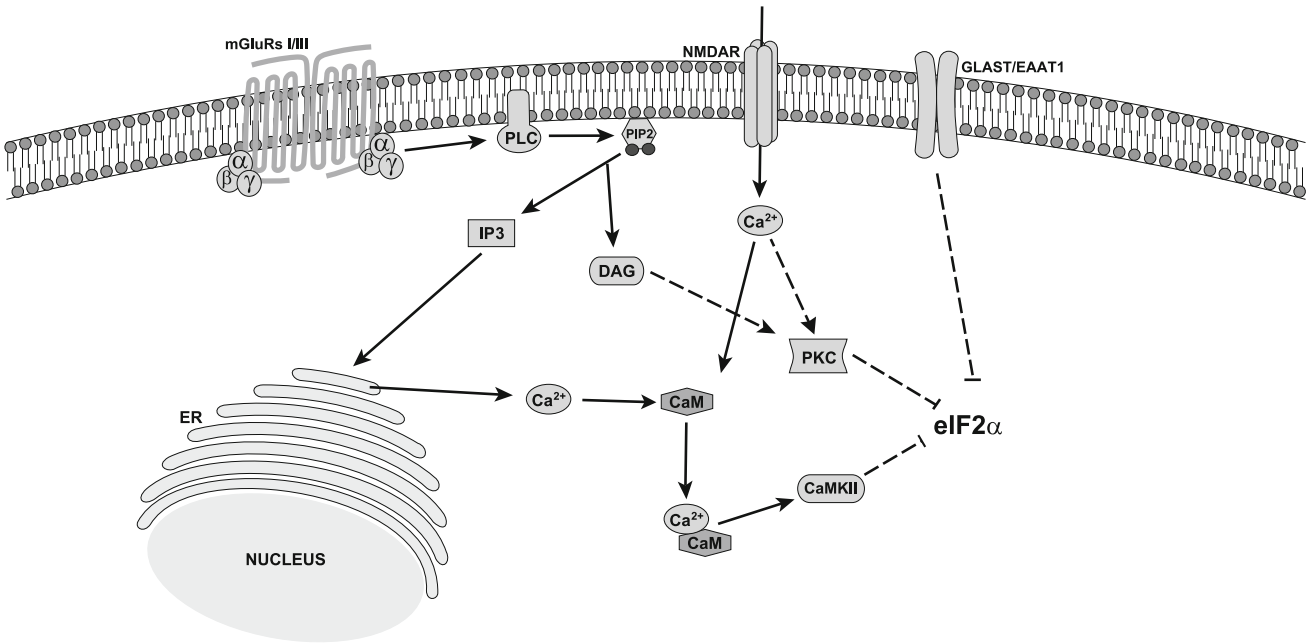

Fig. 7 Model for eIF2α phosphorylation in BGC. Glu binding to mGluRs I/III receptors leads to the activation of PLC (phospholipase C) cleaving PIP3 (phosphatidylinositol 4,5-bisphosphate) into DAG (diacyl glycerol) and IP3 (inositol 1,4,5-trisphosphate). IP3 binds to the ER (endoplasmic reticulum) IP3 receptors raising intracellular Ca^{2+} levels. NMDA receptors activation induces Ca^{2+} influx activating both PKC (protein kinase C) and CaMKII resulting in eIF2α phosphorylation. The activity of the GLAST/EAAT1 also induces eIF2α phosphorylation

stimulation of eEF2 K both in neurons [24, 25] and glia cells [15]. It is tempting to speculate that a transient decrease in protein synthesis as a result of a massive exposure of glia cells to Glu is the related to the metabolic stress of the removal of the neurotransmitter from the synaptic cleft. The calculated Glu concentration in the veccinity of the Bergmann glia membranes is 250 μM [26], if one takes into consideration that the reported K_M of GLAST/EAAT1 is 62 μM in these cells [27] then it is clear that under periods of sustained synaptic activity glial cells reduce their translational process in order to restore the Na^+ gradient compulsory for the transmitter uptake. In fact, this saturation of the Glu transporters is linked to the activation of glia Glu receptors [28].

Interestingly, both receptors and transporters are linked to the increase in Ser 51 eIF2α phosphorylation (Figs. 2, 3) reflecting the importance, in energetic terms, for glial cells to reduce their polypeptide synthesis. As expected, the kinetics for the receptor-mediated versus the transporter-dependent effect are different as their associated Ca^{2+} (receptors) or Na^+ (transporters) fluxes have different kinetics. Whether the signalling mechanisms used by receptors and transporters are the same it is not clear at the moment, but apparently both are linked to an increase in intracellular Ca^{2+} levels, since its removal of the extracellular media as well at is chelation with BAPTA prevents eIF2α phosphorylation.

In summary, we provide here evidence for Glu-dependent decrease in the initiation phase of protein synthesis that is mediated both by receptors and transporters as a response to the elevated Glu concentration in the synaptic space. An schematic representation of the major findings of this communication is presented in Fig. 7. Work currently in progress in our lab is aimed to the characterization of the signalling cascades triggered by Glu that regulate the initiation phase of protein synthesis.

Acknowledgments This work was supported by Grants from Conacyt-Mexico to A.O. (79502 and 123625). M.A.F.-M. and Z.M.-L. are supported by Conacyt-Mexico PhD fellowships. The technical assistance of Luis Cid and Blanca Ibarra is acknowledged.

References

1. Hollmann M, Heinemann S (1994) Cloned glutamate receptors. Annu Rev Neurosci 17:31–108
2. Coutinho V, Knopfel T (2002) Metabotropic glutamate receptors: electrical and chemical signaling properties. Neuroscientist 8(6):551–561
3. Yang CZ et al (2008) Astrocyte and neuron intone through glutamate. Neurochem Res 33(12):2480–2486
4. Somogyi P et al (1990) Subcellular localization of a putative kainate receptor in Bergmann glial cells using a monoclonal antibody in the chick and fish cerebellar cortex. Neuroscience 35(1):9–30
5. Lopez-Bayghen E et al (2007) Cerebellar Bergmann glia: an important model to study neuron-glia interactions. Neuron Glia Biol 3(2):155–167
6. Barrera I et al (2010) Glutamate regulates eEF1A phosphorylation and ribosomal transit time in Bergmann glial cells. Neurochem Int 57(7):795–803
7. Hu D et al (2006) Aging-dependent alterations in synaptic plasticity and memory in mice that overexpress extracellular superoxide dismutase. J Neurosci 26(15):3933–3941
8. Pittenger C, Kandel E (1998) A genetic switch for long-term memory. C R Acad Sci III 321(2–3):91–96
9. Cammalleri M et al (2003) Time-restricted role for dendritic activation of the mTOR-p70S6 K pathway in the induction of late-phase long-term potentiation in the CA1. Proc Natl Acad Sci USA 100(24):14368–14373
10. Sonenberg N, Hinnebusch AG (2009) Regulation of translation initiation in eukaryotes: mechanisms and biological targets. Cell 136(4):731–745
11. Klann E, Dever TE (2004) Biochemical mechanisms for translational regulation in synaptic plasticity. Nat Rev Neurosci 5(12):931–942
12. Krishnamoorthy T et al (2001) Tight binding of the phosphorylated alpha subunit of initiation factor 2 (eIF2α) to the regulatory subunits of guanine nucleotide exchange factor eIF2B is required for inhibition of translation initiation. Mol Cell Biol 21(15): 5018–5030
13. Proud CG (2007) Signalling to translation: how signal transduction pathways control the protein synthetic machinery. Biochem J 403(2):217–234
14. Ortega A, Eshhar N, Teichberg VI (1991) Properties of kainate receptor/channels on cultured Bergmann glia. Neuroscience 41(2–3):335–349
15. Gonzalez-Mejia ME et al (2006) Glutamate-dependent translational regulation in cultured Bergmann glia cells: involvement of p70S6 K. Neuroscience 141(3):1389–1398
16. Barrera I et al (2008) Glutamate-dependent elongation factor-2 phosphorylation in Bergmann glial cells. Neurochem Int 52(6):1167–1175
17. Abe K, Saito H (2001) Possible linkage between glutamate transporter and mitogen-activated protein kinase cascade in cultured rat cortical astrocytes. J Neurochem 76(1):217–223
18. Gegelashvili M et al (2007) Glutamate transporter GLAST/EAAT1 directs cell surface expression of FXYD2/gamma subunit of Na, K-ATPase in human fetal astrocytes. Neurochem Int 50(7–8):916–920
19. Martinez-Lozada Z et al (2011) Signaling through EAAT-1/GLAST in cultured Bergmann glia cells. Neurochem Int 59(6): 871–879
20. Shank RP, Campbell GL (1984) Glutamine, glutamate, and other possible regulators of alpha-ketoglutarate and malate uptake by synaptic terminals. J Neurochem 42(4):1162–1169
21. Pellerin L et al (2007) Activity-dependent regulation of energy metabolism by astrocytes: an update. Glia 55(12):1251–1262
22. Nestler EJ (2001) Molecular basis of long-term plasticity underlying addiction. Nat Rev Neurosci 2(2):119–128
23. Lopez-Bayghen E, Ortega A (2010) Glial cells and synaptic activity: translational control of metabolic coupling. Rev Neurol 50(10):607–615
24. Marin P et al (1997) Glutamate-dependent phosphorylation of elongation factor-2 and inhibition of protein synthesis in neurons. J Neurosci 17(10):3445–3454
25. Scheetz AJ, Nairn AC, Constantine-Paton M (2000) NMDA receptor-mediated control of protein synthesis at developing synapses. Nat Neurosci 3(3):211–216
26. Bergles DE, Dzubay JA, Jahr CE (1997) Glutamate transporter currents in Bergmann glial cells follow the time course of

extrasynaptic glutamate. Proc Natl Acad Sci USA 94(26): 14821–14825
27. Ruiz M, Ortega A (1995) Characterization of an Na(+)-dependent glutamate/aspartate transporter from cultured Bergmann glia. NeuroReport 6(15):2041–2044
28. Dzubay JA, Jahr CE (1999) The concentration of synaptically released glutamate outside of the climbing fiber-Purkinje cell synaptic cleft. J Neurosci 19(13):5265–5274

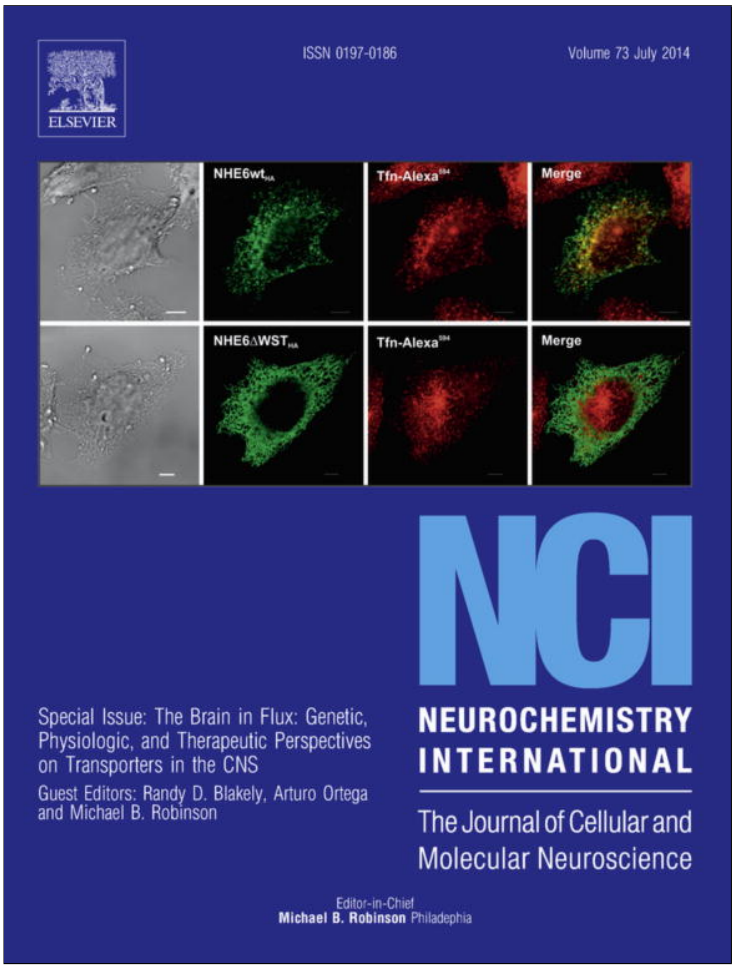

Neurochemistry International 73 (2014) 139–145

Contents lists available at ScienceDirect

Neurochemistry International

journal homepage: www.elsevier.com/locate/nci

GLAST/EAAT1 regulation in cultured Bergmann glia cells: Role of the NO/cGMP signaling pathway

Alberto Balderas [a], Alain M. Guillem [a], Zila Martínez-Lozada [a], Luisa C. Hernández-Kelly [a,b], José Aguilera [b], Arturo Ortega [a,*]

[a] Departamento de Genética y Biología Molecular, Centro de Investigación y de Estudios Avanzados del Instituto Politécnico Nacional, Apartado Postal 14-740, México DF 07000, Mexico

[b] Institut de Neurosciénces i Departament de Bioquímica i Biología Molecular, Universitat Autònoma de Barcelona, Cerdanyola del Vallès, Barcelona, Spain

ARTICLE INFO

Article history:
Available online 6 November 2013

Keywords:
GLAST/EAAT1
Bergmann glia
Nitric oxide
cGMP

ABSTRACT

Glutamate, the major excitatory amino acid, activates a wide variety of signal transduction cascades. Ionotropic and metabotropic glutamate receptors are critically involved in long-term synaptic changes, although recent findings suggest that the electrogenic Na^+-dependent glutamate transporters, responsible for its removal from the synaptic cleft participate in the signaling transactions triggered by this amino acid. Glutamate transporters are profusely expressed in glia therefore most of its uptake occurs in this cellular compartment. In the cerebellar cortex, Bergmann glial cells enwrap glutamatergic synapses and participate in the recycling of its neurotransmitter through the glutamate/glutamine shuttle. It has long been acknowledged that glutamatergic transmission in the cerebellar molecular layer results in cGMP accumulation within Bergmann glia cells. In this context, we decided to investigate a plausible role of the nitric oxide/cGMP-signaling pathway in the regulation of Bergmann glia glutamate transporters. To this end, the well-established model of primary cultures of chick cerebellar Bergmann glial cells was used. Confluent monolayers were exposed to the nitric oxide donor, sodium nitroprusside, or to the non-hydrolysable cGMP analog dbcGMP and the [^{3}H] D-aspartate uptake activity measured. An increase in uptake activity, related to an augmentation in V_{Max}, was detected with both treatments. The signaling cascade includes NO/cGMP/PKG and Ca^{2+} influx through the Na^+/Ca^{2+} exchanger and might be related to the plasma membrane glutamate transporters turnover. Interestingly enough, an inhibitor of the cGMP dependent protein kinase was capable to abolish the sodium nitroprusside induced Ca^{2+} influx. These results provide an insight into the physiological role of cGMP in the cerebellum.

1. Introduction

Excitatory neurotransmission in the vertebrate Central Nervous System (CNS) is mediated mostly by glutamate (Glu). This excitatory amino acid exerts its actions through the activation of two main subtypes of receptors defined in terms of structure and signaling mechanisms: ionotropic (iGluRs) and metabotropic receptors (mGluRs). Three iGluRs have been defined: *N*-methyl-D-aspartate (NMDA), α-amino-3-hydroxy-5-methyl-4-isoaxazolepropionate (AMPA) and kainate (KA) receptors (Hollmann and Heinemann, 1994). Metabotropic receptors have been divided in terms of sequence similarity, signal transduction mechanisms and pharmacology in three groups. Group I receptors are coupled to the stimulation of phospholipase C with the consequent release of intracellular Ca^{2+}, while Groups II and III are coupled to the inhibition of adenylate cyclase. These three groups are activated preferentially by (RS)-3,5-dihydroxyphenylglycine (DHPG) for Group I, (*S*)-4-carboxy-3-hydroxyphenylglycine (*S*)-4C3HPG activates Group II while L-(+)-2-amino-4-phosphonobutyric acid (L-AP4) acts upon Group III (Coutinho and Knopfel, 2002).

A family of sodium-dependent Glu transporters are responsible for the removal of the excitatory transmitter from the synaptic cleft (Danbolt, 2001). These proteins are known as excitatory amino acid transporters (EAATs) and five different subtypes, numbered from 1 to 5 have been described. Although Glu uptake activity has been described in neurons and glia, more than 80% of the total brain removal of this excitatory amino acid from the synaptic cleft, is carried out by glial cells, which express EAAT1/GLAST (Glu/aspartate transporter) and/or EAAT2/Glt-1 (Glu transporter 1). In the cerebellum, the bulk of the Glu uptake takes place in Bergmann glia, which express GLAST/EAAT1, while in most of the other CNS structures, except for retina, Glt-1/EAAT2 is the major Glu carrier, in fact, it is known that this transporter represents roughly 2% of the total brain protein (Lehre and Danbolt, 1998).

* Corresponding author. Address: Departamento de Genética y Biología Molecular, Cinvestav-IPN, Apartado Postal 14-740, México DF 07000, Mexico. Tel.: +52 5 55747 3769; fax: +52 5 55747 3800x5317.
E-mail address: arortega@cinvestav.mx (A. Ortega).

0197-0186/$ - see front matter © 2013 Elsevier Ltd. All rights reserved.
http://dx.doi.org/10.1016/j.neuint.2013.10.011

Bergmann glia cells (BGC) are the most abundant glia cells in the cerebellum, comprising more than 90% of the cerebellar glia. These cells span the entire cerebellar molecular layer and encapsulate neuronal somata, dendrites and axons. BGC are involved in neurotransmitter uptake, K^+ homeostasis, lactate supply and pH regulation due to the expression of a battery of receptors and transporters (Lopez-Bayghen et al., 2007). In terms of glutamatergic transmission, BGC are in a very close proximity to the parallel fiber-Purkinje cell synapses, and are involved in the Glu/glutamine (Gln) shuttle that assures Glu supply to the presynaptic terminals. In this sense, BGC respond to glutamatergic stimulation, as we have been able to characterize over the years (Barrera et al., 2010).

The ability of Glu to induce large increases in the levels of guanosine 3′,5′-cyclic monophosphate (cGMP) in the cerebellum has been known since 1980 (Foster and Roberts, 1980). Exposure of rat cerebellar slices to NMDA, KA or sodium nitroprusside (SNP), an NO donor, results in a robust accumulation of cGMP in Bergmann glia fibers, that is inhibited by methylene blue, by the blockage of nitric oxide synthesis or by the depletion of extracellular Ca^{2+} (De Vente et al., 1990). Interestingly, both subunits of soluble guanylate cyclase (sGC) have been detected in BGC suggesting that these cells may be responsive to NO generated by a NMDA-dependent stimulation of neuronal nitric oxide synthase in granule cells (Ding et al., 2004). To gain insight into the role of cGMP in the physiology of BGC, we decided to evaluate its effects in one of the most characterized functions of BGC, the removal of Glu via GLAST/EAAT1. An augmentation of [^{3}H]-D-Asp uptake was found upon activation of the NO/cGMP pathway, suggesting a rapid up-regulation of the uptake process that might counter-balance the previously characterized reduction in GLAST/EAAT-1 activity by Glu (Gonzalez and Ortega, 2000).

2. Materials and methods

2.1. Materials

Tissue culture reagents were obtained from GE Healthcare (Carlsbad, CA, USA). A23187 (5-(methylamino)-2-({(2*R*,3*R*,6*S*,8*S*,9*R*,11*R*)-3,9,11-trimethyl-8-[(1*S*)-1-methyl-2-oxo-2-(1*H*-pyrrol-2-yl) ethyl]-1,7-dioxaspiro[5.5] undec-2-yl}methyl)-1,3-benzoxazole-4-carboxylic acid), D-aspartate (D-Asp) and Glu were all obtained from Tocris-Cookson (St. Louis, MO, USA). [^{3}H]-D-aspartate and [$^{45}Ca^{2+}$] were from Perkin Elmer (Boston, MA, USA). SNP, methylene blue, dbcGMP and Rp-8-Bromo-β-phenyl-1,N^2-ethenoguanosine 3′,5′-cyclic monophosphorothioate sodium salt hydrate (Rp-8-Br-PET-cGMPS), were obtained from Sigma–Aldrich, Mexico.

2.2. Cell culture and stimulation protocol

Primary cultures of cerebellar BGC were prepared from 14-day-old chick embryos as previously described (Ortega et al., 1991). Cells were plated in 24-well plastic culture dishes in DMEM containing 10% fetal bovine serum, 2 mM Gln, and gentamicin (50 μg/ml) and used on the 4th to 7th day after culture. Before any treatment, confluent monolayers were switched to non-serum DMEM media containing 0.5% bovine serum albumin (BSA) for 30 min and then treated as indicated. Inhibitors were added 30 min before agonists.

2.3. [^{3}H]-D-aspartate influx

Confluent BGC monolayers seeded in 24-well plates were washed three times to remove all non-adhering cells with 0.5 ml aliquots of solution A containing 25 mM HEPES-Tris, 130 mM NaCl, 5.4 mM KCl, 1.8 mM $CaCl_2$, 0.8 mM $MgCl_2$, 33.3 mM glucose and 1 mM NaH_2PO_4 at pH 7.4. When indicated, NaCl was replaced by choline chloride. The [^{3}H]-D-Asp influx was initiated at $t = 0$ by the addition of 0.5 ml solution A containing 0.4 μCi/ml of [^{3}H]-D-Asp. When inhibitors or modulators were tested, they were added 30 min prior to the beginning of the [^{3}H]-D-Asp influx assay. The reaction was stopped by aspirating the radioactive medium and washing each well within 15 s with 0.5 ml aliquots of an ice-cold solution A. For the determination of the kinetic parameters, the cold aspartate concentration was modified to a final 10, 25, 50, 100, 200 μM concentrations and the uptake time was 30 min a time which we have previously shown that uptake is linear (Ruiz and Ortega, 1995). The uptake was stopped as described above. The cells in the wells were then exposed for 2 h at 37 °C to 0.5 ml NaOH 0.1 M and an aliquot of that solution counted in a Beckmann 7800LS scintillation counter in the presence of a scintillation cocktail. Experiments were carried out as a minimum of quadruplicates.

2.4. [^{3}H]-D-aspartate binding

Confluent BGC monolayers seeded in 24-well culture plates were washed three times to remove all non-adhering cells with 0.5 ml aliquots of solution A. In the Na^+-free solution, NaCl was replaced by choline chloride. In the Ca^{2+}-free solution the $CaCl_2$ was supressed and 5 mM EDTA was added. The [^{3}H]-D-Asp binding was initiated at $t = 0$ by the addition of 0.5 ml solution A with or without modifications containing 0.4 μCi/ml of [^{3}H]-D-Asp at 4 °C. Glu was added 30 min and SNP 12 min prior to the beginning of the [^{3}H]-D-Asp binding assay. The assay was stopped by aspirating the radioactive medium and washing each well within 15 s with 0.5 ml aliquots of an ice-cold solution A. The cells in the wells were then exposed for 2 h at 37 °C to 0.5 ml NaOH and an aliquot of that solution counted in a Perkin Elmer TriCarb 2910 TR scintillation counter in the presence of a scintillation cocktail. Experiments were carried out as a minimum of quadruplicates.

2.5. [$^{45}Ca^{2+}$] influx

Confluent BGC monolayers seeded in 24-well plates were washed three times to remove all non-adhering cells with 0.5 ml aliquots of solution A containing 25 mM HEPES-Tris, 130 mM NaCl, 5.4 mM KCl, 1.8 mM $CaCl_2$, 0.8 mM $MgCl_2$, 33.3 mM glucose and 1 mM NaH_2PO_4 at pH 7.4. The SNP-induced influx of [$^{45}Ca^{2+}$] ions was initiated at $t = 0$ by the addition of 0.5 ml solution A containing 1.5 μCi/ml of [$^{45}Ca^{2+}$], and SNP at the specified concentration. When inhibitors or modulators were tested, they were added 30 min prior to the beginning of the [$^{45}Ca^{2+}$] influx assay. The reaction was stopped by aspirating the radioactive medium and washing each well within 15 s with 0.5 ml aliquots of an ice-cold solution A. The cells in the wells were then exposed for 2 h at 37 °C to 0.5 ml NaOH 0.1 M and an aliquot of that solution counted in a Perkin Elmer TriCarb 2910 TR scintillation counter in the presence of a scintillation cocktail. Experiments were carried out at least three times in quadruplicates.

2.6. Statistical analysis

Data are expressed as the mean (average) ± standard error (S.E.). A one-way analysis of variance (ANOVA) was performed to determine significant differences between conditions. When this analysis indicated significance (at the 0.05 level), post-hoc Student–Newman–Keuls test analysis was used to determine which conditions were significantly different from each other with the Prism software.

3. Results

3.1. The NO/cGMP signaling pathway increases [^{3}H]-D-aspartate uptake in Bergmann glial cells

More than thirty years have passed since the establishment of a Glu-dependent, Ca^{2+}-sensitive, increase in cGMP levels in cerebellar slices and the physiological consequence of the rise in the concentration of this nucleotide in glia cells remains obscure. In order to gain insight into the plausible role of NO as a modulator of glia cell function, we decided to concentrate in one established role of glia cells: Glu uptake (Danbolt, 2001). To this end, we exposed confluent BGC monolayers to the NO donor SNP. The results are depicted in Panel A of Fig. 1. A substantial increase in [^{3}H]-D-Asp was found in the presence of SNP. Two fundamental biochemical mechanisms are responsible of NO action: nitration and/or activation of sGC with the rise in cGMP intracellular concentrations. Treatment of the cultured cells with the non-hydrolysable cGMP analog, dbcGMP also results in an augmentation of the Glu uptake activity, similar but not identical the SNP effect (Panel B of Fig. 1). As expected, methylene blue, a guanylate cyclase inhibitor, prevents the SNP increase in [^{3}H]-D-Asp uptake without affecting the dbcGMP response (Panel C of Fig. 1).

3.2. GLAST/EAAT1 is regulated by the NO/cGMP pathway

D-Asp uptake through GLAST/EAAT1 is Na^+-dependent; therefore if the SNP effect is specific for this transporter, the replacement of NaCl in the external solution with an equimolar concentration of choline chloride would prevent the SNP effect. As expected, in a Na^+-free solution, SNP is no longer capable to increase [^{3}H]-D-Asp uptake (Fig. 2, panel A) it favor the idea of a specific effect over GLAST/EAAT1. As a control, cells were treated for 30 min with 1 mM Glu, which we have previously shown that reduces [^{3}H]-D-Asp uptake in a receptor-independent manner (Gonzalez and Ortega, 2000). At this stage, we decided to explore the kinetic parameters of the [^{3}H]-D-Asp uptake process, as a way to gain insight into the biochemical mechanism of the cGMP effect. The results are shown in panel B of Fig. 2. A change in GLAST/EAAT1 K_M is present upon cGMP and SNP that is reflected in an increase in the V_{Max} value, suggesting that an augmentation of available transporters in the plasma membrane. Note that this effect is not present when cells were pre-incubated with MB, the guanylate cyclase blocker blocking SNP effect. To corroborate this hypothesis, [^{3}H]-D-Asp binding experiments were performed in cells treated with SNP in the presence or absence of Na^+ and Ca^{2+}. As shown in Fig. 2C SNP increases the number of transporters in the plasma membrane, in a Ca^{2+}-dependent manner.

3.3. Sodium nitroprusside induces [$^{45}Ca^{2+}$] influx via PKG

The fact that dbcGMP was able to mimic the SNP effect, suggested the involvement of its downstream kinase, the cGMP-dependent protein kinase (PKG). To test this hypothesis, we pre-incubated confluent BGC monolayers with the PKG inhibitor, Rp-8-Br-PET-cGMPS, and then treated them with SNP, and as shown in Fig. 3A, the PKG inhibitor blocks SNP effect, demonstrating the involvement of PKG in the NO signaling in BGC.

It has been reported that the SNP triggered increase in cGMP intracellular levels is Ca^{2+} dependent in cerebellar slices (Linden et al., 1995). In the same vain, Kitao and co-workers demonstrated that SNP and cGMP stimulate Ca^{2+} influx through the activation in reverse mode of Na^+/Ca^{2+} exchanger (NCX) in astrocytes (Kitao et al., 2010). Therefore, we decided to analyze the involvement of Ca^{2+} and the NCX in the SNP effect observed in BGC. With this in mind, cells were treated with 100 μM SNP in normal or Ca^{2+}-free solution A and with the specific NCX inhibitor, KB-R7943 (15 μM). As clearly shown in Fig. 3B, the SNP effect is Ca^{2+}-dependent and sensitive to KB-R7943, suggesting that the NO response (augmentation of plasma membrane transporters) increases Na^+ influx, which activates the NCX leading to an increase in Ca^{2+} influx. To corroborate this idea, [$^{45}Ca^{2+}$] influx experiments were done. As clearly shown in Fig. 3C, exposure of the cultured cells to 100 μM SNP results in a significant increase in [$^{45}Ca^{2+}$] influx that is similar to that induced by the Ca^{2+} ionophore A231887. Pre-incubation of BGC cultures with the PKG inhibitor Rp-8-Br-PET-cGMPS prevents the SNP effect, demonstrating a NO-dependent PKG activation in BGC that in a undefined mechanism participates in the NCX function.

4. Discussion

The process of neurotransmitter removal or inactivation is critically involved in the proper function of the synapses, and the glutamatergic system is not an exemption (Tzingounis and Wadiche, 2007). It has been assumed that the physiological role of glial Glu transporters is restricted to the recycling of the neurotransmitter (Holz and Fisher, 2006), nevertheless, we, and others, have been able to demonstrate the involvement of these proteins as signaling entities (Martinez-Lozada et al., 2011; Abe and Saito, 2001; Martinez-Lozada et al., 2013). In any event, it is clear that the dysfunction of the neurotransmitter transporter systems results in a plethora of neurological and psychiatry disorders ranging from epilepsy to depression (Kanner, 2011; Wankerl et al., 2010).

Glu uptake and its rapid transformation into Gln to complete the Glu/Gln shuttle provides a biochemical framework for the involvement of glia cells in glutamatergic neurotransmission (Shank and Campbell, 1984). The expression and characterization of neurotransmitter receptors in glia cells favored the concept of a *tripartite* synapse (Araque et al., 1999). In this context, glia cells associated to glutamatergic synapses respond to synaptic activity via receptors: Ca^{2+} waves in radial glia cells (Muller et al., 1996) and via transporters: the Glu/Gln shuttle and its associated inward Na^+ current (Owe et al., 2006). Of particular interest, has been the regulation of the glia protein repertoire by Glu through transcriptional and translational control (Balazs, 2006; Gallo and Ghiani, 2000; Lopez-Bayghen and Ortega, 2010; Lopez-Bayghen et al., 2007).

In an effort to advance in our understanding of the role of glia cells in synaptic function we analyzed the plausible effect of NO in the regulation of [^{3}H]-D-Asp uptake activity. We were able to demonstrate that exposure to SNP or dbcGMP results in augmentation in the activity of the sole Glu transporter expressed in these cells: GLAST/EAAT-1 (Ruiz and Ortega, 1995; Danbolt, 2001). Note that the SNP effect is transient whereas the dbcGMP is more sustained (Fig. 1), most possible reflecting its resistance to hydrolysis by the cGMP phosphodiesterase. The extent of [^{3}H]-D-Asp uptake in BGC depends upon the abundance and affinity of GLAST/EAAT1 transporters in the plasma membrane; both SNP and dbcGMP increase V_{Max} values (Panel B of Fig. 2). It is important to mention that at first sight, it could be difficult to reconcile the magnitude of SNP and dbcGMP increase in [^{3}H] D-Asp uptake shown in Fig. 1 with the V_{Max} values reported in panel B of Fig. 3. A plausible explanation for this apparent discrepancy might be linked to the [^{3}H] D-Asp final concentration used in Fig. 1 [35 nM]. This concentration is below the affinity of GLAST/EAAT1 (Fig. 2). Since an augmentation of [^{3}H]-D-Asp uptake in one-point experiments as those in Fig. 1, can be the result of a different affinity of the transporters or to the fact that there could be more transporters in the plasma membrane, it was important to measure the Michaelis–Menten

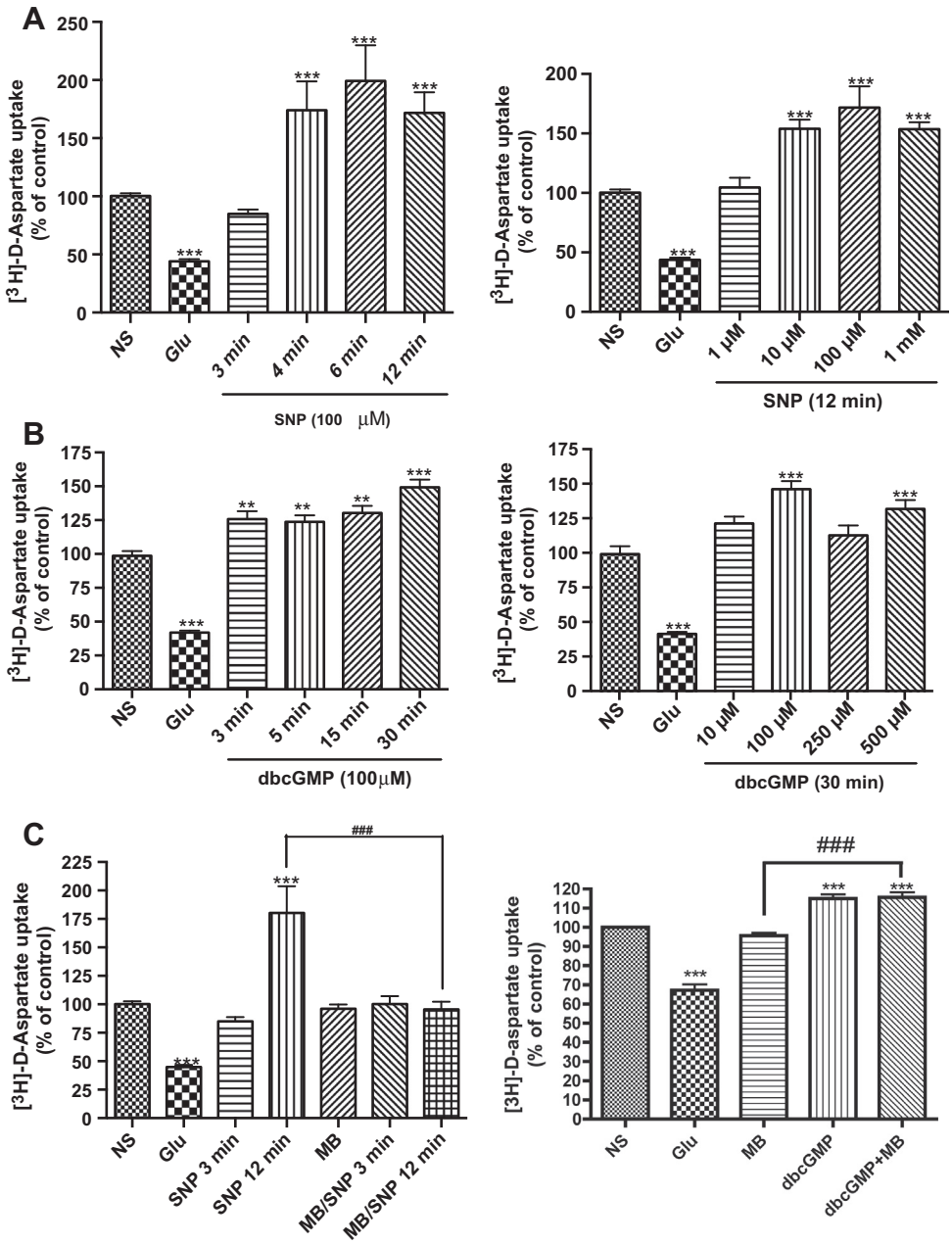

Fig. 1. NO and cGMP increase [^{3}H]-D-Asp uptake. (A) BGC were pre-incubated with the nitric oxide (NO) donor, SNP at a 100 μM concentration for indicated time periods (3, 4, 6 or 12 min); or pre-incubated 12 min with increasing SNP concentrations (1 μM, 10 μM, 100 μM and 1 mM), the [^{3}H]-D-Asp uptake time was 30 min. (B) BGC were pre-treated with the non-metabolizable analog of cGMP, dbcGMP at a 100 μM concentration for the indicated time periods (3, 5, 15 or 30 min); or pre-incubated 30 min with increasing dbcGMP concentrations (10 μM, 100 μM, 250 μM and 500 μM), the [^{3}H]-D-Asp uptake was measured as in panel A. (C) BGC were pre-treated with 100 μM SNP for 3 or 12 min or 100 μM dbcGMP, both in presence or absence of the sGC inhibitor, Methylene blue (MB); the [^{3}H]-D-Asp uptake assay done as in panel A. In all panels cells pre-incubated with 1 mM Glu for 30 min was used as a control of the experiment (Gonzalez and Ortega, 2000). Data are expressed as the mean ± SEM at least of 3 independent experiment, each tested in quadruplicate; a Student's *t*-test with a Dunnett's Multiple comparison test was performed to analyze the data ($^{***}p < 0.001$, $^{**}p < 0.01$). In Panel C a Newman–Keuls Multiple Comparison Test was performed to analyze MB/SNP effect ($^{###}p < 0.001$).

parameters. In fact, what we found is that either SNP or dbcGMP augments V_{Max}, albeit to a different extent probably due to the transient increase in cGMP levels in the cells exposed to SNP.

The amount Gln released by BGC is a function of the intracellular concentration of this neutral amino acid. It should be noted that the affinity of GLAST/EAAT1 is the 13–20 μM range, whereas the affinity of the Gln transporters involved the Gln release is in the 1–2 mM range (Ruiz and Ortega, 1995; Martinez-Lozada et al., 2013), therefore it is not surprising that a high (1 mM) Glu concentration inhibits [^{3}H]-D-Asp uptake (Figs. 1 and 2), (Gonzalez and Ortega, 2000).

It is tempting to speculate that *in vivo*, in periods of intense electrical activity in the cerebellar molecular layer, Glu-dependent increase in NO synthase results in a significant NO production that diffuses and activates soluble guanylate cyclase in BGC with the concomitant increase in cGMP levels. Activated PKG would facilitate the insertion of already synthetized GLAST/EAAT1 in the plasma membrane, increasing by these means the capacity of glial cells to bind Glu and therefore shape the post synaptic excitatory potential (Tzingounis and Wadiche, 2007; Takayasu et al., 2004). In support of our interpretation is the fact that the SNP effect of the increase in [^{3}H]-D-Asp uptake is present already after 4 min of

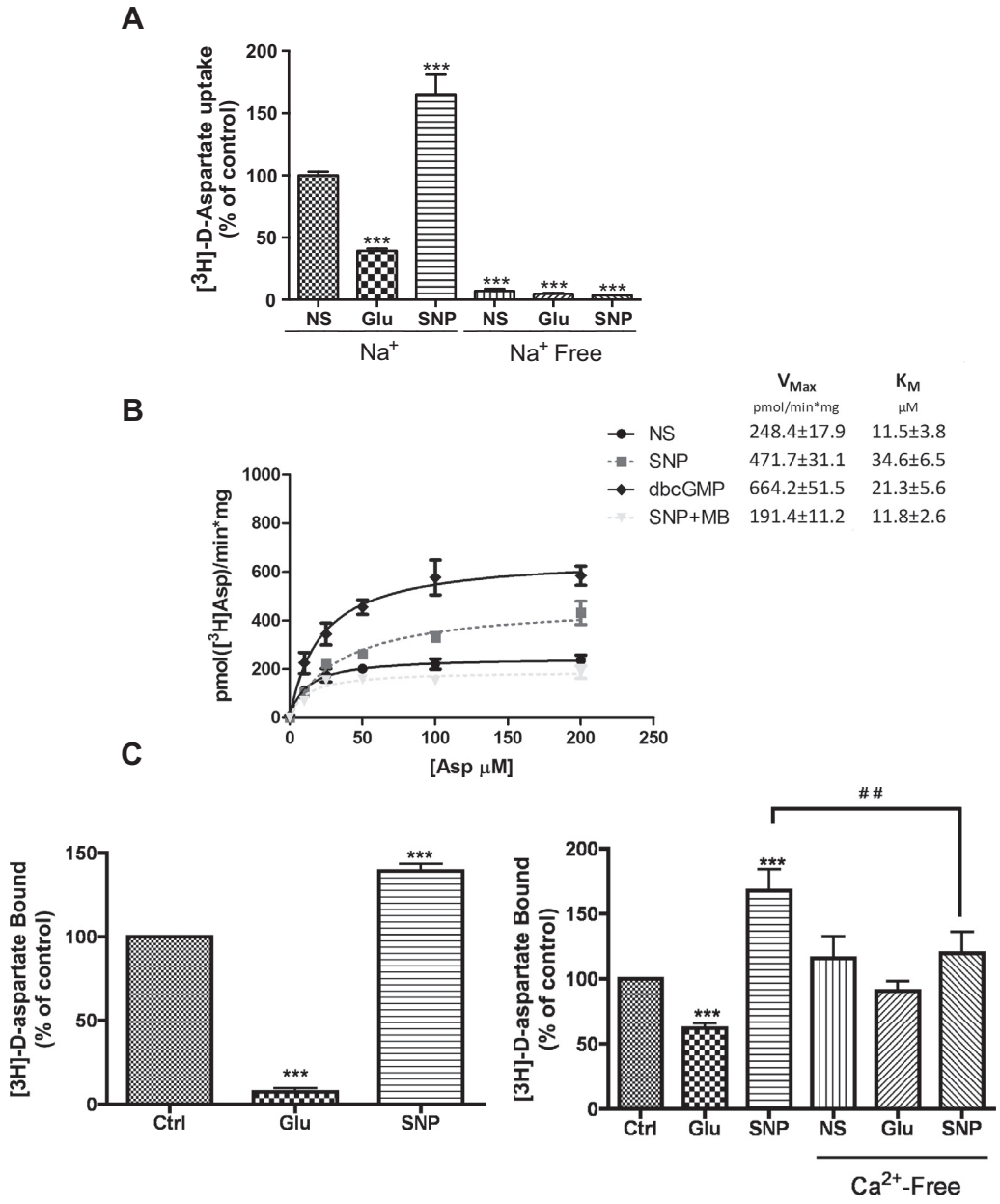

Fig. 2. SNP increases [^{3}H]-D-Asp uptake through the augmentation of available transporters in the plasma membrane. (A) BGC were pre-incubated with 1 mM Glu for 30 min and with 100 μM SNP for 12 min, both in presence or absence of Na^+; [^{3}H]-D-Asp uptake measured as in Fig. 1 in presence or absence of Na^+. Cells treated with 1 mM for Glu 30 min were used as a control of the experiment. Data are expressed as the mean ± SEM of at least 3 independent experiments, each tested in quadruplicate; a Student's *t*-test with a Dunnett's multiple comparison test was performed to analyze the data (***$p < 0.001$). (B) BGC were pre-incubated with 100 μM SNP for 12 min both in presence or absence of the sGC inhibitor, Methylene blue (MB); or with 100 μM dbcGMP for 30 min and the D-[^{3}H]-Asp uptake assay was performed with increasing non-labeled D-Asp concentrations (10 μM, 25 μM, 50 μM, 100 μM and 200 μM) for 30 min. Data are expressed as the mean ± SEM at least of 3 independent experiments, each tested in quadruplicate. Transport kinetics V_{Max} (pmol/min*mg) and K_M (μM) were determined by non-linear regression with the Prism 5 software (GraphPad). (C) BGC were stimulated with 1 mM Glu for 30 min or with 100 μM SNP both in presence or absence of Na^+ and Ca^{2+} (as indicated in the figure). Then a D-[^{3}H]-Asp binding assay was performed at 4 °C. Data are expressed as the mean ± SEM of at least 3 independent experiments, each tested in quadruplicate; a Student's *t*-test with a Dunnett's Multiple comparison test was performed to analyze the data (***$p < 0.001$, **$p < 0.01$). In Panel C a Newman–Keuls Multiple Comparison Test was performed to analyze SNP without Ca^{2+} effect (##$p < 0.01$).

treatment with the NO donor, whereas the Glu effect of reduction of [^{3}H]-D-Asp influx is present only after a Glu stimulation of 30 min. The actual target for PKG phosphorylation is not known at this moment. A direct PKG mediated GLAST/EAAT1 phosphorylation is unlikely given the fact that up to date it has not been possible to ascribe a role for the phosphorylation in the regulation of this protein (Conradt and Stoffel, 1997). Interestingly, all these effects are dependent on a NCX-mediated Ca^{2+} influx (Figs. 2 and 3). At this stage, one could speculate that the traffic of the transporter is mediated by the cytoskeleton, a structure tightly regulated though Ca^{2+}-mediated phosphorylation events. Work in progress in our lab is aimed to the characterization of the molecular mechanism of this regulation.

In summary, a complex set of biochemical transactions are triggered by Glu not only in the post-synaptic neuron but also in the glia cells that regulate the turnover and therefore the availability of releasable Glu in the presynaptic terminal. A model of our present findings is depicted in Fig. 4, the arrival of an action potential to

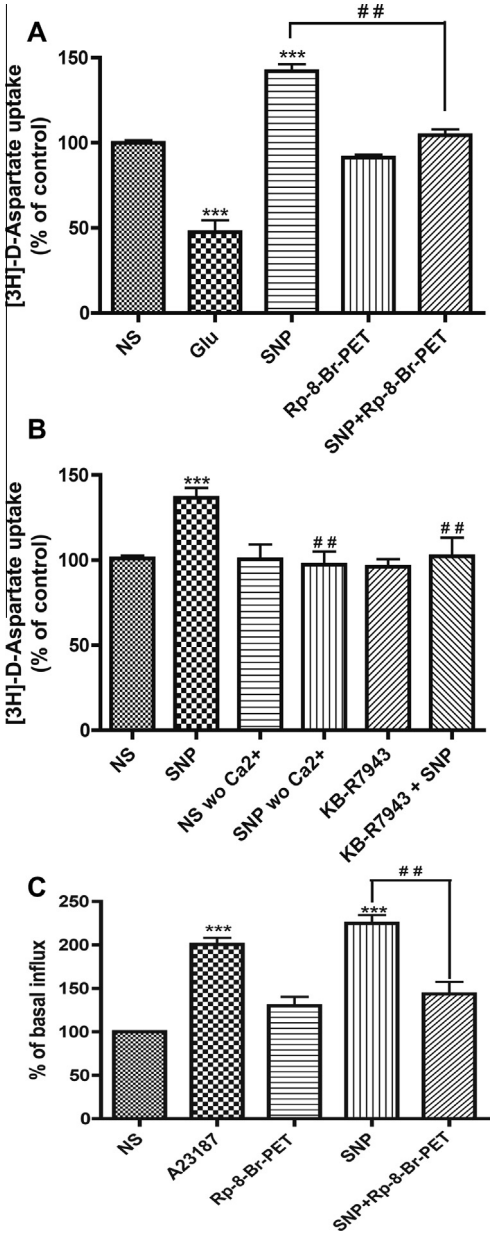

Fig. 3. SNP induced [$^{45}Ca^{2+}$] influx is PKG-dependent. (A) Cells were stimulated with 100 μM SNP for 12 min in presence or absence of PKG inhibitor, Rp-8-Br-PET-cGMPS 10 μM; the [^{3}H]-D-Asp uptake assay done as in Fig. 1. Cells pre-incubated with 1 mM Glu for 30 min were used as a control of the experiment. (B) BGC were treated with 100 μM SNP for 12 min in presence or absence of Ca^{2+}, or pre-incubated for 30 min with the NCX inhibitor, KB-R7943 (15 μM) and then treated with SNP; the [^{3}H]-D-Asp uptake assay done as in panel A. (C) Confluent BGC cultures were pre-exposed for 30 min to the PKG inhibitor, Rp-8-Br-PET-cGMPS 10 μM as indicated, and then incubated with 100 μM SNP and the [$^{45}Ca^{2+}$] uptake performed for 3 min. The Ca^{2+} ionophore A23187 (10 μM) was used as a positive control. Data are expressed as the mean ± SEM of at least 3 independent experiments, each tested in quadruplicate; a Student's *t*-test with a Dunnett's Multiple comparison test was performed to analyze the data ($^{***}p < 0.001$, $^{**}p < 0.01$) also a Newman–Keuls Multiple Comparison Test was performed to analyze SNP effect *vs* SNP + inhibitors ($^{\#\#}p < 0.01$).

the granule cells terminals results in Glu release. Glu activates ionotropic as well as metabotropic receptors in Purkinje cells, leading to the synthesis and release of NO, which would diffuse and activate sGC in Bergmann glia activating guanylate cyclase, augmented cGMP levels activate PKG activation, that together with the increased Na^{+} levels due to the Glu transport, activates of NCX with the resulting Ca^{2+} influx, which then would favor

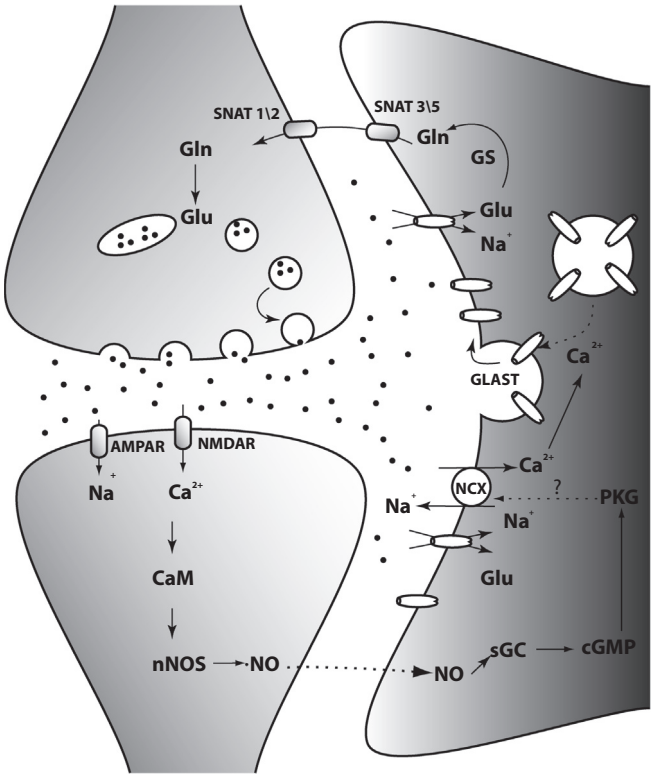

Fig. 4. Current working model. Once granule cells are depolarized, the released Glu activates ionotropic receptors in Purkinje cells, leading to the synthesis and release of NO, which would diffuse and activate sGC in Bergmann glia resulting in an increase in cGMP levels and PKG activation, resulting in the activation of NCX with the resulting Ca^{2+} influx, which then would favor GLAST/EAAT1 containing vesicles movement to plasma membrane to increase GLAST/EAAT1 insertion in the plasma membrane and therefore an augmentation of Glu uptake.

GLAST/EAAT1 containing vesicles movement to plasma membrane to increase GLAST/EAAT1 insertion in the plasma membrane and therefore an augmentation of Glu uptake.

5. Conclusion

Nitric oxide regulates GLAST/EAAT1 through the activation of guanylate cyclase. A role for PKG and Ca^{2+} in this effect could be demonstrated.

Acknowledgements

This work was supported by grants from Conacyt-Mexico to A.O. (79502 and 123625). A.B., A.M.G., and Z.M. are supported by Conacyt-Mexico fellowship. The technical assistance of Luis Cid and Blanca Ibarra is acknowledged.

References

Abe, K., Saito, H., 2001. Possible linkage between glutamate transporter and mitogen-activated protein kinase cascade in cultured rat cortical astrocytes. J. Neurochem. 76, 217–223.
Araque, A., Parpura, V., Sanzgiri, R.P., Haydon, P.G., 1999. Tripartite synapses: glia, the unacknowledged partner. Trends Neurosci. 22, 208–215.
Balazs, R., 2006. Trophic effect of glutamate. Curr. Top. Med. Chem. 6, 961–968.
Barrera, I., Flores-Mendez, M., Hernandez-Kelly, L.C., Cid, L., Huerta, M., Zinker, S., Lopez-Bayghen, E., Aguilera, J., Ortega, A., 2010. Glutamate regulates eEF1A phosphorylation and ribosomal transit time in Bergmann glial cells. Neurochem. Int. 57, 795–803.
Conradt, M., Stoffel, W., 1997. Inhibition of the high-affinity brain glutamate transporter GLAST-1 via direct phosphorylation. J. Neurochem. 68, 1244–1251.
Coutinho, V., Knopfel, T., 2002. Metabotropic glutamate receptors: electrical and chemical signaling properties. Neuroscientist 8, 551–561.

Danbolt, N.C., 2001. Glutamate uptake. Prog. Neurobiol. 65, 1–105.
De Vente, J., Bol, J.G., Berkelmans, H.S., Schipper, J., Steinbusch, H.M., 1990. Immunocytochemistry of cGMP in the cerebellum of the immature, adult, and aged rat: the involvement of nitric oxide. A micropharmacological study. Eur. J. Neurosci. 2, 845–862.
Ding, J.D., Burette, A., Nedvetsky, P.I., Schmidt, H.H., Weinberg, R.J., 2004. Distribution of soluble guanylyl cyclase in the rat brain. J. Comp. Neurol. 472, 437–448.
Foster, G.A., Roberts, P.J., 1980. Pharmacology of excitatory amino acid receptors mediating the stimulation of rat cerebellar cyclic GMP levels in vitro. Life Sci. 27, 215–221.
Gallo, V., Ghiani, C.A., 2000. Glutamate receptors in glia: new cells, new inputs and new functions. Trends Pharmacol. Sci. 21, 252–258.
Gonzalez, M.I., Ortega, A., 2000. Regulation of high-affinity glutamate uptake activity in Bergmann glia cells by glutamate. Brain Res. 866, 73–81.
Hollmann, M., Heinemann, S., 1994. Cloned glutamate receptors. Annu. Rev. Neurosci. 17, 31–108.
Holz, R.W., Fisher, S.K., 2006. Synaptic transmission and cellular signaling: an overview. In: Siegel, G., Wayne, A.R., Brady, S., Price, D. (Eds.), Basic Neurochemistry: Molecular, Cellular and Medical Aspects. Elsevier Academic Press, Canada, pp. 167–181.
Kanner, A.M., 2011. Depression and epilepsy: a bidirectional relation? Epilepsia 52 (Suppl. 1), 21–27.
Kitao, T., Takuma, K., Kawasaki, T., Inoue, Y., Ikehara, A., Nashida, T., Ago, Y., Matsuda, T., 2010. The Na+/Ca^{2+} exchanger-mediated Ca^{2+} influx triggers nitric oxide-induced cytotoxicity in cultured astrocytes. Neurochem. Int. 57, 58–66.
Lehre, K.P., Danbolt, N.C., 1998. The number of glutamate transporter subtype molecules at glutamatergic synapses: chemical and stereological quantification in young adult rat brain. J. Neurosci. 18, 8751–8757.
Linden, D.J., Dawson, T.M., Dawson, V.L., 1995. An evaluation of the nitric oxide/cGMP/cGMP-dependent protein kinase cascade in the induction of cerebellar long-term depression in culture. J. Neurosci. 15, 5098–5105.
Lopez-Bayghen, E., Ortega, A., 2010. Glial cells and synaptic activity: translational control of metabolic coupling. Rev. Neurol. 50, 607–615.
Lopez-Bayghen, E., Rosas, S., Castelan, F., Ortega, A., 2007. Cerebellar Bergmann glia: an important model to study neuron–glia interactions. Neuron Glia Biol. 3, 155–167.
Martinez-Lozada, Z., Guillem, A.M., Flores-Mendez, M., et al., 2013. GLAST/EAAT1-induced glutamine release via SNAT3 in Bergmann glial cells: evidence of a functional and physical coupling. J. Neurochem. 125, 545–554.
Martinez-Lozada, Z., Hernandez-Kelly, L.C., Aguilera, J., Lopez-Bayghen, E., Ortega, A., 2011. Signaling through EAAT-1/GLAST in cultured Bergmann glia cells. Neurochem. Int. 59, 871–879.
Muller, T., Moller, T., Neuhaus, J., Kettenmann, H., 1996. Electrical coupling among Bergmann glial cells and its modulation by glutamate receptor activation. Glia 17, 274–284.
Ortega, A., Eshhar, N., Teichberg, V.I., 1991. Properties of kainate receptor/channels on cultured Bergmann glia. Neuroscience 41, 335–349.
Owe, S.G., Marcaggi, P., Attwell, D., 2006. The ionic stoichiometry of the GLAST glutamate transporter in salamander retinal glia. J. Physiol. 577, 591–599.
Ruiz, M., Ortega, A., 1995. Characterization of an Na(+)-dependent glutamate/aspartate transporter from cultured Bergmann glia. Neuroreport 6, 2041–2044.
Shank, R.P., Campbell, G.L., 1984. Glutamine, glutamate, and other possible regulators of alpha-ketoglutarate and malate uptake by synaptic terminals. J. Neurochem. 42, 1162–1169.
Takayasu, Y., Iino, M., Ozawa, S., 2004. Roles of glutamate transporters in shaping excitatory synaptic currents in cerebellar Purkinje cells. Eur. J. Neurosci. 19, 1285–1295.
Tzingounis, A.V., Wadiche, J.I., 2007. Glutamate transporters: confining runaway excitation by shaping synaptic transmission. Nat. Rev. Neurosci. 8, 935–947.
Wankerl, M., Wust, S., Otte, C., 2010. Current developments and controversies: does the serotonin transporter gene-linked polymorphic region (5-HTTLPR) modulate the association between stress and depression? Curr. Opin. Psychiatry 23, 582–587.

Activation of Sodium-Dependent Glutamate Transporters Regulates the Morphological Aspects of Oligodendrocyte Maturation via Signaling through Calcium/Calmodulin-Dependent Kinase IIβ's Actin-Binding/-Stabilizing Domain

Zila Martinez-Lozada,[1,2] Christopher T. Waggener,[1] Karam Kim,[3] Shiping Zou,[1] Pamela E. Knapp,[1] Yasunori Hayashi,[3,4] Arturo Ortega,[2] and Babette Fuss[1]

Signaling via the major excitatory amino acid glutamate has been implicated in the regulation of various aspects of the biology of oligodendrocytes, the myelinating cells of the central nervous system (CNS). In this respect, cells of the oligodendrocyte lineage have been described to express a variety of glutamate-responsive transmembrane proteins including sodium-dependent glutamate transporters. The latter have been well characterized to mediate glutamate clearance from the extracellular space. However, there is increasing evidence that they also mediate glutamate-induced intracellular signaling events. Our data presented here show that the activation of oligodendrocyte expressed sodium-dependent glutamate transporters, in particular GLT-1 and GLAST, promotes the morphological aspects of oligodendrocyte maturation. This effect was found to be associated with a transient increase in intracellular calcium levels and a transient phosphorylation event at the serine $(S)^{371}$ site of the calcium sensor calcium/calmodulin-dependent kinase type IIβ (CaMKIIβ). The potential regulatory S^{371} site is located within CaMKIIβ's previously defined actin-binding/-stabilizing domain, and phosphorylation events within this domain were identified in our studies as a requirement for sodium-dependent glutamate transporter-mediated promotion of oligodendrocyte maturation. Furthermore, our data provide good evidence for a role of these phosphorylation events in mediating detachment of CaMKIIβ from filamentous (F)-actin, and hence allowing a remodeling of the oligodendrocyte's actin cytoskeleton. Taken together with our recent findings, which demonstrated a crucial role of CaMKIIβ in regulating CNS myelination *in vivo*, our data strongly suggest that a sodium-dependent glutamate transporter–CaMKIIβ–actin cytoskeleton axis plays an important role in the regulation of oligodendrocyte maturation and CNS myelination.

GLIA 2014;62:1543–1558

Key words: myelin, calcium signaling, differentiation, central nervous system, actin cytoskeleton

Introduction

Glutamate (Glu), the major excitatory amino acid, mediates a wide variety of cellular responses in the developing and adult central nervous system (CNS) not only by affecting signal transduction in neurons but also by regulating glia cells, including the myelinating cells of the CNS, oligodendrocytes (Kolodziejczyk et al., 2010). Interestingly, the primary mode of Glu release affecting differentiating cells of

View this article online at wileyonlinelibrary.com. DOI: 10.1002/glia.22699

Published online May 27, 2014 in Wiley Online Library (wileyonlinelibrary.com). Received July 26, 2013, Accepted for publication May 9, 2014.

Address correspondence to Babette Fuss, Department of Anatomy and Neurobiology, Virginia Commonwealth University, PO Box 980709, Richmond, VA. E-mail: bfuss@vcu.edu

From the [1]Department of Anatomy and Neurobiology, Virginia Commonwealth University Medical Center, Richmond, Virginia; [2]Departamento de Toxicología, Centro de Investigación y de Estudios Avanzados del Instituto Politécnico Nacional, México D.F., México; [3]Brain Science Institute, RIKEN, Wako, Saitama, Japan; [4]Saitama University Brain Science Institute, Saitama University, Saitama, Japan.

*Zila Martinez-Lozada and Christopher T. Waggener contributed equally to this work.

Additional Supporting Information may be found in the online version of this article.

the oligodendrocyte lineage during development and under physiological conditions appears to be vesicle exocytosis along unmyelinated axons (Kukley et al., 2007; Ziskin et al., 2007) although release from electrically active axons by reversal of Glu uptake has also been proposed (Kriegler and Chiu, 1993). The prominent release of Glu from unmyelinated axons raises the possibility that Glu, in addition to mediating signaling events at synaptic junctions between axons and NG2-positive progenitor cells (De Biase et al., 2011; Etxeberria et al., 2010; Kukley et al., 2010), may be able to trigger cellular responses in differentiating oligodendrocytes that are involved in the regulation of oligodendrocyte maturation and CNS myelination.

Cells of the oligodendrocyte lineage have been described to express the members of all of the three major Glu-responsive transmembrane protein families (Kolodziejczyk et al., 2010; Matute, 2011). Out of these, metabotropic Glu receptors have been found downregulated as oligodendrocytes differentiate (Deng et al., 2004; Luyt et al., 2006). Ionotropic Glu receptors have primarily been associated with excitotoxicity (Matute, 2011) but they have also been implicated in the regulation of myelination (Lundgaard et al., 2013) and the preservation of neuronal integrity (Fruhbeis et al., 2013). Nevertheless, conditional deletion of the key receptor subunit of the NMDA subtype of iontropic Glu receptors in cells of the oligodendrocyte lineage was not found to lead to an apparent phenotype (De Biase et al., 2011; Guo et al., 2012). Thus, sodium-dependent Glu transporters emerge as good candidates for mediating Glu-evoked responses related to the maturation of differentiating oligodendrocytes. Of the known five mammalian sodium-dependent Glu transporters, also known as excitatory amino acid transporters (EAAT) or members of the solute carrier family 1 (SLC1), three have been found expressed by cells of the oligodendrocyte lineage, namely GLAST (EAAT1, SLC1A3), GLT-1 (EAAT2, SLC1A2), and EAAC1 (EAAT3, SLC1A1) (Arranz et al., 2008; DeSilva et al., 2009; Domercq and Matute, 1999; Kukley et al., 2010; Regan et al., 2007). Although these transporters have been well characterized to remove Glu from the extracellular environment (Beart and O'Shea, 2007; Danbolt, 2001), increasing evidence suggests that they play functional roles beyond extracellular Glu clearance (Flores-Mendez et al., 2013; Lopez-Colome et al., 2012; Martinez-Lozada et al., 2011).

Interestingly, signaling initiated by the activation of sodium-dependent Glu transporters has been proposed to activate calcium/calmodulin-dependent kinase type II (CaMKII) (Flores-Mendez et al., 2013; Martinez-Lozada et al., 2011), and one of the four CaMKII genes, namely CaMKIIβ, has recently been implicated in the regulation of oligodendrocyte maturation and CNS myelination (Waggener et al., 2013). More specifically, CaMKIIβ was implicated in promoting the morphological aspects of oligodendrocyte maturation, which are, to a large extent, regulated by the changes in the cellular cytoskeleton (Bauer et al., 2009), primarily via its actin-binding/-stabilizing domain rather than its well-known kinase catalytic domain. Thus, and based on the above observations, we investigated here a possible role of a sodium-dependent Glu transporter–CaMKIIβ–actin cytoskeleton axis in the regulation of the morphological aspects of oligodendrocyte maturation.

Materials and Methods

Animals

Sprague–Dawley female rats with early postnatal litters were obtained from Harlan Laboratories (Indianapolis, IN). All animal studies were approved by the Institutional Animal Care and Use Committee at Virginia Commonwealth University.

Antibodies

Supernatants from cultured hybridoma cells (clone A2B5; ATCC, Manassas, VA) were used for immunopanning. Anti-GLAST, anti-GLT-1, and anti-EAAC1 (Abcam, Cambridge, MA) antibodies were used for Western blot analysis as well as immunocytochemistry. Anti-CaMKII, anti-pCaMKII $T^{286/7}$ (Cell Signaling Technology, Danvers, MA), anti-pCaMKIIβ S^{371} (generated and characterized by us; Kim et al., in preparation), anti-GAPDH (EMD Millipore, Billerica, MA), and horseradish peroxidase (HRP)-labeled secondary antibodies (Vector Laboratories, Burlingame, CA) were used for Western blot analysis. Supernatants from cultured hybridoma cells (clone O4; gift from S.E. Pfeiffer), anti-myelin basic protein (MBP) antibodies (EMD Millipore, Billerica, MA), and Alexa 488- or Alexa 564-conjugated secondary antibodies (Life Technologies, Grand Island, NY) were used for immunocytochemistry.

Cell Culture

Primary rat oligodendrocyte progenitors were isolated from postnatal day 3 (P3) rat brains by A2B5 immunopanning (Barres et al., 1992; Lafrenaye and Fuss, 2011). Oligodendrocyte progenitors were either used directly in plasmid nucleofection experiments or plated onto fibronectin (10 μg/mL)-coated tissue culture dishes or glass coverslips. Plated oligodendrocyte progenitors were cultured in serum-free differentiation medium (Dulbecco's modified Eagle's medium [DMEM] containing 40 ng/mL tri-iodo-thyronine [T3; Sigma, St Louis, MO] and 1× N2 supplement [Life Technologies, Grand Island, NY]; DMEM/T3/N2). In siRNA-mediated gene silencing experiments, differentiating oligodendrocytes were transfected with siRNAs 24 h after plating. Otherwise, plated oligodendrocyte progenitors were allowed to differentiate for 48 h. Under these conditions, the majority of cells represented postmigratory, premyelinating oligodendrocytes as they expressed the O4 antigen (Sommer and Schachner, 1982; Warrington et al., 1993; data not shown). Such populations of differentiating oligodendrocytes were either directly analyzed or treated as indicated with the following compounds: L-Glu, D-aspartate (Asp), the competitive, nontransportable inhibitor

of sodium-dependent Glu transport DL-*threo*-β-benzyloxyaspartic acid (TBOA), the GLT-1-selective nontransportable inhibitor of Glu/Asp uptake dihydrokainic acid (DHK) (all from R&D Systems, Minneapolis, MN), the selective GLAST inhibitor UCPH-101 (Abcam, Cambridge, MA), the membrane permeable pharmacological inhibitor of CaMKII activity KN-93, or its inactive derivative KN-92 (EMD Millipore, Billerica, MA). In the case of dual treatments, inhibitors were added 30 min prior to the application of L-Glu or D-Asp. Cells were analyzed 6 h after the addition of L-Glu or D-Asp unless stated otherwise. Typically, at least three independent experiments were performed, whereby an independent experiment refers to an experiment in which cells were isolated from a separate P3 rat litter at an independent time point (day) and treated separately from all other independent experiments. In each experiment, triplicate coverslips (cultures) were prepared for all conditions/treatments.

Cells of the immortalized mouse oligodendroglial cell line CIMO were cultured in DMEM/5% fetal calf serum (FCS)/1 μg/mL interferon-γ (EMD Millipore, Billerica, MA) at 33°C (Bronstein et al., 1998) and then used in plasmid nucleofection experiments.

Quantitative (q)RT-PCR Analysis

For the determination of relative mRNA expression levels, qRT-PCR was performed on a CFX96 Real-Time PCR Detection System (Bio-Rad, Hercules, CA) using the iQ SYBR Green Supermix (Bio-Rad, Hercules, CA) and the following gene-specific primer pairs:

Glast: forward (5′-AGCCTGGGGTGTCTTCCACCA-3′), reverse (5′-ACCACAGCCTTGCACTTCAGTGTCT-3′);

Glt-1: forward (5′-TGGCGGCTCCCATCCACCCT-3′), reverse (5′-GGCGGCCGCTGGCTTTAGCA-3′);

Eaac1: forward (5′-GCCCACGAGCTCGGGATGCG-3′), reverse (5′-CACGATGCCCAGTACCACGGC-3′).

Ppia (reference gene): forward: (5′-GGAGACGAACCTGTAGGACG-3′) and reverse: (5′-GATGCTCTTTCCTCCTGTGC-3′)

Pgk1 (reference gene): forward: (5′-ATGCAAAGACTGGCCAAGCTAC-3′) and reverse: (5′-AGCCACAGCCTCAGCATATTTC-3′).

PCR conditions were as follows: 95°C for 3 min followed by 40 cycles of 95°C for 15 s, 58°C for 30 s, and 95°C for 10 s. For comparing the expression levels of the different genes, R_0 values were determined as described by Peirson et al. (2003). To determine the relative expression levels, the $\Delta\Delta C_T$ method was used (Livak and Schmittgen, 2001).

Western Blot Analysis

Cells were homogenized in lysis buffer (150 mM NaCl, 10 mM KCl, 20 mM HEPES [pH 7.0], 1 mM $MgCl_2$, 20% glycerol, and 1% Triton X-100) including the complete protease and phosphatase inhibitor cocktail (Thermo Scientific, Rockford, IL), and 12 μg (30 μg when using anti-GLAST antibodies) were used for Western blot analysis. Bound antibodies were detected using HRP-conjugated secondary antibodies in combination with the ECL Prime Western blotting detection reagent (GE Healthcare Life Sciences, Piscataway, NJ). Chemiluminescent signals were detected by the exposure of photographic film (Kodak BioMax MR, Eastman Kodak, Rochester, NY) and quantified by densitometry using the ImageJ software package (Abramoff et al., 2004).

Immunocytochemistry

For immunocytochemistry using O4 hybridoma supernatants, cells were fixed in 4% of paraformaldehyde/phosphate-buffered saline (PBS), nonspecific binding sites were blocked in 10% FCS/DMEM, and cells were incubated with the supernatant (1:1 diluted in 10% FCS/DMEM) overnight. For immunocytochemical detection of GLAST, GLT-1, EAAC1, or MBP, cells were fixed in 4% of paraformaldehyde/PBS and then permeabilized using 0.5% Triton X-100/0.4 M sucrose/PBS. Subsequently, cells were incubated for 30 min in 10% FCS/DMEM and then overnight with anti-GLAST, anti-GLT-1, anti-EAAC1 (Abcam, Cambridge, MA), or anti-MBP (SMI99; Covance, Princeton, NJ) antibodies. Primary antibodies were detected using Alexa 488- or Alexa 564-conjugated secondary antibodies (Life Technologies, Grand Island, NY) and nuclei were counterstained using Hoechst 33342 (EMD Millipore, Billerica, MA).

siRNA-Mediated Gene Silencing

Differentiating oligodendrocytes were transfected with ON-TARGET*plus* siRNA SMARTpools directed against rat *Glast*, *Glt-1*, or *Eaac1* (Thermo Fisher Scientific, Pittsburg, PA) using Lipofectamine 2000 (Life Technologies, Grand Island, NY). As control, an ON-TARGET*plus* nontargeting siRNA pool (Thermo Fisher Scientific, Pittsburg, PA) was used. Transfection medium containing siRNA–lipofectamine complexes was replaced with serum-free differentiation medium (DMEM/T3/N2) after 3 h and cells were cultured for an additional 72 h. Knockdown of gene expression was assessed by qRT-PCR and Western blot analysis.

Process Morphology Analysis

Oligodendrocyte morphology was analyzed and quantified as described previously in detail (Dennis et al., 2008). Briefly, oligodendrocytes were immunostained using O4 hybridoma cell supernatants and the images of approximately 30 cells were taken for each treatment group in each experiment ($n \geq 3$; i.e. at least 90 cells per condition) using an Olympus BX51 inverted fluorescent microscope (Olympus America, Center Valley, PA). Cells were chosen over the entire field of the coverslip by scanning from the upper left to the lower right. Only cells that displayed the features of a healthy cell (based on the nuclear stain and membrane appearance) and were without overlap with any neighboring cell were selected for analysis. IP Lab imaging software (BD Biosciences Bioimaging, Rockville, MD) was used to determine the network area (total area within the radius of the O4 immunopositive process network minus the cell body). For the bar graphs representing network area, the mean value for cells cultured under control conditions was calculated and set to 100%. Adjusted, that is normalized, values for all cells were then averaged for each experimental condition. For the generation of representative images, confocal laser scanning microscopy was used (Zeiss LSM 510 META NLO; Carl Zeiss Microscopy, LLC, Thornwood, NY). Images represent 2D maximum projections of stacks of 0.5 μm optical sections.

Cell Count Analysis

To determine the number of MBP immunopositive cells, images of four fields per coverslip were taken with a 20× objective using an Olympus BX51 fluorescence microscope equipped with an Olympus DP72 CCD camera (Olympus America, Center Valley, PA). Three coverslips per condition for each of three independent experiments were analyzed, and Hoechst 33342-positive nuclei as well as MBP immunopositive oligodendrocytes were counted using the Cell Counter plugin to the ImageJ software package (Abramoff et al., 2004).

Intracellular Calcium Measurement

The concentrations of intracellular calcium were determined in principal as described previously (Grynkiewicz et al., 1985). Briefly, differentiating oligodendrocytes were loaded with the calcium indicator fura-2 AM ester (2.5 μM) and pluronic F-127 (0.01%) (Life Technologies, Grand Island, NY) in differentiation medium for 30 min at 37°C. Cells were washed and incubated in differentiation medium for an additional 30 min at 37°C. Ratiometric calcium measurements were made at 340 and 380 nm of excitation and 510–520 nm of emission wavelengths with cells cultured in differentiation medium (unless mentioned otherwise) using a Zeiss Observer.Z1 microscope in combination with the Axio VisionRel 4.8 software package (Carl Zeiss Microscopy, LLC, Thornwood, NY). Measurements were taken from at least nine cells per treatment group and experiment and from three independent experiments (i.e., a total of 27 cells per treatment group) before and after the application of the indicated compounds. To calculate intracellular free calcium concentrations (in nM), a calibration curve (Calcium Calibration Buffer Kit, Life Technologies, Grand Island, NY) was used.

Plasmid Nucleofection

A2B5 immunopanned oligodendrocyte progenitors or CIMO cells were nucleofected (Lonza Cologne GmbH, Cologne, Germany) with the following constructs: a plasmid encoding eGFP–CaMKIIβ (Okamoto et al., 2004), a control plasmid encoding eGFP alone, and plasmids encoding eGFP–CaMKIIβ^{allA} or eGFP–CaMKIIβ^{allD} in which alanine or aspartic acid residues replace all serine/threonine residues located within the variable domain (amino acid, 317–396) (Kim et al., in preparation). All the above plasmids have the same plasmid backbone derived from the eukaryotic expression vector pEGFP-C1 (Clontech Laboratories, Mountain View, CA). It is also worth noting that the eGFP tag has been shown not to interfere with CaMKIIβ function (Okamoto et al., 2004, 2007).

To visualize F-actin in CIMO cells, cells were fixed in 4% paraformaldehyde/0.5% glutaraldehyde/0.4 M sucrose/PBS and then incubated with Acti-stain 555 phalloidin (Cytoskeleton, Denver, CO). Colocalization was quantified by determining weighted colocalization coefficients (Manders et al., 1993) using the ZEN software package (Carl Zeiss MicroImaging, LLC, Thornwood, NY) and dual-color confocal images of cellular protrusion that were imaged using a 63× objective and 2× digital zoom. At least 20 cells per condition and experiment were analyzed in three independent experiments (i.e., a total of at least 60 cells per condition).

To visualize F-actin in differentiating oligodendrocytes, a plasmid (pCAGGS backbone; Niwa et al., 1991) encoding Lifeact (Riedl et al., 2008) fused to mRuby (Kredel et al., 2009) was used. For the generation of representative images, confocal laser scanning microscopy was used (Zeiss LSM 510 META NLO; Carl Zeiss Microscopy, LLC, Thornwood, NY). Images represent 2D maximum projections of stacks of 0.5 μm optical sections.

Statistical Analysis

For statistical analysis, the GraphPad Prism software (GraphPad Software, La Jolla, CA) was used. In the case of two or more groups of data composed of variable values, two-tailed Student's *t*-tests or Kruskal–Wallis one-way analyses of variance (ANOVA) combined with Dunn's *post hoc* or Student–Newman–Keuls tests were performed. When comparing a single control group with experimental groups of data, ANOVA with Dunnett's *post hoc* tests was used. In the case data were compared with a set control value (1 or 100%) lacking variability, one-sample *t*-tests were used (Dalgaard, 2008; Skokal and Rohlf, 1995).

Results

Sodium-Dependent Glu Transport, Mediated Primarily by GLAST and GLT-1, Promotes the Morphological Maturation of Differentiating Oligodendrocytes

As introduced above, the sodium-dependent Glu transporter genes *Glast*, *Glt-1*, and *Eaac1* have been found to be expressed by cells of the oligodendrocyte lineage. To confirm such expression in differentiating oligodendrocytes in our culture system, qRT-PCR analysis was performed and revealed relative mRNA expression levels of *Glast* > *Glt-1* > *Eaac1* (Fig. 1A). Further validation was obtained through Western blot analysis and immunocytochemistry (Fig. 1B,C). Notably, in particular GLAST and GLT-1 were readily detectable not only in the cell body but also in the cellular processes.

To assess a potential role of sodium-dependent Glu transporters beyond extracellular Glu clearance, differentiating oligodendrocytes were treated with 100 μM of L-Glu and morphological aspects of oligodendrocyte maturation were assessed via a quantification of the network area as described previously in detail (Dennis et al., 2008). As shown in Fig. 2A–C, L-Glu treatment had a maturation-promoting effect that was seen as early as 2 h and up to 6 h. Importantly, this effect could be blocked by pretreatment with TBOA (Fig. 2A,B), a competitive and nontransportable inhibitor of sodium-dependent Glu transport (Shigeri et al., 2001; Shimamoto et al., 1998). In agreement with previous studies, no obvious effects on cell survival were noted in the presence of the L-Glu and TBOA concentrations used here and within the time frames analyzed (Deng et al., 2006 and data not shown).

To further substantiate that sodium-dependent Glu transporters play a predominant role in the observed maturation-promoting effect exerted by L-Glu, the naturally

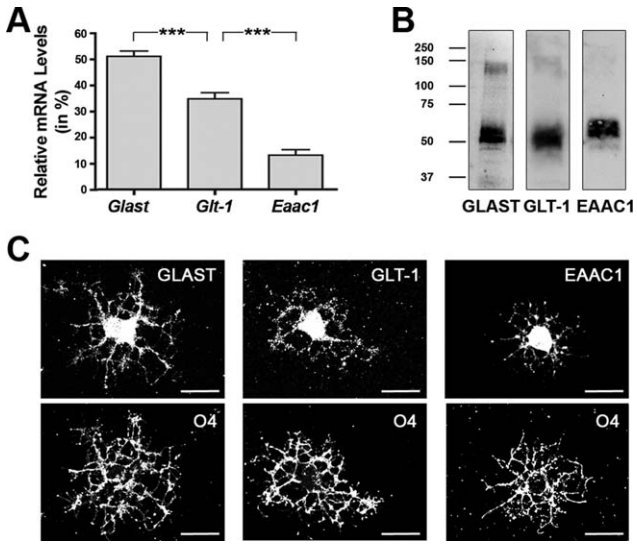

FIGURE 1: Sodium-dependent Glu transporters are expressed in differentiating oligodendrocytes. A: Bar graph representing sodium-dependent Glu transporter mRNA levels as determined by qRT-PCR analysis. Total Glu transporter mRNA levels (*Glast*+*Glt-1*+*Eaac1*) were set to 100% and the values for the individual gene-specific mRNA levels were adjusted accordingly. Data represent means ± SEM ($n = 3$ independent experiments, $^{***}P \leq 0.001$, ANOVA). B: Representative Western blots showing sodium-dependent Glu transporter protein expression. Numbers to the left indicate molecular weights in kDa. C: Representative images of differentiating oligodendrocytes double-immunostained using anti-GLAST, -GLT-1, or -EAAC1 antibodies in combination with O4 hybridoma supernatants. Scale bars: 20 μm.

occurring amino acid D-Asp was used as a Glu-equivalent agonist. Similar to L-Glu, D-Asp is efficiently taken up through the sodium-dependent Glu transporter system (Danbolt and Storm-Mathisen, 1986; Davies and Johnston, 1976; Kanai and Hediger, 1992; Palacin et al., 1998; Pines et al., 1992). In contrast to L-Glu, however, D-Asp does not activate non-NMDA receptor ionotropic and metabotropic Glu receptors (Domercq et al., 2005; Errico et al., 2008; Sugiyama et al., 1989), and it is not metabolized by glutamine synthetase (Bender et al., 1997). Thus, the use of D-Asp eliminates potential confounding effects that may be owing to an activation of AMPA/kainate and/or metabotropic Glu receptors and/or the release of glutamine via the sodium-dependent neutral amino acid transporter system. As shown in Fig. 2D, D-Asp elicited an effect on the oligodendrocyte process network that was comparable to the one seen upon treatment with L-Glu (compare Fig. 2B with 2D).

It has been well demonstrated that morphological maturation of oligodendrocytes occurs during development concurrently with changes in gene expression (Baumann and Pham-Dinh, 2001; Emery, 2010; Pfeiffer et al., 1993). Under experimental conditions, however, molecular mechanisms regulating cellular morphology may be uncoupled from those that regulate gene expression (Buttery and ffrench-Constant, 1999; Kim et al., 2006; Lafrenaye and Fuss, 2011; Osterhout et al., 1999; Waggener et al., 2013). Thus, and to assess a potential role of L-Glu and the activity of sodium-dependent Glu transporters on myelin gene expression, potential changes in *Mbp* expression were assayed using immunocytochemistry. In these experiments, no significant differences in the number of MBP-positive cells were noted (Fig. 2E,F), thus suggesting that the sodium-dependent Glu transporter-mediated effect on oligodendrocyte maturation is primarily associated with the morphological aspects of this process.

As shown in Fig. 1, differentiating oligodendrocytes express more than one of the known sodium-dependent Glu transporter genes. To evaluate the role of individual transporter genes, differentiating oligodendrocytes were transfected with siRNA pools specifically silencing *Glast*, *Glt-1*, or *Eaac1* expression. Knockdown of gene expression was confirmed by Western blot analysis, which revealed a specific reduction in transporter protein levels of at least 70% (Supp. Info. Fig. S1). Importantly, downregulation of a particular transporter gene was not associated with compensatory upregulation of any other transporter gene (Supp. Info. Fig. S1). In addition, no effect on the oligodendrocyte network area was noted upon knockdown of sodium-dependent Glu transporter expression alone (data not shown). However, knockdown of either *Glast* or *Glt-1* expression was found to eliminate the effect of L-Glu on the oligodendrocyte network area (Fig. 2G). For *Eaac1*, the sodium-dependent Glu transporter with much lower mRNA expression levels when compared with *Glast* or *Glt-1*, knockdown of gene expression was seen to only partially attenuate the effect of L-Glu on the oligodendrocyte network area (*siCtrl*+Glu: 157 ± 7%, *siEaac1* + Glu: 136 ± 6%, $P = 0.007$, ANOVA).

Taken together, the abovementioned data demonstrate that L-Glu can promote the morphological aspects of oligodendrocyte maturation via a sodium-dependent L-Glu transporter-mediated mechanism. In addition, they suggest that even a slight decline in the oligodendrocyte-derived expression of sodium-dependent L-Glu transporters can reduce the effect of L-Glu on the maturation of differentiating oligodendrocytes.

Activation of Sodium-Dependent Glu Transporters in Differentiating Oligodendrocytes Leads to a Transient Increase in Intracellular Calcium Levels

Having established that the activation of sodium-dependent Glu transporters promotes the morphological maturation of differentiating oligodendrocytes, we next wished to explore potential downstream signaling events involved in this process. These signaling-related studies were focused on calcium-mediated events as it had been previously demonstrated that Glu transport can activate the reverse mode of the

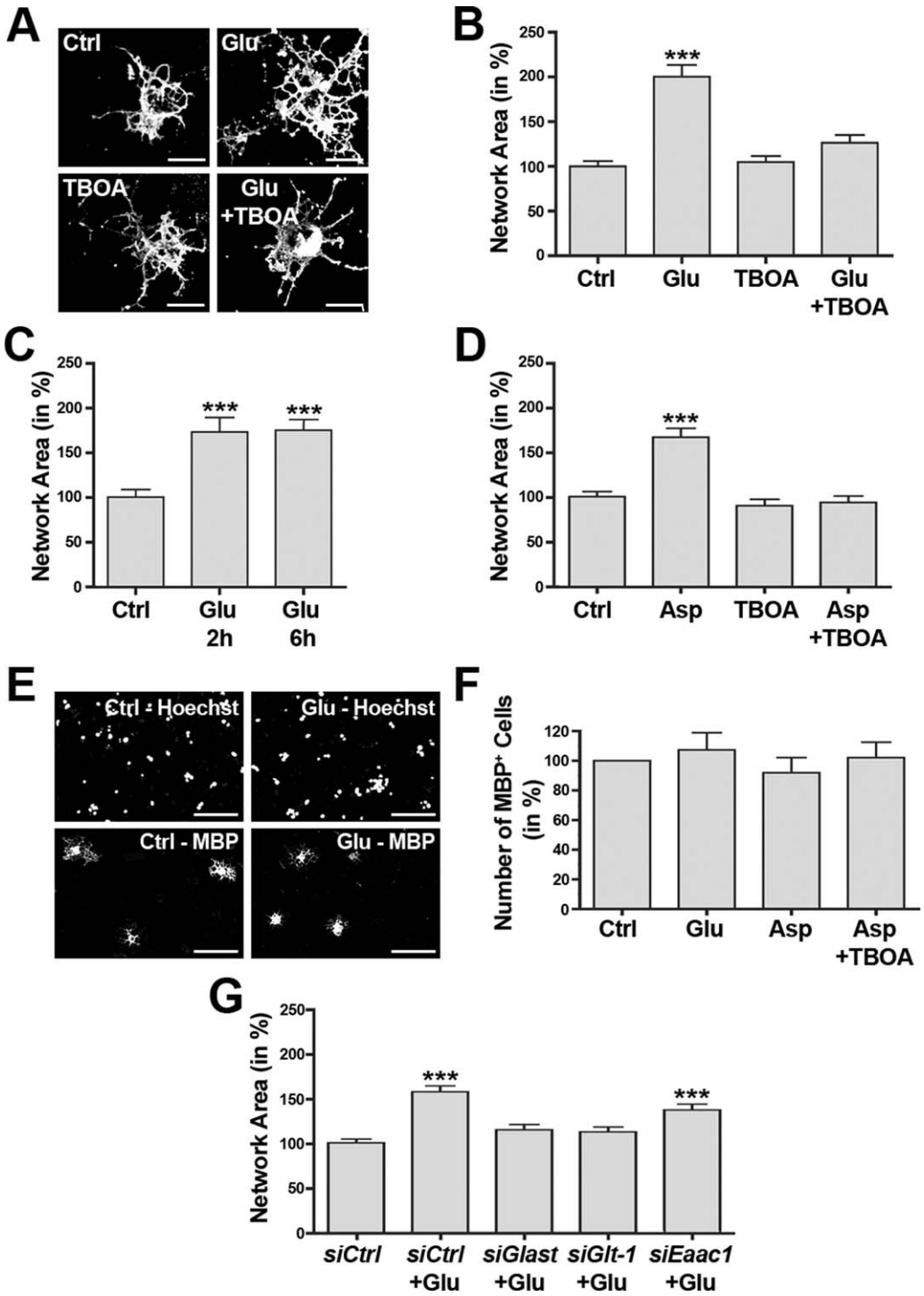

FIGURE 2: Activation of sodium-dependent Glu transporters promotes the morphological aspects of oligodendrocyte differentiation. **A–F**: Differentiating oligodendrocytes were treated for 6 h (unless noted otherwise) as indicated: control (Ctrl), L-Glu (100 μM), a nontransportable inhibitor of sodium-dependent Glu transport (TBOA, 100 μM), and D-Asp (100 μM). A: Representative images of differentiating oligodendrocytes immunostained using O4 hybridoma supernatants. Scale bars: 20 μm. B–D: Bar graphs representing quantitative analyses of oligodendrocyte network areas (Dennis et al., 2008). Data represent means ± SEM (***$P \leq 0.001$ compared with control, ANOVA). E: Representative images of differentiating oligodendrocytes stained with an antibody specific for MBP as well as with Hoechst 33342 (Hoechst) to visualize nuclei. Scale bars: 100 μm. F: Bar graph showing the number of MBP immunopositive cells normalized to the number of Hoechst-positive nuclei. Data represent means ± SEM. ANOVA revealed no statistically significant difference ($P \leq 0.05$). **G**: Bar graph showing oligodendrocyte network areas upon siRNA-mediated knockdown of individual sodium-dependent Glu transporters (as indicated) and subsequent treatment with L-Glu (100 μM). Data represent means ± SEM (***$P \leq 0.001$ compared with *siCtrl* nontreated, ANOVA).

sodium/calcium exchanger and hence lead to a transient increase in intracellular calcium levels (Lopez-Colome et al., 2012; Martinez-Lozada et al., 2011; Rojas et al., 2007). To assess the effect of an activation of sodium-dependent Glu transporters on intracellular calcium levels, D-Asp was used as a Glu-equivalent agonist, and the measurements of calcium were taken within the first minutes of the experiment, that is at an early stage of oligodendrocyte maturation. It is worth noting that the cells shown in Fig. 2A were imaged 6 h after Glu application, that is subsequent to a period of significant process outgrowth. As shown in Fig. 3, D-Asp treatment elicited a transient increase in intracellular calcium levels that appeared to occur first within cellular processes (Fig. 3A). This D-Asp-induced transient increase in free intracellular calcium levels was found to be dose dependent (Fig. 3B) and absent in the presence of TBOA (Fig. 3C). In addition, no such increase was observed in the absence of extracellular calcium (Fig. 3B).

To assess the functional contributions of each of the two main sodium-dependent Glu transporters expressed by differentiating oligodendrocytes, namely GLAST and GLT-1, DHK, a nontransportable inhibitor of L-Glu uptake selective for GLT-1 (Arriza et al., 1994), and UCPH-101, a nonsubstrate inhibitor selective for GLAST (Abrahamsen et al., 2013; Erichsen et al., 2010), were used. As shown in Fig. 3D, the D-Asp-mediated transient increase in intracellular calcium levels was completely abolished in the presence of DHK but only partially blocked in the presence of UCPH-101. Such a more prominent functional role of GLT-1 compared with GLAST in differentiating oligodendrocytes could be further validated by performing Glu uptake assays (data not shown).

Taken together, the abovementioned data support the idea that in differentiating oligodendrocytes L-Glu/D-Asp activates sodium-dependent Glu transporters and in particular GLT-1, which in turn mediates a transient increase in intracellular calcium levels via entry from the extracellular environment.

The Maturation-Promoting Effect of Sodium-Dependent Glu Transporters in Differentiating Oligodendrocytes is Mediated by a Transient Phosphorylation Event Within CaMKIIβ's Actin-Binding/-Stabilizing Domain

Our recent data provided good evidence for a critical role of the calcium sensor CaMKIIβ and in particular its actin-binding/-stabilizing domain in regulating oligodendrocyte maturation and CNS myelination (Waggener et al., 2013). Thus, CaMKIIβ and its actin-binding/-stabilizing domain may be directly involved in the sodium-dependent Glu transporter-mediated effect described here. Indeed, pretreatment of differentiating oligodendrocytes with KN-93, a membrane-permeable pharmacological inhibitor of CaMKIIβ's kinase catalytic as well as actin-binding/-stabilizing activity (Lin and Redmond, 2008; Sumi et al., 1991), was found to block the maturation-promoting effect of L-Glu on the oligodendrocyte process network (Fig. 4A). It is worth noting that KN-93 treatment alone and thus a continuous inhibition of CaMKII activity attenuated the morphological maturation of differentiating oligodendrocytes (Fig. 4A). This effect has been previously described and was found not to be associated with a change in cellular viability (Waggener et al., 2013).

To further assess the effect of L-Glu on CaMKII and in particular CaMKIIβ's actin-binding/-stabilizing domain in differentiating oligodendrocytes, phosphorylation events at CaMKII's $T^{286/7}$ and CaMKIIβ's S^{371} site were analyzed. CaMKII's $T^{286/7}$ site represents CaMKII's autophosphorylation site, which regulates autonomous CaMKII kinase catalytic activity and calcium-/calmodulin-binding affinity (Coultrap and Bayer, 2012). Owing to sequence conservation, phosphorylation events at this site could be detected only by pan pCaMKII $T^{286/7}$ antibodies. CaMKIIβ's S^{371} phosphorylation site is located within CaMKIIβ's unique actin-binding/-stabilizing domain (Kim et al., 2011; Lin and Redmond, 2009; Okamoto et al., 2007; O'Leary et al., 2006; Sanabria et al., 2009), and antibodies specifically recognizing this site have been generated by us. These antibodies were found not to recognize CaMKIIβ S^{371A}, a mutant form of CaMKIIβ that cannot be phosphorylated at its S^{371} site (data not shown). As shown in Fig. 4B,C, treatment of differentiating oligodendrocytes with L-Glu led to a significant increase in phosphorylation at CaMKIIβ's S^{371} site. This effect was time dependent and transient as an increase in phosphorylation was not seen prior to 30 min of treatment and beyond 4 h (Fig. 4C,F). No such increase in phosphorylation was observed at CaMKII's autophosphorylation ($T^{286/7}$) site within 15–60 min of L-Glu treatment (Fig. 4E), nor was a change in total protein levels of CaMKIIβ noted (Fig. 4D). Importantly, the effect of L-Glu on the phosphorylation at CaMKIIβ's S^{371} site could be blocked by pretreatment with TBOA (Fig. 4G).

To further assess the contribution of individual sodium-dependent Glu transporter genes in this L-Glu-mediated increase in pCaMKIIβ S^{371} levels, differentiating oligodendrocytes were transfected with siRNA pools specifically targeting *Glast*, *Glt-1*, or *Eaac1* expression. Similar to those observed for the effect of gene-specific knockdown of sodium-dependent Glu transporter expression on the oligodendrocyte network area (Fig. 2F), knockdown of *Glast* or *Glt-1* expression eliminated the effect of L-Glu on the phosphorylation of CaMKIIβ's S^{371} site, whereas the effect of a

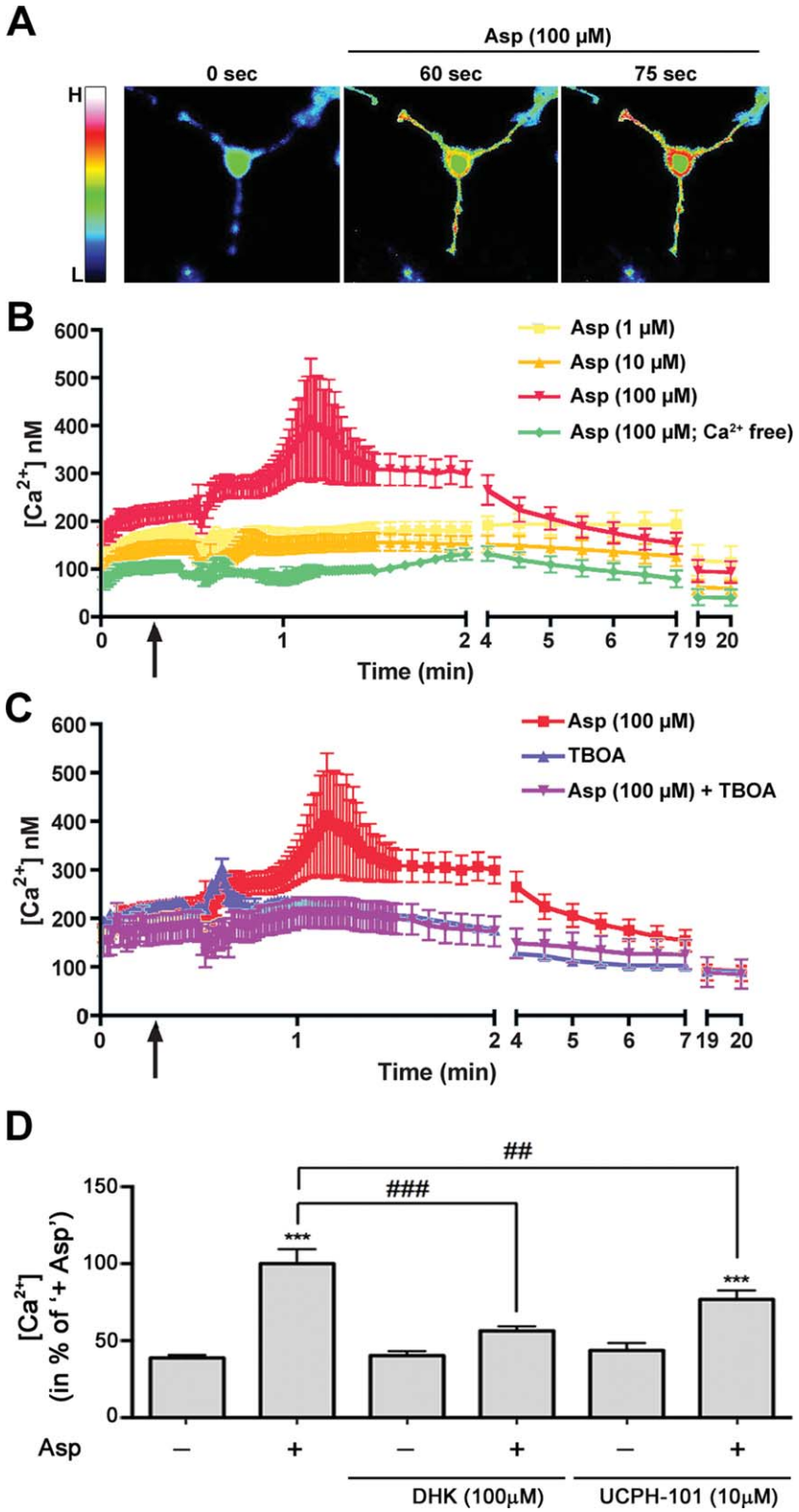

FIGURE 3: The activation of sodium-dependent Glu transporters increases intracellular calcium levels in the processes of early-stage differentiating oligodendrocytes. **A**: Representative pseudo-colored images of fura-2 AM fluorescence ratio measurements upon treatment with D-Asp. The bar to the left represents a relative color scale indicating low (L) and high (H) calcium levels. **B,C**: Time course of changes in free intracellular calcium concentrations [Ca^{2+}] upon different treatments as indicated in the inset shown in the upper right. Start of treatment is indicated by the arrow. The graphs represent means ± SEM. **D**: Bar graph showing a quantitative analysis of free intracellular calcium concentrations [Ca^{2+}] at the time point of highest response to D-Asp. The mean value for D-Asp-treated cells (+Asp) was set to 100% and the remaining values were calculated accordingly. Treatments are indicated along the *x*-axis. Data represent means ± SEM (***$P \leq 0.001$ compared with control [untreated], $^{###}P \leq 0.001$ and $^{##}P \leq 0.01$ compared with "+Asp," ANOVA).

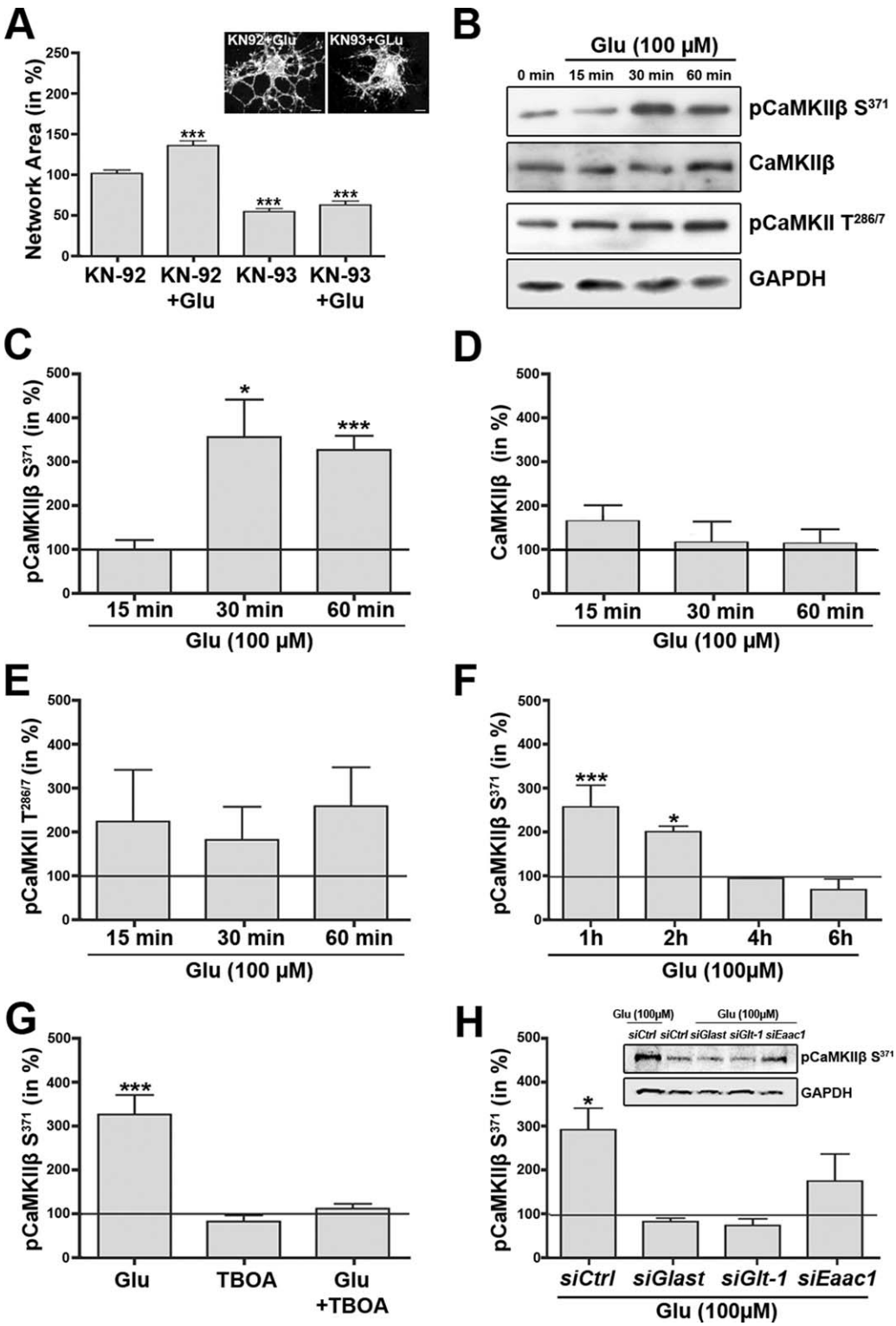

FIGURE 4: Activation of sodium-dependent Glu transporters leads to a transient phosphorylation event at CaMKIIβ's S^{371} site. **A**: Bar graph showing a quantitative analysis of the oligodendrocyte network area (Dennis et al., 2008). Cells were pretreated with the pharmacological CaMKII inhibitor KN-93 or its inactive derivative KN-92 and then incubated in the absence or presence (+Glu) of 100 µM of L-Glu. The mean values for control cells (pretreated with KN-92 and incubated in the absence of L-Glu) were set to 100% and the experimental values were calculated accordingly. Data represent means ± SEM (***$P \leq 0.001$ compared with control, ANOVA). The inset (upper right) shows representative images of differentiating oligodendrocytes treated with KN-92 plus L-Glu (left) or KN-93 plus L-Glu (right), and immunostained using O4 hybridoma supernatants. Scale bars: 5 µm. **B, inset in H**: Representative Western blots showing CaMKII phosphorylation (pCaMKIIβ S^{371}, pCaMKII $T^{286/7}$) or total CaMKIIβ protein levels. GAPDH protein levels are shown representatively for the Western blot for which anti-pCaMKII $T^{286/7}$ (B) or anti-pCaMKIIβ S^{371} (inset in H) antibodies were used. **C–H**: Bar graphs showing the levels of pCaMKIIβ S^{371} (C,F–H), total CaMKIIβ (D), or pCaMKII $T^{286/7}$ (E) at different time points after the addition of L-Glu (C–F), at the time point of 60 min after the addition of L-Glu and prior pretreatment with or without TBOA (G) or after transfection with siRNA pools as indicated and L-Glu treatment for 60 min (H). All CaMKII protein levels were normalized to GAPDH protein levels. The mean-normalized values for control (nontreated) cells were set to 100% (horizontal line) and the experimental values were calculated accordingly. Data represent means ± SEM of three independent experiments (***$P \leq 0.001$, *$P \leq 0.05$ compared with control, ANOVA).

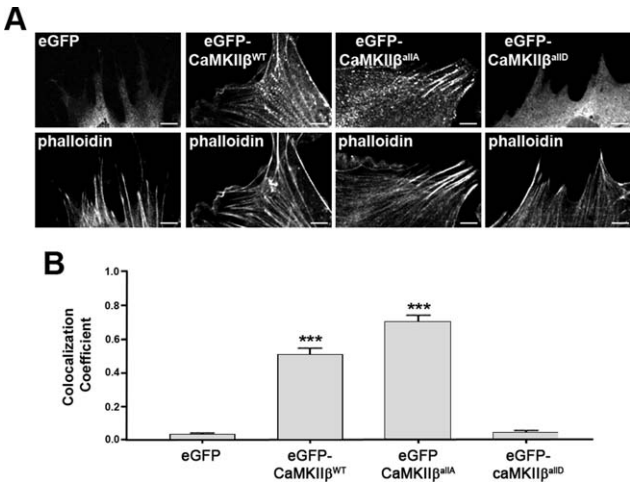

FIGURE 5: Phosphorylation events within CaMKIIβ's actin-binding/-stabilizing domain regulate the association of CaMKIIβ with F-actin. A: Representative images of CIMO cells nucleofected with plasmids encoding eGFP fusion proteins of CaMKIIβ (WT or mutant form as indicated) and stained for F-actin (phalloidin). Scale bars: 5 μm. B: Bar graph showing the weighted colocalization coefficients for eGFP fusion proteins and phalloidin. Data represent means ± SEM (*$P \leq 0.001$ compared with eGFP, ANOVA).**

knockdown of Eaac1 expression appeared less pronounced (Fig. 4H).

Our data described so far demonstrate that in differentiating oligodendrocytes, L-Glu can activate sodium-dependent Glu transporters, which in turn can mediate a transient increase in intracellular calcium levels, a transient phosphorylation event within CaMKIIβ's actin-binding/-stabilizing domain (S^{371} site) and a promotion of the morphological aspects of oligodendrocyte maturation.

Phosphorylation Events Within CaMKIIβ's Actin-Binding/-Stabilizing Domain Regulate the Association of CaMKIIβ with F-Actin and the Effect of L-Glu on the Oligodendrocyte Process Network

Our recent data, investigating the role of CaMKIIβ in the structural plasticity of dendritic spines, demonstrated that upon increases in intracellular calcium levels and serine (including S^{371})/threonine phosphorylation events within CaMKIIβ's actin-binding/-stabilizing domain CaMKIIβ detaches from F-actin (Kim et al., 2011). These data raised the possibility that sodium-dependent Glu transporter-mediated phosphorylation events within CaMKIIβ's actin-binding/-stabilizing domain may affect the oligodendrocyte process network via a change in CaMKIIβ's association with F-actin. To assess this idea, eGFP fusion proteins of CaMKIIβ mutant forms were generated in which the serine/threonine residues within the actin-binding/-stabilizing domain are either nonphosphorylatable (eGFP–$CaMKII\beta^{allA}$) or their phosphorylated state is mimicked (eGFP–$CaMKII\beta^{allD}$). In addition, eGFP–$CaMKII\beta^{WT}$ and eGFP–$CaMKII\beta^{K43R}$, a mutant that is impaired in ATP binding and thus inactive with regard to its kinase catalytic but not actin-binding activity (Okamoto et al., 2007), were used. To validate the proposed involvement of phosphorylation events within CaMKIIβ's actin-binding/-stabilizing domain on CaMKIIβ's association with F-actin, nucelofection studies were performed in cells of the oligodendroglial cell line CIMO. As shown in Fig. 5, nonphosphorylatable eGFP–$CaMKII\beta^{allA}$ as well as eGFP–$CaMKII\beta^{WT}$ largely colocalized with F-actin. In contrast, the phospho-mimetic eGFP–$CaMKII\beta^{allD}$ showed little colocalization with F-actin and appeared similar to eGFP distributed diffusely and throughout the cytoplasm.

Having established the F-actin-binding characteristics of the different forms of CaMKIIβ, we performed conucleofection experiments using a plasmid encoding Lifeact fused to mRuby in differentiating oligodendrocytes. Lifeact is a 17-amino-acid peptide, which binds to F-actin without interfering with actin organization and dynamics (Riedl et al., 2008) and thus allows reliable visualization of F-actin-rich structures. Using this approach, $CaMKII\beta^{allA}$ and eGFP–$CaMKII\beta^{WT}$ were readily detectable within F-actin-enriched regions located within cellular processes of differentiating oligodendrocytes (Fig. 6A, arrows). In contrast, eGFP–$CaMKII\beta^{allD}$ was similar to eGFP found predominantly localized to the cell body (Fig. 6A).

To further assess the role of the phosphorylation state of CaMKIIβ's actin-binding/-stabilizing domain and thus its level of association with F-actin in the L-Glu-mediated promotion of the morphological aspects of oligodendrocytes maturation, the effect of the expression of the different eGFP–CaMKIIβ forms on the oligodendrocyte network area was evaluated. As shown in Fig. 6B, the expression of nonphosphorylatable eGFP–$CaMKII\beta^{allA}$ blocked the maturation-promoting effect of L-Glu treatment. No such effect was observed when eGFP–$CaMKII\beta^{WT}$ or eGFP–$CaMKII\beta^{K43R}$ were expressed, suggesting that the L-Glu-mediated maturation-promoting effect may not require CaMKIIβ's kinase catalytic activity. Importantly and consistent with our previous findings (Waggener et al., 2013; Fig. 4A), constitutive expression of the phospho-mimetic eGFP–$CaMKII\beta^{allD}$ attenuated the morphological maturation of differentiating oligodendrocytes, likely owing to a dominant-negative effect with regard to F-actin binding. In addition, it eliminated the effect of L-Glu treatment on the oligodendrocyte process network.

Taken together, the abovementioned data support the idea that transient phosphorylation within CaMKIIβ's actin-binding/-stabilizing domain leading to transient detachment of CaMKIIβ from F-actin is a required step in the molecular mechanism that promotes the morphological aspects of

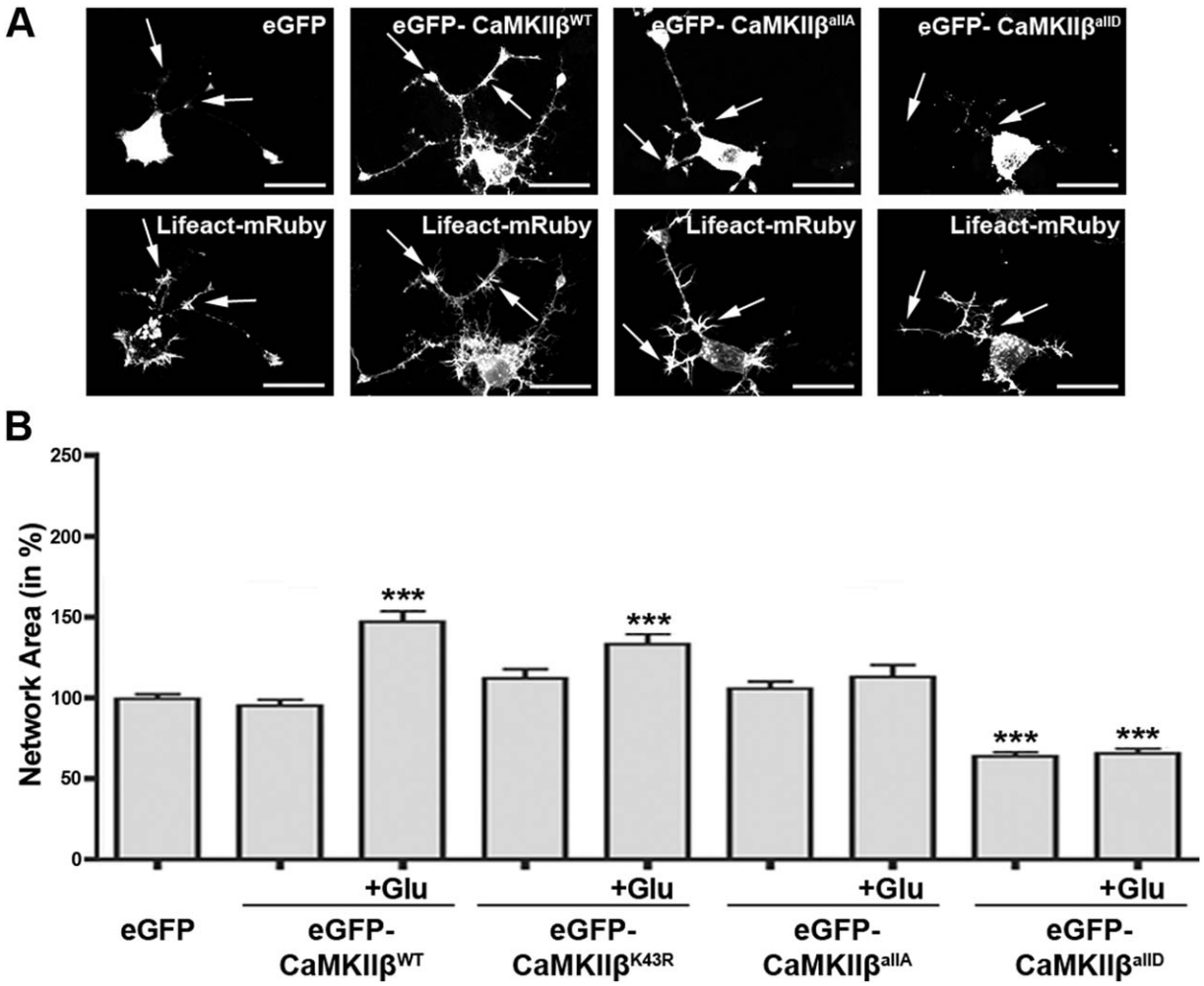

FIGURE 6: Phosphorylation events within CaMKIIβ's actin-binding/-stabilizing domain regulate the Glu-mediated promotion of the morphological aspects of oligodendrocyte maturation. A: Representative images of differentiating oligodendrocytes conucleofected with plasmids encoding an eGFP fusion protein of CaMKIIβ (WT or mutant form as indicated) and Lifeact–mRuby. Arrows point toward F-actin-enriched regions along cellular processes as visualized via Lifeact–mRuby fluorescence. Scale bars: 20 μm. B: Bar graph showing a quantitative analysis of the oligodendrocyte network area (Dennis et al., 2008). Cells were nucleofected as indicated and then incubated in the absence or presence (Glu) of 100 μM of L-Glu. The mean values for control cells (nucleofected with an eGFP-encoding plasmid and incubated in the absence of L-Glu) were set to 100% and the experimental values were calculated accordingly. Data represent means ± SEM (*$P \leq 0.001$ compared with control, ANOVA).**

oligodendrocyte maturation via an activation of sodium-dependent Glu transporters. Notably, constitutive (vs. transient) phosphorylation within CaMKIIβ's actin-binding/-stabilizing domain appears to have an opposing effect, that is to attenuate oligodendrocyte maturation.

Discussion

The studies described here investigated the role of sodium-dependent Glu transporters in the regulation of oligodendrocyte maturation. Based on the data presented and in combination with the ascribed function of CaMKIIβ's actin-binding/-stabilizing domain in the regulation of dendritic spine morphology (Okamoto et al., 2009), we propose the following model for the role of sodium-dependent Glu transporters in the regulation of oligodendrocyte maturation (Fig. 7). Under basal conditions, CaMKIIβ is, in differentiating oligodendrocytes, to a large extent, associated with the actin cytoskeleton. Glu release from, for example, unmyelinated axonal segments activates oligodendroglial sodium-dependent Glu transporters, which in turn activates the reverse mode of oligodendroglial sodium/calcium exchangers, resulting in a transient increase in intracellular calcium levels (Fig. 7A). This increase in intracellular calcium levels leads to phosphorylation events within CaMKIIβ's actin-binding/-stabilizing domain (including CaMKIIβ's S^{371} site), inactivation of CaMKIIβ's actin-binding activity and detachment of CaMKIIβ from the actin cytoskeleton. Such transient inactivation of CaMKIIβ's actin-binding activity opens a time window during which actin cytoskeleton remodeling events and actin polymerization are favored (Hoffman et al., 2013;

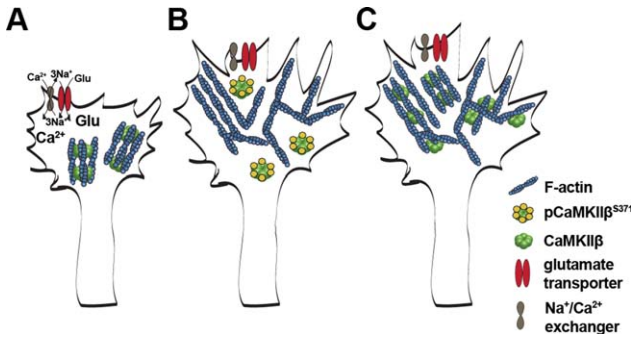

FIGURE 7: Proposed model for the role of a sodium-dependent Glu transporter-CaMKIIβ-actin cytoskeleton axis in the regulation of oligodendrocyte maturation. A: L-Glu **stimulates sodium-dependent Glu transporter activity, which in turn leads to an increase in intracellular sodium (Na^+) levels, activation of the reverse mode of the sodium/calcium exchanger, and a transient increase in intracellular calcium (Ca^{2+}) levels. B: The transient increase in intracellular calcium levels leads to phosphorylation events within CaMKIIβ's actin-binding/-stabilizing domain ($pCaMKII\beta^{S371}$), detachment of CaMKIIβ from F-actin, and the opening of a time window during which cytoskeletal rearrangements and morphological remodeling can occur. C: Upon deactivation (dephosphorylation), CaMKIIβ binds to F-actin and hence stabilizes the newly arranged cytoskeleton. Such cycles of activation and deactivation of CaMKIIβ's actin-binding activity allow reorganization of the actin cytoskeleton while at the same time preventing its uncontrolled disintegration. Adapted from Okamoto et al., Physiology, 2009, 24, 357–366.**

Okamoto et al., 2007; Sanabria et al., 2009) (Fig. 7B). This dynamic phase is followed by a phase of actin cytoskeleton stabilization via reactivation of CaMKIIβ's actin-binding activity through dephosphorylation (Fig. 7C). It is worth noting that the actin-binding activity of CaMKIIβ appears to be independent of its kinase catalytic activity, a concept that is supported by recent *in vitro* and *in vivo* studies (Borgesius et al., 2011; van Woerden et al., 2009). Interestingly, actin-binding properties have also been described for other members of the CaMKII gene family. These are, however, mediated by a structure–function domain different from the one identified in CaMKIIβ and analyzed here (Caran et al., 2001; Hoffman et al., 2013). Thus, further studies will be necessary to evaluate a potential contribution of CaMKII isozymes other than CaMKIIβ in the molecular mechanism described here. Importantly, and in contrast to its physiological role as proposed above, inactivation of CaMKIIβ's actin-binding properties in a constitutive (vs. transient) fashion appears to attenuate the morphological maturation of differentiating oligodendrocytes, an effect that is likely mediated by destabilization of the actin cytoskeleton over an extended period of time (Waggener et al., 2013). Thus, it is cycles of activation and deactivation of CaMKIIβ's actin-binding activity that allow reorganization of the actin cytoskeleton and a promotion of the morphological aspects of oligodendrocyte maturation. This idea is further supported by recent findings, demonstrating that balanced activation and deactivation of the actin filament severing and depolymerizing factor cofilin regulates the function of the myelinating cells of the peripheral nervous system, namely Schwann cells (Sparrow et al., 2012).

In addition to the abovementioned data, functional significance of oligodendroglial sodium-dependent Glu transporters for Glu uptake has been well demonstrated (Arranz et al., 2008; DeSilva et al., 2009; Domercq et al., 2005; Pitt et al., 2003; Regan et al., 2007). Consistent with our observations made when assessing calcium levels in differentiating oligodendrocytes upon treatment with D-Asp (Fig. 3), it has been shown that, at least in isolated optic nerve preparations, uptake of D-Asp occurs particularly within oligodendrocyte processes. This observation led to the idea that Glu homeostasis may be tightly regulated at the zones where axons and oligodendrocyte processes meet and in a fashion that may be analogous to what has been described for the tripartite synapse (Arranz et al., 2008). At the tripartite synapse, a so-called "Glu/glutamine shuttle" has been described (Martinez-Lozada et al., 2013; Rodriguez and Ortega, 2012; Uwechue et al., 2012) in which, upon its uptake, Glu is converted to glutamine by the enzymatic activity of glutamine synthetase. Glutamine is then released via sodium-dependent neutral amino acid transporters to be retaken up by neurons and to serve as a precursor for Glu synthesis. Glutamine synthetase is well known to be expressed by cells of the oligodendrocyte lineage (D'Amelio et al., 1990; Tansey et al., 1991; Warringa et al., 1988), and microarray studies indicate the expression of, in particular, the system *N*-amino acid transporter 2 (SNAT2 or SLC38A2) in differentiating oligodendrocytes (Cahoy et al., 2008). Nevertheless, more detailed studies will be necessary to clearly demonstrate that such a Glu/glutamine shuttle exists at axon–oligodendrocyte process interaction zones.

Our studies revealed a prominent expression of the sodium-dependent Glu transporter gene *Glast* in differentiating oligodendrocytes. This finding is in agreement with the previous observations made in tissue culture as well as *in vivo* in both rodents and humans (DeSilva et al., 2009; Domercq et al., 1999; Pitt et al., 2003; Regan et al., 2007; Vallejo-Illarramendi et al., 2006). In addition, a low-level expression of *Eaac1* is consistent with the reported presence of few *Eaac1*-positive cells in the developing optic nerve (Domercq et al., 1999). In contrast, the expression of *Glt-1* in cells of the oligodendrocyte lineage appears more complicated as it has *in vivo* and in rodents been described to be developmentally regulated and to be predominant at stages at which oligodendrocytes are premyelinating (Desilva et al., 2007; DeSilva et al., 2009; Domercq et al., 1999). However, in human tissue the expression of *Glt-1* has been reported to

occur in mature oligodendrocytes (Pitt et al., 2003; Werner et al., 2001). More importantly, our data suggest that on a functional level GLT-1 is the more prominent sodium-dependent Glu transporter in differentiating oligodendrocytes although GLAST also contributes to Glu-mediated uptake and transient increases in intracellular calcium levels. Such a predominant functional sodium-dependent Glu transporter role of GLT-1 in cells of the oligodendrocyte lineage is in agreement with previous findings made in rodents and humans (Pitt et al., 2003; Regan et al., 2007). However, a predominant role of EAAC1 in Glu uptake in maturing oligodendrocytes has also been described (DeSilva et al., 2009). Thus, additional studies will be necessary to more precisely define individual sodium-dependent Glu transporter contributions in cells of the oligodendrocyte lineage. Also, noteworthy is the finding that development in mice with single knockouts for *Glast*, *Glt-1*, or *Eaac1* occurs without apparent CNS gross phenotypes (Peghini et al., 1997; Tanaka et al., 1997; Watase et al., 1998), whereas double *Glast*/*Glt-1* knockout mice die *in utero* and show multiple developmental brain defects (Matsugami et al., 2006). These data indicate that during CNS development the loss of one sodium-dependent Glu transporter may be compensated for functionally by at least one of the remaining transporters, that is by a mechanism that could further complicate a delineation of individual roles for individual sodium-dependent Glu transporters.

Our model shown in Fig. 7 is suggestive of pivotal roles for oligodendroglial sodium/calcium exchangers and intracellular calcium levels in the regulation of oligodendrocyte maturation. This idea is supported by recent findings, implicating the sodium/calcium exchanger NCX3 in the regulation of oligodendrocyte differentiation (Boscia et al., 2012). In addition, process outgrowth has been found to be regulated by intracellular calcium levels in differentiating oligodendrocytes (Yoo et al., 1999). Interestingly, in our studies (Fig. 3), intracellular calcium levels remained slightly above the control levels after the initial rise. Such a calcium response is consistent with the previously described calcium responses mediated by signaling through sodium-dependent Glu transporters in astrocytes (Rojas et al., 2007). In the case of astrocytes, the initial rise in intracellular calcium concentration was found to be amplified by calcium release from ryanodine-sensitive calcium stores (Rojas et al., 2007), which are also expressed by cells of oligodendrocyte lineage (Simpson et al., 1998).

In the major demyelinating disease in human, multiple sclerosis (MS), a block in oligodendrocyte differentiation is considered one of the main causes of inefficient remyelination and repair (Chang et al., 2002; Fancy et al., 2010; Kremer et al., 2011; Kuhlmann et al., 2008). Interestingly, changes in sodium-dependent Glu transporter protein levels have been reported for white-matter areas surrounding MS lesions (Pitt et al., 2003; Vallejo-Illarramendi et al., 2006; Werner et al., 2001) and Glu levels have been found elevated in MS brains (Srinivasan et al., 2005; Trapp and Stys, 2009; Werner et al., 2001). Such changes in Glu homeostasis have been implicated in mediating excitotoxicity (Matute, 2011; Pitt et al., 2003). However, it has also been suggested that mature rodent as well as human oligodendrocytes are largely resistant to such Glu-mediated injury (Kolodziejczyk et al., 2009; Rosenberg et al., 2003; Wosik et al., 2004). Thus, and in light of our findings, it is tempting to speculate that the changes in Glu homeostasis and sodium-dependent Glu transporter signaling may primarily contribute to the differentiation block seen in MS rather than mediate oligodendrocyte cell death.

Acknowledgment

Grant sponsor: The NIH-NINDS.; Grant sponsor: NIH; Grant number: R01DA17310; Grant sponsor: Conacyt-Mexico.; Grant sponsor: Conacyt-Mexico.; Grant sponsor: Grant-in-Aid for Scientific Research and Grant-in-Aid for Scientific Research on the Innovative Area "Foundation of Synapse and Neurocircuit Pathology" from the Ministry of Education, Culture, Sports, Science, and Technology of Japan.; Grant sponsor: NIH-NINDS Center Core; Grant number: 5 P30 NS047463; Grant sponsors: Takeda Pharmaceuticals Co. Ltd.; Fujitsu Laboratories.

Microscopy was performed at the VCU Department of Anatomy and Neurobiology Microscopy Facility. Special thanks go to Steve Pfeiffer and Jeff Bronstein for providing the O4 hybridoma and CIMO cells, respectively.

References

Abrahamsen B, Schneider N, Erichsen MN, Huynh TH, Fahlke C, Bunch L, Jensen AA. 2013. Allosteric modulation of an excitatory amino acid transporter: The subtype-selective inhibitor UCPH-101 exerts sustained inhibition of EAAT1 through an intramonomeric site in the trimerization domain. J Neurosci 33:1068–1087.

Abramoff MD, Magelhaes PJ, Ram SJ. 2004. Image processing with ImageJ. Biophoton Int 11:36–42.

Arranz AM, Hussein A, Alix JJ, Perez-Cerda F, Allcock N, Matute C, Fern R. 2008. Functional glutamate transport in rodent optic nerve axons and glia. Glia 56:1353–1367.

Arriza JL, Fairman WA, Wadiche JI, Murdoch GH, Kavanaugh MP, Amara SG. 1994. Functional comparisons of three glutamate transporter subtypes cloned from human motor cortex. J Neurosci 14:5559–5569.

Barres BA, Hart IK, Coles HS, Burne JF, Voyvodic JT, Richardson WD, Raff MC. 1992. Cell death and control of cell survival in the oligodendrocyte lineage. Cell 70:31–46.

Bauer NG, Richter-Landsberg C, ffrench-Constant C. 2009. Role of the oligodendroglial cytoskeleton in differentiation and myelination. Glia 57: 1691–1705.

Baumann N, Pham-Dinh D. 2001. Biology of oligodendrocyte and myelin in the mammalian central nervous system. Physiol Rev 81:871–927.

Beart PM, O'Shea RD. 2007. Transporters for L-glutamate: An update on their molecular pharmacology and pathological involvement. Br J Pharmacol 150: 5–17.

Bender AS, Woodbury DM, White HS. 1997. The rapid L- and D-aspartate uptake in cultured astrocytes. Neurochem Res 22:721–726.

Borgesius NZ, van Woerden GM, Buitendijk GH, Keijzer N, Jaarsma D, Hoogenraad CC, Elgersma Y. 2011. BetaCaMKII plays a nonenzymatic role in hippocampal synaptic plasticity and learning by targeting alphaCaMKII to synapses. J Neurosci 31:10141–10148.

Boscia F, D'Avanzo C, Pannaccione A, Secondo A, Casamassa A, Formisano L, Guida N, Annunziato L. 2012. Silencing or knocking out the Na(+)/Ca(2+) exchanger-3 (NCX3) impairs oligodendrocyte differentiation. Cell Death Differ 19:562–572.

Bronstein JM, Hales TG, Tyndale RF, Charles AC. 1998. A conditionally immortalized glial cell line that expresses mature myelin proteins and functional GABA(A) receptors. J Neurochem 70:483–491.

Buttery PC, ffrench-Constant C. 1999. Laminin-2/integrin interactions enhance myelin membrane formation by oligodendrocytes. Mol Cell Neurosci 14:199–212.

Cahoy JD, Emery B, Kaushal A, Foo LC, Zamanian JL, Christopherson KS, Xing Y, Lubischer JL, Krieg PA, Krupenko SA, Thompson WJ, Barres BA. 2008. A transcriptome database for astrocytes, neurons, and oligodendrocytes: A new resource for understanding brain development and function. J Neurosci 28:264–278.

Caran N, Johnson LD, Jenkins KJ, Tombes RM. 2001. Cytosolic targeting domains of gamma and delta calmodulin-dependent protein kinase II. J Biol Chem 276:42514–42519.

Chang A, Tourtellotte WW, Rudick R, Trapp BD. 2002. Premyelinating oligodendrocytes in chronic lesions of multiple sclerosis. N Engl J Med 346:165–173.

Coultrap SJ, Bayer KU. 2012. CaMKII regulation in information processing and storage. Trends Neurosci 35:607–618.

Dalgaard P. 2008. Introductory Statistics with R. New York: Springer.

D'Amelio F, Eng LF, Gibbs MA. 1990. Glutamine synthetase immunoreactivity is present in oligodendroglia of various regions of the central nervous system. Glia 3:335–341.

Danbolt NC. 2001. Glutamate uptake. Prog Neurobiol 65:1–105.

Danbolt NC, Storm-Mathisen J. 1986. Na+-dependent "binding" of D-aspartate in brain membranes is largely due to uptake into membrane-bounded saccules. J Neurochem 47:819–824.

Davies LP, Johnston GA. 1976. Uptake and release of D- and L-aspartate by rat brain slices. J Neurochem 26:1007–1014.

De Biase LM, Kang SH, Baxi EG, Fukaya M, Pucak ML, Mishina M, Calabresi PA, Bergles DE. 2011. NMDA receptor signaling in oligodendrocyte progenitors is not required for oligodendrogenesis and myelination. J Neurosci 31: 12650–12662.

Deng W, Wang H, Rosenberg PA, Volpe JJ, Jensen FE. 2004. Role of metabotropic glutamate receptors in oligodendrocyte excitotoxicity and oxidative stress. Proc Natl Acad Sci USA 101:7751–7756.

Deng W, Yue Q, Rosenberg PA, Volpe JJ, Jensen FE. 2006. Oligodendrocyte excitotoxicity determined by local glutamate accumulation and mitochondrial function. J Neurochem 98:213–222.

Dennis J, White MA, Forrest AD, Yuelling LM, Nogaroli L, Afshari FS, Fox MA, Fuss B. 2008. Phosphodiesterase-Ialpha/autotaxin's MORFO domain regulates oligodendroglial process network formation and focal adhesion organization. Mol Cell Neurosci 37:412–424.

DeSilva TM, Kabakov AY, Goldhoff PE, Volpe JJ, Rosenberg PA. 2009. Regulation of glutamate transport in developing rat oligodendrocytes. J Neurosci 29:7898–7908.

Desilva TM, Kinney HC, Borenstein NS, Trachtenberg FL, Irwin N, Volpe JJ, Rosenberg PA. 2007. The glutamate transporter EAAT2 is transiently expressed in developing human cerebral white matter. J Comp Neurol 501: 879–890.

Domercq M, Etxebarria E, Perez-Samartin A, Matute C. 2005. Excitotoxic oligodendrocyte death and axonal damage induced by glutamate transporter inhibition. Glia 52:36–46.

Domercq M, Matute C. 1999. Expression of glutamate transporters in the adult bovine corpus callosum. Brain Res Mol Brain Res 67:296–302.

Domercq M, Sanchez-Gomez MV, Areso P, Matute C. 1999. Expression of glutamate transporters in rat optic nerve oligodendrocytes. Eur J Neurosci 11:2226–2236.

Emery B. 2010. Regulation of oligodendrocyte differentiation and myelination. Science 330:779–782.

Erichsen MN, Huynh TH, Abrahamsen B, Bastlund JF, Bundgaard C, Monrad O, Bekker-Jensen A, Nielsen CW, Frydenvang K, Jensen AA, Bunch L. 2010. Structure-activity relationship study of first selective inhibitor of excitatory amino acid transporter subtype 1: 2-Amino-4-(4-methoxyphenyl)−7-(naphthalen-1-yl)−5-oxo-5,6,7,8-tetrahydro-4H-chrom ene-3-carbonitrile (UCPH-101). J Med Chem 53:7180–7191.

Errico F, Rossi S, Napolitano F, Catuogno V, Topo E, Fisone G, D'Aniello A, Centonze D, Usiello A. 2008. D-aspartate prevents corticostriatal long-term depression and attenuates schizophrenia-like symptoms induced by amphetamine and MK-801. J Neurosci 28:10404–10414.

Etxeberria A, Mangin JM, Aguirre A, Gallo V. 2010. Adult-born SVZ progenitors receive transient synapses during remyelination in corpus callosum. Nat Neurosci 13:287–289.

Fancy SP, Kotter MR, Harrington EP, Huang JK, Zhao C, Rowitch DH, Franklin RJ. 2010. Overcoming remyelination failure in multiple sclerosis and other myelin disorders. Exp Neurol 225:18–23.

Flores-Mendez MA, Martinez-Lozada Z, Monroy HC, Hernandez-Kelly LC, Barrera I, Ortega A. 2013. Glutamate-dependent translational control in cultured Bergmann glia cells: eIF2alpha phosphorylation. Neurochem Res 38:1324–1332.

Fruhbeis C, Frohlich D, Kuo WP, Amphornrat J, Thilemann S, Saab AS, Kirchhoff F, Mobius W, Goebbels S, Nave KA, Schneider A, Simons M, Klugmann M, Trotter J, Krämer-Albers EM. 2013. Neurotransmitter-triggered transfer of exosomes mediates oligodendrocyte-neuron communication. PLoS Biol 11:e1001604.

Grynkiewicz G, Poenie M, Tsien RY. 1985. A new generation of Ca2+ indicators with greatly improved fluorescence properties. J Biol Chem 260:3440–3450.

Guo F, Maeda Y, Ko EM, Delgado M, Horiuchi M, Soulika A, Miers L, Burns T, Itoh T, Shen H, Lee E, Sohn J, Pleasure D. 2012. Disruption of NMDA receptors in oligodendroglial lineage cells does not alter their susceptibility to experimental autoimmune encephalomyelitis or their normal development. J Neurosci 32:639–645.

Hoffman L, Farley MM, Waxham MN. 2013. Calcium-calmodulin-dependent protein kinase II isoforms differentially impact the dynamics and structure of the actin cytoskeleton. Biochemistry 52:1198–1207.

Kanai Y, Hediger MA. 1992. Primary structure and functional characterization of a high-affinity glutamate transporter. Nature 360:467–471.

Kim HJ, DiBernardo AB, Sloane JA, Rasband MN, Solomon D, Kosaras B, Kwak SP, Vartanian TK. 2006. WAVE1 is required for oligodendrocyte morphogenesis and normal CNS myelination. J Neurosci 26:5849–5859.

Kim K, Hayashi M, Narayanan R, Suzuki A, Matsuura K, K. O, Hayashi Y. 2011. CaMKII gates rapid structural plasticity in hippocampal dendirtic spines. Program No 87207/E3 2011. Neuroscience Meeting Planner Washington, DC: Society for Neuroscience, Online.

Kolodziejczyk K, Hamilton NB, Wade A, Karadottir R, Attwell D. 2009. The effect of N-acetyl-aspartyl-glutamate and N-acetyl-aspartate on white matter oligodendrocytes. Brain 132:1496–1508.

Kolodziejczyk K, Saab AS, Nave KA, Attwell D. 2010. Why do oligodendrocyte lineage cells express glutamate receptors? F1000 Biol Rep 2:57.

Kredel S, Oswald F, Nienhaus K, Deuschle K, Rocker C, Wolff M, Heilker R, Nienhaus GU, Wiedenmann J. 2009. mRuby, a bright monomeric red fluorescent protein for labeling of subcellular structures. PLoS One 4:e4391.

Kremer D, Aktas O, Hartung HP, Kury P. 2011. The complex world of oligodendroglial differentiation inhibitors. Ann Neurol 69:602–618.

Kriegler S, Chiu SY. 1993. Calcium signaling of glial cells along mammalian axons. J Neurosci 13:4229–4245.

Kuhlmann T, Miron V, Cuo Q, Wegner C, Antel J, Bruck W. 2008. Differentiation block of oligodendroglial progenitor cells as a cause for remyelination failure in chronic multiple sclerosis. Brain 131:1749–1758.

Kukley M, Capetillo-Zarate E, Dietrich D. 2007. Vesicular glutamate release from axons in white matter. Nat Neurosci 10:311–320.

Kukley M, Nishiyama A, Dietrich D. 2010. The fate of synaptic input to NG2 glial cells: Neurons specifically downregulate transmitter release onto differentiating oligodendroglial cells. J Neurosci 30:8320–8331.

Lafrenaye AD, Fuss B. 2011. Focal adhesion kinase can play unique and opposing roles in regulating the morphology of differentiating oligodendrocytes. J Neurochem 115:269–282.

Lin YC, Redmond L. 2008. CaMKIIbeta binding to stable F-actin in vivo regulates F-actin filament stability. Proc Natl Acad Sci USA 105:15791–15796.

Lin YC, Redmond L. 2009. Neuronal CaMKII acts as a structural kinase. Commun Integr Biol 2:40–41.

Livak KJ, Schmittgen TD. 2001. Analysis of relative gene expression data using real-time quantitative PCR and the 2(-Delta Delta C(T)) method. Methods 25:402–408.

Lopez-Colome AM, Martinez-Lozada Z, Guillem AM, Lopez E, Ortega A. 2012. Glutamate transporter-dependent mTOR phosphorylation in Muller glia cells. ASN Neuro 4:e00095.

Lundgaard I, Luzhynskaya A, Stockley JH, Wang Z, Evans KA, Swire M, Volbracht K, Gautier HO, Franklin RJ, Attwell D, Káradóttir RT. 2013. Neuregulin and BDNF induce a switch to NMDA receptor-dependent myelination by oligodendrocytes. PLoS Biol 11:e1001743.

Luyt K, Varadi A, Durant CF, Molnar E. 2006. Oligodendroglial metabotropic glutamate receptors are developmentally regulated and involved in the prevention of apoptosis. J Neurochem 99:641–656.

Manders EMM, Verbeek FJ, Aten JA. 1993. Measurement of co-localization of objects in dualcolor confocal images. J Microsc 169:375–382.

Martinez-Lozada Z, Guillem AM, Flores-Mendez M, Hernandez-Kelly LC, Vela C, Meza E, Zepeda RC, Caba M, Rodriguez A, Ortega A. 2013. GLAST/EAAT1-induced glutamine release via SNAT3 in Bergmann glial cells: Evidence of a functional and physical coupling. J Neurochem 125:545–554.

Martinez-Lozada Z, Hernandez-Kelly LC, Aguilera J, Lopez-Bayghen E, Ortega A. 2011. Signaling through EAAT-1/GLAST in cultured Bergmann glia cells. Neurochem Int 59:871–879.

Matsugami TR, Tanemura K, Mieda M, Nakatomi R, Yamada K, Kondo T, Ogawa M, Obata K, Watanabe M, Hashikawa T, Tanaka K. 2006. From the cover: Indispensability of the glutamate transporters GLAST and GLT1 to brain development. Proc Natl Acad Sci USA 103:12161–12166.

Matute C. 2011. Glutamate and ATP signalling in white matter pathology. J Anat 219:53–64.

Niwa H, Yamamura K, Miyazaki J. 1991. Efficient selection for high-expression transfectants with a novel eukaryotic vector. Gene 108:193–199.

Okamoto K, Bosch M, Hayashi Y. 2009. The roles of CaMKII and F-actin in the structural plasticity of dendritic spines: A potential molecular identity of a synaptic tag? Physiology 24:357–366.

Okamoto K, Nagai T, Miyawaki A, Hayashi Y. 2004. Rapid and persistent modulation of actin dynamics regulates postsynaptic reorganization underlying bidirectional plasticity. Nat Neurosci 7:1104–1112.

Okamoto K, Narayanan R, Lee SH, Murata K, Hayashi Y. 2007. The role of CaMKII as an F-actin-bundling protein crucial for maintenance of dendritic spine structure. Proc Natl Acad Sci USA 104:6418–6423.

O'Leary H, Lasda E, Bayer KU. 2006. CaMKIIbeta association with the actin cytoskeleton is regulated by alternative splicing. Mol Biol Cell 17:4656–4665.

Osterhout DJ, Wolven A, Wolf RM, Resh MD, Chao MV. 1999. Morphological differentiation of oligodendrocytes requires activation of Fyn tyrosine kinase. J Cell Biol 145:1209–1218.

Palacin M, Estevez R, Bertran J, Zorzano A. 1998. Molecular biology of mammalian plasma membrane amino acid transporters. Physiol Rev 78:969–1054.

Peghini P, Janzen J, Stoffel W. 1997. Glutamate transporter EAAC-1-deficient mice develop dicarboxylic aminoaciduria and behavioral abnormalities but no neurodegeneration. EMBO J 16:3822–3832.

Peirson SN, Butler JN, Foster RG. 2003. Experimental validation of novel and conventional approaches to quantitative real-time PCR data analysis. Nucleic Acids Res 31:e73.

Pfeiffer SE, Warrington AE, Bansal R. 1993. The oligodendrocyte and its many cellular processes. Trends Cell Biol 3:191–197.

Pines G, Danbolt NC, Bjoras M, Zhang Y, Bendahan A, Eide L, Koepsell H, Storm-Mathisen J, Seeberg E, Kanner BI. 1992. Cloning and expression of a rat brain L-glutamate transporter. Nature 360:464–467.

Pitt D, Nagelmeier IE, Wilson HC, Raine CS. 2003. Glutamate uptake by oligodendrocytes: Implications for excitotoxicity in multiple sclerosis. Neurology 61:1113–1120.

Regan MR, Huang YH, Kim YS, Dykes-Hoberg MI, Jin L, Watkins AM, Bergles DE, Rothstein JD. 2007. Variations in promoter activity reveal a differential expression and physiology of glutamate transporters by glia in the developing and mature CNS. J Neurosci 27:6607–6619.

Riedl J, Crevenna AH, Kessenbrock K, Yu JH, Neukirchen D, Bista M, Bradke F, Jenne D, Holak TA, Werb Z, Sixt M, Wedlich-Soldner R. 2008. Lifeact: A versatile marker to visualize F-actin. Nat Methods 5:605–607.

Rodriguez A, Ortega A. 2012. The glia connection of the glutamate/glutamine shuttle. Am J Neurosci 3:32–38.

Rojas H, Colina C, Ramos M, Benaim G, Jaffe EH, Caputo C, DiPolo R. 2007. Na+ entry via glutamate transporter activates the reverse Na+/Ca2+ exchange and triggers Ca(i)2+-induced Ca2+ release in rat cerebellar Type-1 astrocytes. J Neurochem 100:1188–1202.

Rosenberg PA, Dai W, Gan XD, Ali S, Fu J, Back SA, Sanchez RM, Segal MM, Follett PL, Jensen FE, Volpe JJ. 2003. Mature myelin basic protein-expressing oligodendrocytes are insensitive to kainate toxicity. J Neurosci Res 71:237–245.

Sanabria H, Swulius MT, Kolodziej SJ, Liu J, Waxham MN. 2009. {beta}CaMKII regulates actin assembly and structure. J Biol Chem 284:9770–9780.

Shigeri Y, Shimamoto K, Yasuda-Kamatani Y, Seal RP, Yumoto N, Nakajima T, Amara SG. 2001. Effects of threo-beta-hydroxyaspartate derivatives on excitatory amino acid transporters (EAAT4 and EAAT5). J Neurochem 79:297–302.

Shimamoto K, Lebrun B, Yasuda-Kamatani Y, Sakaitani M, Shigeri Y, Yumoto N, Nakajima T. 1998. DL-threo-beta-benzyloxyaspartate, a potent blocker of excitatory amino acid transporters. Mol Pharmacol 53:195–201.

Simpson PB, Holtzclaw LA, Langley DB, Russell JT. 1998. Characterization of ryanodine receptors in oligodendrocytes, type 2 astrocytes, and O-2A progenitors. J Neurosci Res 52:468–482.

Skokal RR, Rohlf FJ. 1995. Biometry: The principle and practice in biological research. New York: W. H. Freeman and Company.

Sommer I, Schachner M. 1982. Cell that are O4 antigen-positive and O1 antigen-negative differentiate into O1 antigen-positive oligodendrocytes. Neurosci Lett 29:183–188.

Sparrow N, Manetti ME, Bott M, Fabianac T, Petrilli A, Bates ML, Bunge MB, Lambert S, Fernandez-Valle C. 2012. The actin-severing protein cofilin is downstream of neuregulin signaling and is essential for Schwann cell myelination. J Neurosci 32:5284–5297.

Srinivasan R, Sailasuta N, Hurd R, Nelson S, Pelletier D. 2005. Evidence of elevated glutamate in multiple sclerosis using magnetic resonance spectroscopy at 3 T. Brain 128:1016–1025.

Sugiyama H, Ito I, Watanabe M. 1989. Glutamate receptor subtypes may be classified into two major categories: A study on Xenopus oocytes injected with rat brain mRNA. Neuron 3:129–132.

Sumi M, Kiuchi K, Ishikawa T, Ishii A, Hagiwara M, Nagatsu T, Hidaka H. 1991. The newly synthesized selective Ca2+/calmodulin dependent protein

kinase II inhibitor KN-93 reduces dopamine contents in PC12h cells. Biochem Biophys Res Commun 181:968–975.

Tanaka K, Watase K, Manabe T, Yamada K, Watanabe M, Takahashi K, Iwama H, Nishikawa T, Ichihara N, Kikuchi T, Okuyama S, Kawashima N, Hori S, Takimoto M, Wada K. 1997. Epilepsy and exacerbation of brain injury in mice lacking the glutamate transporter GLT-1. Science 276:1699–1702.

Tansey FA, Farooq M, Cammer W. 1991. Glutamine synthetase in oligodendrocytes and astrocytes: New biochemical and immunocytochemical evidence. J Neurochem 56:266–272.

Trapp BD, Stys PK. 2009. Virtual hypoxia and chronic necrosis of demyelinated axons in multiple sclerosis. Lancet Neurol 8:280–291.

Uwechue NM, Marx MC, Chevy Q, Billups B. 2012. Activation of glutamate transport evokes rapid glutamine release from perisynaptic astrocytes. J Physiol 590:2317–2331.

Vallejo-Illarramendi A, Domercq M, Perez-Cerda F, Ravid R, Matute C. 2006. Increased expression and function of glutamate transporters in multiple sclerosis. Neurobiol Dis 21:154–164.

van Woerden GM, Hoebeek FE, Gao Z, Nagaraja RY, Hoogenraad CC, Kushner SA, Hansel C, De Zeeuw CI, Elgersma Y. 2009. BetaCaMKII controls the direction of plasticity at parallel fiber-Purkinje cell synapses. Nat Neurosci 12:823–825.

Waggener CT, Dupree JL, Elgersma Y, Fuss B. 2013. CaMKIIbeta regulates oligodendrocyte maturation and CNS myelination. J Neurosci 33:10453–10458.

Warringa RA, van Berlo MF, Klein W, Lopes-Cardozo M. 1988. Cellular location of glutamine synthetase and lactate dehydrogenase in oligodendrocyte-enriched cultures from rat brain. J Neurochem 50:1461–1468.

Warrington AE, Barbarese E, Pfeiffer SE. 1993. Differential myelinogenic capacity of specific developmental stages of the oligodendrocyte lineage upon transplantation into hypomyelinating hosts. J Neurosci Res 34:1–13.

Watase K, Hashimoto K, Kano M, Yamada K, Watanabe M, Inoue Y, Okuyama S, Sakagawa T, Ogawa S, Kawashima N, Hori S, Takimoto M, Wada K, Tanaka K. 1998. Motor discoordination and increased susceptibility to cerebellar injury in GLAST mutant mice. Eur J Neurosci 10:976–988.

Werner P, Pitt D, Raine CS. 2001. Multiple sclerosis: Altered glutamate homeostasis in lesions correlates with oligodendrocyte and axonal damage. Ann Neurol 50:169–180.

Wosik K, Ruffini F, Almazan G, Olivier A, Nalbantoglu J, Antel JP. 2004. Resistance of human adult oligodendrocytes to AMPA/kainate receptor-mediated glutamate injury. Brain 127:2636–2648.

Yoo AS, Krieger C, Kim SU. 1999. Process extension and intracellular Ca2+ in cultured murine oligodendrocytes. Brain Res 827:19–27.

Ziskin JL, Nishiyama A, Rubio M, Fukaya M, Bergles DE. 2007. Vesicular release of glutamate from unmyelinated axons in white matter. Nat Neurosci 10:321–330.

Neurochemical Research

Glutamate-dependent translational control through ribosomal protein S6 phosphorylation in cultured Bergmann glial cells

--Manuscript Draft--

Manuscript Number:	NERE-D-14-00555R1
Full Title:	Glutamate-dependent translational control through ribosomal protein S6 phosphorylation in cultured Bergmann glial cells
Article Type:	Original
Keywords:	ribosomal protein S6., glutamate receptors., translational control., Bergmann glia
Corresponding Author:	Arturo Ortega, PhD Cinvestav-IPN Mexico City, DF MEXICO
Corresponding Author Secondary Information:	
Corresponding Author's Institution:	Cinvestav-IPN
Corresponding Author's Secondary Institution:	
First Author:	Marco Flores-Mendez, PhD
First Author Secondary Information:	
Order of Authors:	Marco Flores-Mendez, PhD
	Miguel Escalante-Lopez, MSc
	Zila Martinez-Lozada, PhD
	Luisa C Hernandez-Kelly, MSc
	Mustapha Najimi, PhD
	Ettiene Sokal, MD, PhD
	Arturo Ortega, PhD
Order of Authors Secondary Information:	

CENTRO DE INVESTIGACION Y DE ESTUDIOS AVANZADOS DEL I.P.N.

Dr.Arturo Ortega Soto
Investigador Titular
Depto.Toxicología

Febraury 10, 2015

Prof. Jan Albrecht
Associate Editor
Neurochemical Research

Dear Professor Albrecht,

Please find enclosed the revised version of the manuscript entitled: "**Glutamate-dependent translational control through ribosomal protein S6 phosphorylation in cultured Bergmann glial cells**".

A detailed account of our answers to the various points raised by the reviewers follows:

Reviewer # 1

The referee raises the pertinent question of a plausible involvement of NMDA receptores in Glutamate-dependent rpS6 phosphorylation , and suggest us to perform experiments treating the cells in a media without Mg^{2+} and/or the presence of a Ca^{2+} quelator. We totally agree and in the revised version, we show the results of such a protocol (Panel C, Figure 3). In a Mg^{2+}-devoid solution, 500 μM NMDA+ 10 μM glycine does not increase rpS6 phosphorylation. As expected, pre-exposures of the cultured cells to BAPTA results in an even smaller degree of rpS6 phosphorylation. These results make us confident that the Bergmann glia NMDA receptors are not involved in the Glutamate-detected response, making unnecessary to pretreat the cells with MK801 as suggested.

Reviewer # 2

1. The referee raises the point of the levels of phosphorylated rpS6 in nucleus and citoplasm and suggest us to better explain these results. In fact, a 15 min of Glu exposure results in an increase in phosphorylated rpS6 protein in both compartments. It is tempting to assume that once phosphorylated rpS6 is targeted, at least in part, to the nuclei compartment, maily since MEK and mTOR blockage reduces completely the levels of rpS6 phosphorylation. A detailed description of this phenomena is underway in our lab and it is beyond the scope of this communication. Nervertheless, we have modified both the results and the discussion to make this point clear (page 11). (As suggested by the reviewer we have corrected the text in results section, it is now mentioned that the ratio between nuclear/cytoplasmic levels is mantained in the non-phosphorylated/phosphorylated forms of rpS6, suggesting an increase in total rpS6 levels

unpon Glu exposure).

2. The reviewer asks us to discuss the relevance of Glu-induced rpS6 phosphorylation in the context of protein synthesis and the identity of some of the proteins that are translated in response to Glu in Bergmann glia. Preliminary data from our lab has begun to emerge, Glu treatment increases the amount of polysomal mRNA quantity. We speculate that among the proteins actively translated upon Glu are components of the Glu/glutamine shuttle. We are working in this direction and we mention these preliminary evidences in the discussion (page 11, 2nd paragraph)Flores-Mendez.

3. The referee prompt us to extend the description of the signaling pathway in the context of our previous findings, we agree and have modified the discussion in the revised version. In the same context, the reviewer suggest that the rather high Glu concentrations capable to elict the rpS6 response are quite high, in this context, Glu concentrations upon high frequency Glu stimulation have been calculated to be in the range of the effective concentrations of this study. In fact Glu transporters profusely expressed in glial membranes surrounding glutamatergic synapses have K_M in the micromolar range (Ruiz and Ortega, *NeuroReport* 6:2041., Danbolt, *Prog*. *Neurobiol*. **65:** 1).

4. The referee ask us about the involvement of metabotropic Glu receptors in rpS6 phosphorylation. In this context, we have previosly shown that cultured Bergmann glia express metabotropic glutamate receptors of the group I (mGluR1 and mGluR5) (López *et al*., *Mol*. *Brain Res* **58:** 40. DHPG (3,5-dihydroxyphenylglycine), is a potent agonist of these receptors and as shown in panel A of Figure 3, no significant increase in rpS6 phosphorylation was detected upon exposure to DHPG.

We very much hope that you find our answers adequate and that now our manuscript is ready for publication in *Neurochemical Research*.

Sincerely,

Arturo Ortega, Ph.D.
Depto. Toxicología
Cinvestav-IPN
Apartado Postal 14-740
México D.F. 07000
MEXICO
Tel.: (525) 747-3800
Email: arortega@cinvestav.mx

Reviewer # 1

The referee raises the pertinent question of a plausible involvement of NMDA receptores in Glutamate-dependent rpS6 phosphorylation , and suggest us to perform experiments treating the cells in a media without Mg^{2+} and/or the presence of a Ca^{2+} quelator. We totally agree and in the revised version, we show the results of such a protocol (Panel C, Figure 3). In a Mg^{2+}-devoid solution, 500 μM NMDA+ 10 μM glycine does not increase rpS6 phosphorylation. As expected, pre-exposures of the cultured cells to BAPTA results in an even smaller degree of rpS6 phosphorylation. These results make us confident that the Bergmann glia NMDA receptors are not involved in the Glutamate-detected response, making unnecessary to pretreat the cells with MK801 as suggested.

Reviewer # 2

1. The referee raises the point of the levels of phosphorylated rpS6 in nucleus and citoplasm and suggest us to better explain these results. In fact, a 15 min of Glu exposure results in an increase in phosphorylated rpS6 protein in both compartments. It is tempting to assume that once phosphorylated rpS6 is targeted, at least in part, to the nuclei compartment, maily since MEK and mTOR blockage reduces completely the levels of rpS6 phosphorylation. A detailed description of this phenomena is underway in our lab and it is beyond the scope of this communication. Nervertheless, we have modified both the results and the discussion to make this point clear (page 11). (As suggested by the reviewer we have corrected the text in results section, it is now mentioned that the ratio between nuclear/cytoplasmic levels is mantained in the non-phosphorylated/phosphorylated forms of rpS6, suggesting an increase in total rpS6 levels unpon Glu exposure).

2. The reviewer asks us to discuss the relevance of Glu-induced rpS6 phosphorylation in the context of protein synthesis and the identity of some of the proteins that are translated in response to Glu in Bergmann glia. Preliminary data from our lab has begun to emerge, Glu treatment increases the amount of polysomal mRNA quantity. We speculate that among the proteins actively translated upon Glu are components of the Glu/glutamine shuttle. We are working in this direction and we mention these preliminary evidences in the discussion (page 11, 2nd paragraph)Flores-Mendez.

3. The referee prompt us to extend the description of the signaling pathway in the context of our previous findings, we agree and have modified the discussion in the revised version. In the same context, the reviewer suggest that the rather high Glu concentrations capable to elict the rpS6 response are quite high, in this context, Glu concentrations upon high frequency Glu stimulation have been calculated to be in the range of the effective concentrations of this study. In fact Glu transporters profusely expressed in glial membranes surrounding glutamatergic synapses have K_M in the micromolar range (Ruiz and Ortega, *NeuroReport* 6:2041., Danbolt, *Prog. Neurobiol.* **65:** 1).

4. The referee ask us about the involvement of metabotropic Glu receptors in rpS6 phosphorylation. In this context, we have previosly shown that cultured Bergmann glia express metabotropic glutamate receptors of the group I (mGluR1 and mGluR5) (López *et al*., *Mol. Brain Res* **58:** 40. DHPG (3,5-dihydroxyphenylglycine), is a potent

agonist of these receptors and as shown in panel A of Figure 3, no significant increase in rpS6 phosphorylation was detected upon exposure to DHPG.

Glutamate-dependent translational control through ribosomal protein S6 phosphorylation in cultured Bergmann glial cells

Marco Flores-Méndez[1], Miguel Escalante-López[1], Zila Martínez-Lozada[1], Luisa C. Hernández-Kelly[1], Mustapha Najimi[2], Ettiene Sokal [2] and Arturo Ortega[1]

[1]Laboratorio de Neurotoxicología, Departamento de Toxicología, Centro de Investigación y de Estudios Avanzados del Instituto Politécnico Nacional, Apartado Postal 14-740, México D.F. 07300, México, and [2]Laboratory of Pediatric Hepatology and Cell Therapy, Institut de Recherche Expérimentale et Clinique , Cliniques Universitaires St. Luc, Université Catholique de Louvain, Brussels 1200, Belgium.

Correspondence

Arturo Ortega, PhD
Departamento de Toxicología
Cinvestav-IPN
Apartado Postal 14-740
México DF 07300
México
Tel. 52 55 5747 5410
Email. arortega@cinvestav.mx

Abstract

Glutamate (Glu) the main excitatory neurotransmitter of the Central Nervous System regulates gene expression at different levels through the activation of specific membrane receptors and transporters expressed in neurons and glia cells. A membrane to nucleus signaling cascade triggered by this neurotransmitter has been described in cultured cerebellar Bergmann glia cells isolated from chick embryos. Furthermore, it has also been described that Glu receptors activation is linked to a modulation of [^{35}S]-methionine incorporation into newly synthesized polypeptides. In order to gain insight into the signal transduction cascades that participate in this effect, in the present study we characterized the phosphorylation of a critical component of the translational machinery, namely the ribosomal protein S6.

The phosphorylation sites in rpS6 have been mapped to five clustered residues, Ser235, Ser236, Ser240, Ser244 and Ser247. Nevertheless, Ser236 phosphorylation is the primary phosphorylation site. The kinases responsible of this modification are p70^{S6K} and p90^{RSK}. rpS6 phosphorylation increases the affinity of 40s subunit for mRNAs and thus facilitates translational initiation. Glutamate exposure of cultured cerebellar Bergmann glia cells results in a time-and dose-dependent increase in rpS6 phosphorylation. This effect is mainly observed at cytoplasm, and involves the phosphoinositol-3 kinase (PI3-K)/ protein kinase B (PKB) pathway. Our results favor the notion of a continuous neuronal signaling to glia cells that regulates the proteome of these cells not only at the transcriptional levels but also at the level of protein synthesis.

Key words: ribosomal protein S6, glutamate receptors, translational control, Bergmann glia

1. Introduction

Excitatory neurotransmission in the vertebrate Central Nervous System (CNS) is mediated largely by glutamate (Glu). The signaling transactions activated by this amino acid are mediated by specific membrane receptors that have been commonly divided into two groups according their signaling properties. Ionotropic Glu receptors (iGluRs) are ligand-gated ion channels that have been classified as N-methyl-D-aspartate (NMDA), □-amino-3-hydroxy-5-methyl-4-isoaxazolepropionate (AMPA) and kainate [1] receptors [2]. In contrast, metabotropic receptors (mGluRs) are G-protein coupled receptors that are described in terms of sequence similarity, signal transduction mechanisms and pharmacology. Group I receptors are coupled to the stimulation of phospholipase C with the consequent release of intracellular Ca^{2+}, while Groups II and III are coupled to the inhibition of adenylate cyclase. These three groups are activated preferentially by (RS)-3,5-dihydroxyphenylglycine (DHPG) for Group I, (S)-4-Carboxy-3-hydroxyphenylglycine (S)-4C3HPG activates Group II while L-(+)-2-amino-4-phosphonobutyric acid (L- AP4) acts upon Group III [3].

Bergmann glia cells (BGC), the most abundant non-neuronal population of the cerebellum, span the molecular layer covering completely excitatory and inhibitory synapses [4]. This characteristic localization is related their involvement in neurotransmitter uptake and turnover, K^+ homeostasis, lactate supply and pH regulation [5]. In terms of glutamatergic transmission, BGC are in a very short proximity to the parallel fiber-Purkinje cell synapses, and participate in the Glu/glutamine shuttle that assures the proper neurotransmitter supply to presynaptic terminals. In this sense, BGC respond to glutamatergic stimulation, as we have been able to characterize over the years [6].

It has long been established that transcription and translation are essential for long-term memory [7]. Activity-dependent gene expression regulation stabilizes the synaptic changes that underlie the late phase of long-term potentiation [1]. In this regard, it should be noted that most studies focused in gene expression regulation are devoted to the study of this process at the transcriptional level. Nevertheless, the rate of protein synthesis has a crucial role in synaptic plasticity [8]. Translational control offers the possibility of a rapid response to external stimulus without mRNA synthesis and transport. Therefore, immediacy is the most conspicuous advantage of translational over transcriptional control.

Eukaryotic ribosomes are composed of two subunits that are designed as 40S (small) and 60S (large). The 40S subunit is composed of a single RNA molecule, 18S ribosomal (r) RNA and 33 proteins; whereas the 60S

subunit has three RNA molecules, 5S, 5.8S and 28S rRNAs and also 46 proteins. Of all the ribosomal proteins, the ribosomal protein S6 (rpS6) has attracted much attention, since it is the first ribosomal protein shown to undergo an inducible phosphorylation [9]. This protein is involved in 40S ribosomal subunit biogenesis, it enters the nucleus (nucleolus) where it is assembled with other proteins and rRNA into a pre-40S subunit. Thereafter, small rpS6-containing ribosomal subunits are exported to cytosol where they fuse to form mature ribosomes [10]. Several reports have demonstrated that rpS6 is phosphorylated in response a numerous physiological, pathological and pharmacological stimuli. It should be noted that rpS6 takes part in mRNA binding and therefore, its phosphorylation might have an important regulatory role in translation initiation [11]. The phosphorylation sites in rpS6 have been mapped to S235, S236, S240 and S244 and a role for the mammalian target of rapamycin (mTOR) and the mitogen-activated protein kinase (MAPK) signaling pathways has been described [12]. For example, a well-established mTOR substrate is in fact, S6 kinase (S6K), which phosphorylates rpS6 at S235/236 and 240/244 [13]. Alternatively, p42/p44 MAPK activation phosphorylates and thus activates of RSK (ribosomal S6 kinase) that phosphorylates rpS6 exclusively at S235/236 [14].

In the present study, we analyzed rpS6 phosphorylation at Ser235/236 after glutamate treatment in Bergmann glia cells. Our results demonstrate that both S6K and RSK are capable to phosphorylate rpS6, although it is clear that S6K is the major kinase involved in glutamate-dependent phosphorylation. Also, we demonstrate here that phosphorylated rpS6 is mostly present at cytoplasm and a kinetic analysis shows that the time in which the maximal phosphorylation takes place, a correlation with an increase in the polysomal fraction is present, suggesting that rpS6 could play a major role in glutamate-dependent translational control in Bergmann glia.

2. Materials and Methods

2.1 Materials

Tissue culture reagents were obtained from GE Healthcare (Carlsbad, CA, USA). DL-TBOA (DL-threo-b-Benzyloxyaspartic acid), THA (threo-□hydroxyaspartate), CNQX (6,7-Dinitroquinoxaline-2,3-dione), LAP5 (L-(+)-2-Amino-5-phosphonopentanoic acid); D-aspartate (Asp), W7 (*N*-(6-Aminohexyl)-5-chloro-1-naphtha lene sulfonamide hydrochloride and Glu were all obtained from Tocris-Cookson (St. Louis, MO USA). Polyclonal anti phospho-rpS6 (Ser 235/236) and anti rpS6 were purchased from Cell Signaling Technology (Denvers, MA). Monoclonal anti-actin antibody was kindly donated by Prof. Manuel Hernández (Cinvestav-IPN). Horseradish peroxidase-linked anti-rabbit antibodies, and the enhanced chemiluminescence reagent (ECL), were obtained from Amersham Biosciences (Buckinghamshire, UK). All other chemicals were purchased from Sigma (St. Louis, MO, USA).

Cell culture and stimulation protocol

Primary cultures of cerebellar BGC were prepared from 14-day-old chick embryos as previously described [15]. Cells were plated in 6-well plastic culture dishes in DMEM containing 10% fetal bovine serum, 2 mM glutamine, and gentamicin (50 μg/ml) and used on the 4^{th} to 7^{th} day after culture. Before any treatment, confluent monolayers were switched to non-serum DMEM media containing 0.5% bovine serum albumin (BSA) for 2 h and then treated as indicated. Inhibitors were added 30 min before agonists. The cells were treated with Glu analogues added to culture medium for the indicated time periods.

SDS-PAGE and Western blots

Cells from confluent monolayers were harvested with phosphate-buffer saline (PBS) (10 mM K_2HPO_4/KH_2PO_4, 150 mM NaCl, pH 7.4) containing phosphatase inhibitors (10 mM NaF, 1 mM Na_2MoO_4 and 1 mM Na_3VO_4). The cells were lysed with RIPA buffer (50 mM Tris-HCl, 1 mM EDTA, 150 mM NaCl, 1mM phenylmethylsufonyl fluoride, 1mg/ml aprotinin, 1mg/ml leupeptin, 1% NP-40, 0.25% sodium deoxycholate, 10 mM NaF, 1 mM Na_2MoO_4 and 1 mM Na_3VO_4 pH 7.4). Cell lysates were denaturized in Laemmli's sample buffer, and equal amount of proteins (50 □g as determined by the Bradford method) were resolved through a 15% SDS-PAGE and then electroblotted to nitrocellulose membranes. Blots were stained

with Ponceau S stain to confirm that protein content was equal in all lanes. Membranes were soaked in PBS to remove the Ponceau S and incubated in TBS containing 3% dried skimmed milk and 0.1% Tween 20 for 30 min to block the excess of non-specific protein binding sites. Membranes were then incubated overnight at 4˚C with the particular primary antibodies indicated in each Figure, followed by secondary antibodies. Immunoreactive polypeptides were detected by chemiluminescence and exposed to X-ray films. Densitometry analyses were performed and data analyzed with Prism, GraphPad Software (San Diego, CA, USA).

Staining Procedures

BGC primary cultures were grown on poly-L-lysine-treated (0.01 mg/ml) glass coverslips following the procedure described above. Cells were fixed by exposure for 10 min to methanol at -20º C and washed twice with PBS containing 0.5% Triton X-100 (washing solution). Non-specific binding was prevented by incubation with 1% BSA in PBS (blocking solution) for 1 h. Cells were exposed to a 1:50 dilution of the primary antibodies anti-rpS6 and anti-phospho-rpS6 in blocking solution overnight at 4°C. Then, cells were washed three times with washing solution and incubated with a 1:200 dilution of the fluorescent-labeled secondary antibodies dissolved in blocking solution. After washing out secondary antibodies, cell preparations were mounted with Vectashield (Vector Laboratories, Burlingame, CA, USA) and examined with an inverted fluorescence microscope (Zeiss Axioscope 40).

Subcellular fractionation

To isolate cytosolic and nuclear protein extracts, cells were pelleted and resuspended in 500 µL of TM buffer (10 mM Tris-HCl, pH 7.4, 2 mM $MgCl_2$, 0.5 mM phenylmethylsufonyl fluoride, 1 mg/mL aprotinin, 1 mg/mL leupeptin, 10 mM NaF, 1 mM Na_2MoO_4 and 1 mM Na_3VO_4) and incubated for 10 min on ice; 500 µL of 1%(v/v) Triton X-100 was then added and the homogenate incubated on ice for 10 min. Cellular membrane debris was removed by 30 strokes in a Dounce homogenizer. Nuclei were separated from cytosol by centrifugation at 5000 rpm for 15 min at 4 ◦C. The supernatant was saved as the cytosolic fraction and the pellet resuspended in 100 µL of sucrose buffer I [0.32 M sucrose, 10 mM Tris-HCl, pH 8.0, 3 mM $CaCl_2$, 2 mM $Mg(CH_3COO)_2$, 0.1 mM EDTA, 1 mM DTT, 0.5 mM PMSF and 0.5% NP-40] and 100 µL of sucrose buffer II [2 M sucrose, 10 mM Tris-HCl, pH 8.0, 5 mM $Mg(CH_3COO)_2$, 0.1mM EDTA, 1 mM DTT and 0.5

mM phenylmethylsufonyl fluoride]. The nuclei suspension was transferred into a new tube with 200 μL of sucrose buffer II; after nuclei suspension, 800 □L of sucrose buffer I was added and then centrifuged at 16000 rpm for 60 min at 4 ◦C. The nuclear pellet was suspended in lysis buffer (50 mM Tris-HCl, pH 8.0, 150 mM NaCl, 1%Triton X-100, 1 mM phenylmethylsufonyl fluoride, 1 mg/mL aprotinin, 1 mg/mL leupeptin, 10 mM NaF, 1 mM Na_2MoO_4 and 1 mM Na_3VO_4), sonicated and centrifuged at 13000 rpm for 2 min at 4 ◦C, with supernatant retained as nuclear protein fraction.

Statistical analysis

Data are expressed as the mean values (average) +/- the standard error (S.E.). A nonparametric one-way ANOVA (Kruskal–Wallis test) was performed to determine significant differences between conditions. When these analyses indicated significance (at the 0.05 level), a Dunn's post hoc test was used to determine which conditions were significantly different from each other with Prism, GraphPad Software (San Diego, CA, USA).

Results

Glu induces rpS6 phosphorylation in Bergmann glial cells

In previous reports, we observed that Glu treatment decreases [^{35}S]-methionine incorporation in BGC [16]. Such treatment leads eEF2 Thr56 phosphorylation thus preventing its binding to the ribosomes [17]. This treatment also induced eIF2α phosphorylation on Ser51 blocking as well the initiation phase of protein synthesis [18]. After all of these events, a recovery of [^{35}S]-methionine incorporation and a decrease in both eEF2 and eIF2α phosphorylation takes place. In this context, resumption of protein synthesis is favored, therefore we decided to explore if Glu treatment could be linked to the Ser235/236 rpS6 phosphorylation. As a first approach, we exposed confluent BGC monolayers to a fixed 1 mM Glu concentration for 15 min and as depicted in panel A of Figure 1, a clear increase in Ser235/236 rpS6 phosphorylation was found, with no apparent change in rpS6 levels. Immunocytochemical evidence of Glu-dependent phosphorylation is shown in panels B and C.

As expected, Glu dependent-rpS6 phosphorylation is time-dependent (Fig. 2A). All subsequent experiments were done after 15 min of glutamatergic stimulation. In order to support a physiological relevance of this phosphorylation, we treated BGC cultures with increasing Glu concentrations (Fig. 2B) and a clear dose-dependency could be established with an EC_{50} of 502.4 μM (Fig. 2C), suggesting a receptor-mediated effect.

Signaling of the Glu-mediated rpS6 phosphorylation

Through the use of pharmacological tools, the profile of the Glu response was determined. BGC were exposed to different glutamatergic agonists. As shown in Fig 3A, only the agonist AMPA augments rpS6phosphorylation. As expected, pre-treatment with AMPA receptors antagonist 6-cyano-7-nitroquinoxaline-2,3-dione (CNQX) prevents any further Glu-stimulatory effect (Fig. 3B). Moreover NMDA do not have an effect in rpS6 phosphorylation even in a media without Mg+, neither BAPTA-AM an intracellular Ca2+ chelator (Fig. 3C), ruling out the participation of NMDA receptors.

It has been well established that AMPA receptors activation in BGC is linked to the MAPK and PI3K/mTOR signaling pathways resulting $p90^{RSK}$ and $p70^{S6K}$ activation [19,20,16,21,22] leading to Ser235/236 rpS6 phosphorylation. In order to delineate the signaling events triggered by Glu that results in rpS6

phosphorylation, we decided to use a MAPK inhibitor (PD98059) and an mTOR inhibitor (rapamycin). Although both of these blockers reduces rpS6 phosphorylation, apparently $p70^{S6K}$ plays a major role in this event (Fig. 3D).

Phosphorylated rpS6 is localized mainly to the cytoplasm

rpS6 participates in ribosome biogenesis, therefore it has a nuclear and a cytoplasmic localization [23]. To shed some light into a plausible role of phosphorylation in rpS6 subcellular distribution, we decided to perform subcellular fractionation of control and treated cells. The results are shown in Fig 4A, rpS6 is present in the nucleus as well as in the cytoplasm. Within the nucleus a small fraction of rpS6 is phosphorylated, under control conditions and exposure to Glu results in an increase in rpS6 phosphorylation in both subcellular domains.

Discussion

Protein synthesis is one of the most energy-demanding cellular processes. It consumes almost 5% of the human caloric intake. Therefore, translational control is a sophisticated phenomenon that requires extensive biochemical machinery that could ensure rapid regulation of the protein repertoire that does not involve nuclear pathways nor mRNA synthesis and transport. In this scenario, the dynamic phosphorylation status of translation factors becomes a key feature of translational control [24].

The input of glia cells to brain physiology has only begun to be recognized and the concept of tripartite synapases is nowadays common [25]. Nevertheless, most of the work is centered in establishing how astrocytes sense neuronal activity and through the release of gliotransmitters and/or biological active molecules modulate synaptic transmission [26]. Less abundant is the knowledge of the molecular mechanisms triggered by neurotransmitters in glial cells shaping their function to provide a favored biochemical environment to ensure a continuous and even enhanced synaptic transmission. Two examples of this coupling are the Glu/glutamine and the astrocyte-neuronal lactate shuttles. The former provides proper neurotransmitter (Glu) supply [27] and the latter ensures the required energy to sustain neurotransmission [28]. Interestingly these two biochemical shuttles are triggered by the removal of the neurotransmitter from the synaptic cleft through glial excitatory amino acid transporters (GLAST/EAAT1 and GLT-1/EAAT2).

Despite of these facts, glial cells harbor Glu receptors that also are activated as a result of neuronal Glu release [29]. It has long been demonstrated that glial Glu receptors are linked to transcriptional gene expression regulation [30], although a systematic study of the identity and function of the Glu-regulated genes is lacking. Concerning BGC, a transcriptional profile of these cells at two developmental stages has been published [31].

While most studies have focused into the molecular mechanisms of gene expression regulation at the transcriptional level, covalent modifications of preexisting proteins and regulation of protein synthesis is fundamental in our understanding of gene expression regulation. Previous studies in our lab have been able to demonstrate a Glu-dependent translational control in BGC, with a biphasic effect in overall protein synthesis after Glu treatment [16]. We have also reported a physical interaction between PI3-K and the ionotropic Glu receptors of BGC, resulting in the activation of PKB/GS3K-β signaling pathway [21] with the subsequent

phosphorylation of the mechanistic (former mammalian) target of rapamycin mTOR [20] and the phosphorylation/dephosphorylation of some eukaryotic translational factors [18] and other components of the translational machinery under glutamatergic exposure.

rpS6 is phosphorylated on evolutionarily conserved serine residues by $p70^{S6K}$ and $p90^{RSK}$. The former represents a direct effector of the TORC1 while the other involves a distinct pathway of rpS6 phosphorylation that is mediated by MAPK [32]. It has been proved that MAPK, PI3-K, and mTOR pathways converge at the level of rpS6 phosphorylation to control metabolic signaling in CD8 T Cells [33].

In order to gain insight into this problem, the results presented in this communication represent an effort to continue the characterization of the Glu-dependent translational control in a cell preparation that represents glia cells that are in intimate contact with glutamatergic neurons. We were able to establish a Glu-dependent rpS6 phosphorylation that is time and dose dependent basically mediated through AMPA receptors activation and the downstream participation of MAPK and TORC1 pathways (Fig 3).

With the idea to understand the physiological role of rpS6 phosphorylation activated by Glu, we decided to evaluate the subcellular distribution of the phosphorylated protein, which is known to be different depending on the cell type. To our surprise, we could detect the phosphorylated protein both in nucleus and in cytoplasm, favoring the notion that neuronal signaling continuously shape astrocytic functions since in one hand, it has a biphasic effect on global protein synthesis, [16,18] and in the other hand it might be involved in ribosomal assembly. Interestingly, the ratio between nuclear/cytoplasmic levels is mantained in the non-phosphorylated/phosphorylated forms of rpS6, suggesting an increase in total rpS6 levels unpon Glu exposure (223.3±24.74 while for cytoplasm is 218.2±9.082 (Fig 4B)). In fact, preliminary data from our lab suggests that Glu treatment increases the amount of polysomal mRNA quantity. We speculate that among the proteins actively translated upon Glu are signaling molecules as rpS6 as well as components of the Glu/glutamine shuttle. Work currently in progress should shed light into this issue.

In summary, we provide here evidence for a receptor-mediated, Glu-dependent rpS6 phosphorylation that might be important not only for protein synthesis regulation but also for ribosomal biogenesis. Work currently in progress in our labs is aimed as to characterize the signal transduction pathways involved in nuclear rpS6 phsophorylation. A summary of our findings is depicted in Fig 5.

REFERENCES

1. Pittenger C, Kandel E (1998) A genetic switch for long-term memory. C R Acad Sci III 321 (2-3):91-96
2. Hollmann M, Heinemann S (1994) Cloned glutamate receptors. Annu Rev Neurosci 17:31-108. doi:10.1146/annurev.ne.17.030194.000335
3. Coutinho V, Knopfel T (2002) Metabotropic glutamate receptors: electrical and chemical signaling properties. Neuroscientist 8 (6):551-561
4. Somogyi P, Eshhar N, Teichberg VI, Roberts JD (1990) Subcellular localization of a putative kainate receptor in Bergmann glial cells using a monoclonal antibody in the chick and fish cerebellar cortex. Neuroscience 35 (1):9-30
5. Lopez-Bayghen E, Rosas S, Castelan F, Ortega A (2007) Cerebellar Bergmann glia: an important model to study neuron-glia interactions. Neuron glia biology 3 (2):155-167. doi:10.1017/s1740925x0700066x
6. Barrera I, Flores-Mendez M, Hernandez-Kelly LC, Cid L, Huerta M, Zinker S, Lopez-Bayghen E, Aguilera J, Ortega A (2010) Glutamate regulates eEF1A phosphorylation and ribosomal transit time in Bergmann glial cells. Neurochemistry international 57 (7):795-803. doi:10.1016/j.neuint.2010.08.017
7. Hu D, Serrano F, Oury TD, Klann E (2006) Aging-dependent alterations in synaptic plasticity and memory in mice that overexpress extracellular superoxide dismutase. The Journal of neuroscience : the official journal of the Society for Neuroscience 26 (15):3933-3941. doi:10.1523/jneurosci.5566-05.2006
8. Klann E, Dever TE (2004) Biochemical mechanisms for translational regulation in synaptic plasticity. Nature reviews Neuroscience 5 (12):931-942. doi:10.1038/nrn1557
9. Gressner AM, Wool IG (1974) The phosphorylation of liver ribosomal proteins in vivo. Evidence that only a single small subunit protein (S6) is phosphorylated. The Journal of biological chemistry 249 (21):6917-6925
10. Tschochner H, Hurt E (2003) Pre-ribosomes on the road from the nucleolus to the cytoplasm. Trends in cell biology 13 (5):255-263
11. Ruvinsky I, Meyuhas O (2006) Ribosomal protein S6 phosphorylation: from protein synthesis to cell size. Trends in biochemical sciences 31 (6):342-348. doi:10.1016/j.tibs.2006.04.003
12. Krieg J, Hofsteenge J, Thomas G (1988) Identification of the 40 S ribosomal protein S6 phosphorylation sites induced by cycloheximide. The Journal of biological chemistry 263 (23):11473-11477
13. Fingar DC, Richardson CJ, Tee AR, Cheatham L, Tsou C, Blenis J (2004) mTOR controls cell cycle progression through its cell growth effectors S6K1 and 4E-BP1/eukaryotic translation initiation factor 4E. Molecular and cellular biology 24 (1):200-216
14. Roux PP, Shahbazian D, Vu H, Holz MK, Cohen MS, Taunton J, Sonenberg N, Blenis J (2007) RAS/ERK signaling promotes site-specific ribosomal protein S6 phosphorylation via RSK and stimulates cap-dependent translation. The Journal of biological chemistry 282 (19):14056-14064. doi:10.1074/jbc.M700906200
15. Ortega A, Eshhar N, Teichberg VI (1991) Properties of kainate receptor/channels on cultured Bergmann glia. Neuroscience 41 (2-3):335-349

16. Gonzalez-Mejia ME, Morales M, Hernandez-Kelly LC, Zepeda RC, Bernabe A, Ortega A (2006) Glutamate-dependent translational regulation in cultured Bergmann glia cells: involvement of p70S6K. Neuroscience 141 (3):1389-1398. doi:10.1016/j.neuroscience.2006.04.076
17. Barrera I, Hernandez-Kelly LC, Castelan F, Ortega A (2008) Glutamate-dependent elongation factor-2 phosphorylation in Bergmann glial cells. Neurochemistry international 52 (6):1167-1175. doi:10.1016/j.neuint.2007.12.006
18. Flores-Mendez MA, Martinez-Lozada Z, Monroy HC, Hernandez-Kelly LC, Barrera I, Ortega A (2013) Glutamate-dependent translational control in cultured Bergmann glia cells: eIF2alpha phosphorylation. Neurochemical research 38 (7):1324-1332. doi:10.1007/s11064-013-1024-1
19. Aguirre A, Lopez-Bayghen E, Ortega A (2002) Glutamate-dependent transcriptional regulation of the chkbp gene: signaling mechanisms. Journal of neuroscience research 70 (1):117-127. doi:10.1002/jnr.10394
20. Zepeda RC, Barrera I, Castelan F, Suarez-Pozos E, Melgarejo Y, Gonzalez-Mejia E, Hernandez-Kelly LC, Lopez-Bayghen E, Aguilera J, Ortega A (2009) Glutamate-dependent phosphorylation of the mammalian target of rapamycin (mTOR) in Bergmann glial cells. Neurochemistry international 55 (5):282-287. doi:10.1016/j.neuint.2009.03.011
21. Morales M, Gonzalez-Mejia ME, Bernabe A, Hernandez-Kelly LC, Ortega A (2006) Glutamate activates protein kinase B (PKB/Akt) through AMPA receptors in cultured Bergmann glia cells. Neurochemical research 31 (3):423-429. doi:10.1007/s11064-005-9034-2
22. Millan A, Arias-Montano JA, Mendez JA, Hernandez-Kelly LC, Ortega A (2004) Alpha-amino-3-hydroxy-5-methyl-4-isoxazolepropionic acid receptors signaling complexes in Bergmann glia. J Neurosci Res 78 (1):56-63. doi:10.1002/jnr.20237
23. Rosner M, Fuchs C, Dolznig H, Hengstschlager M (2011) Different cytoplasmic/nuclear distribution of S6 protein phosphorylated at S240/244 and S235/236. Amino acids 40 (2):595-600. doi:10.1007/s00726-010-0684-2
24. Hershey JW, Sonenberg N, Mathews MB (2012) Principles of translational control: an overview. Cold Spring Harbor perspectives in biology 4 (12). doi:10.1101/cshperspect.a011528
25. Perea G, Araque A (2010) GLIA modulates synaptic transmission. Brain research reviews 63 (1-2):93-102. doi:10.1016/j.brainresrev.2009.10.005
26. Navarrete M, Araque A (2011) Basal synaptic transmission: astrocytes rule! Cell 146 (5):675-677. doi:10.1016/j.cell.2011.08.006
27. Bak LK, Schousboe A, Waagepetersen HS (2006) The glutamate/GABA-glutamine cycle: aspects of transport, neurotransmitter homeostasis and ammonia transfer. Journal of neurochemistry 98 (3):641-653. doi:10.1111/j.1471-4159.2006.03913.x
28. Pellerin L, Magistretti PJ (2012) Sweet sixteen for ANLS. Journal of cerebral blood flow and metabolism : official journal of the International Society of Cerebral Blood Flow and Metabolism 32 (7):1152-1166. doi:10.1038/jcbfm.2011.149
29. Balakrishnan S, Dobson KL, Jackson C, Bellamy TC (2014) Ectopic release of glutamate contributes to spillover at parallel fibre synapses in the cerebellum. The Journal of physiology 592 (Pt 7):1493-1503. doi:10.1113/jphysiol.2013.267039
30. Gallo V, Ghiani CA (2000) Glutamate receptors in glia: new cells, new inputs and new functions. Trends in pharmacological sciences 21 (7):252-258

31. Koirala S, Corfas G (2010) Identification of novel glial genes by single-cell transcriptional profiling of Bergmann glial cells from mouse cerebellum. PloS one 5 (2):e9198. doi:10.1371/journal.pone.0009198
32. Meyuhas O (2008) Physiological roles of ribosomal protein S6: one of its kind. International review of cell and molecular biology 268:1-37. doi:10.1016/S1937-6448(08)00801-0
33. Salmond RJ, Emery J, Okkenhaug K, Zamoyska R (2009) MAPK, phosphatidylinositol 3-kinase, and mammalian target of rapamycin pathways converge at the level of ribosomal protein S6 phosphorylation to control metabolic signaling in CD8 T cells. Journal of immunology 183 (11):7388-7397. doi:10.4049/jimmunol.0902294
34. Cammalleri M, Lutjens R, Berton F, King AR, Simpson C, Francesconi W, Sanna PP (2003) Time-restricted role for dendritic activation of the mTOR-p70S6K pathway in the induction of late-phase long-term potentiation in the CA1. Proceedings of the National Academy of Sciences of the United States of America 100 (24):14368-14373. doi:10.1073/pnas.2336098100
2336098100 [pii]

Figure Legends

Figure 1. *Glutamate induces rpS6phosphorylation in BGC.* Panel A: Confluent BGC monolayers were treated with 1 mM Glu for 15 min. Total protein extracts were subjected to Western blot analysis. The membranes were incubated with specific antibodies that recognize rpS6 phosphorylated and total rpS6. NS, non-stimulated. The immunopositive polypeptides were visualized with peroxidase-conjugated goat anti-rabbit IgGs, using ECL kit. An autoradiography of a typical experiment is shown. Panel B: Representative immunofluorescence of BGC treated with 1 mM Glu for 15 min. Cells were immunostained with the antibody that recognizes total rpS6. Panel C: Immunolocalization of phosphorylated rpS6 (green). Nuclei were counterstained with DAPI (blue).

Figure 2. *rpS6 phosphorylation is time and dose-dependent*. Panel A: BGC monolayers were treated for different time periods with a 1 mM Glu concentration. Panel B: BGC cultures were treated with increasing Glu concentrations for 15 min. The levels of rpS6 phosphorylation were detected via Western blot with anti-phospho rpS6 antibodies and were normalized with total levels of rpS6. Panel C: Non-linear regression of the data obtained in Panel B. Data are expressed as mean ± SE from at least three independent experiments. An autoradiography of a typical experiment is shown. Statistical analysis was performed comparing against data obtained from non-stimulated [11] cells using non-parametric one-way ANOVA (Kruskal-Wallis test) and Dunn's post hoc test (***P*<0.01, ****P*<0.001).

Figure 3. *Signaling pathways involved in Glu-dependent rpS6 phosphorylation*. Panel A: BGC monolayers were incubated for 15 min with the indicated Glu-receptors agonists, 500 µM AMPA, 500 µM KA, 500 µM NMDA plus 10 µM Gly, 25 µM DHPG and 500 µM L-AP4. Panel B: BGC cultures were incubated with the AMPA receptor antagonist, CNQX (50 µM) for 30 min before a 1 mM Glu exposure (15 min). Panel C: BGC were incubated for 15 min with 500 µM NMDA plus 10 µM Gly in the presence or absence of an intracellular Ca^{2+} chelator (BAPTA-AM 25µM) in Mg^{2+} free media. Panel D: BGC were incubated with MEK inhibitor PD98059 (10 µM) or with mTOR inhibitor Rapamycin (100 nM) for 30 min before 1 mM Glu exposure (15 min). The levels of rpS6 phosphorylation were detected via Western blot. Data are expressed as

mean ± SE from at least three independent experiments. An autoradiography of a typical experiment is shown. Statistical analysis was performed comparing data of each condition against non-stimulated [11] using a non-parametric one-way ANOVA (Kruskal-Wallis test) and Dunn's post hoc test (*P<0.05, **P<0.01, ***P<0.001).

Figure 4. *Glutamate increases the rpS6 phosphorylation at cytoplasm*. Subcellular fractionation of BGC treated with Glu for 15 min. The levels of cytoplasmic or nuclear phosphorylated rpS6 protein were detected via Western blot with anti-phospho rpS6 and anti-total rpS6 antibodies. Anti-lamin A/C and anti-GAPDH antibodies were used as controls of nuclear and cytoplasmic extracts, respectively. Data are expressed as mean ± SE from at least three independent experiments. An autoradiography of a typical experiment is shown. Statistical analysis was performed comparing against data obtained from non-stimulated [11] cells using non-parametric one-way ANOVA (Kruskal-Wallis test) and Dunn's post hoc test (*P<0.05, **P<0.01).

Figure 5. *Signaling of rpS6 phosphorylation in Bergmann glial cells*. Glu released from the parallel fibers depolarizes the BGC triggering not only a significant Ca^{2+} influx but also a membrane to nuclei cascade. Interestingly, AMPA receptors are involved in this process and become tyrosine phosphorylated leading to the recruitment and activation of transduction molecules such as the focal adhesion kinase PI-3K, leading to activation of MAPK and mTOR pathways, which in turn trigger the $p90^{RSK}$ and $p70^{S6K}$ activation resulting in rpS6 phosphorylation at Ser235/236.

Figure 1

Click here to download Figure: Fig 1.eps

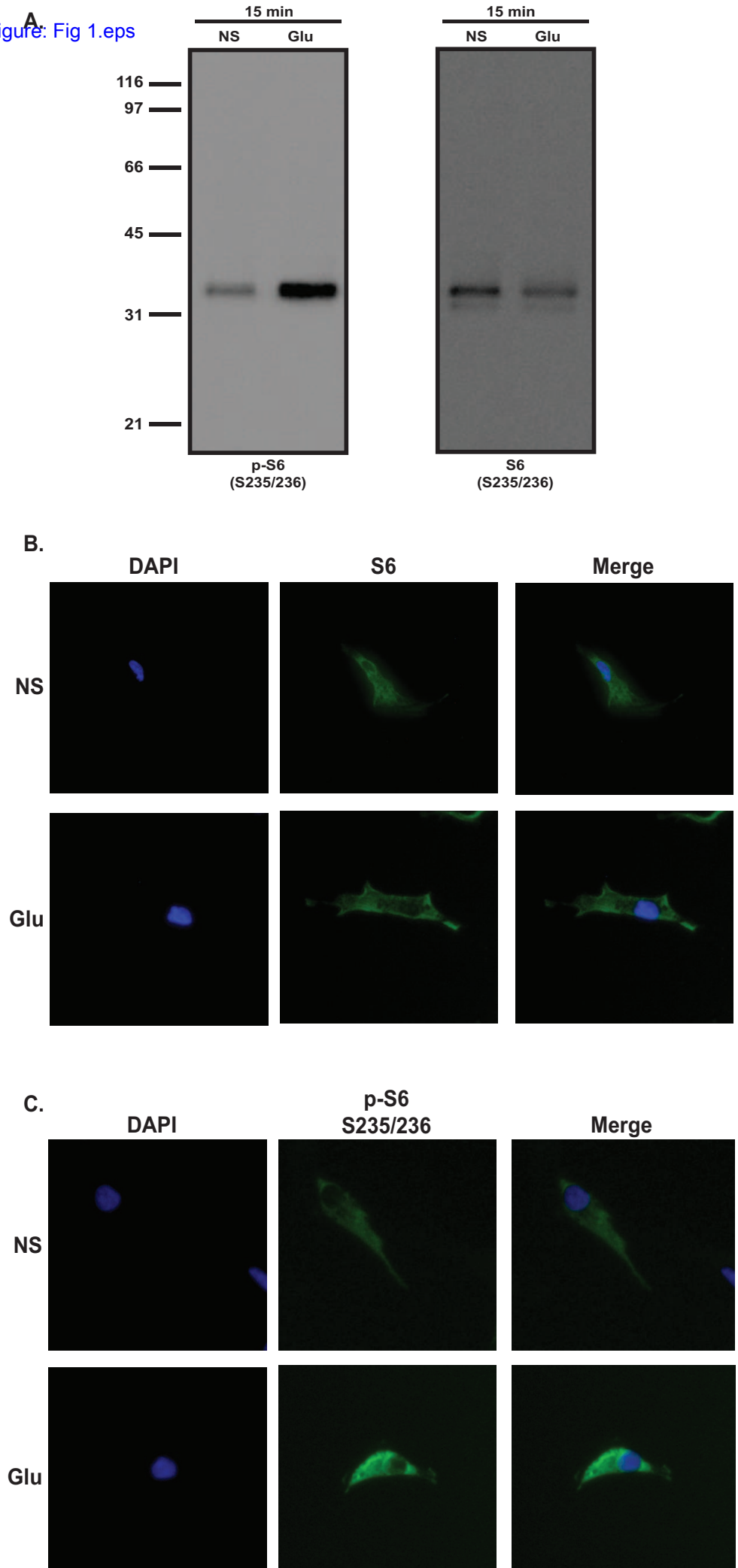

Figure2
Click here to download Figure: Fig 2.eps

Fig. 2

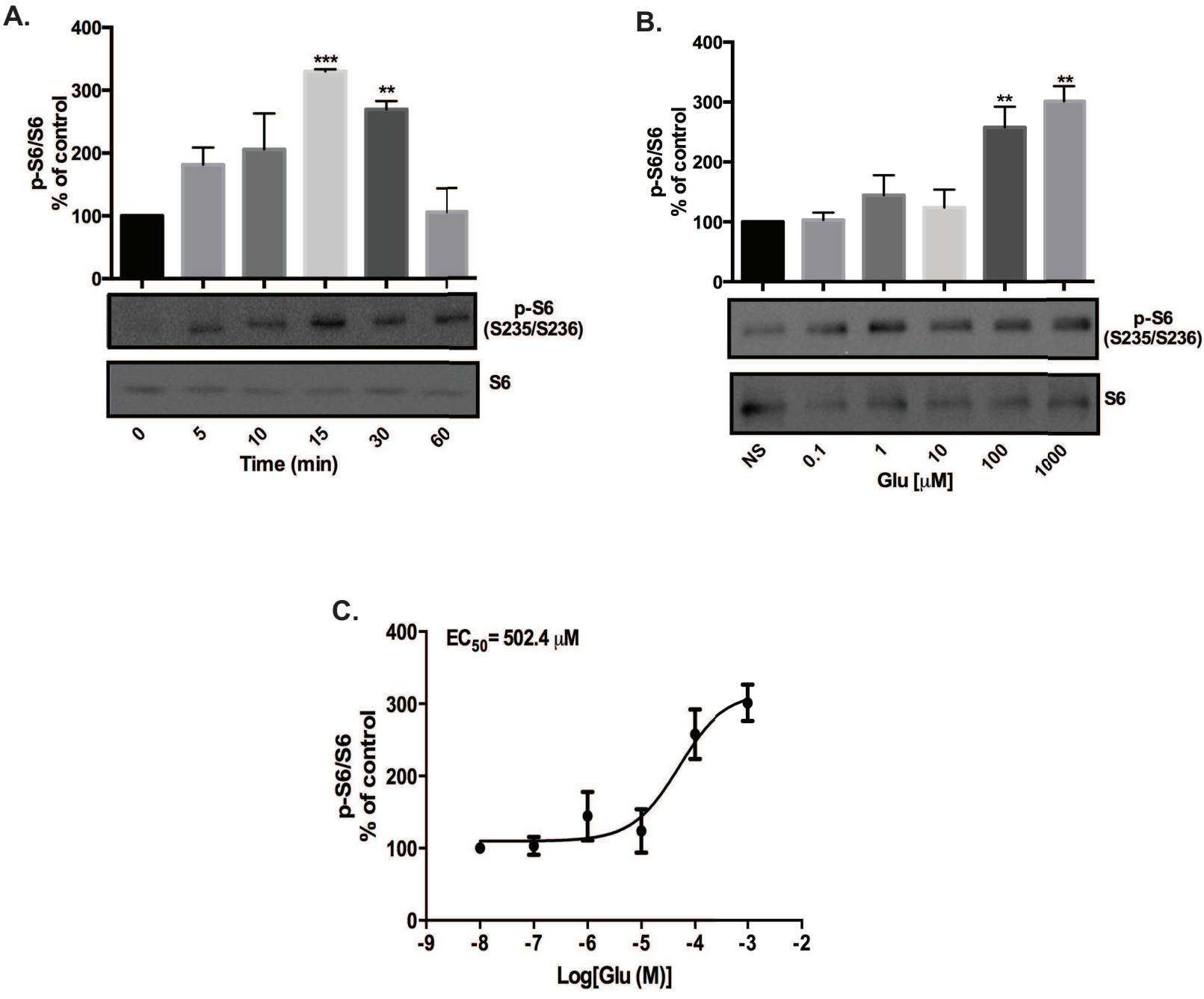

Figure3
Click here to download Figure: Fig 3.eps

Fig. 3

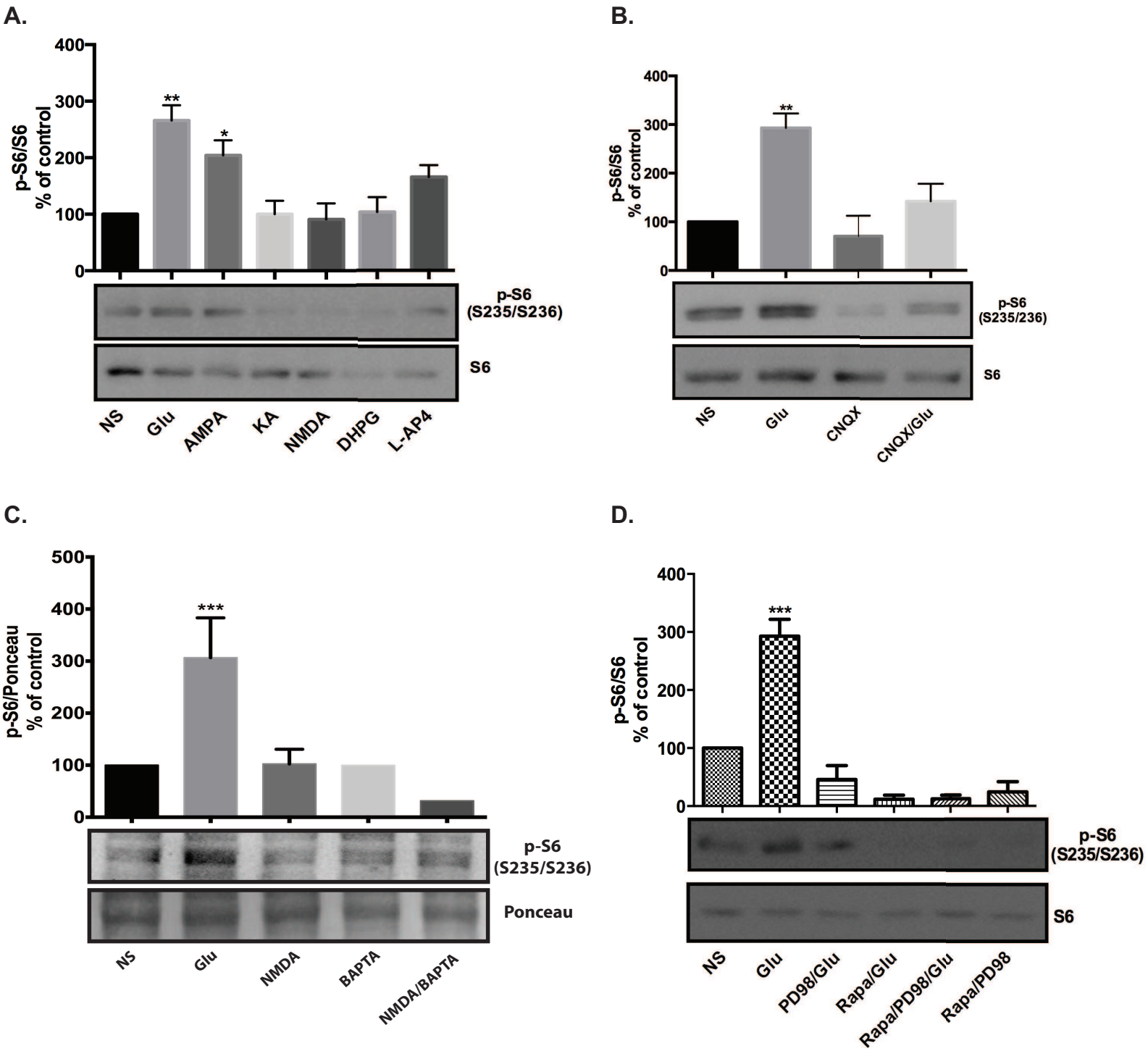

Figure4
Click here to download Figure: Fig 4.eps

Fig. 4

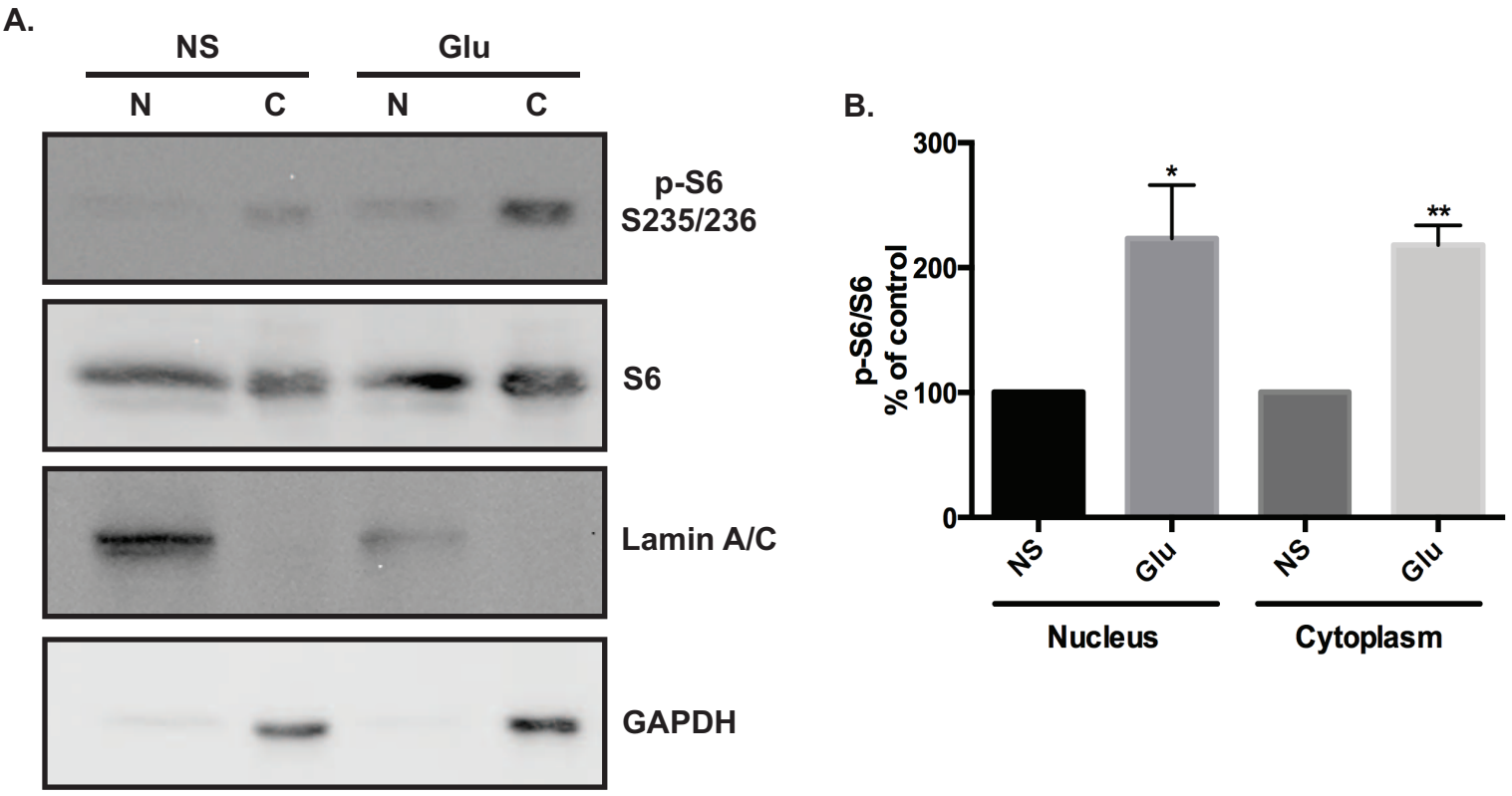

Figure5
Click here to download Figure: Fig 5.eps

Fig. 5

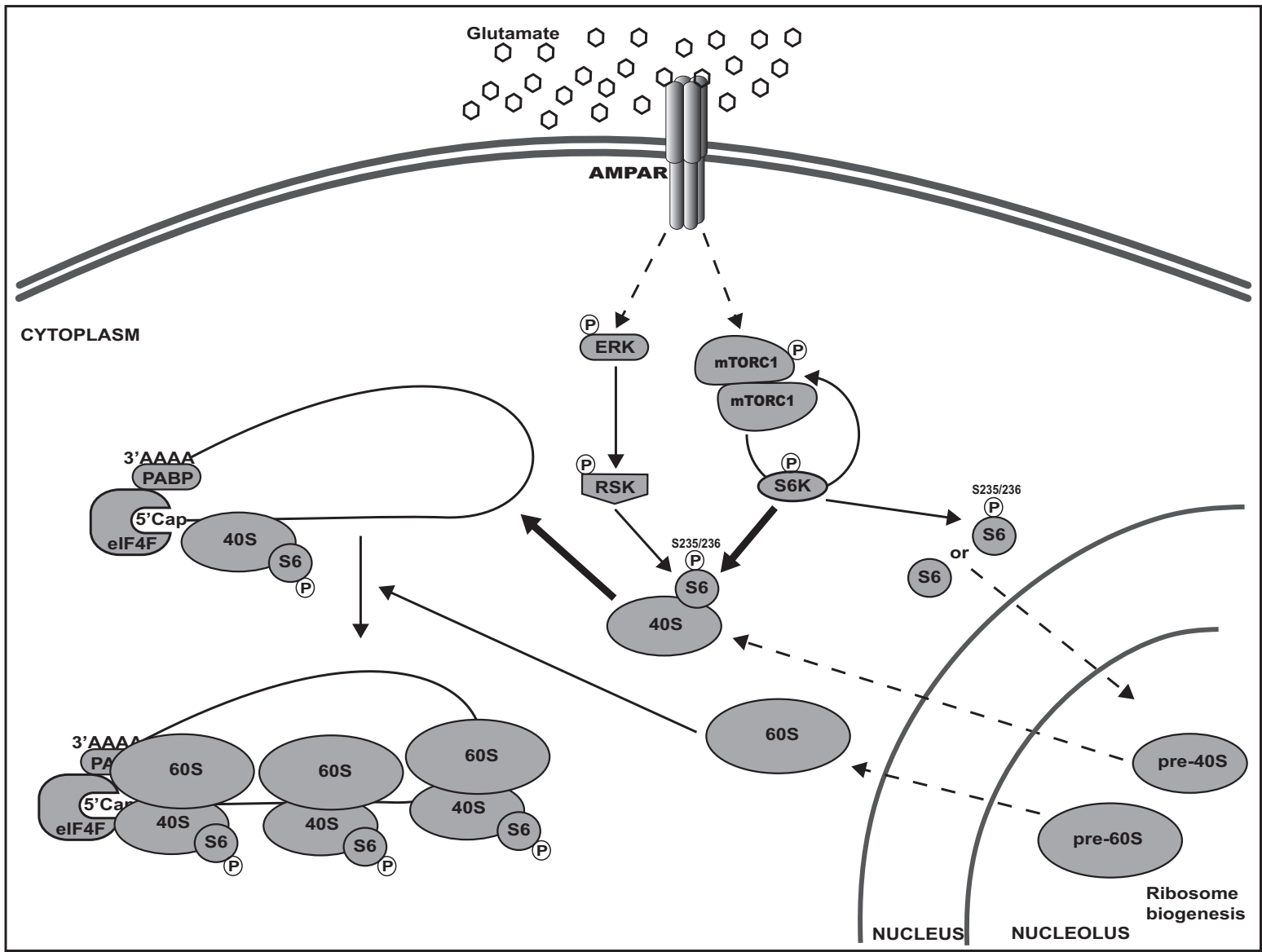

From: Arne Schousboe <em@editorialmanager.com>
To: Arturo Ortega <arortega@cinvestav.mx>
Reply-To: Arne Schousboe <arne.schousboe@sund.ku.dk>
Date: 12 de febrero de 2015 12:26:31 GMT-6
Subject: **Decision on your manuscript**

CC: arne.schousboe@sund.ku.dk

Dear arortega:

I am pleased to inform you that your manuscript, "Glutamate-dependent translational control through ribosomal protein S6 phosphorylation in cultured Bergmann glial cells" has been accepted for publication in Neurochemical Research.

You will receive an e-mail from Springer in due course with regards to the following items:

1. Offprints
2. Colour figures
3. Transfer of Copyright

Please remember to quote the manuscript number, NERE-D-14-00555R1, whenever inquiring about your manuscript. Thank you.

Congratulations and best regards,

Arne Schousboe, D.Sc.
Editor-in-Chief
Neurochemical Research